DOCTOR OF PHILOSOPHY

Elucidating the biological function of the uncharacterised protein FAM83G/PAWS1

Role in Wnt signalling through its interaction with Caseine Kinase 1α

Bozatzi, Polyxeni

Award date:
2018

Elucidating the biological function of the uncharacterised protein FAM83G/PAWS1: Role in Wnt signalling through its interaction with Caseine Kinase 1α

Polyxeni Bozatzi

January 2018

A thesis submitted for the degree of Doctor of Philosophy.

MRC Protein Phosphorylation and Ubiquitylation Unit,

University of Dundee

Contents

List of figures

List of tables

Declarations

I declare that the following thesis is based on the results of investigations conducted by myself, and that this thesis is of my own composition. Work other than my own is clearly indicated in the text by reference to the relevant researchers or to their publications. This dissertation has not in whole, or in part, been previously submitted for a higher degree.

Polyxeni Bozatzi

I certify that Polyxeni Bozatzi has spent the equivalent of at least nine terms in research work in the Medical Research Council Protein Phosphorylation and Ubiquitylation Unit (MRC-PPU), School of Life Sciences, University of Dundee and that she has fulfilled the conditions of the Ordinance General No. 14 of the University of Dundee and is qualified to submit the accompanying thesis in application for the degree of Doctor of Philosophy.

Gopal P. Sapkota

Acknowledgments

First and foremost, I would like to thank my supervisor, Gopal Sapkota, who gave me the opportunity to work on a very interesting and exciting project. I am grateful for his support, guidance, advice and trust that he placed in me over the last few years.

I also want to thank everyone in the Sapkota lab including Tim, Luke H, Luke F, Theresa, Kevin, Karen and Sascha, for making the lab a fun and friendly place to work in. Special thanks go to Tim, who was the only person in the lab when I started my PhD, and became like my daily supervisor. I learnt a lot from his expertise in science and beyond, and his enthusiasm together with his scientific input has been a source of inspiration for me; and to Luke F, not only for making us laugh and maintaining a lively environment in the lab, but for being a great friend, too. I am also grateful to all the students and post-docs that I worked with, and with whom I shared many wonderful times over the last four years.

All the support and administrative staff from MRC-PPU, as well as those from the SLS, were of great help and I would like to thank all of them for making our lives a lot easier. Many thanks to the DSTT staff for the reagents they produced. I am particularly grateful to Tom Macartney and Nikki Wood for all the constructs they made for my project. I would also like to thank David Campbell, Joby Varghese and Bob Gourlay for mass spectrometry analysis. I owe many thanks to our collaborators from Jim Smith's lab in the Francis Crick Institute, with special thanks to Kevin Dingwell for all the *Xenopus* studies, that were a major contribution to the progress of this thesis. I also need to thank my thesis committee, Karim Labib and Ulrich Zachariae for their advice and guidance throughout my PhD.

A huge thanks to the new friends that I made during my PhD: Nikoleta and Stelios for welcoming me to Dundee, Kristina for reminding me to never give up, Jo and Sascha for being my gym buddies and good friends outside the lab, the ISE teachers for keeping us fit and sane, and Fede for his constant support throughout my PhD and life stages in general. I am grateful to my friends from home and especially to Έλενα for being my best friend and for always being there for me even if we are miles apart, and to Βαγγέλη who was there for me during some of the toughest times.

Last but certainly not least, I would like to thank my family in Greece and especially my parents for their endless love and support throughout every stage of my education. Without them I would never be able to do this. Μαμά και μπαμπά ό,τι έγινα το χρωστάω σε εσάς. Αυτή η διατριβη είναι αφιερωμένη σε σας.

Thesis Summary

PAWS1/FAM83G, a member of the poorly characterised FAM83 family of proteins that share the conserved domain of unknown function DUF1669, was identified as an interactor of the SMAD1 transcription factor. Because BMP signalling plays a fundamental role during embryogenesis, collaboration with Jim Smith (The Francis Crick Institute, London) led to the discovery that ectopic expression of PAWS1 mRNA in *Xenopus* embryos leads to a complete duplication of body axis. In similar assays, such a phenotype is associated with either the inhibition of canonical (SMAD4-dependent) BMP signalling or the activation of canonical Wnt/β-catenin signalling. PAWS1 has been reported to modulate only non-canonical BMP signalling and not influence canonical BMP signalling, findings which were also validated in *Xenopus* embryos and PAWS1-knockout U2OS cells in this thesis. Therefore, focus turned to investigating potential roles of PAWS1 in the regulation of the canonical Wnt/β-catenin signalling pathway.

The canonical Wnt/β-catenin signalling pathway plays critical roles during embryogenesis, stem cell self-renewal and in adult tissue homeostasis and is often misregulated in developmental defects, including skin and hair abnormalities, and cancer. In the absence of Wnt signals, sequential phosphorylation of the transcriptional co-factor β-catenin by CK1 and GSK3 results in the ubiquitylation of β-catenin, priming it for degradation via the proteasome. Upon Wnt-activation, β-catenin is stabilised and translocates to the nucleus, where it associates with TCF and LEF and regulates the expression of Wnt-target genes. Although the fundamental steps in Wnt signalling are established, many gaps remain in our understanding of the precise regulation of the pathway. It is demonstrated in this thesis that PAWS1 activates Wnt signalling in both *Xenopus* embryos and human cells. Furthermore, in PAWS1-knockout U2OS cells Wnt signalling is attenuated. Collectively, these data uncover a role for PAWS1 as a novel regulator of canonical Wnt/β-catenin signalling.

In search of molecular mechanisms through which PAWS1 regulates Wnt/β-catenin signalling, a proteomic approach on endogenous PAWS1 revealed the Ser/Thr protein kinase CK1α as a robust PAWS1 interactor. PAWS1 interacts and colocalises with endogenous CK1α. CK1 isoforms are key regulators of Wnt signalling and they phosphorylate many components of the pathway, however their precise regulation in cells, despite being critically important, is poorly understood. After mapping

CK1-interaction sites to key residues within the conserved DUF1669 domain of PAWS1, it was possible to demonstrate that the interaction between PAWS1 and CK1α is critical for PAWS1 to activate Wnt signalling in both *Xenopus* embryos and U2OS cells. Although the phosphorylation of β-catenin on Ser45, which is reported to be phosphorylated by CK1 isoforms, appears to be unaltered by PAWS1-deficiency, the Wnt3A-induced nuclear translocation of β-catenin is slightly inhibited in PAWS1 knockout U2OS cells. It is likely that PAWS1 controls Wnt signalling by directing CK1α to key subcellular locations and substrates upon Wnt stimulation to regulate the nuclear translocation of β-catenin. Consistent with this hypothesis, a global phosphoproteomics analysis of wild type and PAWS1$^{-/-}$ U2OS cells has revealed differential phosphorylation of proteins that may be regulated by the PAWS1:CK1α interaction.

Interestingly, PAWS1 appears to control levels of endogenous CK1α protein and *vice versa*, although the mechanisms by which each achieves this are still unclear. The findings that the DUF1669 domain of PAWS1 interacts with CK1α led to the discovery that all FAM83 members bind to different CK1 isoforms through an identical mechanism. This has led to the hypothesis that FAM83 members serve as anchoring proteins for CK1 isoforms, and in doing so, they regulate CK1 subcellular localisation and substrate accessibility in cells.

Regulation of PAWS1 by post-translational modifications remains poorly defined. A proteomic approach identified calcium and calmodulin-dependent kinase isoforms D and G (CaMK2D and CaMK2G) as two novel interactors of PAWS1. CaMK2 enzymes are activated in response to calcium signals to control cytoskeletal rearrangements and cell movement. PAWS1 has been implicated in actin cytoskeletal dynamics and cell migration, through its dynamic interaction with the adapter protein CD2AP at the cell periphery. Here, PAWS1 has been shown to be phosphorylated at Ser356 by CaMK2D in cells and this phosphorylation event is demonstrated to be important for PAWS1-dependent cell migration.

Lastly, several PAWS1 mutations have been recently linked with the pathogenesis of skin diseases in dogs and humans. However, how these mutations relate to PAWS1 function in cells and potentially cause the disease phenotypes remain elusive. In this thesis, initial steps have been taken to address the potential impact of these pathogenic mutants on PAWS1 function.

Abbreviations

ºC	Celsius degrees
a.u.	arbitrary units
Ab	antibody
ACN	acetonitrile
AD	Alzheimer's disease
ADDA	Alpha-adducin
ADHD	attention-deficit/hyperactivity disorder
AHNK	neuroblast differentiation-associated protein
AI	amelogenesis imperfecta
ALK	activin-receptor-like-kinase
AMP	ampicillin
A-P	anterior-posterior
APC	adenomatous polyposis coli
APS	ammonium persulfate
AR	androgen receptor
ASNS	asparagine synthetase
ATP	adenosine 5’-triphosphate sodium salt
BafA1	Bafilomycin A1
BAMBI	BMP and Activin receptor membrane bound inhibitor
BICC1	bicaudal C homolog 1
BMP	bone morphogenetic protein
BMPR1	bone morphogenetic protein receptor type 1
bp	base pair
C	cytoplasmic
CaM	calmodulin
CaMK2	calcium/calmodulin kinase 2
Cas9	CRISPR associated protein 9
CCNA1	cyclin A1
CD2AP	CD2-associated protein
CDK	cyclin-dependent kinase
cDNA	complementary deoxyribonucleic acid
Chk1	Checkpoint kinase 1
CK	casein kinase
CM	conditioned medium
CNS	central nervous system
cpm	counts per minute
CRISPR	clustered regularly interspaced short palindromic repeat
Cs	cytoskeletal
C-terminal	carboxy-terminal
cyto	cytoplasmic
Da	dalton
DAG	diacylglycerol
DAPI	4',6-diamidino-2-phenylindole
DDX	DEAD-box RNA helicase

DD	death domain
DED	death effector domain
dH_2O	distilled water
DISCC	death-inducing-signalling-complex
DMEM	Dulbecco's modified Eagle's medium
DMP	dimethyl pimelimidate dihydrochloride
DMSO	dimethyl sulfoxide
DNA	deoxyribonucleic acid
dNTP	Deoxynucleotide triphosphate
Drosophila	*Drosophila melanogaster*
DSB	double-stranded break
DSP	dithiobis (succinimidyl propionate)
DSTT	division of signal transduction therapy
DTT	dithiothreitol
DUF1669	domain of unknown function 1669
D-V	dorsoventral
DVL	dishevelled
E.coli	*Escherichia coli*
ECL	enhanced chemiluminescence
EDTA	ethylenediaminetetraacetate
EGFR	epidermal growth factor receptor
EGTA	ethyleneglycol bis (2-aminoethylether)-N'N'tetraacetic
ER	endoplasmic reticulum
FACS	flow-cytometry associated cell sorting
FAM83	family with sequence similarity 83
FASPS	familial advanced phase sleep syndrome
FBS	foetal bovine serum
FGF	fibroblast growth factor
FGFR	fibroblast growth factor receptor
FT	flow-through extracts
FZD	Frizzled
g	grams or gravity
G418	geneticin
GAPDH	glyceraldehyde 3-phosphate dehydrogenase
G-CK	genuine casein kinase
GFP	green fluorescent protein
Gli	glioma-associated oncogene homolog
GRK2	G-protein coupled receptor kinase 2
gRNA	guide ribonucleic acid
GSK3	glycogen synthase kinase 3
GST	glutathione S-transferase
h	hours
HA	haemagglutinin
HaCaT	human keratinocyte
HEK	human embryonic kidney
HEPES	4-(2-Hydroxyethyl)piperazine-1-ethanesulfonic acid
HFH	hereditary footpad hyperkeratosis
Hh	Hedgehog

HCl	Hydrochloric acid
HMMR	hyaluronan mediated motility receptor
HPLC	high-performance liquid chromatography
HRP	horseradish peroxidase
IC50	half maximal inhibitory concentration
ID1	inhibitor of differentiation 1
IF	immunofluorescence
IGF	insulin-like growth factor
IgG	immunoglobulin G
IMiD	immunomodulatory drug
IP	immunoprecipitation
IPTG	isopropyl thio-β-D-galactoside
IRES	internal ribosome entry sites
JNK	JUN-N-terminal kinase
KD	kinase dead
kDa	kilodalton
KI	Knock-in
Km	Michaelis-Menten constant
KO	knockout
L	litre
L3-CM	L-Wnt3A producing cells condition medium
LB	Luria-Bertani medium
LC3	Microtubule-associated protein 1A/1B-light chain 3
L-CM	L cells conditioned medium
LC-MS/MS	liquid chromatography coupled to high-resolution tandem mass spectrometry
LDLR	low density lipoprotein receptor
LEF	lymphoid enhancer factor
Lena	Lenalidomide
LGR5	leucine-rich repeat-containing G-protein coupled receptor 5
LRP5/6	low-density-lipoprotein receptor-related proteins 5 and 6
luc	luciferase
m	milli or meter
M	molar or membrane
MDM2	murine double minute clone 2
MDS	myelodysplastic syndrome
min	minutes
MMP	matrix metalloproteinase
mol	mole
MOPS	3-(N-morpholino) propanesulfonic acid
MRC PPU	Medical Research Council Protein Phosphorylation and Ubiquitylation Unit
mRNA	messenger ribonucleic acid
MS	mass spectrometry
MUSK	muscle skeletal receptor Tyr kinase
MW	molecular weight
n	nano or number
N	nuclear
n.s.	no statistical significance
NaCl	sodium chloride

NCI	national cancer institute
NEDD9	neural precursor cell expressed developmentally down-regulated protein 9
NFAT	nuclear factor associated with T cells
NLS	nuclear localisation signal
nm	nanometer
N-terminal	amino-terminus
Nups	nucleoproteins
OD	optical density
p	pico
p-	phospho
PAGE	polyacrylamide gel electrophoresis
PAI-1	plasminogen activator inhibitor-1
PAWS1	Protein Associated With SMAD1
PBS	phosphate-buffered saline
PC3	prostate cancer cell line
PCP	planar cell polarity
PCR	polymerase chain reaction
PEI	polyethylenimine
PER1/2	period(in) 1/2
PKA	protein kinase A
PKC	protein kinase C
PLD	phospholipase D
PP2A	protein phosphatase 2A
PPK	palmoplantar keratoderma
PTEN	phosphatase and tensin homolog
PTK7	protein Tyr kinase 7
PVDF	polyvinylidene difluoride
PyrPam	pyrvinium pamoate
qPCR	quantitative reverse transcription polymerase chain reaction
RanBP3	ran binding protein 3
RAS	rat sarcoma protein family
Res	rescue
RNA	ribonucleic acid
RNAi	ribonucleic acid interference
ROCK	RHO-associated kinase
ROR	receptor Tyr kinase-like orphan receptor
rpm	revolutions per minute
RXR	retinoid X receptor
RYK	receptor Tyr kinase
SD	standard deviation
SDS	sodium dodecyl sulphate
sec	seconds
SEM	standard error of the mean
SHH	Sonic Hedgehog
siRNA	small interfering ribonucleic acid
SLS	School of Life Sciences
SMAD1	mothers against DPP homologue 1
Smo	Smoothered

TAE	Tris-acetate-EDTA
TBS	tris-buffered saline
TBST	tris-buffered saline with Tween 20
TCF	T cell factor
TFA	trifluoracetic acid
TEMED	tetramethylethylenediamine
TGFBI	transforming growth factor beta induced
TGFβ	transforming growth factor β
TKI	tyrosine kinase inhibitor
TMT	tandem mass tag
tris	tris(hydroxymethyl)methylamine
Triton X-100	t-octylphenoxypolyethoxyethanol-X-100
TTBK	tau tubulin kinase
Tween 20	polyethylene glycol sorbitan monolaurate
Ub	ubiquitin
URP	unfolded protein response
UV	ultraviolet
V	volts
v/v	volume to volume
VRK	vaccinia related kinase
w/v	weight to volume
WASF3	Wiskott-Aldrich syndrome protein family member 3
Wls	Wntless
wly	wooly
WRE	Wnt-responsive element
WT	wild type
x	*Xenopus*
XIRP1	Xin actin-binding repeat-containing protein 1
XNLA	*Xenopus laevis*
Xnr	*Xenopus* nodal-related factor
β-TrCP	β-transducin repeat-containing protein
µ	micro

Amino acid code

amino acid	three letter code	one letter symbol
Alanine	Ala	A
Arginine	Arg	R
Asparagine	Asn	N
Aspartic acid	Asp	D
Cysteine	Cys	C
Glutamic acid	Glu	E
Glutamine	Gln	Q
Glycine	Gly	G
Histidine	His	H
Isoleucine	Ile	I
Leucine	Leu	L
Lysine	Lys	K
Methionine	Met	M
Phenylalanine	Phe	F
Proline	Pro	P
Serine	Ser	S
Threonine	Thr	T
Tryptophan	Trp	W
Tyrosine	Tyr	Y
Valine	Val	V
any amino acid	Xaa	X

List of Publications

Bozatzi P, Dingwell KS, Wu KZL, Cooper F, Cummins TD, Hutchinson LD, Vogt J, Wood NT, Macartney TJ, Varghese J, Gourlay R, Campbell DG, Smith JC and Sapkota GS. (2018) PAWS1 controls Wnt signalling through association with Casein Kinase 1α. EMBO Rep. Apr;19(4). Pii: e44807

Bozatzi P and Sapkota GP (2018) The FAM83 family of proteins: From pseudo-PLDs to anchors for CK1 isoforms. Biochemical Society Transductions (In press)

Fulcher LJ, **Bozatzi P**, Tachie-Menson T., Wu KZL, Cummins TD, Bufton JC, Pinkas DM, Dunbar K, Shrestha S, Wood NT, Weidlich S, Macartney TJ, Varghese J, Gourlay R, Campbell DG, Dingwell KS, Smith JC, Bullock AN and Sapkota GS (2018) The DUF1669 domain of FAM83 family proteins anchor casein kinase 1 isoforms. Science signalling (In press)

Hutchinson LD, **Bozatzi P**, Macartney TJ, and Sapkota GP (2018) Generation of endogenous BMP transcriptional reporter cells through CRISPR/Cas9 genome editing. Methods Mol Biol (In Press)

Cummins TD, Wu KZL, **Bozatzi P**, Dingwell KS, Macartney TJ, Wood NT, Varghese J, Gourlay R, Campbell DG, Prescott A, Griffis E, Smith JC, Sapkota GP. (2018) PAWS1 controls cytoskeletal dynamics and cell migration through association with the SH3 adaptor CD2AP. J Cell Sci. 2018 Jan 10;131(1)

Fulcher, L. J., Macartney, T., **Bozatzi, P**., Hornberger, A., Rojas-Fernandez, A. and Sapkota, G. P. (2016) An affinity-directed protein missile system for targeted proteolysis. Open Biol. Oct6;(10)

1. Introduction

1.1 Overview of FAM83G/PAWS1

The human FAM83G protein is a 91 kDa protein composed of 823 amino acids. It is encoded by the *FAM83G* gene, located on Chromosome 17p11.2. *FAM83G* belongs to the poorly characterized FAM83 family (Family with sequence similarity 83) of genes, which are conserved in vertebrates. The FAM83 family consists of eight members (FAM83A-H), which share the conserved domain of unknown function (DUF1669) at their N-terminus (Fig 1-1). To date, very little is known about the biological roles of the FAM83 proteins and much less about the DUF1669.

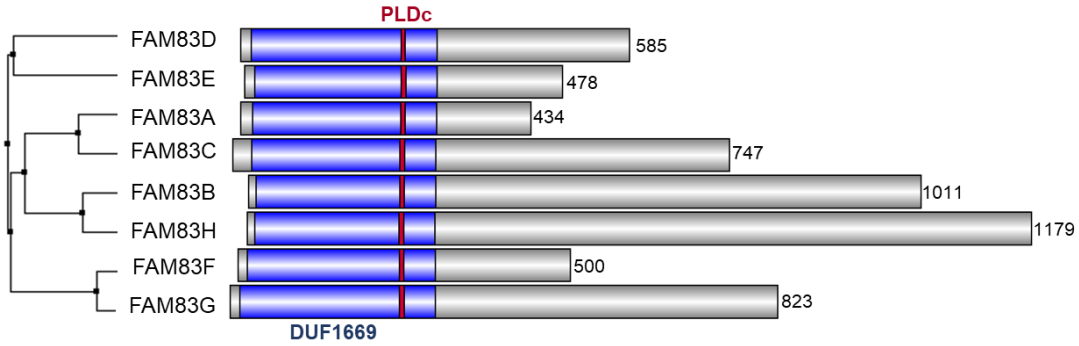

Figure 1- 1 Schematic overview of the human FAM83 proteins.

The relative size and the location of the conserved DUF1669 domain is highlighted in blue. The PLDc-like motif which lies within the DUF1669 is highlighted in pink. The phylogenetic tree was constructed in Jalview based on the conserved DUF1669 domain.

The Sapkota lab identified FAM83G as an interacting partner of the transcription factor SMAD1 and thus it was renamed as PAWS1 (Protein Associated With SMAD1) (Vogt, Dingwell et al. 2014). SMAD1 is an intracellular mediator of the bone morphogenetic protein (BMP) signalling pathway. BMP signalling regulates many cellular processes, such as differentiation, proliferation, motility and apoptosis, during embryonic development and in adult tissues (Shi and Massague 2003) During embryogenesis, BMP signalling is first seen during gastrulation, when the cell fate patterning happens(Little and Mullins 2006). In vertebrates, BMPs pattern ventral cell fates, whereas repression of BMP signalling is required for dorsal cell fates (Holley, Jackson et al. 1995). Expression of BMPs in the ventral animal pole, in combination with

expression of BMP antagonists in the dorsal side, create a gradient of BMP signalling along the dorsal-ventral axis, to ensure proper embryonic development (De Robertis and Kuroda 2004). Abnormal BMP signalling is associated not only with developmental abnormalities but also with many human diseases, including bone defects and cancer (Massague, Blain et al. 2000, Shi and Massague 2003).

BMPs bind to BMP receptor complexes, leading to the phosphorylation of the transcription factors SMAD1, 5 and 8. These SMADs are then associated with SMAD4 and they translocate into the nucleus (canonical BMP signalling pathway), where they modulate the transcription of target genes, such as *ID1* and *SMAD6* (Ishida, Hamamoto et al. 2000, Lopez-Rovira, Chalaux et al. 2002). Alternatively, it has been shown that in cells that lack SMAD4 expression, BMPs can signal independently of SMAD4 and can regulate the transcription of about a hundred genes involved in the suppression of cell proliferation and chemotaxis, including *NEDD9*, *ASNS* and *PTEN* (Beck and Carethers 2007, Perron and Dodd 2009). This is often referred to as non-canonical BMP signalling pathway and to date it remains poorly characterised.

PAWS1 was shown to form a macromolecular complex with SMAD1 independent of SMAD4 or BMP stimulation (Vogt, Dingwell et al. 2014). It was further shown that the manipulation of PAWS1 levels by over-expression and siRNA knock-down approaches, did not affect the BMP-induced phosphorylation of SMAD1, nor the expression of canonical BMP-target genes (Vogt, Dingwell et al. 2014). PAWS1 is the first non-SMAD BMP type I receptor substrate, as it was found to be phosphorylated by BMPR1A (ALK3) at Ser610, Ser614 and Ser616 *in vitro*. BMP stimulation was also found to induce PAWS1 phosphorylation at Ser610 in HaCaT cells (human keratinocytes). Mutation of Ser610 to Ala did not affect the PAWS1 interaction with SMAD1 but did impact the transcription of the PAWS1-target genes *NEDD9* and *ASNS* upon BMP stimulation (Vogt, Dingwell et al. 2014).

Preliminary work, using RNA-sequencing, showed that introduction of PAWS1 in PC3 prostate cancer cells, which lack endogenous PAWS1 expression due to hypermethylation of its promotor, was found to regulate the transcription of over 800 genes, in a SMAD4-independent manner [Table 1-1; (Vogt 2013) PhD thesis, http://discovery.dundee.ac.uk]. However, most of these genes were regulated by PAWS1 independent of BMP stimulation, suggesting that PAWS1 also acts in pathways other than BMP signalling. It is presently unknown how PAWS1 regulates transcription of so many target genes, and whether the association with SMAD1 is required for this. Although there

are no apparent or predicted DNA-binding motifs on PAWS1, it is still unclear whether PAWS1 can potentially act as a transcription factor or transcription co-factor.

PAWS1 up-regulated		PAWS1 down-regulated	
CAMK2B	CHRM3	AFF2	ADCY1
GJB2	HPGD	ALDH2	AR
KCNK13	LGR5	BEX1	CCNA1
MMP1	MMP13	CNTN1	CXorf57
MPZL2	MUC3A	FREM2	GABRA3
NPY1R	PCDHB8	GABRG3	MAGEA3
PCDHGB2	PPP2R2C	MAGEA6	NEO1
PROKR1	REG4	NEURL	PDGFRA
SH2D1B	TSPAN8	PDZRN3	TUB
TGFBI	ZNF100	WASF3	RFXAP

Table 1- 1 Top 40 PAWS1-regulated genes in PC3 cells

PAWS1-dependenent genes were identified by RNA-sequencing and validated by RT-PCR. (Red: >10fold, black: >5fold, blue: >4fold) (By Vogt PhD thesis, *http://discovery.dundee.ac.uk*).

Remarkably, bioinformatic analysis of the 800 genes that showed transcriptional regulation by PAWS1 revealed that these genes could not be assigned to any single, known signalling pathway, suggesting that PAWS1 might be involved in multiple pathways in cells. The majority of the genes whose expression was significantly altered by PAWS1 are reported as mis-expressed or functionally compromised in cancer. Moreover, PAWS1 protein expression was shown to be absent from over 60% of the cancer cell lines in the National Cancer Institute (NCI) panel (Vogt PhD thesis, http://discovery.dundee.ac.uk). In line with this, hundreds of PAWS1 mutations have been identified in various human cancers. According to the online COSMIC database by the Sanger Institute, over half of PAWS1 mutations are missense substitutions with the majority of them found in skin tissue (http://cancer.sanger.ac.uk/cosmic/gene/analysis?ln=FAM83G#overview).

Another study in the literature reporting on PAWS1 function describes a recessive missense mutation (R52P) on PAWS1 in dogs that suffer from hereditary footpad

hyperkeratosis (HFH). HFH is characterised by epidermal hyperplasia and hair follicular abnormalities (Drogemuller, Jagannathan et al. 2014, Sayyab, Viluma et al. 2016) The affected dogs develop hard and cracked footpads, which become severely debilitating over time. Hyperkeratosis is a serious condition in humans and it is associated with defects in the genes encoding keratins (Cheng, Syder et al. 1992). Through communication with Prof. I. McLean (University of Dundee), who works on skin diseases, a novel putative mutation (G640R) in human PAWS1 was identified in patients with benign trichilemmal cysts, which originate from hair follicles. More recently, another recessive mutation on PAWS1 (A34E) was published and it was associated with palmoplantar keratoderma, a condition characterised by abnormal thickening of the palms and soles, and exuberant scalp hair (Maruthappu, McGinty et al. 2017) (Fig 1-2).

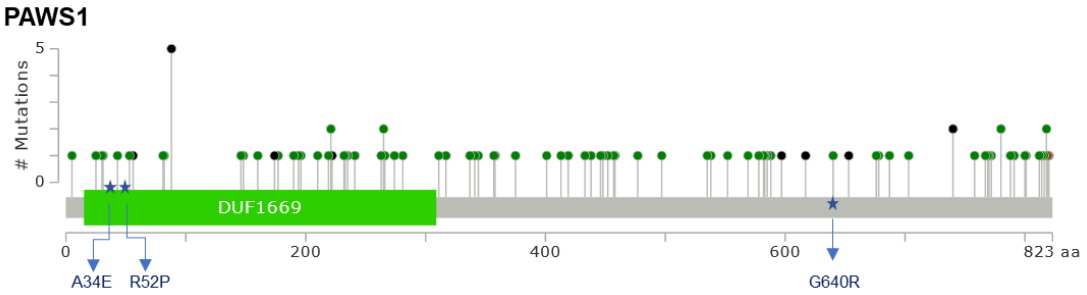

Figure 1- 2 Schematic representation of the PAWS1 protein with the locations of the reported mutated residues.

Missence mutations are shown in green, truncating in black and in-frame in brown. The stars highlight the residues that are found to be mutated in skin disease. Figure was adapted from *www.cbioportal.org.*

Finally, Radden *et al.* (2013) reported a 955 bp deletion of the genomic DNA that transcribes the *PAWS1* gene in mice with the wooly mutation (wly) (Radden, Child et al. 2013). The phenotypic characterisation of the affected mice was limited to observations of matted and rough coat in 3-4-week-old pups and giant hair follicles during the first stage of the hair growth cycle in 5-week-old pups (The Jackson Laboratory; https://www.jax.org/strain/004774) but this was not followed up by any further investigation into PAWS1 protein expression or function.

Taken together, it appears that all the pathological conditions associated with PAWS1 affect the skin or the hair. Therefore, one can hypothesise that PAWS1 plays an important role in the development or homeostasis of the skin and the hair follicles. Hence,

it would be pertinent to investigate potential implications of PAWS1 in the molecular pathways that are known to govern these processes. During skin development, Wnt signalling is critical for the determination of epidermal cell fate of the ectoderm (Wilson and Hemmati-Brivanlou 1995). Activation of Wnt signalling in ectodermal cells leads to FGF inhibition followed by the induction of BMPs expression, which were shown to be epidermal inducers (Wilson and Hemmati-Brivanlou 1995). In the postnatal skin, active Wnt signalling is required for the development of the hair follicle (Andl, Reddy et al. 2002). Notably, the hair follicles, in addition to their role in hair production, also have self-renewal properties due to the presence of pluripotent stem cells and this process is also regulated by the Wnt signalling pathway (Lim and Nusse 2013). Hyperactivation of Wnt signalling has been linked to skin tumours (Malanchi, Peinado et al. 2008, Yang, Andl et al. 2008). Furthermore, patients with mutations in the Wnt genes were reported to display palmoplantar hyperkeratosis and hair growth abnormalities (Adaimy, Chouery et al. 2007, Petrof, Fong et al. 2011). Collectively, the evidence above raises the tantalising possibility that PAWS1 might function in the Wnt signalling pathway.

Thus far, the main limitation of assigning a biochemical role to PAWS1 is the lack of any obvious functional domains within its protein sequence. Therefore, it is important to discuss the functional insights gleaned from other FAM83 members and try to understand the potential role of the conserved DUF1669 domain that unites all FAM83 family members.

1.2 The Fam83 family of proteins

The FAM83 (FAMily with sequence similarity 83) family of proteins consists of 8 members (A to H), which were clustered together based on sequence similarity of a conserved DUF1669 domain (Pfam PF07894) of unknown function. Often, sequence similarity implies similar biological and biochemical functions (Joshi and Xu 2007). The conserved globular DUF1669 domain lies at the very N-termini of the FAM83 members. Outside the DUF1669 domain there is no detectable sequence similarity among the family members and the most of C-terminal section of every FAM83 member is predicted to consist of non-globular, disordered regions (Fig 1-3; Appendix Fig A-1). Domains are defined as functional and/or structural units of a protein (Sheehan 2011). Thus, grouping together proteins based on the presence of a domain can provide a useful starting point to form testable hypotheses, especially when there is a lack of any functional information. Therefore, identifying the role(s) of the DUF1669 domain, its structure and function in cells, is critical for the biological characterisation of the FAM83 family.

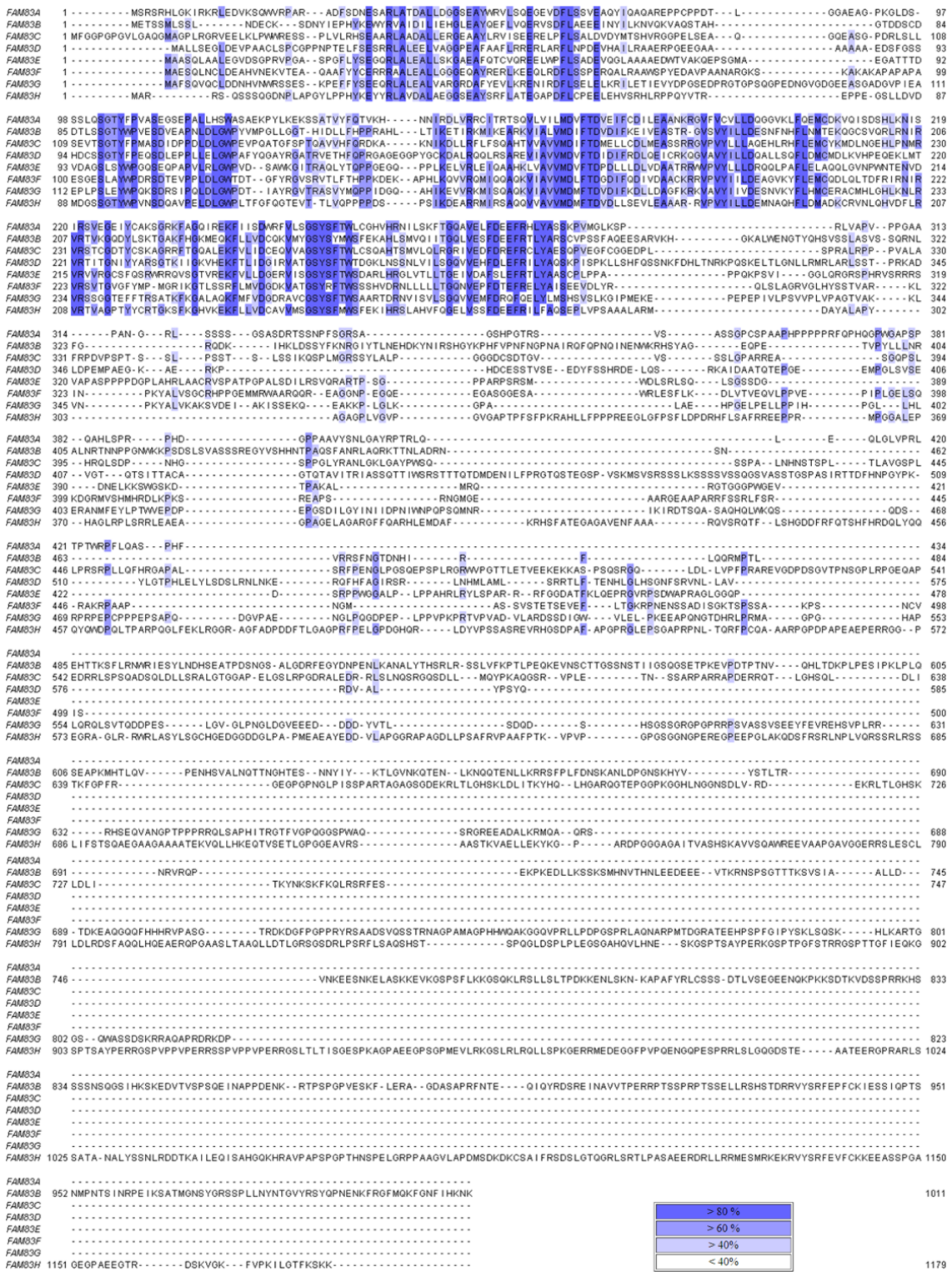

Figure 1- 3 Multiple sequence alignment of the human FAM83 proteins.

Alignment was performed with ClustalO in Jalview 2.10.3 and colouring indicates the % of sequence identity.

Often, domains of unknown function (DUFs), by definition are understudied. However, many DUFs are present in essential proteins and they are highly conserved, implying critical roles in biology (Luo, Gamage et al. 2016, Tong, Chen et al. 2016) .The

limited three-dimensional protein structure, phenotypic and protein-protein interaction data, has hampered the reliable assignment of a functional annotation of these predicted but uncharacterised protein DUF domains. This is the reason why there is not much information available regarding the biological and the biochemical properties of the FAM83 family.

The FAM83 genes are conserved in vertebrates but are absent in more primitive organisms. The observations that FAM83 genes are mutated in various cancers (Lee, Hu et al. 2008, Cipriano, Graham et al. 2012, Wang, Liu et al. 2013, Cipriano, Miskimen et al. 2014, Mao, Liu et al. 2016, Walian, Hang et al. 2016, Wang, Hu et al. 2016, Kim, Park et al. 2017, Perez-Pena, Alcaraz-Sanabria et al. 2017, Snijders, Lee et al. 2017) have made this novel family of genes an interesting topic for pursuing further biological research, aimed at identifying their functions in health and disease.

1.2.1 Are FAM83 proteins pseudo-PLDs?

According to annotation databases (UniProt, SMART), the DUF1669 domain displays a short sequence of amino acids that resembles the phospholipase D catalytic motif (PLDc). Phospholipase D (PLD) is an enzyme which hydrolyses the most abundant membrane lipid, phosphatidylcholine, to choline and phosphatidic acid. Phosphatidic acid is rapidly converted into diacylglycerol by phosphatidic phosphatase, which then activates protein kinase C isoforms. PLDs are involved in phospholipid metabolism, intracellular signal transduction and vesicle trafficking (Jenkins and Frohman 2005). There are six PLD isoforms in humans: PLD1 and PLD2 which share about 50% sequence similarity, the endoplasmic reticulum transmembrane PLD3 and PLD4, PLD5, which so far is considered inactive enzyme, and PLD6, which is also called mitoPLD (Nelson and Frohman 2015). The conventional phospholipase catalytic motif comprises the conserved consensus sequence motif His-x-Lys-x-x-x-x-Asp (also referred to as HKD), where x denotes any amino acid (Sung, Roper et al. 1997). Human PLD1 and PLD2 have two HKD motifs, which are critical for their enzymatic activity (Sung, Roper et al. 1997), whereas the rest of the human PLD isoforms have only one HKD motif. It was suggested that one His of the HKD motif acts as the nucleophile that attacks a phosphate group of a lipid substrate while the second His protonates the remaining group, allowing a water molecule or primary alcohol to complete the hydrolysis reaction (Leiros, Secundo et al. 2000, Xie, Ho et al. 2000). Often, the histidine of the HKD motif is mutated to Ala for neutralizing the catalytic activity (Yang and Roberts 2002). Notably, PLD6 is phylogenetically closer to the bacterial endonuclease Nuc, which also contains a single

HKD motif (Choi, Huang et al. 2006). The resolved crystal structure of Nuc showed that it forms a dimer to assemble into a functional complex (Stuckey and Dixon 1999).

To date no PLD catalytic activity has been attributed to FAM83 proteins. This is supported by the fact that unlike the PLD enzymes, all FAM83 proteins except FAM83D have a *pseudo* HKD motif in which the first His residue is replaced by another amino acid (Fig 1-4). Moreover, unlike PLDs, in all FAM83 proteins there is only one HKD motif. It is therefore unlikely that FAM83 proteins retain any PLD enzymatic activity. However, based on the presence of an inactive PLD motif, FAM83 proteins could be classified as pseudo PLDs. Their sequence similarity with the PLD catalytic motif might still imply that they have retained related direct or indirect signalling function. Pseudoenzymes usually arise from gene duplication events and during evolution they lose the key catalytic sites, thereby gaining new functions (Adrain and Freeman 2012). As the signalling events become more complex in the higher eukaryotes, it is possible that the pseudoenzymes still function in the same signalling pathways as the active enzyme counterparts, as regulators of allosteric activation or suppression (Murphy, Farhan et al. 2017). Currently, the only example that FAM83 proteins assume such a role was reported by Cipriano et al (2014) who showed that overexpression of FAM83B leads to increased PLD activity in human mammary epithelial cells, through hyperactivation of the epidermal growth factor receptor (EGFR) (Cipriano, Bryson et al. 2014).

Another piece of evidence to support a putative pseudo-PLD role for the FAM83 family of proteins comes from the crystal structures of the DUF1669 domains of FAM83A and FAM83B. During the course of my PhD, a collaboration with Dr A. Bullock (University of Oxford) was set up to resolve the crystal structures of the FAM83 proteins. The Bullock lab crystallised the human FAM83A and FAM83B DUF1669 domains (PDB 4URJ and 5LZK, unpublished). Both structures displayed dimerization, with the architecture of the pseudo HKD motif almost identical to that of the HKD motifs from the crystal structures of *Streptomyces sp.* PLD, and the *Salmonella typhimurium* Nuc endonuclease (Fig 1-5). However, there were many unique features noted. For example, the DUF1669 cleft was found to be more open and funnel-like compared to the cylindrical cleft of the PLD catalytic core, suggesting that FAM83 DUF1669 domain could accommodate larger ligands than a phospholipid (Fig 1-5). Furthermore, unique structural motifs that were observed in FAM83 proteins that were absent from PLD, including beta-hairpins (Fig 1-4, 1-5). It is yet to be determined if these structural motifs are involved in protein folding or if they are important for mediating interactions with other proteins, or

DNA (Leon, Tecklenburg et al. 2008). Other than the similarities in the position of the catalytic cleft residues, the overall structures of DUF1669 and PLDs were significantly different. These findings also suggest that FAM83 proteins might form homo- or hetero-dimers, which despite the absence of catalytic residues, might be both necessary and important for proper biological function in response to different biological signals.

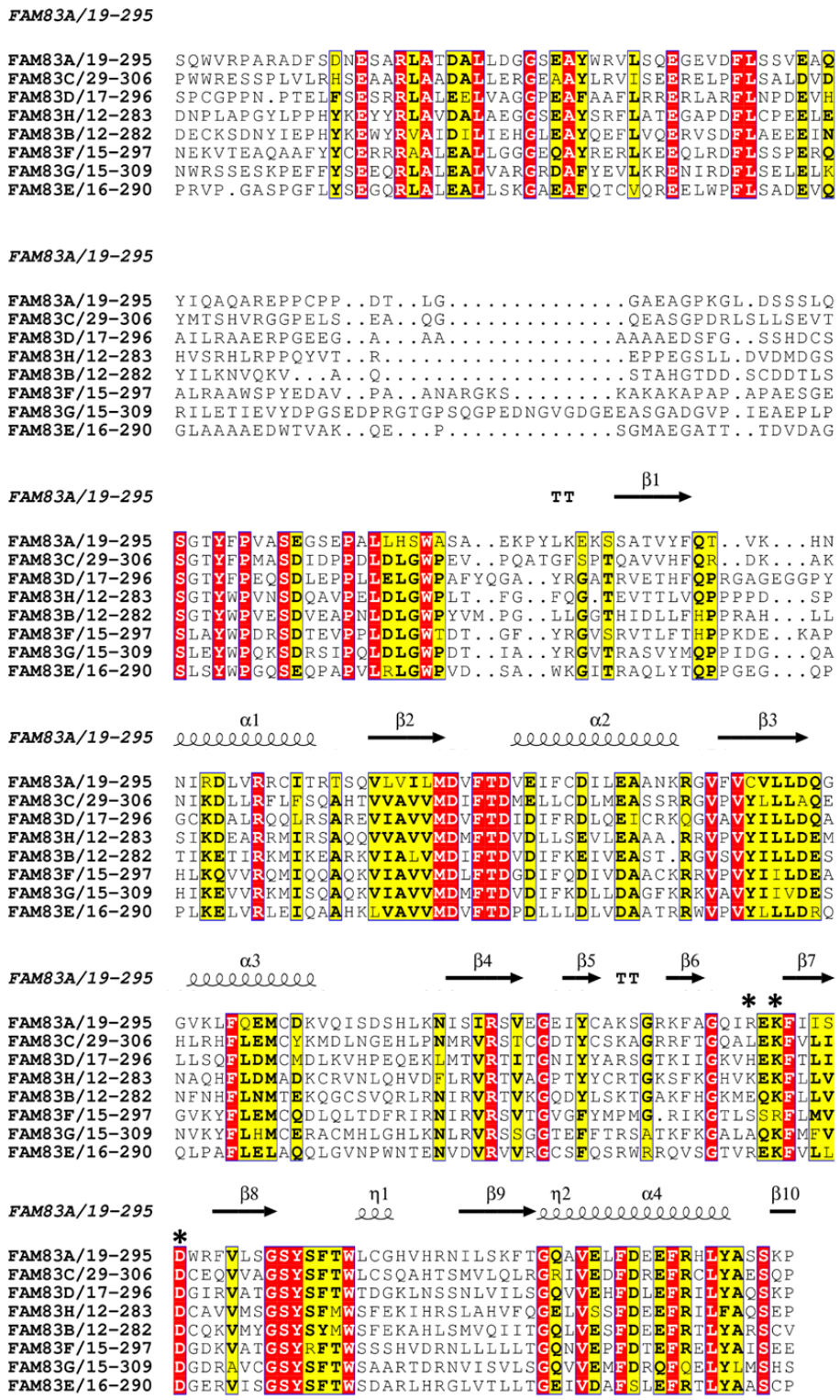

Figure 1- 4 Sequence alignment of the DUf1669 domain of the FAM83 proteins, covering the region of FAM83A that was used for crystallography.

Multiple alignment was performed with T-Coffee software. The secondary structure elements on top of the sequences were obtained with the ESPript program based on the PDB entry 4URJ (squiggle: α-helix, arrow: b-strand, TT: strict β-turn). Identical and similar residues are boxed in red and yellow, respectively (Robert and Gouet 2014). The asterisks indicate the HKD motif.

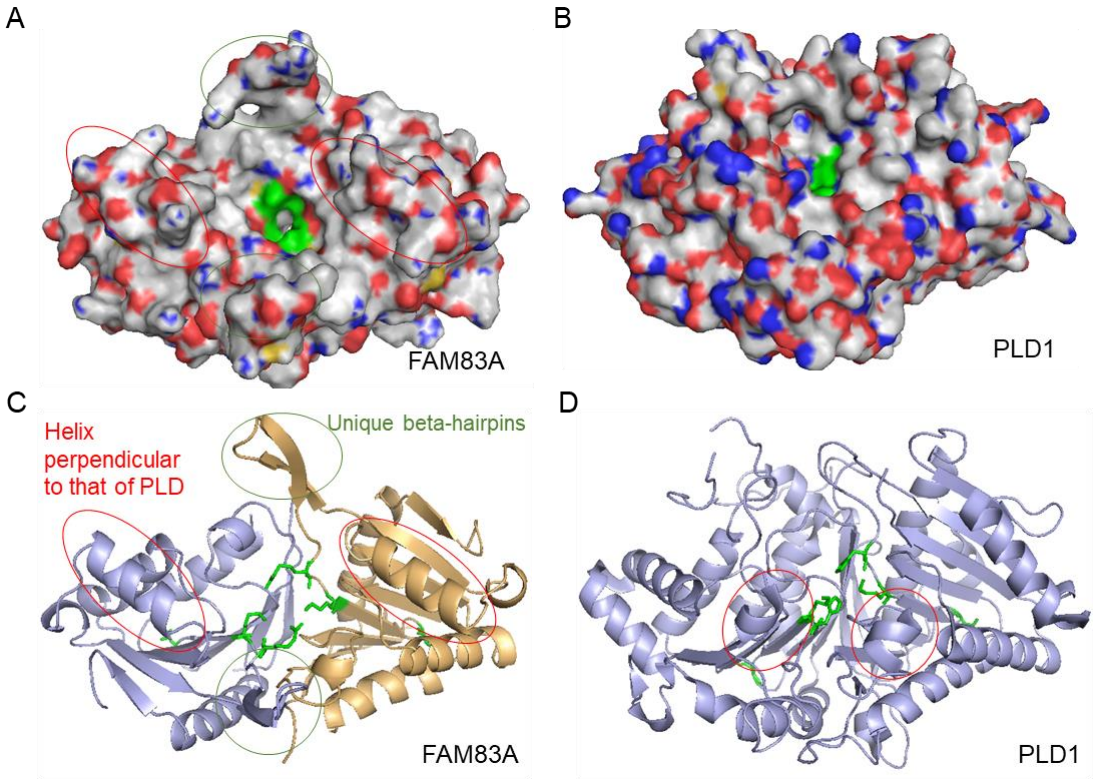

Figure 1- 5 Crystal structure of the DUF1669 domain.

A. Structure of the FAM83A DUF1669 domain that was resolved in collaboration by Dr A. Bullock (Oxford). The structure reveals a unique dimer with a PLD-like fold which brings the putative PLD catalytic motif together at the catalytic cleft (green).

B. PLD1 structure (from PDB entry1FO1).

C. Ribbon diagram depicting the folding of the FAM83A DUF1669 domain into a dimer with two helices perpendicular to those in the PLD1 which form the catalytic cleft (green).

D. Ribbon diagram depicting the folding of the PLD1 (adopted from Leiros et al. 2000).

1.2.2 The biological niche of FAM83 proteins

Having reviewed the literature on FAM83G (1.1), I will now focus on the rest of the FAM83 proteins.

1.2.2.1 FAM83A and FAM83B

FAM83A and FAM83B have both been reported to be oncogenes as their expression was found to be significantly elevated in various human tumours compared to normal tissue (Snijders, Lee et al. 2017). Cancer cells with elevated FAM83A and FAM83B expression were shown to display resistance to tyrosine kinase inhibitors (TKI) (Lee, Meier et al. 2012, Cipriano, Bryson et al. 2014). Tyrosine kinases, such as EGFR and FGFR, are frequently activated in human cancers and they promote cell proliferation, growth and survival through activation of the RAS/RAF/MEK/ERK and PI3K/AKT pathways (Fig 1-6). Ablation of either FAM83A or FAM83B showed decreased growth and proliferation of cancer cells compared to healthy non-cancer controls (Lee, Meier et al. 2012). It was suggested that FAM83A interacts with c-RAF and the p85 subunit of PI3K upon EGF-stimulation, leading to its oncogenic transduction (Lee, Meier et al. 2012). However, the above data have not yet been validated in a non-over-expression system. FAM83B was shown to substitute for RAS in activating both MAPK and PI3K/AKT signalling pathways. In FAM83B over-expressing cells, c-RAF was found to interact with FAM83B, an event that then prevented the c-RAF interaction with 14-3-3 proteins, which negatively regulates the pathway, thereby resulting in increased c-RAF localisation at the plasma membrane and sustained MAPK signalling (Cipriano, Graham et al. 2012, Cipriano, Miskimen et al. 2013) (Fig 1-6).

On the grounds that both FAM83A and B were suggested to play a role in EGFR-TKI resistance and cancer progression, it was proposed that FAM83 members could comprise a novel family of oncogenes that could be promising targets for drug discovery (Cipriano, Graham et al. 2012, Lee, Meier et al. 2012, Cipriano, Miskimen et al. 2013). Although the above studies highlighted the biological significance and pathogenic roles of FAM83A/B, none of them illuminated their biochemical roles, nor the mechanisms through which they act. Ideally, the above observations would be strengthened with studies performed under physiological conditions, in which the endogenous protein levels are kept in homeostatic balance and not affected by over-expression and with genetic evidence from FAM83A/B-null cells obtained from genome editing techniques.

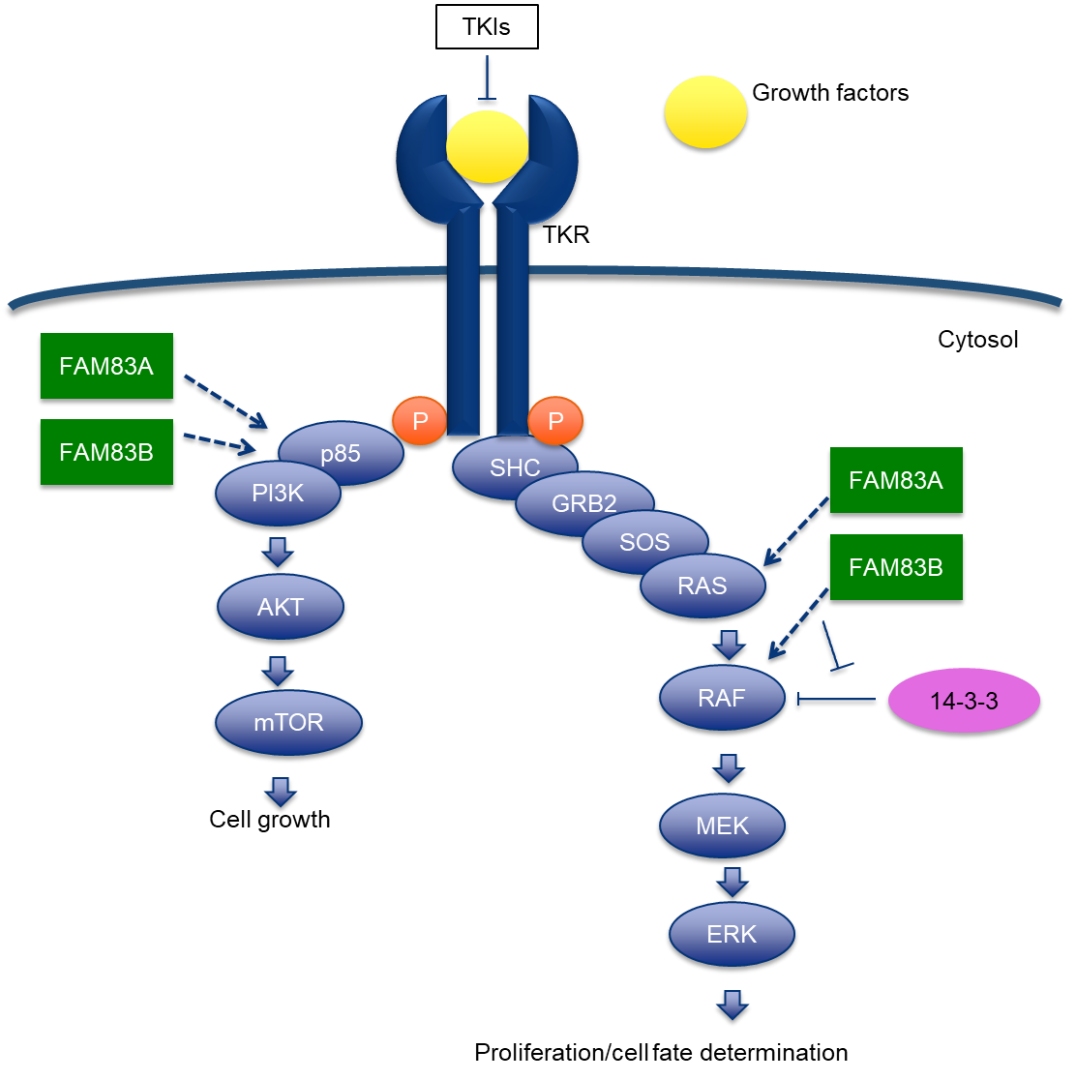

Figure 1- 6 Proposed model by which FAM83A and FAM83B may modulate Tyrosine Kinase signalling.

Growth factors such as EGF and FGF bind to their tyrosine kinase receptors (TKs) resulting in receptor dimerization, autophosphorylation and activation. In a simplified model, the signal is then transduced via the RAS/RAF/MEK/ERK pathway or PI3K/AKT/mTOR pathway resulting in cell transformation. Lee et al., 2012 suggested that FAM83A binds PI3K p85 subunit and RAF, sustaining the activation of the pathway. Cipriano et al., 2013 suggested that FAM83B interacts with RAF, preventing the RAF interaction with 14-3-3 proteins that negatively regulate the pathway, and thus sustaining downstream ERK signaling. Like FAM83A, FAM83B was also shown to interact with p85 sustaining PI3K signaling. By acting downstream of the receptor activation, FAM83A and FAM83B might alter the cellular responses to TKIs as they could bypass the inhibition of growth signaling caused by TKIs (Modified from Cipriano et al., 2013; Lee et al., 2012).

1.2.2.2 FAM83D

FAM83D or CHICA was identified in a proteomic study of the human spindle apparatus and shown to be involved in mitosis (Sauer, Korner et al. 2005). It was then found to be required for the proper organisation of the metaphase plate via its association with the chromokinesin KID (Santamaria, Nagel et al. 2008), the dynein light chain 1 motor pretein and microtubule-binding protein HMMR (Dunsch, Hammond et al. 2012). It was shown to be cell cycle regulated and phosphorylated in mitosis (Santamaria, Nagel et al. 2008). Depletion of FAM83D from cells resulted in shorter spindles and chromosome alignment defects (Santamaria, Nagel et al. 2008).

Like the other FAM83 genes, FAM83D has been reported to have prognostic significance in different human cancers, suggesting that higher FAM83D mRNA could correlate with lower survival (Walian, Hang et al. 2016, Perez-Pena, Alcaraz-Sanabria et al. 2017). It has also been reported that FAM83D promotes cell proliferation in hepatocellular carcinoma through activating cell cycle progression by activating the MEK/ERK signalling pathway (Wang, Han et al. 2015), and by downregulating the tumour suppressor gene FBXW7 in various cancer types (Wang, Liu et al. 2013).

1.2.2.3 FAM83H

FAM83H is the largest protein of the FAM83 family and it has been reported to be mutated in amelogenesis imperfecta (AI) (Kim, Lee et al. 2008, Lee, Hu et al. 2008, Ding, Estrella et al. 2009, Hart, Becerik et al. 2009, Hyun, Lee et al. 2009, Lee, Lee et al. 2009, Wright, Frazier-Bowers et al. 2009, Kweon, Lee et al. 2013, Xin, Wenjun et al. 2017). Amelogenesis imperfecta (AI) is a group of diverse inherited disorders that cause dental enamel defects (Lee, Hu et al. 2008). Although several reports have shown the relationship between AI and mutations in FAM83H, there is still a complete lack of insight into the biochemical properties by which FAM83H is involved in amelogenesis. Studies by Kuga *et al.* (Kuga, Kume et al. 2013, Kuga, Kume et al. 2016, Kuga, Sasaki et al. 2016) proposed a possible mechanism by which FAM83H mutations impact AI showing that human ameloblastoma cells transfected with FAM83H mutant DNAs resulting in truncated FAM83H protein, displayed aberrant desmosome formation and a disorganized keratin cytoskeleton. This was shown to be mediated through interaction with and inhibition of Casein Kinase 1 (CK1) (Kuga, Sasaki et al. 2016). They had earlier identified CK1 as an interacting protein of FAM83H, and suggested that this association regulated the keratin cytoskeleton in colorectal cancer cells (Kuga, Kume et al. 2013). In agreement with this, it was then proposed that in metastatic cancer cells with

compromised keratin cytoskeleton, FAM83H and CK1 translocated to nuclear speckles together with the scaffold protein SON where they potentially regulate invasion phenotypes of cancer cells (Kuga, Kume et al. 2016).

More recently, FAM83H expression was linked to tumorigenesis as it was shown to be under the transcriptional regulation of the *MYC* oncogene, in liver cancer, and knock-down of FAM83H down-regulated proliferation and survival of cancer cells (Kim, Park et al. 2017).

1.2.2.4 FAM83C, E and F

The functions of the rest of the FAM83 members remain to be characterised and there is currently no literature on the functions of FAM83C and E. FAM83F was found to be up-regulated both at the protein and mRNA levels in patients with oesophageal squamous cell carcinoma (Mao, Liu et al. 2016). However, there is no biochemical function attributed to FAM83F protein so far.

Overall, as described above, there is emerging evidence indicating that FAM83 proteins are involved in diverse cellular processes, which could possibly be attributed to their diverse C-termini. Of note, most FAM83 protein functions are implicated in promoting cancer and tumorigenesis (Snijders, Lee et al. 2017). Various signalling pathways that are activated during tumour formation are critical during early embryonic development (Yang and Weinberg 2008). Among those pathways are the Wnt, BMP, Hedgehog and Notch signalling (Kelleher, Fennelly et al. 2006). Thus, a collaboration was initiated between our laboratory and the developmental biologists in Prof J. Smith's lab (The Francis Crick Institute, previously NIMR London), to investigate the role of PAWS1 in the molecular pathways during development. Work from J. Vogt (Vogt PhD thesis, http://discovery.dundee.ac.uk) and Dr K. Dingwell (Smith lab, The Francis Crick Institute, London), provided the first insights into the physiological activity of FAM83 proteins *in vivo*, starting with PAWS1 as discussed below.

1.3 The first physiological indications of PAWS1 function

In light of the fact that PAWS1 interacts with SMAD1 and is involved in BMP signalling, it was speculated that PAWS1 might act during early embryogenesis. To test this hypothesis, the *Xenopus laevis* embryogenesis model, which is an established experimental model to study vertebrate embryogenesis, was employed. *Xenopus* is a genus of African clawed frogs and it is a genetically similar vertebrate experimental model to humans. It was observed that microinjection of PAWS1 mRNA at the ventral

marginal zones of 4-cell stage *X. laevis* embryos, resulted in the formation of a complete secondary body axis at the tadpole stage. Such dorsalised phenotypes, characterised by a secondary axis formation, are often caused by either BMP inhibitors such as Chordin, (Sasai, Lu et al. 1994) or canonical Wnt signalling activators such as Wnt8 (Du, Purcell et al. 1995, Larabell, Torres et al. 1997).

1.4 Wnt and BMP signalling control early embryogenesis of Xenopus laevis

Following the sperm entrance at the animal pole of the egg, a rapid movement of the egg content is initiated. This internal re-organisation of the yolk characterises the specification of the dorso-ventral (D-V) axis (Rowning, Wells et al. 1997) (Fig 1-7A). The cytoplasmic content that moves towards the opposite site of sperm entry, has dorsal determinants such as Dishevelled and GSK3-binding protein that together with maternal Wnt signalling lead to the stabilization and nuclear translocation of β-catenin, activating its transcription activity and defining the dorsal side of the embryo (Larabell, Torres et al. 1997). The site of the sperm entry will mark the future ventral part of the embryo (Vincent, Oster et al. 1986). In the blastula stage, the dorsally accumulated β-catenin acts synergistically with Veg1 and VegT which are expressed vegetally and form a gradient of Nodal related proteins (Xnr) from the dorsal region, defined as Nieuwkoop center to the ventral one (Agius, Oelgeschlager et al. 2000) (Fig 1-7B). Depletion of the β-catenin mRNA leads to the loss of dorsal structures (Heasman, Crawford et al. 1994), whereas injection of β-catenin antibodies induces axis duplication in *Xenopus* embryos (McCrea, Brieher et al. 1993). Xnrs are potent mesoderm inducers. High Xnr concentration induces the overlying cells to become dorsal mesoderm and this is the region specified as Spemman-Mangold organiser where gastrulation is initiated (Fig 1-7B). Low Xnr concentrations induce ventral mesoderm. The Spemman organizer induces the expression of the BMP antagonists Chordin, Noggin and Follistatin (De Robertis and Kuroda 2004). Micro-injection of BMP inhibitors induces an ectopic partial secondary axis (Sasai, Lu et al. 1994, Graff 1997). In addition to BMP inhibitors, the Spemman organizer also induces the expression of the Wnt inhibitors Cerberus, Frzb, Dickkopf and Crescent (Bouwmeester, Kim et al. 1996, Leyns, Bouwmeester et al. 1997, Wang, Krinks et al. 1997, Glinka, Wu et al. 1998, Piccolo, Agius et al. 1999, Pera and De Robertis 2000). The inhibition of both BMP and Wnt signalling at the dorsal side promotes the formation of the most anterior part of the embryo, the cement gland, eyes and nasal placodes (Bouwmeester, Kim et al. 1996, Kiecker and Niehrs 2001).

Opposite of the Spemman organiser, the ventral gastrula centre displays high BMP activity, which induces the formation of lateral plate mesoderm and blood islands (Bier and De Robertis 2015). Proteins such as Bambi, Xlr, Sizzled, CV2 and Tsg are secreted from the ventral centre and act as BMP agonists (De Robertis and Kuroda 2004). The BMP gradient across the D-V axis is kept by opposite transcriptional regulation in the dorsal and ventral centre (Reversade and De Robertis 2005). In the posterior part, an opposite gradient of Wnt signals is established from gastrulation to early development, defining the anterior-posterior axis (A-P) (Hikasa and Sokol 2013).

Upstream of the BMP signals, Wnt signals, like xWnt8, act to maintain the ventral cell fates (Itoh and Sokol 1999). Over expression of several Wnt ligands and Wnt pathway components, as the β-catenin mentioned above, induces the formation of a secondary axis in *Xenopus* embryos (McCrea, Brieher et al. 1993, Baker, Beddington et al. 1999). It is remarkable that the same β-catenin mechanism is employed for the induction of two very distinct embryonic parts in early *Xenopus* development; at an earlier stage, it specifies the dorsal axis from the Spemman organiser whereas it modulates the ventral mesoderm development later on.

In summary, two distinct signalling centres shape the D-V patterning during early *Xenopus* embryonic development (Fig 1-7), namely the dorsal signalling centre, which displays high Wnt/β-catenin activity and secretes BMP antagonists, and the ventral signalling centre, where BMP signalling functions. Perturbations of these signalling pathways impact D-V patterning. For example, activation of the Wnt signalling pathway results in a dorsalised phenotype characterised by the formation of a secondary axis, whereas activation of the BMP signalling leads to ventralised embryos. Microinjection of cloned mRNAs or the use of antisense DNA nucleotides, are commonly used by developmental biologists to examine their effect on body axis formation. These methods can reveal novel regulators of Wnt and BMP pathways according to the resulting dorsalised or ventralised phenotypes.

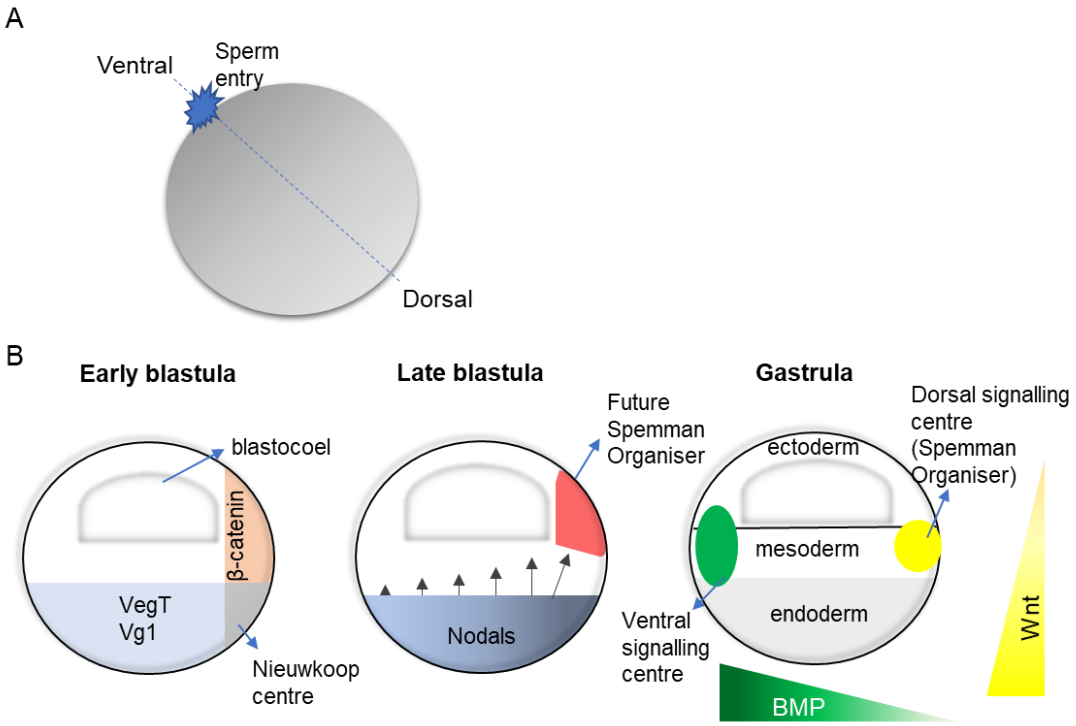

Figure 1- 7 Organiser formation in early *Xenopus* embryo

A. Sperm entry in the oocyte initiates the internal re-organisation of the yolk which determines the dorso-ventral axis of the embryo.

B. At the early blastula stage, the Nieuwkoop centre is formed at the dorsal-most and ventral-most region of the embryo, where the VegT/Vg1 and β-catenin signalling meet. A gradient of Nodal signalling at late blastula is formed. High Nodal signalling induces the Spemman organiser at the dorsal side whereas low Nodal signalling is needed for the induction of the ventral signalling centre. At gastrula, the ventral and dorsal signalling centres maintain a BMP and Wnt signalling gradient required for the D-V patterning of the embryo. Figure adapted from De Robertis and Kuroda, 2008.

1.5 The Wnt signalling pathway

The Wnt signalling pathway is an evolutionarily conserved signal transduction pathway in metazoan animals (Loh, van Amerongen et al. 2016). Research into Wnt signalling has a long history of over 35 years. Its name is derived from the *Drosophila* segment polarity gene *wingless* and its vertebrate homologue *integrated* or *int-1* (Nusse and Varmus 2012).

Wnts are secreted Cys-rich glycoproteins, which are encoded by 19 different genes in humans (Kikuchi, Yamamoto et al. 2011). Binding of Wnts to their cell membrane receptors initiates intracellular signalling cascades, which have been traditionally classified as canonical (β-catenin dependent) and non-canonical (β-catenin-independent) Wnt signalling. There are more than 15 Wnt receptors and co-receptors, including members of Frizzled (FZD), the highly homologous low-density-lipoprotein receptor-related proteins 5 and 6 (LRP5/6), receptor Tyr kinase-like orphan receptor (ROR), protein Tyr Kinase 7 (PTK7), receptor Tyr kinase (RYK), muscle skeletal receptor Tyr kinase (MUSK) and proteoglycan families (Niehrs 2012). The combination of different Wnt ligands with receptors and co-receptors designates the downstream signalling output (Grumolato, Liu et al. 2010). The presence of multiple extracellular Wnt agonists and antagonists adds another level of complexity and regulation to the Wnt signalling pathway (summarised in Fig 1-8).

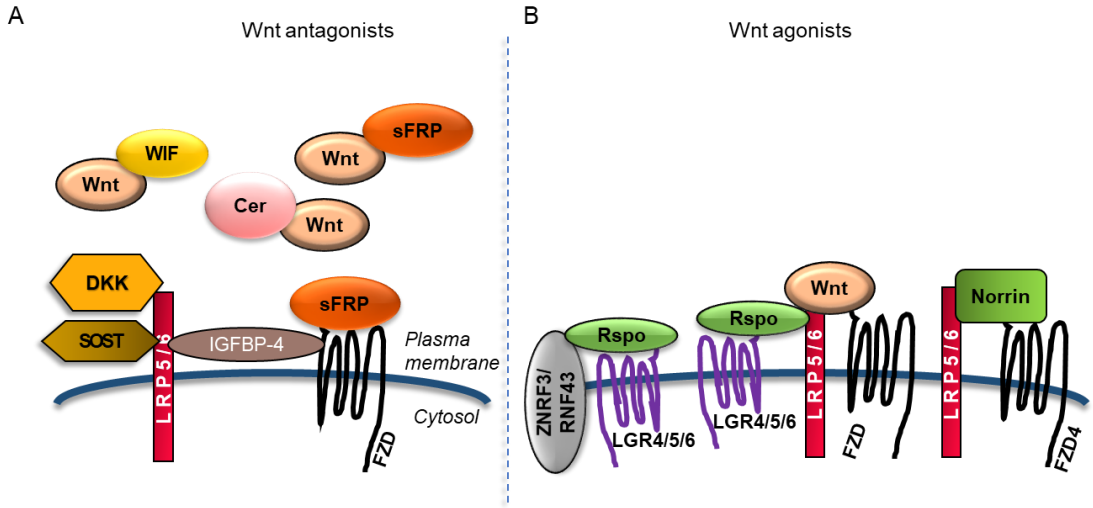

Figure 1- 8 Wnt antagonists and agonists

A. Dickkopf (DKK) and SOST binding to LRP5/6 disrupts the Wnt-induced FZD–LRP6 complex formation. Insulin-like growth-factor binding protein 4 (IGFBP-4) binds to LRP5/6 and FZD, thereby preventing signal transduction by Wnt. secreted Frizzled-related proteins (sFRPs), Wnt-inhibitory factor (WIF) and Cerberus (Cer) sequester Wnt, thereby inhibiting Wnt signalling. sFRPs may also inhibit Wnt signalling by binding to FZD.

B. Wnts are the primary agonists and form a complex with LRP5/6 and FZD to activate signalling. Norrin acts similarly to Wnt, but binds specifically to FZD4. R-spondinS (Rspo) are vertebrate-specific proteins that bind to Leucine-rich repeat-containing G-protein coupled receptors 4, 5, 6 (LGR 4/5/6) and the E3 ligases ZNRF3/RNF43. This induces receptor endocytosis so the internalised ZNRF3/RNF43 are unable to ubiquitinate Wnt receptors for degradation, sustaining thereby Wnt signalling. Figure modified from (Cruciat and Niehrs 2013).

1.5.1 The canonical (β-catenin-dependent) signalling

The canonical Wnt signalling pathway is the best characterised Wnt pathway to date. The transcriptional co-activator β-catenin plays a central role in mediating the Wnt pathway and it regulates several cell responses to Wnt signals (Fig 1-9). In the absence of Wnt ligands, β-catenin is captured by the so-called β-catenin destruction complex (Stamos and Weis 2013). The destruction complex consists of the scaffold proteins Axin and adenomatous polyposis coli (APC), the kinases glycogen synthase kinase 3 (GSK3) and Casein kinase 1 (CK1), the protein phosphatase PP2A and the SKP1-CUL1-F-box protein (SCF) E3 ubiquitin-protein ligase complex β-transducin repeat-containing protein (β-TrCP) (Liu, Kato et al. 1999). Within the destruction complex β-catenin is phosphorylated by CK1 at Ser45, which primes it for subsequent sequential phosphorylation by GSK3 at Thr41, Ser37 and Ser33 (Liu, Li et al. 2002). APC binds to phosphorylated β-catenin and protects it against de-phosphorylation by PP2A (Su, Fu et

al. 2008). Subsequently, phosphorylated β-catenin is targeted for ubiquitylation by β-TrCP followed by proteasomal degradation (Liu, Li et al. 2002, Wu and He 2006). Binding of Wnts to the FZD/LRP5/6 receptors, leads to the translocation of Axin to the activated LRP5/6 receptor, where it binds to its phosphorylated tail. However, the precise mechanisms that regulate Axin translocation have not been elucidated yet. Then, the destruction complex becomes saturated with phosphorylated β-catenin and as a result, the newly synthesised and unphosphorylated, therefore stabilised β-catenin accumulates in the cytosol and subsequently translocates into the nucleus (Li, Ng et al. 2012). In the nucleus, the T cell factor (TCF) binds and represses the Wnt-target genes in unstimulated cells together with the transcriptional co-repressor Groucho. Generally, upon Wnt activation, the nuclear β-catenin displaces Groucho and binds to TCF and lymphoid enhancer-binding factor (LEF), recruiting the transcriptional co-activators Bcl9 and Pygopus (Cavallo, Cox et al. 1998, Kramps, Peter et al. 2002) and the histone modifiers Brg1 and CBP (Stadeli, Hoffmans et al. 2006), thereby initiating the transcription of many Wnt-target genes (Fig 1-9).

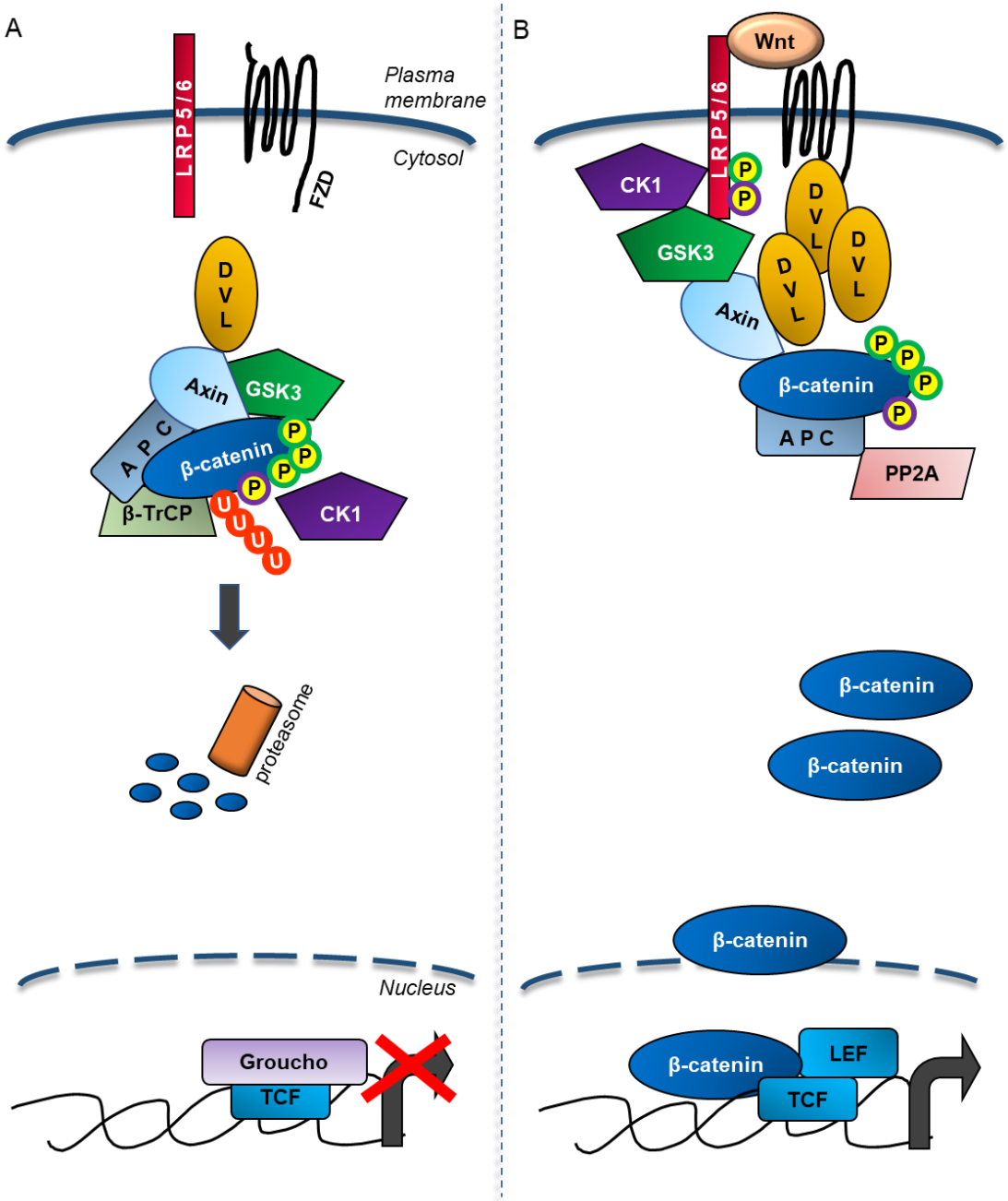

Figure 1- 9 Overview of the canonical Wnt signalling pathway

A. In the absence of Wnt ligands, β-catenin is captured by the destruction complex, which is mainly composed of Axin, APC, GSK3, CK1 and β-TrCP. Sequential phosphorylation of β-catenin by CK1 and GSK3 leads to its ubiquitination by β-TrCP followed by its degradation by the proteasome, so that the cytosolic levels of β-catenin remain low. In the nucleus, binding of Groucho to TCF blocks the transcription of Wnt-target genes.

B. Wnt ligands bind to their receptors, causing phosphorylation of LRP5/6 and the formation of the Wnt signalosome which is mainly composed of polymerised DVL and Axin which recruits the whole destruction complex to the membranes. β-catenin is stabilised in the cytosol and enters the nucleus where it displaces Groucho from TCF and together with LEF they activate the TCF target genes.

1.5.2 The non-canonical (β-catenin-independent) signalling

Non-canonical Wnt signalling refers to the Wnt-triggered pathways that do not involve β-catenin, but signal through other factors, that trigger different transcriptional or non-transcriptional responses. The non-canonical pathway is further sub-divided into several, poorly studied branches. Among these, the two most characterised ones are the Planar Cell Polarity (PCP) pathway and the Wnt/Ca^{2+} pathway (Semenov, Habas et al. 2007).

In the PCP pathway, Wnts signal through the FZD receptors without the need for the LRP5/6 co-receptors (Fig 1-10A). The activated cascade includes the small GTPases RAC1 and RHOA and the kinases JUN-N-terminal kinase (JNK) and Rho-associated kinase (ROCK). This pathway results in cytoskeletal rearrangements, which govern cell motility, migration and cell polarity as well as transcriptional activation of the JNK-dependent transcription targets such as cJUN (Simons and Mlodzik 2008) (Fig 1-10A). In vertebrates, the PCP pathway is primarily involved in embryonic development during gastrulation, where it modulates cell movements, and in adult tissues, where it regulates cell polarity and ciliary function (Simons and Mlodzik 2008).

The other non-canonical Wnt pathway is the Wnt/Ca^{2+} pathway (Fig 1-10B). Wnt binding to FZD activates G-proteins, which then activate phospholipase C (PLC). This leads to accumulation of diacylglycerol (DAG) and inositol triphosphate (IP3), which triggers intracellular Ca^{2+} release. Intracellular calcium accumulation activates several Ca^{2+}-sensitive proteins, such as protein kinase C (PKC), calcium/calmodulin-dependent kinase 2 (CaMK2) and the protein phosphatase calcineurin, which then de-phosphorylates and activates the transcriptional regulator nuclear factor associated with T cells (NFAT) (Sheldahl, Slusarski et al. 2003) (Fig 1-10B). In *Xenopus* embryos, NFAT promotes ventral cell fates (Saneyoshi, Kume et al. 2002) and enhances the expression of numerous genes in neurons, cardiac and skeletal muscle cells, and promotes pro-inflammatory gene expression in lymphocytes (De Boer, Mordvinov et al. 1999).

In addition to the Wnt signalling pathways described above, several other Wnt-FZD combinations as well as Wnt-binding to receptors other than FZD, trigger different β-catenin-independent responses (Bovolenta, Rodriguez et al. 2006, Inoki, Ouyang et al. 2006, Schambony and Wedlich 2007). These pathways might be activated in a tissue-specific manner and they could share overlapping components with the canonical and non-canonical Wnt signalling pathways. Because the main focus of this

thesis is the canonical Wnt signalling pathway, in the next section it will be discussed in more detail how the pathway is modulated by its core components, during each stage of the signalling cascade, in addition to the biology related to it.

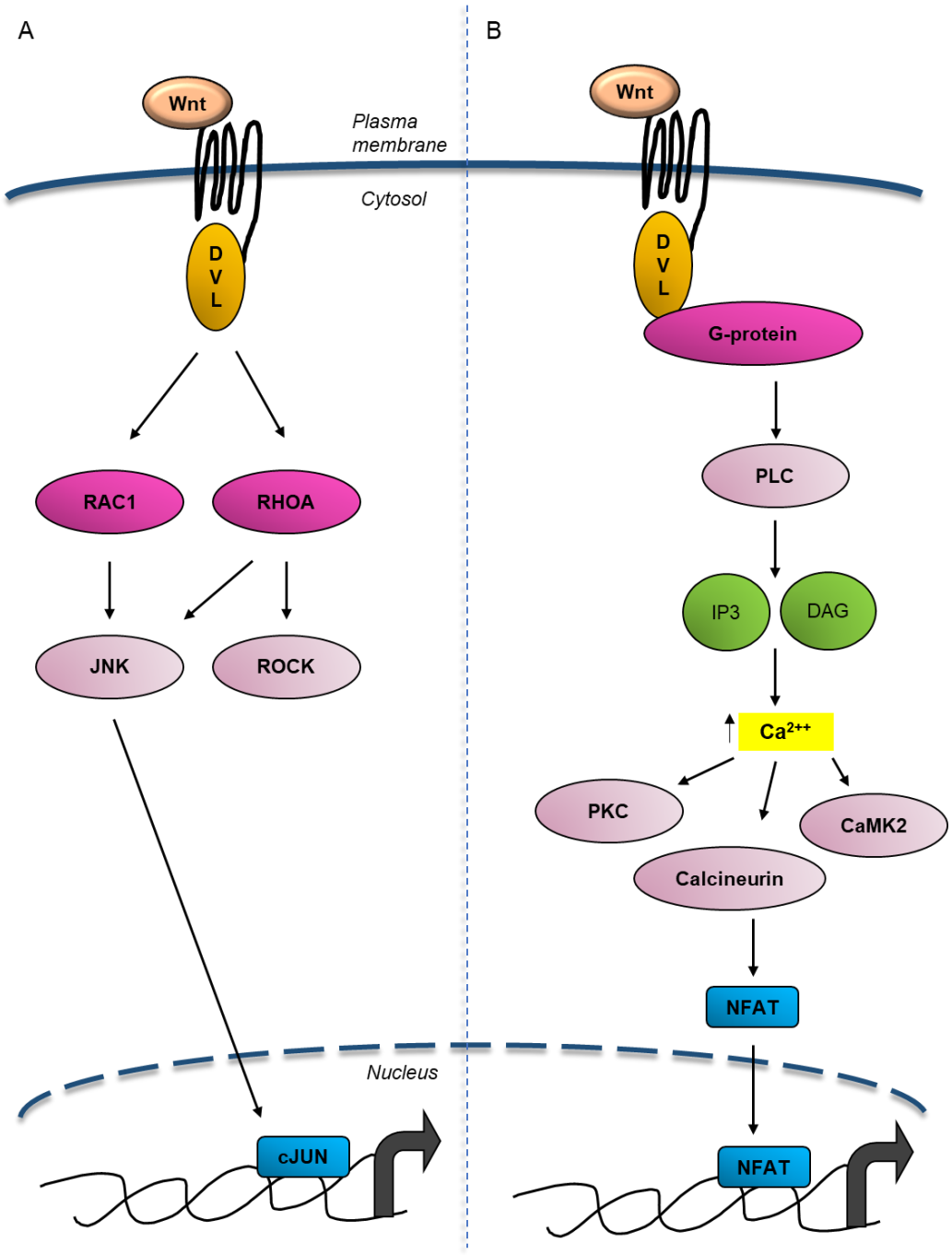

Figure 1- 10 Simplified overview of the PCP and the Wnt/Ca^{2+} signalling pathways.

A. The PCP pathway: Wnt binding to FZD leads to the activation of RAC1 and RHOA which in turn activate JNK and ROCK kinases resulting in the activation of the downstream target genes in the nucleus.

B. The Wnt/Ca^{2+} pathway: Activation of the Wnt/Ca^{2+} pathway signals through PLC which leads to the accumulation of IP3 and DAG that trigger the intracellular Ca^{2+} release. Ca^{2+} accumulation activates PKC, CaMK2 and Calcineurin which then activates NFAT which activates its target genes in the nucleus.

1.5.3 Modulation of the canonical Wnt signalling

1.5.3.1 Wnt secretion

During their synthesis, all Wnt proteins are modified with the attachment of the lipid palmitoleic acid. This is performed by the palmitoyl transferase Porcupine (Porc) on the endoplasmic reticulum. The lipid on the Wnts serves as a binding site to the FZD receptor, but also adds hydrophobicity properties so that Wnts are tethered to membranes (Janda, Waghray et al. 2012). Palmitoylated Wnts are then transported to the plasma membrane by the transmembrane protein Wntless/Evi (Wls) to be secreted (Banziger, Soldini et al. 2006, Bartscherer, Pelte et al. 2006)..

1.5.3.2 The binding of Wnts to their receptors and the formation of the Wnt signalosome

As discussed earlier, Wnts bind to their receptors FZD/LRP5/6 on the surface of the target cells. FZDs have a 7-transmembrane domain and a cysteine-rich extracellular domain, which binds Wnts (Bu, Li et al. 2017). How different Wnts bind to different FZDs is not fully understood. Binding of Wnt to FZD causes the dimerization of FZD with the single-pass transmembrane proteins LRP5/6, promoting a conformational change of both receptors (Cong, Schweizer et al. 2004). It has been hypothesised that extracellular Wnt binds to FZD dimers, which then form complexes with LRP dimers, for canonical Wnt signalling activation (DeBruine, Xu et al. 2017). The extracellular part of LRP5/6 consists of YWTD (Tyr, Trp, Thr and Asp)-type β-propeller domains, epidermal growth factor (EGF)-like domains and LDLR domains, which bind extracellular ligands but it is still not known whether Wnt ligands bind LRPs or not (Semenov, Habas et al. 2007). The intracellular domains of LRP are critical for signal transduction upon Wnt stimulation (Tamai, Zeng et al. 2004, Zeng, Tamai et al. 2005). The conformational change on receptors caused by Wnt-binding, allows for immediate sequential LRP phosphorylation by GSK3 and CK1γ at PPPSP repeats (Davidson, Wu et al. 2005, Zeng, Tamai et al. 2005). Next, the Axin complex is recruited to the membrane, promoting the Wnt signalosome formation (Bilic, Huang et al. 2007). The formation of signalosomes is a hallmark of signal transduction pathways. An extracellular signal mediates the recruitment of cytoplasmic polymerised proteins to the activated transmembrane receptors, where they are assembled in large dynamic protein clusters (Gammons, Renko et al. 2016).

The formation of the Wnt signalosome depends on the polymerisation of the cytoplasmic protein Dishevelled (DVL), which is recruited to FZD upon Wnt stimulation

(Cong, Schweizer et al. 2004). DVL is an evolutionarily conserved component of the Wnt pathway and it gets polymerised via its N-terminal DIX domain, promoting the formation of large protein clusters beneath the plasma membrane and mediating signal transduction by cytoplasmic effectors (Gammons, Renko et al. 2016). Polymerisation of DVL is critical for Wnt signal transduction, as mutations that block polymerisation fail to transduce the Wnt response in mammalian cells (Schwarz-Romond, Fiedler et al. 2007). DVL recruits Axin to the plasma membrane via direct binding through their respective DIX domains (Schwarz-Romond, Merrifield et al. 2005). Therefore, the whole β-catenin destruction complex is relocated to the plasma membrane, resulting in its disruption or inactivation of its function, which in turn leads to the accumulation and nuclear translocation of active/non-phosphorylated β-catenin. There are several models (as discussed below) describing the mechanisms of complex inactivation although most of them were formulated on over-expression-based studies (Li, Ng et al. 2012).

1.5.3.3 Inactivation of the destruction complex

By immunoprecipitating the endogenous form of Axin, Li *et al.* (2012) demonstrated that the destruction complex is functionally active upon Wnt stimulation despite its recruitment to the plasma membrane. In other words, there is no change on the phosphorylation status of β-catenin following Wnt signalling (Li, Ng et al. 2012). However, the destruction complex-associated β-catenin is no longer subjected to ubiquitylation and proteasomal degradation due to immediate dissociation of the β-TrCP ligase from the complex. At the same time, β-catenin stabilisation may be further promoted by phosphorylated LRP PPPSP motifs, which act as pseudo-substrates for the Axin-bound GSK3, inhibiting its kinase activity (Stamos, Chu et al. 2014). Consequently, there is an accumulation of non-phosphorylated β-catenin in the cytosol, which then translocates into the nucleus to activate Wnt-responsive target genes. An alternative model by Kim *et al.* (2013) suggests that phosphorylation of Axin by GSK3 is inhibited upon its membrane translocation following Wnt stimulation. The protein phosphatase 1 (PP1) de-phosphorylates Axin, altering Axin's conformation, preventing its association with β-catenin and phospho-LRP, thereby resulting in disassembly of the destruction complex (Kim, Huang et al. 2013). The identification of a consensus model that describes the mechanisms of the destruction complex regulation might be further hampered by the transient nature of the protein-protein interactions within the complex. Nevertheless, conclusions based on overexpression studies should be considered with caution given the dual activating and inhibitory role of some of the pathway components, as slight changes

in their protein levels might significantly perturb the downstream outcome. On the contrary, kinetic analysis of the pathway and quantitative approaches may provide a better understanding on how the signalling functions physiologically.

1.5.3.4 The nuclear/cytosolic shuttling of β-catenin

One of the least understood stages of the canonical Wnt signalling pathway is the nuclear import and export of β-catenin. There is no evidence supporting the presence of a NLS (nuclear localisation signal) or importin-mediated nuclear entry of β-catenin. On the contrary, it was shown recently that β-catenin interacts with nucleoporins (Nups) that mediate bidirectional translocation through the nuclear envelope pores (Sharma, Johnson et al. 2014). However, whether Wnt signalling itself regulates the β-catenin localisation remains unknown. The only indirect evidence so far comes from studies by Wu *et al.* (2008), who showed that phosphorylation of β-catenin at Ser191 and Ser 605 by JNK after Wnt stimulation is essential for the nuclear translocation of β-catenin (Wu, Tu et al. 2008). Of note, APC and Axin were reported to regulate β-catenin localisation (Henderson and Fagotto 2002, Cong and Varmus 2004). Ran binding protein 3 (RanBP3), which binds to β-catenin in a Ran-GTP-dependent manner was also reported to participate in the nucleocytoplasmic transport of β-catenin (Hendriksen, Fagotto et al. 2005). Nevertheless, research on this topic is more complicated, as most of the cellular β-catenin pool has been reported to be present at the plasma membrane, where it forms adherens junctions through its association with α-catenin and E-cadherin (Gottardi and Gumbiner 2004, Baum and Georgiou 2011, Tan, Gardiner et al. 2012).

On the other hand, the interaction of β-catenin with binding partners, such as LEF, TCF1, 2, 3 and 4 and BCL9 inside the nucleus enhances its nuclear retention, resulting in positive regulation of the pathway (Krieghoff, Behrens et al. 2006, Jamieson, Sharma et al. 2011). There, β-catenin associates with multiple TCF and non-TCF transcription factors to activate the transcription of target genes. The genes that are traditionally defined as direct β-catenin targets contain the TCF binding motif 5'-AGATCAAAGG-3' (van de Wetering, Cavallo et al. 1997), which is also known as Wnt-responsive element (WRE). Notably, WRE has been exploited by researchers who created artificial reporters with multiple WRE repeats upstream of the luciferase gene (Veeman, Axelrod et al. 2003). These reporters can be transfected into cells to provide a quick way to measure Wnt-dependent transcriptional activity, through luciferase activity measurement (TOPflash assay). Although the activation of Wnt-target genes is highly context-dependent (cell- and developmental stage- specific), one main marker for proper Wnt activation is the

expression of *Axin2* (Jho, Zhang et al. 2002). Activation of Wnt-target genes including *Axin2*, *DKK1* and *Naked*, or suppression of *LRP6* and *FZD*, can also participate in negative feedback loops that dampen the pathway. In contrast, the activation of LEF/TCF reinforces the signal via a positive feedback loop (Logan and Nusse 2004, Arce, Yokoyama et al. 2006). Indisputably, the key output of Wnt signalling is the re-programming of the target cells via the activation of transcriptional programs which govern growth (*FGF4*, *VEGF*), proliferation (*Cyclin D1*, *MYC*), differentiation (*Siamois*, *Brachyury*) and adhesion (*E-Cadherin*) in the developing cell or during adult tissue homeostasis (Reya and Clevers 2005).

1.5.3.5 The biological outcomes of the canonical Wnt activation

As emphasised earlier, Wnt signalling plays a pivotal role in defining the body axis formation and cell fate decisions during early embryonic development. It controls the balance between cell proliferation and differentiation. This is highlighted through the fact that mutations of components of the canonical Wnt pathway are linked to developmental defects including abnormalities in the central nervous system (Thomas and Capecchi 1990, Wang, Thekdi et al. 2002), kidney defects (Stark, Vainio et al. 1994) lung and hair follicle abnormalities (Li, Rheaume et al. 2007) as well as focal dermal hypoplasia (Grzeschik, Bornholdt et al. 2007).

In addition to its prominent role in embryonic development, Wnt signalling remains active in self-renewing tissues throughout the adult life. Nowadays, one of the most attractive areas of research on Wnt signalling is investigating its role in specification and maintenance of the stem cells in various tissues and organs. Stem cells are pluripotent cells that are able to both self-renew and differentiate into specialised cell types. It was first shown in 1998 that loss of the β-catenin binding partner TCF4 leads to the depletion of the stem cells compartment of the small intestine (Korinek, Barker et al. 1998). Since then, Wnt signals have been reported to play major roles in the maintenance of pluripotency of almost all stem cell types (ten Berge, Kurek et al. 2011).

Finally, mutations in the destruction complex components have been individually implicated in human tumours. APC is the most commonly mutated gene in colorectal carcinoma (Sparks, Morin et al. 1998). Loss of APC function from colon cancer cell lines is associated with constitutive β-catenin-TCF4 interaction and activation of downstream target genes (Korinek, Barker et al. 1998). Other colorectal tumours without APC mutations were found to carry mutations in the N-terminal part of β-catenin, near its CK1 and GSK3 phosphorylation sites (Sparks, Morin et al. 1998). Similar mutations on

β-catenin were identified in uterine endometrium (Fukuchi, Sakamoto et al. 1998), ovarian (Palacios and Gamallo 1998), stomach (Park, Oh et al. 1999), lung (Sunaga, Kohno et al. 2001) and liver cancer (Miyoshi, Iwao et al. 1998). Furthermore, mutations on Axin1 and Axin2 were identified in several tumours, such as hepatocellular carcinoma (Satoh, Daigo et al. 2000), adenocarcinomas (Koppert, van der Velden et al. 2004) and colorectal cancer (Liu, Dong et al. 2000). Of note, most of these mutations are described as activators of the Wnt signalling via β-catenin stabilisation. Such mutations may lock the Wnt pathway into a constitutively active state independent of Wnt stimuli, thereby resulting in stem cell-like phenotypes and neoplasia (Ewan and Dale 2008).

Therefore, there has been a lot of interest from the pharmaceutical industry for designing anticancer therapeutics that target members of the Wnt signalling pathway. An example is the Porcupine inhibitor LGK794, which blocks Wnt palmitoylation and therefore its secretion. LGK794 is currently in clinical trials for patients with solid malignancies (https://clinicaltrials.gov/ct2/show/NCT01351103). However, a major challenge of targeting the Wnt pathway is that it is utilised by both cancer and healthy tissues of multiple organs. Furthermore, Wnt signalling cross-talks with other pathways that are critical for healthy tissue homeostasis, such as the EGF (Lu, Ghosh et al. 2003), Notch (Gu, Watanabe et al. 2013) and Sonic Hedgehog (SHH) (Kim, Shin et al. 2010) signalling pathways. In addition to this, many of the Wnt pathway components have dual roles in both activation and dampening of the Wnt signal transduction. Examples of this are the Casein Kinase 1 (CK1) isoforms, which are discussed in more detail below. Ultimately, a deeper understanding of the precise regulation of the Wnt pathway, including the specificity of protein-protein interactions of its components, is necessary in order to devise successful pharmacological interventions.

1.6 The Casein Kinase 1 (CK1) family of proteins

1.6.1 The Casein Kinases

The term ‘casein kinase’ has been widely used to describe three different classes of protein kinases that can phosphorylate casein *in vitro*. The secreted milk protein casein was the first phosphoprotein to be identified in 1883. This was the first indication of the existence of the protein kinases (Tagliabracci, Pinna et al. 2013). Some 70 years later, Burnett and Kennedy described the phosphate transfer from ATP to purified casein in liver homogenates (Burnett and Kennedy 1954). The enzymes responsible for catalysing casein phosphorylation were named Casein Kinase 1 (CK1) and Casein Kinase 2 (CK2) (Burnett and Kennedy 1954, Pinna, Clari et al. 1969). However, these are now considered

misnomers because casein, which is a secreted protein, is not a physiological substrate for either enzyme found inside the cells. A genuine casein kinase (G-CK) was isolated from the Golgi-enriched fractions of the mammary gland, where casein is synthesised, but for decades it remained an 'orphan' enzyme (Lasa-Benito, Marin et al. 1996). Only recently the G-CK was identified as Fam20C (Family with sequence similarity 20C), which belongs to a new branch of the human kinome tree, termed the four-jointed family of secreted protein kinases (Tagliabracci, Engel et al. 2012, Tagliabracci, Wen et al. 2016). This family of secreted kinases has been shown to phosphorylate casein as well as other proteins in the extracellular matrix of bone and teeth (Tagliabracci, Engel et al. 2012, Tagliabracci, Wen et al. 2016).

Apart from their ability to phosphorylate casein *in vitro*, CK1, CK2 and Fam20C are very distinct and have little in common. CK1 and CK2 are pleiotropic enzymes that control a plethora of substrates, and impact a diverse range of biological processes. For the purpose of this thesis, I will focus on the CK1 family, which I will discuss in more detail in the following sections.

1.6.2 The CK1 biology

The CK1 family consists of a group of Serine/Threonine protein kinases that form a small branch in the human kinome tree (Fig 1-11). CK1 proteins are evolutionarily conserved and are present in organisms that range from bacteria, fungi and plants to mammals (Rowles, Slaughter et al. 1991, Fish, Cegielska et al. 1995, Gross and Anderson 1998). In humans, there are seven CK1 isoforms encoded by different *CSNK1* genes (α, αL, γ1, γ2, γ3, δ and ε), with several splice variants also reported for some (Fig 1-11, 1-12). The N-terminal kinase domain is highly conserved among all the isoforms but their C-terminal region is significantly different (Fig 1-12).

CK1α and CK1αL display high sequence similarity (over 90%), with only 25 amino acids different over the whole protein sequences. Their kinase domains and the ATP-binding site are almost identical (Fig 1-12). For this reason, there has been a lot of confusion in distinguishing these two gene products and often the name CK1α is commonly used indistinguishably for both. The only reference to CK1αL is by Xu *et al.* (2008), who identified CK1αL as the only isoform to phosphorylate the osmo-sensitive transcription factor OREBP, thereby regulating its nucleocytoplasmic trafficking upon hypertonic stress (Xu, Wong et al. 2008). CK1δ and CK1ε are more closely related to each other, displaying almost 85% sequence similarity, than to CK1α andCK1αL. The

three CK1γ isoforms differ significantly from the rest of the family as they are the only ones that carry a palmitoylation site at their C-terminus, which anchors them to the plasma membrane, whereas all the other CK1 isoforms localise to the cytoplasm and nucleus (Davidson, Wu et al. 2005).

CK1 members are thought to be constitutively active (Rivers, Gietzen et al. 1998). They show a preference for acidic substrates (D/E-x-x-S/T), although in many cases the preference for the acidic amino acid in position n-3 (where n denotes the CK1 phoshorylation residue) can be replaced by a phosho-Ser or a phospho-Thr (Flotow *et al.*, 1990). Since the CK1 phosphorylation consensus motif is common in many target proteins, the enzymatic activity of the CK1 isoforms must be spatiotemporally regulated. Additionally, some CK1 substrates, such as β-catenin, do not possess the consensus phosphorylation motif. The wide range of CK1 targets is further appreciated by the diverse substrates that have been reported over the years. These include transcription factors, adhesion proteins, cytoskeletal components, membrane receptors, ribosomal proteins, vesicle-associated proteins, metabolic enzymes and other signalling molecules, such as adaptors, scaffold proteins and protein kinases and phosphatases (Knippschild, Gocht et al. 2005, Cheong and Virshup 2011). However, as a complete phospho-proteome landscape for each CK1 isoform has not yet been reported, we might still be looking at a subset of the total CK1 substrates. It is evident that the spectrum of CK1 substrates is very wide and combined with the fact that CK1 isoforms are ubiquitously expressed, there must be precise and tight regulation of both CK1 isoform activity and localisation in cells.

Given the diverse range of target substrates that CK1 isoforms phosphorylate, it is not surprising that CK1 isoforms are involved in controlling many cellular processes. Among these are: regulation of cell cycle progression, cell proliferation, circadian rhythm, response to DNA damage, and apoptosis (see below 1.6.5). The CK1 family influences many signalling pathways to modulate these diverse biological processes. Dysfunction of CK1 activity is thus associated with many diseases, including cancer. For this reason, the CK1 family has gained some interest from the pharmaceutical industry, leading to the development of small molecules that modulate its activity. To date, a few small molecules that inhibit CK1 kinase activity have been developed, but all of them lack selectivity (see 1.6.5.4).

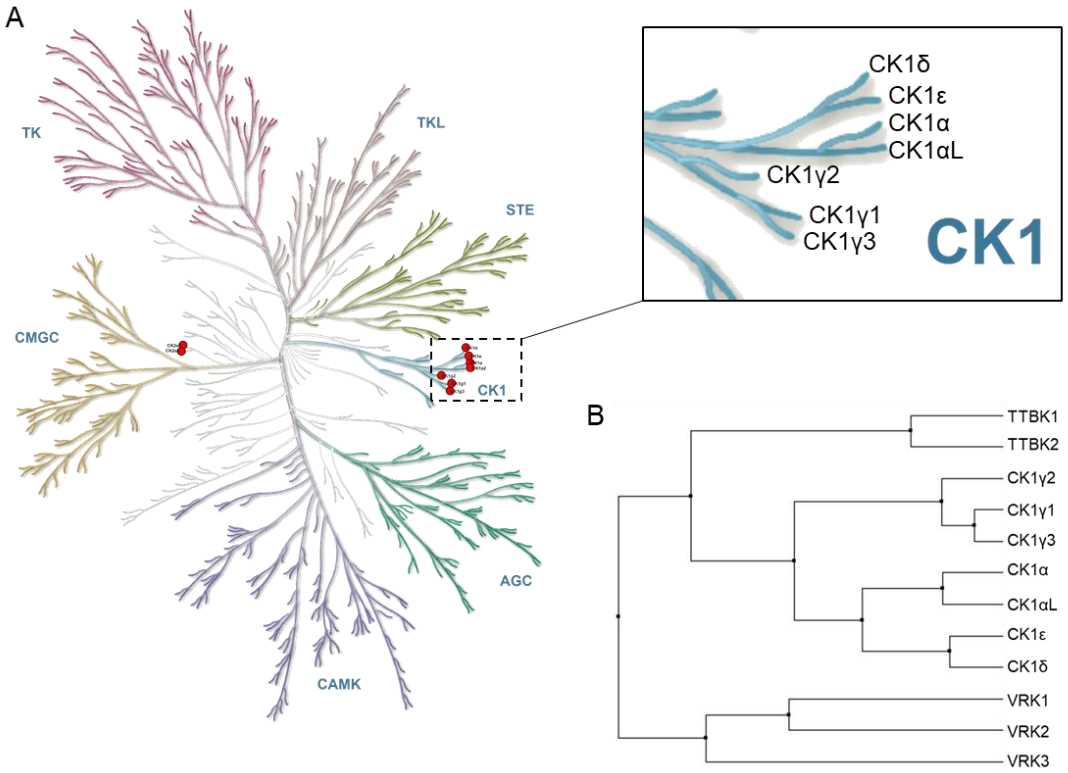

Figure 1- 11 The human CK1 family

A. The red circles highlight the position of the casein kinases in the human kinome tree (modified from *https://www.cellsignal.com/contents/science-protein-kinases/protein-kinases-human-protein-kinases-overview/kinases-human-protein*). A zoom in the dotted box show the CK1 isoforms.

B. Phylogenetic relation of the human CK1 family members. The phylogenetic tree was constructed with Jalview based on sequence alignment of their kinase domain that was performed with ClustalO.

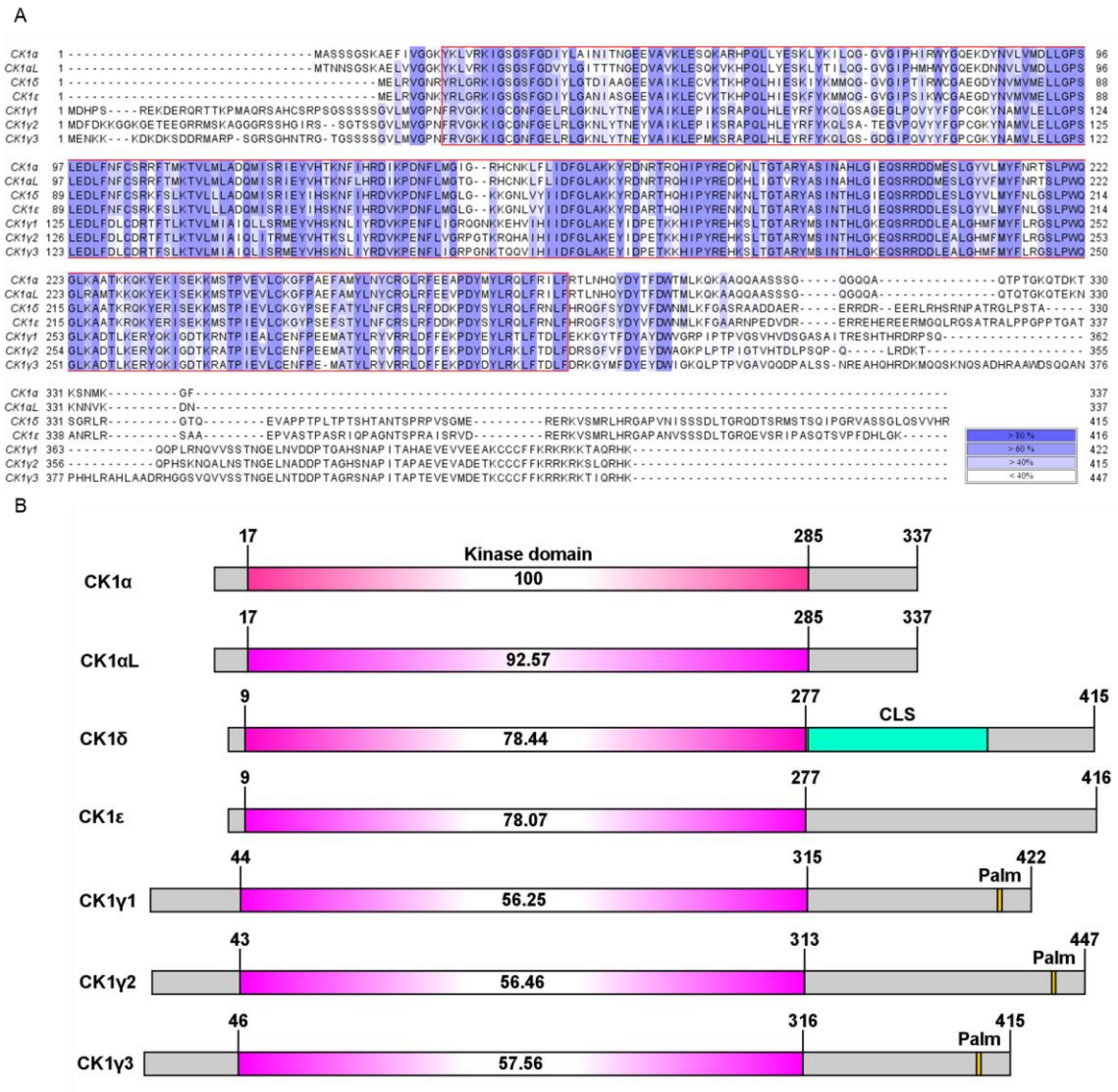

Figure 1- 12 The human CK1 isoforms have a conserved N-terminal kinase domain

A. Multiple sequence alignment of the main human CK1 isoforms was performed with ClustalO in Jalview 2.10.3 and colouring indicates the % of sequence identity.

B. Schematic overview of the human CK1 isoforms. The conserved kinase domain is depicted in pink. The percentage amino-acid identity within the kinase domains of each isoform to that of CK1α kinase domain is indicated. NLS: nuclear localisation signal; CLS: centrosomal localisation signal; Palm: Palmitoylation site.

1.6.3 Regulation of CK1 activity

Although the CK1 isoforms are ubiquitously expressed, the levels of expression and activity of each isoform across different cell lines and tissues differ widely (Nakajo, Hagiwara et al. 1987, Fu, Chakraborti et al. 2001, Davidson, Wu et al. 2005, Lohler, Hirner et al. 2009). The mechanisms that regulate their expression and activation are not fully elucidated. Extracellular signals, such as Wnt, insulin, topoisomerase inhibitors, irradiation and viral transformation can potentially increase CK1 activity (Knippschild, Gocht et al. 2005). The crystal structure of mammalian CK1δ provides some insights into the mechanism of its enzymatic regulation, as it was shown to form homo-dimers that could potential inhibit ATP binding, thereby potentially impairing its kinase activity (Longenecker, Roach et al. 1998). However, this hypothesis has not been validated yet. Currently, it is thought that substrate specificity is achieved via (i) post-translational modifications of CK1 isoforms, including auto-phosphorylation, (ii) interaction with scaffold proteins (iii) regulated subcellular localisation/compartmentalisation and (iv) substrate phosphorylation priming.

CK1δ and CK1ε have been reported to be negatively regulated via auto-phosphorylation (Gietzen and Virshup 1999). The phosphorylated part on their C-terminus might act as a pseudo-substrate, which inhibits their catalytic activity. The presence of phosphatases is thought to keep these kinases active in cells (Rivers, Gietzen et al. 1998). However, the specific phosphatases that accomplish this have not been identified yet. It is still not clear if the other CK1 isoforms are regulated through autophosphorylation. Notably, CK1α and CK1γ have a short C-terminal domain, which makes it unlikely for autophosphorylation to be a regulatory mechanism for their activity, even though autophosphorylation sites have also been also found on these isoforms in *in vitro* studies (Budini, Jacob et al. 2009).

Apart from autophosphorylation, phosphorylation by other cellular kinases can also negatively regulate the kinase activity of CK1 isoforms. In particular, CK1δ has been found to be phosphorylated by Protein Kinase A (PKA) (Giamas, Hirner et al. 2007), checkpoint kinase 1 (Chk1) (Bischof, Randoll et al. 2013), cyclin-dependent kinase 2 (CDK2/E) and cyclin-dependent kinase 5 (CDK5/p35) (Ianes, Xu et al. 2016) which in turn reduces its activity. Interestingly, over-expression of a CK1δ phospho-mutant (S370A) enhances the formation of an ectopic secondary body axis in *Xenopus laevis* embryos (Giamas, Hirner et al. 2007).

Interaction between CK1 and scaffold proteins can potentially regulate the kinase activity, as scaffold proteins can dictate substrate proximity to the particular CK1 isoform. In the Wnt signalling pathway for example, CK1α binds Axin, which serves as a scaffold that brings CK1 to close proximity with its substrates β-catenin and APC (Ha, Tonozuka et al. 2004). Furthermore, CK1 isoforms form high molecular weight complexes by binding to proteins which contain an F-x-x-x-F motif. This CK1 binding motif was first identified in NFAT1 and PER1/2 proteins, in which mutation of the two phenylalanines abolishes their interaction with CK1 (Okamura, Garcia-Rodriguez et al. 2004). Specifically, the F-x-x-x-F motif on NFAT1 serves as a docking site for CK1 which then regulates its own phosphorylation. The molecular basis through which CK1 recognises the F-x-x-x-F motif has not been established yet. It is still unclear whether the F-x-x-x-F motif is necessary and sufficient for any protein substrate to interact with CK1. Thus, although reversible phosphorylation implies transient interaction between the kinase and its substrate, CK1 isoforms might form tight interactions with some of their targets - a feature that could potentially enhance the rate of their phosphorylation.

An alternative mechanism for CK1 regulation was suggested by Cruciat *et al.* (2013), in which the ATP-dependent DEAD-box RNA helicases 3 (DDX3) acts as an allosteric activator of CK1ε by enhancing its catalytic velocity (Cruciat, Dolde et al. 2013). In this study, Wnt stimulation promoted the interaction between DDX3 and CK1ε, which in turn stimulated its kinase activity towards its substrates, such as Dvl2. The enzymatic activity of DDX3 is not required for CK1 association and activation and the authors suggest that this multifunctional protein is a new regulatory subunit of CK1 isoforms (Cruciat, Dolde et al. 2013). However, it is still unclear how DDX3 is recruited to CK1 upon Wnt stimulation and how the binding to CK1 enhances the kinase activity. Another example of allosteric activation of CK1 has been shown with the small molecule Pyrvinium pamoate, a drug used in the clinic to inhibit Wnt signalling (Thorne, Hanson et al. 2010) and a more recently identified compound SSTC3 (Li, Orton et al. 2017) (see 1.6.6). However, the mechanisms of their actions are yet to be determined.

Furthermore, the subcellular localisation of CK1 determines the access to specific substrates and therefore defines the CK1 function and regulation (Knippschild, Kruger et al. 2014). This is probably the most critical mode of regulation, as it limits the substrate availability and accessibility. Considering the broad range of potential substrates that CK1 targets in the cell, such spatio-temporal mechanisms may help explain how substrate selectivity is achieved. One example of spatio-temporal regulation of CK1 activity is the

association of CK1α with distinct cellular structures and compartments at different stages of the cell cycle (Behrend, Stoter et al. 2000).

Finally, CK1 activity towards some of its targets might depend on the phosphorylation status of its substrates (Flotow, Graves et al. 1990). For instance, it has been shown that efficient phosphorylation of α-synuclein at S129 by CK1 requires priming phosphorylation at Y125 by an unknown kinase in mammalian cells (Kosten, Binolfi et al. 2014). Another example of a priming phosphorylated residue for CK1-mediated phosphorylation was shown upon induction of the unfolded protein response (UPR) due to viral infection (Bhattacharya, HuangFu et al. 2010). UPR was shown to promote phosphorylation of the interferon α receptor (IFNAR1) at S532 by an unknown kinase, which acts as a priming event for subsequent phosphorylation of IFNAR1 by CK1 for the recruitment of β-TrCP ligase that degrades the receptor (Bhattacharya, HuangFu et al. 2010).

1.6.4 CK1 isoforms are both positive and negative regulators of Wnt signalling

CK1 isoforms mediate the phosphorylation of several components of canonical Wnt signalling, resulting in either inhibition or activation of the pathway (Cruciat 2014). The first implication of CK1 in Wnt signalling was in 1999 when Peters *et al.*, showed that overexpression of CK1α, δ and ε causes axis duplication in *Xenopus* embryos (Peters, McKay et al. 1999). It was thus believed that CK1 has a positive role in Wnt signalling activation. The same year, it was shown that overexpression of CK1ε in human cells leads to β-catenin stabilisation and Wnt-target genes activation and it was suggested that CK1ε is in the same complex with Axin, GSK3β and DVL (Sakanaka, Leong et al. 1999). Later it was confirmed that CK1δ and CK1ε interact with DVL and phosphorylate multiple components of the destruction complex including, Axin and β-catenin (Ikeda, Kishida et al. 1998, Kishida, Hino et al. 2001, Gao, Seeling et al. 2002). Subsequently, it was suggested that in response to Wnt signals, CK1ε (or CK1δ) is activated, binds and phosphorylates DVL at S139 and S142 which in turn promote the dissociation of the phosphatase PP2A from the destruction complex, resulting in stabilisation of β-catenin and enhancement of Wnt signalling (Cheng, Syder et al. 1992, Gao, Seeling et al. 2002, Cong, Schweizer et al. 2004, Klimowski, Garcia et al. 2006). Furthermore, it has been suggested that CK1ε-mediated phosphorylation of DVL increases the affinity of DVL for the Wnt receptor complex and enhances the recruitment of Axin, which is required for the Wnt signallosome assembly (Del Valle-Perez, Arques et al. 2011).

Apart from DVL, Wnt signals induce the phosphorylation of LRP6 by CK1γ at T1479 (Davidson, Wu et al. 2005). As mentioned earlier this phosphorylation step is required for the formation of the Wnt signalosome in human cells. Additionally, it is thought that CK1-mediated LRP6 phosphorylation is required for subsequent phosphorylation of LRP6 by GSK3 at its five PPPSPxS motifs that lie downstream of the T1479 residue (Zeng, Tamai et al. 2005, MacDonald, Yokota et al. 2008). It was shown that at least four of these motifs must be phosphorylated for β-catenin stabilisation to occur (MacDonald, Yokota et al. 2008). Because these phosphorylation events are strictly Wnt-dependent, T1479 phosphorylation by CK1γ is widely used to monitor acute Wnt signalling with a T1479 phosho-specific antibody (Bilic, Huang et al. 2007). CK1γ might also phosphorylate the second Ser of the PPPSPxS motif although CK1α, δ and ε have also been implicated in this Wnt-induced phosphorylation of LRP6, contributing to the recruitment of the Axin complex to the cell membrane and thus suggesting a redundancy and overlapping role of CK1 isoforms in early Wnt responses (Zeng, Tamai et al. 2005).

Biochemical studies have revealed that CK1ε binds and phosphorylates TCF3 in the cytoplasm of *Xenopus* eggs and mammalian cells (Lee, Salic et al. 2001). It was shown that TCF3 inhibits β-catenin phosphorylation by GSK3, potentially by sequestering β-catenin away from the Axin:GSK3 complex. TCF3 phosphorylation by CK1ε was demonstrated to be both necessary and sufficient for its interaction with and subsequent stabilisation of β-catenin. Inhibition of CK1ε acts negatively on TCF3-β-catenin binding, increasing the β-catenin degradation levels (Lee, Salic et al. 2001).

On the other hand, CK1 isoforms can also be negative regulators of the Wnt signalling. The best characterised mode of their action is at the level of the β-catenin destruction complex (Liu, Li et al. 2002). Although the phosphorylation of β-catenin at Ser45 is attributed to CK1, it is not clear which isoform (α, δ or ε) is mainly responsible for this event or if the CK1 isoforms can act redundantly. All three isoforms have been identified as potential components of the destruction complex and they all phosphorylate β-catenin *in vitro* (Amit, Hatzubai et al. 2002). Other than β-catenin, CK1δ and ε have been reported to phosphorylate Axin and APC, which enhance β-catenin degradation in human cells (Gao, Seeling et al. 2002). In the nucleus CK1ε interacts with, and phosphorylates LEF, thereby preventing its association with β-catenin and the transcription of its target genes (Hammerlein, Weiske et al. 2005).

Lastly, CK1 isoforms act in feedback loops to either re-activate or cease Wnt signalling. For example, phosphorylation of DVL by CK1ε promotes DVL binding to the

E3-ubiquitin ligase HUWE1, which interacts with the DIX domain that is responsible for DVL polymerisation. Inhibition of DVL polymerisation thus blocks the assembly of Wnt signalosome complex and ultimately inhibits Wnt signalling (de Groot, Ganji et al. 2014). Furthermore, Wnt stimulation induces the phosphorylation of more CK1 substrates on the cell membrane, including E-cadherin and its binding partner p120-catenin. In the adherens junctions, E-cadherin is stabilised by p120 but it also mediates the interaction between p120 and LRP6. Phosphorylation of E-cadherin and p120 upon Wnt stimulation, disrupts the interaction of E-cadherin with p120 and LRP6. Consequently, p120-catenin-bound CK1ε is released from the signalling complex, which in turn prevents further DVL phosphorylation by CK1ε, terminating the initial signalling (Del Valle-Perez, Arques et al. 2011). In conclusion, local modulation of CK1 isoforms can have different effects on the outcome of Wnt signalling.

1.6.5 Roles of CK1 beyond Wnt signalling

1.6.5.1 CK1 and circadian rhythm

One of the most ancient mechanisms of timekeeping, from plants to humans, is modulated by the activity of CK1 (van Ooijen, Hindle et al. 2013). CK1 was the first enzyme that was found to regulate circadian rhythm in *Drosophila*, through phosphorylation of the transcription factor PERIOD (PER) (Kloss, Price et al. 1998, Price and Kalderon 2002). In the mammalian brain and in the periphery, oscillatory transcriptional feedback includes the positive regulator complex CLOCK:BMAL, which activates the transcription of PER1 and PER2, which in turn form heterodimers with CRY and negatively regulate CLOCK:BMAL, thereby completing one circadian circle (Shanware, Hutchinson et al. 2011). CK1δ or CK1ε-dependent phosphorylation of PER1 and PER2 induces their degradation by the β-TrCP-containing E3 ligases and the proteasome, ultimately leading to initiation of a new cycle (Eide, Woolf et al. 2005). Recent studies have shown that the activity of CK1δ against PER degradation is regulated via phosphorylation by different kinases including cyclin-dependent kinases (Eng, Edison et al. 2017). Mutations of the phosphorylation sites on CK1δ and CK1ε, leading to increased kinase activity, have a protective role in the development of familial advanced phase sleep syndrome (FASPS) (Shanware, Hutchinson et al. 2011). Moreover, FASPS patients carry a missense mutation on the binding site of PER to CK1ε which results in PER hypo-phosphorylation and thus a negative regulation on the patients' circadian rhythm. Corroborating evidence from CK1ε null mutant mice support the role of CK1 in circadian rhythm regulation as the free-running periods of the locomotor activity rhythm

of the CK1ε$^{-/-}$ mice was shown to be significantly longer than wild type controls (Meng, Logunova et al. 2008, Etchegaray, Machida et al. 2009). Similarly, CK1δ$^{+/-}$ mice exhibit longer circadian period compared to wild type controls, while CK1δ$^{-/-}$ were embryonic lethal (Etchegaray, Machida et al. 2009). Collectively there is strong evidence supporting that the critical roles CK1δ and CK1ε play in maintaining the daily circadian cycle length.

1.6.5.2 CK1 in cell cycle progression

The eukaryotic cell cycle is divided into two main phases: interphase, which is the stage that the cell develops between two divisions, and M phase, in which the cell divides to create two genetically identical daughter cells. Interphase is divided into the G1 phase, in which the cell grows and prepares for DNA replication, the S phase, where the DNA is replicated and the G2 phase, in which the cell prepares for division. The M phase is divided into mitosis, when DNA is condensed and separated into two nuclei, and cytokinesis, in which the cellular context is segregated and the cell divides into two (Cooper 2000). Checkpoint mechanisms, mediated by for example, cyclin-dependent kinases, regulate the completion of each phase and the progression to another. The yeast homologue of CK1 was the first to be found to have a role in the regulation of cell cycle progression and cell division (Hoekstra, Liskay et al. 1991). In mammals, the precise roles of CK1 isoforms in the cell cycle are not very well understood. CK1α, δ and ε localise to the centrosome and mitotic spindle, where they might function to control mitotic progression (Sillibourne, Milne et al. 2002). Furthermore, CK1δ displays high affinity for microtubules and the spindle apparatus from mitotic cell extracts after DNA damage, suggesting a regulatory role of CK1δ in mitosis (Behrend, Stoter et al. 2000). Inhibition of CK1δ/ε activity with the IC261 inhibitor (see 1.6.5.4) has been associated with mitotic defects, caused by dysregulation of checkpoint control, which inhibits cytokinesis resulting in mitotic arrest (Behrend, Milne et al. 2000). Antibodies against CK1α block cell cycle progression during M phase in mouse oocytes, suggesting a role of CK1α in chromosomal segregation and mitotic spindle formation (Brockman, Gross et al. 1992, Gross and Anderson 1998).

1.6.5.2 CK1 in apoptosis

Programmed cell death is an evolutionarily conserved pathway which is critical during embryonic development and in the maintenance of adult tissue homeostasis. In short, various death receptors, such as FAS, TNFR1 and DR4/5 transduce the extrinsic apoptotic signal for the formation of the intracellular Death-Inducing-Signalling-Complex (DISC), consisting of proteins with death domains (DD) and death effector

domains (DED). These proteins then recruit caspases for propagation of the apoptotic signal. A considerable amount of literature has been published on the role of CK1 in apoptosis through different molecular pathways. Most of these studies are based on the use of CK1 inhibitors or RNAi approaches. CK1 isoforms can phosphorylate the tumour necrosis factor receptor p75 and negatively regulate p75-mediated apoptosis (Beyaert, Vanhaesebroeck et al. 1995). Inhibition of CK1 isoforms or knock-down of CK1α sensitises tumour cells to TRAIL-induced apoptosis mainly by recruiting FADD and procaspase-8 to the receptor complex (Izeradjene, Douglas et al. 2004). Furthermore, CK1 can phosphorylate the pro-apoptotic protein Bid and inhibition of its activity is associated with Fas-mediated apoptosis, whereas hyperactive CK1 delays apoptosis (Desagher, Osen-Sand et al. 2001). Recent research has demonstrated that the inhibition of CK1δ and CK1ε with the IC261 inhibitor (see 1.6.5.4) leads to decreased expression of anti-apoptotic proteins and increased apoptotic sensitivity of pancreatic tumour cells (Brockschmidt, Hirner et al. 2008). Finally, CK1α has been proposed as a negative regulator of apoptosis induced by agonists of retinoid X receptors (RXRs) (Zhao, Qin et al. 2004). Agonists of RXRs are potent inducers of growth arrest and apoptosis in many cancer cells (Altucci and Gronemeyer 2001). CK1α was shown to negatively regulate RXR agonist-mediated apoptosis through interaction with and phosphorylation of RXR (Zhao, Qin et al. 2004).

1.6.5.3 CK1 in Hedgehog signalling

Members of the Hedgehog (Hh) family of signalling proteins mediate several processes during embryonic development, including organogenesis, chondrogenesis and polarity in the central nervous system (CNS) and in adult tissue homeostasis (Ingham and McMahon 2001). Uncontrolled activation of Hh pathway has been associated with tumorigenesis (Barakat, Humke et al. 2010). CK1 isoforms were found to play a dual role in both receptor activation (Chen, Sasai et al. 2011) and inhibition of the Hh-target gene transcription (Shi, Li et al. 2014). In mammals, activation of Hh signalling results in the transcription of Hh-target genes through the activation of the glioma-associated oncogene homolog (Gli) transcription factors. In the absence of Hh, PKA phosphorylates Gli, priming it for subsequent phosphorylation by GSK3 and CK1 (Price and Kalderon 2002, Shi, Li et al. 2014). Phosphorylated Gli is then ubiquitinated by the E3 ligase β-TrCP and targeted for proteolytic processing, which creates the truncated transcriptional repressor (GliR), which inhibits the activation of Hh-target genes. Activation of Hh signalling

induces the phosphorylation of the Hh receptor Smoothened (Smo) by CK1and G-protein coupled receptor kinase 2 (GRK2), leading to the activation of Hh-target genes.

1.6.5.4 CK1 in neurodegeneration

CK1 isoforms have been suggested to regulate synaptic transmission in the brain (Chergui, Svenningsson et al. 2005). In mice, it was shown that all the CK1 isoforms are distributed in different regions of the brain and inhibiting their kinase activity results in increased neuronal excitation in response to the neurotransmitter glutamate. Therefore, it was proposed that CK1 isoforms might be negative regulators of the glutamatergic synaptic transmission in nerve cells (Chergui, Svenningsson et al. 2005).

Furthermore, there has been a positive correlation between the mRNA and protein levels of CK1δ and neurofibrillary lesions in the brains of patients with neurodegenerative diseases, such as Alzheimer's disease (AD) (Kuret, Johnson et al. 1997, Schwab, DeMaggio et al. 2000, Yasojima, Kuret et al. 2000). A hallmark of AD is hyper-phosphorylation of the microtubule-associated protein tau. Tau hyper-phosphorylation is accompanied by tau aggregation into filaments, which correlate with neuronal cell loss and cognitive decline (Bramblett, Goedert et al. 1993). It was found that CK1δ binds and phosphorylates Tau, which then dissociates from microtubules resulting in microtubule destabilisation and neuronal death (Li, Yin et al. 2004).

Finally, CK1δ was shown to regulate dopamine neurotransmission *in vivo* (Zhou, Rebholz et al. 2010). Genetically modified mice that overexpress CK1δ specifically in the forebrain, exhibited decreased levels of dopamine receptors, lower anxiety-like behaviours and hyperlocomotion compared to wild type mice (Zhou, Rebholz et al. 2010). Although the exact mechanisms of CK1δ function are not known, the CK1δ overexpression mouse model showed characteristics similar to the behaviour of attention-deficit/hyperactivity disorder (ADHD) patients suggesting that CK1δ could be involved in ADHD progression in humans.

1.6.5.5 CK1 and cancer

In view of all that has been mentioned so far, it is evident that CK1 can impact tumorigenesis and cancer. In addition to its dual role in Wnt and in Hh signalling and its inhibitory role in apoptosis, CK1 isoforms are involved in p53 phosphorylation, thereby mediating tumorigenesis via different signal transduction pathways. p53 is a short-lived transcription factor that is stabilised and activated upon stress, such as DNA damage, causing cell cycle arrest for DNA repair or the initiation of apoptosis (Horn and Vousden

2007). The ubiquitin ligase murine double minute clone 2 (MDM2 or HDM2) mediates p53 ubiquitylation and degradation in normal tissue, retaining the p53 protein in low physiological levels (Horn and Vousden 2007). Huart *et al.* (2009) found that CK1α phosphorylates p53 in cells infected with viral DNA and this blocks the interaction between p53 and MDM2, leading to p53 stabilisation (Huart, MacLaine et al. 2009). Another binding partner of p53, MDMX is also a CK1α substrate and inhibition of CKα activity, leads to decreased MDMX phosphorylation and activation of p53 (Chen, Li et al. 2005). Under normal conditions, CK1δ phosphorylates MDM2, abrogating its interaction with p53 and thus stabilising and activating p53 (Winter, Milne et al. 2004). Hence, under different conditions, CK1α and δ can positively or negatively regulate p53 activity either by direct phosphorylation or by phosphorylating its binding partners MDM2 and MDMX.

An overview of the RNA levels of CK1 isoforms in different tumours, based on different databases, was performed by Schittek and Sinnberg (2014) (Schittek and Sinnberg 2014). This shows that the RNA levels of CK1δ and CK1ε are mainly up-regulated in various tumour types whereas CK1γ is downregulated. CK1α RNA is more variable as it is up-regulated in brain and prostate tumours, in lymphomas and in leukemia, but it is down-regulated in melanomas and in bladder and lung cancer. However, confirmation of these data at the protein level, and determination of kinase activity levels are required for defining any biological significance that explains the differences among the various tumour types. Nevertheless, these differences potentially highlight the context-specific nature of CK1 isoform activity. Indeed, recent studies showed that in RAS-mutant cancer cells, CK1α levels are increased and that CK1α targets the tumour suppressors FOXO3A and FOXO4, priming them for proteasomal degradation in the nucleus (Cheong, Zhang et al. 2015, Zhang, Virshup et al. 2017). Conversely, pharmacological or RNAi-mediated inhibition of CK1α activity, stabilises FOXO4 and induces apoptosis (Zhang, Virshup et al. 2017).

Furthermore, it has been suggested that CK1 isoforms have a negative role in FGF signalling because they can phosphorylate SPROUTY2, allowing it to interact with GRB2 and inhibit downstream signalling (Yim, Ghosh et al. 2015). In gastric cancer cells with high FGF expression, CK1ε expression is down-regulated, suggesting that CK1ε is an inhibitor of the FGF signalling pathway through activation of the negative regulator SPROUTY2 (Yim, Ghosh et al. 2015).

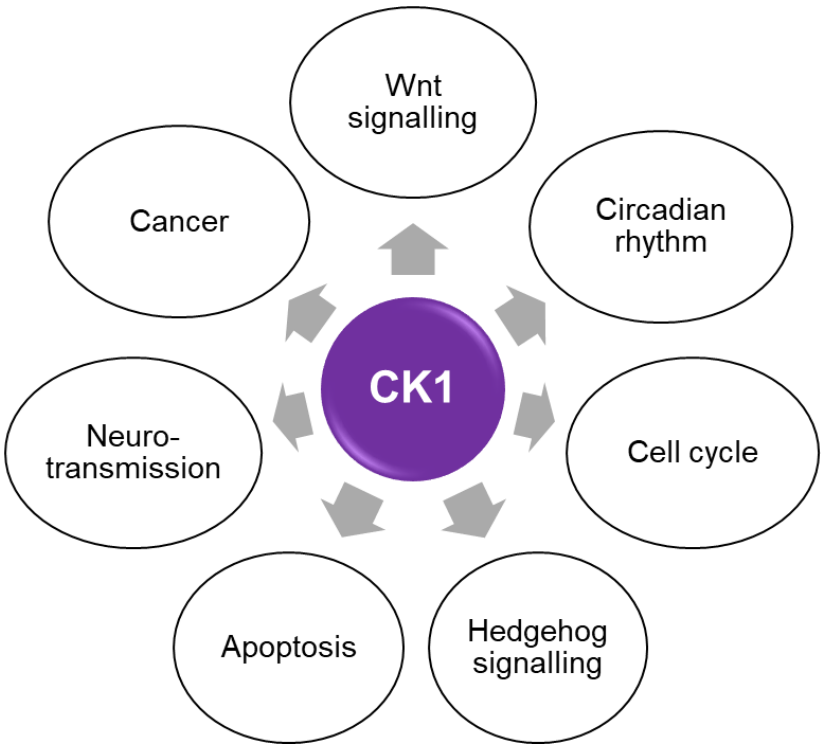

Figure 1- 13 The major biological functions of CK1

1.6.6 Pharmacological targeting of CK1 isoforms

Given the many roles of CK1 in human disease and tumorigenesis, there has been a lot of interest in the last few decades in developing selective small molecules that inhibit CK1 kinase activity (Table 1-2). However, the development of inhibitors capable of selectively targeting each CK1 isoform remains challenging. The first characterised CK1 inhibitor was the ATP-competitive quinoline derivative CK1-7 (N-(2-amino-ethyl)-5-chloroisoquinoline-8-sulfonamide), which does not show any specificity for CK1 isoforms (Chijiwa, Hagiwara et al. 1989). The next CK1 inhibitor, IC261, was developed in 2000 and was derived from iodolinone (Mashhoon, DeMaggio et al. 2000). IC261 is also an ATP-competitive inhibitor and it is the first compound that showed selectivity towards CK1δ and ε. IC261 also inhibits the polymerization of microtubules and enhances apoptosis in a CK1-independent manner (Cheong and Virshup 2011, Stoter, Kruger et al. 2014). More recently, it was demonstrated that the same IC261 concentration used for blocking 50% of CK1δ/ε activity also inhibits sodium channels (Fohr, Knippschild et al. 2017). The first ATP-competitive inhibitor that showed improved potency and selectivity for the δ isoform was the imidazole derivative, D4476 (4-[4-(2,3-dihydro-benzo[1,4]dioxin-6-yl)-5-pyridin-2-yl-1H-imidazol-2-yl]benzamide) (Rena, Bain et al. 2004). However, low doses of D4476 also inhibit the TGFβ receptor ALK5 and p38 (Rena, Bain et al. 2004). More recently, D4476 was found to inhibit CK1α and also showed high therapeutic efficacy on acute myeloid leukemia and multiple myeloma cells (Jaras, Miller et al. 2014, Hu, Song et al. 2015). Several other compounds have been reported to inhibit CK1 isoforms but all of them lack specificity as they have many off-target effects (Table 1-2). However, the most promising one seems to be the immunomodulatory drug (IMiD) Lenalidomide (Lena) which is used for the treatment of myelodysplastic syndrome (MDS) with deletion of chromosome 5q (del(5q)). Lena binds CRBN, the substrate adaptor of the $CRL4^{CRBN}$ E3 ubiquitin ligase, inducing ubiquitylation and degradation of its substrates (Kronke, Fink et al. 2015). CK1α was found to bind CRBN in the presence of Lena and to be subsequently subjected to proteasomal degradation. Interestingly, the *CSNK1A1* gene, which encodes CK1α, is located in the deleted 5q region of the MDS patients and the levels of CK1α expression in the affected cells are 50% lower than the healthy controls. It was demonstrated that these lower expression levels of CK1α account for the increased sensitivity of these cancer cells to Lena compared to healthy controls (Kronke, Fink et al. 2015).

Novel approaches for targeting kinases nowadays also involve activators instead of inhibitors, depending on the disease context. The first CK1 activator described in the literature is the FDA-approved anthelmintic drug Pyrvinium Pamoate (PyrPam) (Thorne, Hanson et al. 2010). It was shown that PyrPam binds to all CK1 isoforms but selectively activates CK1α. It was suggested that PyrPam alters CK1 conformation, which then impacts the kinase activity leading to inhibition of Wnt signalling through enhanced β-catenin phosphorylation. However, a subsequent study by Venerando *et al.* (2013) showed a role for PyrPam in downregulation of the Akt pathway, which subsequently inhibits the Wnt pathway independent of CK1α (Venerando, Girardi et al. 2013). Nevertheless, these results do not rule out a potential role of CK1α misregulation in the Akt pathway. More recently, the small molecule SSTC3 was identified as a CK1α activating Wnt inhibitor (Li, Orton et al. 2017). SSTC3 binds to CK1α and enhances its kinase activity. It blocks Wnt-induced axis duplication phenotypes in *Xenopus* embryos and displays stronger efficacy in cells with low levels of CK1α expression, such as in colorectal tumours (Li, Orton et al. 2017).

Inhibitor	Isoform targeted	in vitro IC50 (μM)	Off-targets	References
CK1-7	α/δ/ε	6.00	ERK8/SGK1/MNK1/ AMPK/PIM1/PIM3	Chijiwa et al., 1989; Bain et al., 2007
IC261	δ/ε	2.50	CK1α/PIM1/PIM3	Mashhoon et al., 2000; Bain et al., 2007
D4476	δ	0.30	CK1α/ALK5/p38	Rena et al., 2004
DAA	δ	0.30	CK2	Cozza et al., 2008
R-DRF053	δ/ε	0.01	CDKs	Oumata et al., 2008
PF-670462	δ/ε	0.013/0.08	PKA/PKC/p38/GSK3β	Walton et al., 2009
PF-4800567	δ/ε	0.032/0.7	EGFR	Walton et al., 2009
CR8	δ/ε	Not reported	CDKs/GSK3α/β	Bettayeb et al., 2008; Delehouze et al., 2014
Hua-1h	γ	0.02	CK1α/δ	Hua et al., 2012
Bischof-5	δ/ε	0.04/0.199	CK1α	Bischof et al., 2012
SR-653234	δ/ε	0.16/0.54	FLT3/CDKs	Bibian et al., 2013
SR-1277	δ/ε	0.049/0.26	FLT3/CDKs	Bibian et al., 2013
SR-3029	δ/ε	0.044/0.26	FLT3/CDKs	Bibian et al., 2013
Richter-1	δ/ε	0.02/0.21	CK1α/CK1αL/FLT3	Richter et al., 2014
Richter-2	δ/ε	0.14/0.52	CK1αL/CK1γ/FLT3/ CLK/DYRK1B/ DYRK2/MLCK	Richter et al., 2014
Halekotte 11-b	δ	0.04	CK1ε/CK1α/p38/JNK/ RIPK/LCK	Halekotte et al., 2017

Table 1- 2 Pharmacological molecules targeting CK1

Aims of the thesis

Previously, PAWS1 had been identified as an interactor of SMAD1 and shown to impact the non-canonical BMP pathway. PAWS1 also regulated transcription of many genes independent of BMP signalling, suggesting roles beyond BMP signalling. In collaboration with Jim Smith (The Francis Crick Institute, London) it was shown that ectopic expression of PAWS1 mRNA in *Xenopus* embryos resulted in complete axis duplication (two-head phenotype) at the tadpole stage, while PAWS1 depletion led to embryonic defects and lethality. In the developing *Xenopus* embryo, opposing gradients of BMP and Wnt activities help pattern the dorso-ventral axis, with the highest levels of BMP or Wnt signalling promoting formation of the most ventral tissues and most dorsal tissues, respectively. Therefore, either inhibiting BMP or activating Wnt signalling forcefully in *Xenopus* embryos could lead to such two-head phenotypes. With these developments in place, the main aims of this thesis were to:

- Elucidate the signalling pathways (either BMP or Wnt; or both) that PAWS1 impacts to mediate axis duplication during *Xenopus* embryogenesis.

This aim was tackled by employing a collaborative approach, in which *Xenopus* embryogenesis assays were performed by Dr. Kevin Dingwell (Jim Smith lab at the Francis Crick Institute) and human cell-line based assays were performed in Dundee. Cutting-edge technologies, including the use of CRISPR/Cas9 genome editing, were employed to assess the impact of PAWS1 on BMP and Wnt signalling.

- Establish the molecular mechanisms by which PAWS1 regulates the Wnt signalling pathway.

As soon as it was evident that PAWS1 activated Wnt signalling in *Xenopus* embryos and human cell lines, it became important to establish the molecular mechanisms by which it did so. This was addressed by employing a proteomic approach to identify key PAWS1 interactors that could explain the activation of Wnt signalling, using PAWS1-GFP knockin U2OS cells generated with CRISPR/Cas9 – a cell line which allowed robust enrichment of the endogenous PAWS1 interactome following subjection of cell extracts to immunoprecipitations with GFP beads. Validation of key targets were performed by biochemical and cell-based assays and the information gleaned was exploited collaboratively to assess the mechanisms in *Xenopus* embryo assays.

- Explore the post-translational regulation of PAWS1 function by novel interacting protein kinases.

Regulation of PAWS1 by post-translational modifications is poorly understood. From endogenous PAWS1 proteomics data, novel interactors, in particular protein kinases, were identified. These interacting proteins, particularly those with intrinsic catalytic activity, hinted at possible roles in PAWS1 function. These were characterised further.

- Examine the role of pathogenic PAWS1 mutations on its function.

Several mutations in PAWS1 have been identified that appear to cause various skin and hair morphological conditions, including hereditary footpad hyperkeratosis and trichillemal cysts. How the mutations impact PAWS1 function is not known.

2. Materials and methods

2.1 Materials

2.1.1 Chemicals and other reagents

The chemicals used in this thesis are listed in table 2-1.

Reagent	Source
4-(2-Hydroxyethyl)piperazine-1-ethanesulfonic acid (HEPES)	Sigma-Aldrich
4',6-diamidino-2-phenylindole (DAPI)	Thermo Fisher Scientific
A23187	Sigma-Aldrich
Acetic acid	Sigma-Aldrich
Acetone	Sigma-Aldrich
Acetonitrile (HPLC grade)	Rathburn Chemicals
Acrylamide:bis-acrylamide 40% (w/v) 29:1	Flowegene Bioscience
Adenosine 5'-triphosphate (ATP)	Roche
Agarose (electrophoresis grade)	Thermo Fisher Scientific
Ammonium bicarbonate	BDH
Ammonium hydroxide (NH_4OH)	Sigma-Aldrich
Ammonium persulphate (APS)	Sigma-Aldrich
Ampicillin	ForMedium
Ataluren	Selleckchem
Autocamtide-3 derived inhibitory peptide (AC3-I)	Anaspec
Baffilomycin A1	Enzo
BAPTA-AM	Sigma-Aldrich
Blasticidin	Thermo Fisher Scientific
BMP2 (#355-BM)	R&D Systems
BMP4 (#314-BP-010)	R&D Systems
Bortezomib	LC Laboratories
Bovine serum albumine (BSA)	Sigma-Aldrich
Bromophenol blue	Sigma-Aldrich
C18 columns	Thermo Fisher Scientific
C18 StageTip	3M Empore
CellTiter 96® AQueous One Solution Cell Proliferation Assay	Promega
CHIR99021	Axon
CK1tide	DSTT
Coelenterazine (CTZ) native	Nanolight
Compartment protein extraction kit (#2145)	Merck
Complete protease inhibitor cocktail tablets	Roche
Coomassie protein assay reagent (Bradford reagent)	Thermo Fisher Scientific
D4476	DSTT

Reagent	Source
Dimethyl sulphoxide (DMSO)	Sigma-Aldrich
Dithiobis succunimidyl propionate (DSP)	Thermo Fisher Scientific
Dithiothreitol (DTT)	Sigma-Aldrich
D-luciferin	Synchem
DNeasy Blood and Tissue (#69504)	Qiagen
Doxycycline (hydrochloride)	Sigma-Aldrich
Dulbecco's modified Eagle medium (DMEM)	Thermo Fisher Scientific
Dulbecco's phosphate buffer saline (PBS)	Thermo Fisher Scientific
EGF (#236-EG-200)	R&D Systems
Enhanced Chemiluminescence (ECL) reagent	GE Healthcare
Ethanol	Sigma-Aldrich
Ethylene glycol-bis(β-aminoethyl ether)-N,N,N',N'-tetraacetic acid (EGTA)	Sigma-Aldrich
Ethylenediaminetetraacetic acid (EDTA)	ForMedium
FGF2 (#8910F)	CST
FGF4 (#100-31)	Peprotech
FLAG-agarose	Sigma-Aldrich
Foetal bovine serum (FBS)	Labtech
Formic acid	Sigma-Aldrich
Gelatin (from porcine skin)	Sigma-Aldrich
Geneticin (G418)	Thermo Fisher Scientific
GFP-Trap agarose beads	Chromotek
Glutathione	Sigma-Aldrich
Glutathione-sepharose	GE Healthcare
Glycerol	VWR
Glycine	VWR
HA-agarose	Sigma-Aldrich
Hexadimethrine bromide (polybrene)	Sigma-Aldrich
Hydrochloric acid (HCl)	VWR
Hygromycin-B	Thermo Fisher Scientific
IGF (#8917LF)	CST
Immobilon-P Polyvinylidene fluoride (PVDF) 0.45 µm membrane,	Merck
InstantBlue Commasie stain	Expendeon
Iodoacetamide	Sigma-Aldrich
Ionomycin	Sigma-Aldrich
iScript cDNA synthesis kit	BioRad
Isobaric Tandem Mass Tag™ 6plex reagent	Thermo Fisher Scientific
Isopropanol	Sigma-Aldrich
Isopropyl β-D1-thiogalactopyranoside (IPTG)	Sigma-Aldrich
Kanamycin	Sigma-Aldrich
KOD hot start polymerase kit	Toyobo
LDS sample buffer (4x)	Thermo Fisher Scientific

Reagent	Source
L-glutamine	Sigma-Aldrich
Lipofectamine RNAiMAX	Thermo Fisher Scientific
Lithium Chloride	BDH
Lithium dodecyl sulphate (LDS) sample buffer 4x	Invitrogen
Luria Bertani broth (LB) and LB agar plates	Central Technical Service team, University of Dundee
Lysozyme chicken egg	Thermo Fisher Scientific
Magnesium Acetatate	Sigma-Aldrich
Magnesium cloride (MgCl2)	Sigma-Aldrich
Methanol	VWR
NE-PER nuclear and cytoplasmic extraction kit	Thermo Fisher Scientific
NiNTA raisin	Qiagen
Nonidet P-40 substitute	Sigma-Aldrich
NuPAGE Novex 4-12% Bis-Tris polyaclylamide gels	Thermo Fisher Scientific
Opti-MEM	Thermo Fisher Scientific
Orange G	Sigma-Aldrich
Paraformaldehyde 4% (v/v)	Sigma-Aldrich
Passive Lysis buffer 5x	Promega
Penicillin/streptomycin	Thermo Fisher Scientific
Plasmid Maxi, Midi and Mini kits	Qiagen
Polyethylenimine (PEI)	Polysciences
Polyoxyethylene(23) lauryl ether (Brij-35)	Sigma-Aldrich
Ponceau S	Sigma-Aldrich
Precision Plus Protein^{TM} All Blue Standards	BioRad
Prolong Gold mounting reagent	Thermo Fisher Scientific
Protein G-sepharose	GE Healthcare
Puromycin	Sigma-Aldrich
RNeasy kit	Qiagen
Sep-Pak SPE cartridges	Waters
Sequencing grade modified trypsin	Promega
SKF 96365	Abcam
Skimmed milk powder	Marvel
Sodium 2-glycerophosphate	Sigma-Aldrich
Sodium Chloride (NaCl)	VWR
Sodium ethylene glycol tetra acetic acid (EGTA)	Sigma-Aldrich
Sodium fluoride	Sigma-Aldrich
Sodium orthovanadate (Na3VO4)	Sigma-Aldrich
Sodium pyrophosphate	Sigma-Aldrich
SsoFast Evagreen Supermix	BioRad
StrataClone Blunt PCR Cloning Kit	Agilent
Sucrose	VWR
SuperSignal West Pico Chemiluminescent Substrate	Thermo Fisher Scientific
SYBR Safe	Thermo Fisher Scientific

Reagent	Source
Tetramethylethylenediamine (TEMED)	Sigma-Aldrich
TGFB1	R&D Systems
TiO_2 beads	GL Sciences
t-octylphenoxypolyethoxyethanol (Triton) X-100	Sigma-Aldrich
TransFectin	BioRad
Triethylammonium bicarbonate	Sigma-Aldrich
Tris (hydroxymethyl) aminomethane (Tris)	BDH
Trypsin/EDTA	Thermo Fisher Scientific
Urea	Sigma-Aldrich
Wnt3A (#5036-WN)	R&D Systems
X-gal	Sigma-Aldrich
Zeocin	Thermo Fisher Scientific
γ^{32}P-ATP	PerkinElmer

Table 2- 1 Reagents used in this thesis

2.1.2 Buffers and solutions

Commonly used buffers and solutions, as well as their composition are listed in table 2-2.

Buffer/Solution	Composition
8-12% acrylamide resolving gels	375 mM Tris/HCl (pH 8.6), 0.1% SDS (w/v) and 8-12% (w/v) acrylamide. 0.1% (w/v) ammonium persulfate (APS) and 0.1% (v/v) TEMED were used to polymerise the gels.
Bacterial Cell lysis buffer	50 mM Tris/HCl pH 7.5, 300 mM NaCl, 10% (v/v) glycerol, 1 mg/ml lysozyme, 10 μg/ml DNAase, 0.075% (v/v) β-mercaptoethanol, 1 tablet of Complete protease inhibitor cocktail (tablet was added just prior to use)
Binding assay buffer	50 mM Tris-HCl pH 7.5, 150 mM NaCl, 0.03% (v/v) Brij-35, 1 mM EGTA, 1 mM DTT
Blocking solution	5% (w/v) milk powder, TBST
BSA primary antibody solution	5% (w/v) BSA, TBST, 0.02% (w/v) sodium azide
Buffer A	50 mM Tris-HCl pH 7.5, 0.1 mM EGTA
Cell freezing medium	50% (v/v) FBS, 40% DMEM,10% DMSO
GST-tag protein elution buffer	50 mM Tris-HCl pH 7.5, 0.03% (v/v) Brij-35, 0,1 mM EGTA, 20 mM glutathione, pH 7.5
GST-tag protein wash buffer	50 mM Tris-HCl pH 7.5, 250 mM NaCl, 0.03% (v/v) Brij-35, 0.1 mM EGTA, 0.1% (v/v) β-mercaptoethanol
His-tag protein binding buffer	500 mM NaCl, 10 mM Imidazole in PBS
His-tag protein dialysis buffer	25 mM Tris-HCl pH 7.4, 150 mM NaCl
His-tag protein elution buffer	1 mM DTT, 250 mM Imidazole in PBS

Buffer/Solution	Composition
Hypotonic lysis buffer	10 mM Tris-HCl (pH 7.4), 2 mM EDTA, 10 mM KCl, 1 tablet of Complete protease inhibitor cocktail
IF blocking solution	3% (w/v) BSA, 0.1% (v/v) Triton X-100 in PBS
IF quenching buffer	10 mM Hepes pH 7.4, DMEM
Kinase assay buffer	50 mM Tris pH 7.5, 0.1 mM EGTA, 10 mM Magnesium Acetate (or $MgCl_2$), 2 mM DTT
LB plates	1% (w/v) tryptone peptone, 0.5% (w/v) yeast extract, 86 mM NaCl, 2% (w/v) bactoagar, 100 μg/ml ampicillin or 25 μg/ml kanamycin after autoclaving for 20 min
Luciferase assay buffer (2x)	50 mM Tris/Phosphate, pH 7.8, 16 mM $MgCl_2$, 1 mM ATP, 30% (v/v) Glycerol, 1% (w/v) BSA, 0.25 mM D-Luciferin, 8 μM Sodium Pyrophosphate
Luria Bertani broth (LB)	1% (w/v) tryptone peptone, 0.5% (w/v) yeast extract, 86mM NaCl, 100 μg/ml ampicillin or 25 μg/ml kanamycin after autoclaving for 20 min
Lysis buffer with DSP	40 mM HEPES pH 7.4, 120 mM NaCl, 1 mM EDTA pH 8.0, 10 mM sodium β-glycerophosphate, 50 mM sodium fluoride, 1 mM sodium orthovanadate, 5 mM sodium pyrophosphate, 1% (v/v) Triton X-100, 1 tablet of complete protease inhibitors per 25 ml lysis buffer, 2.5 mg/ml DSP (in DMSO) (DSP was added just prior to use)
Mammalian cell lysis buffer	50 mM Tris-HCl pH 7.5, 1 mM EGTA pH 8, 1 mM EDTA pH 8, 1 mM activated Na3VO4, 10 mM Na β-glycerophosphate, 50 mM NaF, 5 mM Na Pyrophosphate, 270 mM, Sucrose, 1% (v/v) Nonidet P-40 and a protease inhibitor cocktail (1 tablet per 25 ml buffer)
MOPS running buffer (Purchased from Formedium)	50 mM MOPS, 50 mM Tris base, 0.1% (w/v) SDS, 1 mM EDTA, pH 7.7
PEI	1 mg/ml PEI in 25 mM HEPES, pH 7.5
Phosphate-buffered saline (PBS)	137 mM NaCl, 2.7 mM KCl, 4.3 mM Na_2HPO_4, 1.47 mM KH_2PO_4, pH 7.4
Renilla assay buffer (3x)	0.06 mM PTC124 (in DMSO), 0.01 mM CTZ, 45 mM Na_2EDTA, 30 mM Na-pyrophosphate, 1.425 M NaCl
Sample buffer (5x)	312.5 mM Tris-HCl, pH 6.8, 50% (v/v) glycerol, 10% (w/v) SDS, 0.10% (w/v) bromophenol blue, 5% (v/v) β-mercaptoethanol
SDS-PAGE buffer	25 mM Tris/HCl pH 8.3, 192 mM glycine, 0.1% (v/v) SDS
Stacking gel	125 mM Tris/HCl (pH 6.8), 0.1% SDS (w/v) and 4% acrylamide (w/v). 0.075% (w/v) ammonium persulfate (APS) and 0.1% (v/v) TEMED were used to polymerise the gels
TAE buffer	40 mM Tris-Acetate pH 8, 1mM EDTA
TBST buffer	50 mM Tris-HCl, pH 7.5, 0.15 M NaCl and 0.1 % Tween 20
Transfer Buffer	25 mM Tris/HCl pH 8.3, 192 mM glycine, 20% (v/v) methanol
Tris-buffered saline (TBS)	20 mM Tris/HCl pH 7.5, 150 mM NaCl
Urea lysis buffer	8 M Urea, 2% (w/v) SDS, 250mM NaCl, 50mM HEPES pH 8.5, PhosSTOP (Roche), 2 mM Sodium orthovanadate 10 mM Na B glycerophosphate, 5 mM Na pyrophosphate, 50 mM NaF, 1 tablet of Complete protease inhibitor cocktail (tablet was added just prior to use)

Table 2- 2 Buffers and solutions used in this thesis

2.1.3 Antibodies

All the non-commercial antibodies were raised in sheep or rabbit (Table 2-3) by the Division of Signal Transduction and Therapy (DSTT), School of Life Sciences, University of Dundee. The antigens used to generate the antibodies are also indicated (Table 2-3). The antibodies were affinity purified on CH Sepharose covalently coupled to the antigens used to raise the antibodies. For the purification of phospho-specific antibodies, the antibodies purified on the column containing the phospho-peptide immunogen were passed through a peptide column made with the non-phosphorylated form of the peptide immunogen. The antibodies that did not bind to the non-phosphorylated peptide column were collected and used. Antibodies were eluted with 50 mM glycine pH 2.5 and were then dialyzed for 16 hours in PBS.

Species-specific HRP-coupled secondary antibodies were obtained from either Thermo Fisher Scientific or CST. The antibodies used for immunofluorescence are listed in Table 2-4. Alexa Fluor® 488 donkey anti-sheep IgG (A11015) and Alexa Fluor® 594 goat anti-rabbit IgG (A11012) were used at 1:1000 dilution for immunofluorescence studies and purchased from Thermo Fisher Scientific.

Antibody	Company	Cat Number	Ab dilution	Ab conditions
active β-catenin	Millipore	#05-665	1:500	milk
AXIN1	CST	#2074	1:1000	BSA
AXIN2	CST	#76G6	1:1000	BSA
CaMK2D	Abcam	#ab181052	1:1000	BSA
CK1α	Bethyl Laboratories	#A301-991A-M	1:1000	BSA
CK1δ	CST	#12417	1:1000	milk
CK1ε	CST	#12448	1:1000	BSA
EGFR	CST	#4267	1:1000	BSA
FLAG-HRP	Sigma	#8592	1:5000	milk
GAPDH	CST	#2118	1:5000	BSA
GSK3-α	CST	#9315S	1:1000	BSA
GSK3-α/β	Santa Cruz	#sc-7291	1:1000	BSA
HA-HRP	Roche	2013819001	1:5000	milk
Lamin A/C	CST	#2032	1:1000	BSA
LC3	MBL	#PM036	1:1000	BSA
LRP6	CST	#C47E12	1:1000	BSA
Myc tag	Sigma	9E10 #M5546	1:1000	BSA
PAWS1 (residues 715-815 from human PAWS1)	DSTT	DU 33022	1:2000	milk
phospho-CaMK2 T286	Novusbiologicals	NBP1-64741	1:1000	BSA

Antibody	Company	Cat Number	Ab dilution	Ab conditions
phospho-LRP6 S1490	CST	#2568	1:1000	BSA
phospho-PAWS1 S365 *(CYALYKAKS*VDEIAKI)*	DSTT	RA0400 (3rd bleed)	1:500	milk
phospho-SMAD1 S463/S465	CST	#9516	1:1000	BSA
phospho-SMAD2 S465/S467	CST	#3108	1:1000	BSA
phospho-SMAD3 S423/S425	CST	#9520	1:1000	BSA
phospho-β-catenin S33/37/T42	CST	#9561	1:1000	BSA
phospho-β-catenin S45	CST	#9564	1:1000	BSA
SLC5A10	Abcam	#ab167156	1:1000	BSA
SMAD1 (residues 144-268 from human SMAD1)	DSTT	DU 19291	1:1000	milk
SMAD2/3	CST	#3102	1:1000	BSA
Ubiquitin	Dako	Z0458	1:1000	milk
Vimentin	CST	#5741	1:1000	BSA
α-tubulin	Thermo Fisher Scientific	#MA1-80189	1:10000	BSA
β-catenin	CST	#D10A8	1:1000	BSA

Table 2- 3 Antibodies used for Western Blotting in this thesis

Antibody	Company	Cat Number	Ab dilution
PAWS1	Abcam	ab121750	1:250
CK1α	Santa Cruz	sc6477	1:100
Phospho-SMAD1 S463/465	CST	#9511	1:1000

Table 2- 4 Antibodies used for immunofluorescence in this thesis

2.1.5 Primers

Human and *Xenopus* qPCR primers (Table 2-5) were designed using PerlPrimer software and generated by Thermo Fisher Scientific. For genomic sequence amplification, primers (Table 2-5) were designed with a melting temperature (T_m) of 60 ºC.

Target	Sequence (5' - 3')
AXIN2	F- TACACTCCTTATTGGGCGATCA
	R- TTGGCTACTCGTAAAGTTTTGGT
CYCLIN D1	F- GCTGCGAAGTGGAAACCATC
	R- CCTCCTTCTGCACACATTTGAA
CK1α	F- GAGGCAGCTATTCCGCATTC
	R- TGGGGAGAAACAAATGCTGC
GAPDH	F- TGCACCACCAACTGCTTAGC

Target	Sequence (5' - 3')
	R- GGCATGGACTGTGGTCATGAG
β-ACTIN	F- CCAACCGCGAGAAATGACC
	R- GGAGTCCATCACGATGCCAG
ID1	F- AGGCTGGATGCAGTTAAGGG
	R- GGTCCTTTTCACCAGCAAGCT
SIAMOIS	F- AACCACTTTCCACTCTCCCC
	R- GAAGTCAGTTTGGGTAGGGC
VNT1	F- GCATCTCCTTGGCATATTTGG
	R- TTCCCTTCAGCATGGTTCACC
MSX1	F- GCAGGAACATCACACAGTCC
	R- GGGTGGGCTCATCCTTCT
TGFBI	F- ATCACCAACAACATCCAGCA
	R- CCGTTACCTTCAAGCATCGT
WASF3	F- CATGCTGAAGACATATTTGGTGAG
	R- TCCTGTAGTGAGACCTCTTCC
MMP13	F- CAGTCTTTCTTCGGCTTAGAGG
	R- GGGTGTAATTCACAATTCTGTAGG
LGR5	F- TCTTCACCTCCTACCTGGACCT
	R- GGCGTAGTCTGCTATGTGGTGT
CCNA1	F- CCCTATGCTGGTAGATTCATCTC
	R- GTGCCTTATTTCAGCTTCCCT
AR	F- CCTGGCTTCCGCAACTTACAC
	R- GGACTTGTGCATGCGGTACTC
CHORDIN	F- AACTGCCAGGACTGGATGGT
	R- GGCAGGATTTAGAGTTGCTTC

Table 2- 5 qPCR primers used in this thesis

Target	Sequence (5' - 3')
PAWS1-GFP	F- TAGGGATAAAGACGGCTTCCCAGG
	R- TGTTGTAGTTGTACTCCAGCTTGT
PAWS1 luciferase reporter	F- CAAGCTGGGAGTACAACTACAACAGC
	R- GAGAGGAAGTCTCGGATGTTCTCC
PAWS1 luciferase reporter 1 (N-term)	F- CAGCAGTGCCCGGGCAGGCGGCGCCATGGAAGATGCCAAAAACATTAAGA
	R- TCTTAATGTTTTTGGCATCTTCCATGGCGCCGCCTGCCCGGGCACTGCTG
PAWS1 luciferase reporter 2 (C-term)	F- TGACGTGGAGGAGAATCCCGGCCCAGCtTTCagcCAaGTGCAGTGTCTGG
	R- CCAGACACTGCACtTGgctGAAaGCTGGGCCGGGATTCTCCTCCACGTCA

Table 2- 6 Genomic PCR primers used for sequencing in this thesis

2.1.6 siRNA oligonucleotides

All siRNA oligonucleotides were purchased from Dharmacon. The product references for siRNAs against human CK1α are J-003957-13, J-003957-14, J-003957-15 and J003957-16, against human CaMK2D siRNAs are J-004042-08, J-004042-09, J-004042-10, and J-004042-11, and against human CaMK2G siRNAs are J-004536-07, J-004536-08, J-004536-09 and J-004536-10.

2.1.7 Plasmids

All plasmids encoding mammalian expression constructs were cloned into pCMV5, pBABE-puro, pCS2+ or pcDNA/Frt/TO vectors with N-terminal or C-terminal FLAG, haemagglutinin (HA) or green fluorescent protein (GFP) tags. pcDNA-Frt/TO plasmids (Thermo Fisher Scientific) were used to generate stable doxycycline-inducible U2OS cell lines following manufacturer's protocol. pBABE-puro constructs were used to generate stable cell lines to achieve appropriate protein expression close to physiological levels.

For bacterial protein expression, appropriate constructs were cloned into pGEX6P1 vectors with N- or C-terminal GST- or 6xHis- tags.

All human-origin plasmids used in this thesis are listed in Table 2-7 and were generated by the DSTT (University of Dundee) cloning team. All DNA constructs used were verified by DNA sequencing, performed by DNA Sequencing & Services using Applied Biosystems Big-Dye Ver 3.1 chemistry on an Applied Biosystems model 3730 automated capillary DNA sequencer. The details of all plasmids used in this thesis, which are publicly available to the research community worldwide, can be found on ***https://mrcppureagents.dundee.ac.uk/***. Super 8x TOPFlash (#12456) and Super 8x FOPFlash (#12457) were gifts from Prof Randall Moon (University of Washington, USA) via Addgene. pCS2 NFAT-mCherry was provided by Kevin Dingwell (Crick Institute, London). Renilla-luciferase was obtained from the J. Massagué lab (MSKCC).

Xenopus Addgene constructs pCS2AxinMT (#16298) and pCS2 GSK3β 9SA (#16333) were a kind gift from Peter Klein, pCS2LRP6-m5 (#27283) from Xi He; pCS2 b-catenin-GFP (#16839) and xCK1ε D128N (#16726) from Randall Moon; CK1α (#23355) from William Hahn and David Root; and pCS2C-cadherin (#17023) from Barry Gumbiner. The ORFs of *Xenopus* FAM83G (xPAWS1; Image Clone MGC:98851 Source Bioscience), CK1δ (image clone #5571715 Source Bioscience), CK1ε (Image Clone #6316339, Source Bioscience) were cloned into pENTR-D-TOPO (Thermo Fisher

Scientific) vector and then transferred into pCS2_N-MT (myc-tag), pCS2_N-HA, pCS2_C-HA, pCS2_cmCherryHA destination vectors using LR clonase (Thermo Fisher Scientific).

2.1.8 Proteins

N-terminally GST-tagged proteins were expressed and affinity purified by the Protein Production Team (DSTT, University of Dundee). These include GST-CK1α (DU329), GST-CK1α D136N (DU28371), GST-CaMK2D and GST-β-catenin. FAM83A (DUF1669)-GST was provided by Dr Alex Bullock (Oxford). GST-PAWS1-6xHis and GST-PAWS1$^{F296A/F300A}$ were expressed and purified by the author as described below (2.2.3.10).

Protein	Vector	DU number
PAWS1 R52P-GFP	pBabe	28090
PAWS1 G640R-GFP	pBabe	28091
PAWS1 A34E	pBabe	28382
PAWS1 S356AE	pBabe	28380
PAWS1	pBabe	33460
PAWS1 F296A	pBabe	28044
PAWS1 F300A	pBabe	28045
PAWS1 F296A/F300A	pBabe	28046
PAWS1 S356A	pBabe	42136
PASW1S356E	pBabe	28380
PAWS1 G640R	pBabe	24545
PAWS1 R52P	pBabe	24544
PAWS1 D262A	pBabe	24843
PAWS1 GFP-KI sense gRNA	pBabe	48793
GFP	pBabe	33932
Frt/TO-PAWS1-GFP	pcDNA5	42816
Frt/TO-GFP	pcDNA5	41455
PAWS1 S614A-FLAG	pCMV	28377
FAM83G S356A-FLAG	pCMV	28378
FLAG-CK1γ	pCMV	5580
GFP-CAMK2D	PCMV5	28369
GFP-CAMK2G	pCMV5	28424
FLAG-PAWS1	pCMV5	33274
FLAG-PAWS1 F296A/F300A	pCMV5	28026
FLAG-PAWS1 F296A	pCMV5	28024
FLAG-PAWS1 F300A	pCMV5	28025
FLAG-TTBK2	pCMV5	28024
HA-CK1A	pCS2+	28216
HA-CK1A D136N	pCS2+	28217
HA-CK1ε	pCS2+	28190

Protein	Vector	DU number
HA-CK1δ	pCS2+	28189
HA-vector	pCMV5	44059
PAWS1-GFP donor	pEX-K4	48585
GST-PAWS1-6His	pGEXP-1	28293
GST-PAWS1 S614A	pGEXP-1	33321
GST-PAWS1 F296A/F300A	pGEXP-1	28049
GST-PAWS1 F296A	pGEXP-1	28047
PAWS1 GFP-KI antisense gRNA	pX335	48826
FLAG-CAMK2D	pcDNA	24985
FLAG-vector	pCMV5	44060
GST-CAMK2D	pGEX6P-1	33795

Table 2- 7 List of human plasmids used in this thesis

2.2 Methods

2.2.1 Mammalian cell culture

2.2.1.1 Cell culture

U2OS osteosarcoma, human embryonic kidney HEK293, retrovirus production HEK293-FT cells, HaCaT human keratinocytes, mouse fibroblast L-cells that stably overexpress Wnt3A (L3; ATCC: CRL-2647), or L cells (L; ATCC: CRL-2648) were grown in Dulbecco's Modified Eagle's Medium (DMEM) supplemented with 10% (v/v) FBS, 2mM L-glutamine, 100 units/ml penicillin and 100 μg/ml streptomycin. U2OS TRex cells were maintained in growth medium supplemented with 15 μg/ml blasticidin and 100 μg/ml zeocin. All cells were maintained at 37 ºC in a humidified atmosphere with 5% CO_2. Cell media was pre-warmed at 37 ºC prior to use and all procedures were carried out in aseptic conditions.

Cells were grown to 80-90% confluency in a 10 or 15 cm culture dish. For passaging the cells, the medium was aspirated from the dish, cells were washed once with sterile PBS and then incubated with 1-2 ml trypsin/EDTA at 37 ºC until all cells were detached from the culture dish. Cells were re-suspended in culture medium and cell clumps were broken by pipetting up and down several times. The cell number in the suspension was counted using Countess™ automated cell counter (Thermo Scientific) and then cells were seeded into new culture dishes at required densities.

2.2.1.2 Freezing/thawing cells

Confluent cells were detached from the culture dish using trypsin/EDTA and resuspended in growth medium. The cell suspension was briefly centrifuged (3 min, 1000

rpm) to pellet the cells. The medium was then aspirated and cells were re-suspended in cell freezing medium (Table 2-2). Cells were equally split into 1 ml cryovials and stored in a cell-freezing chamber (Mr. Frosty™ Freezing Container; ThermoFosher Scientific) for 24 h at -80 ºC. The cryovials were then transferred into liquid nitrogen for long-term storage.

To thaw cells, cryovials were placed in a 37 ºC water bath for 2 min and cells were re-suspended in 5 ml of culture medium, followed by brief centrifugation to pellet the cells. The freezing medium was aspirated off and cells were resuspended in 5 ml culture medium and transferred into a 6-cm dish.

2.2.1.3 Cell transfections

Transient cDNA plasmid transfections were carried out at ~60% confluence. For one 10 cm culture dish, 2.5 µg of plasmid DNA was mixed with 20 µl of PEI in 1 ml Opti-MEM. The mixture was immediately vortexed for 10 sec and left to stand for 20 min at room temperature. The DNA/PEI suspension was then added dropwise to the cells, which were incubated for 24-48 h post-transfection.

2.2.1.4 RNA interference (RNAi)

Cells were seeded at ~1 x 10^5 cells per well in 6-well cell culture dishes. Cells were transfected with 5, 10 or 20 nM of the relevant small interfering RNA (siRNA) oligonucleotides using 4 µl Lipofectamine RNAiMAX or TransFectin per well in Opti-MEM, as recommended by the manufacturers. After 16 h, the transfection medium was removed and replaced with normal DMEM culture medium. Cells were lysed 48 h post-transfection.

2.2.1.5 Retroviral infection

Stable cell lines were generated by retroviral infection in accordance with the appropriate biological safety regulations. To generate the retrovirus particles encoding the protein of interest, 6 µg of the pBabe-puro plasmid encoding the protein of interest was incubated with 3.8 µg of GAG/POL and 2.2 µg of vesicular stomatitis virus G (VSV-G) expression plasmids in 300 µl Opti-MEM. In a separate mix, 24 µl of PEI was added to 300 µl Opti-MEM. Both mixes were vortexed for 10 sec and incubated for 5 min at room temperature. Then, they were combined, vortexed for 10 sec and incubated for a further 15 min at room temperature. The transfection mix was added drop-wise to a 10-cm dish of ~70% confluent HEK293-FT cells. 16 h post-transfection, fresh medium was added to the cells. 24 h later, the retroviral medium was collected and filtered through

0.45 μm filters. Target cells (~60% confluent) were infected with the optimised titre of the retroviral medium, which was diluted in fresh medium containing 8 μg/ml polybrene (final) for 4 h to assist retroviral infection (Hesse et al., 1978). The retroviral infection medium was then replaced with fresh medium and 20 h later the medium was again replaced with fresh medium containing 2 μg/ml puromycin for selection of cells which had integrated the cDNA construct. Cell survival was dependent on the stable integration of the cDNA resistant marker. Successfully infected cells were used for experiments following complete death of non-infected cells placed in selection medium in parallel. The expression of protein of interest was confirmed by Western blotting.

2.2.1.5 Generation of doxycycline-inducible Flp-IN U2OS cells

Flp-IN TRex U2OS cell lines were maintained in growth medium supplemented with 15 μg/ml blasticidin and 100 μg/ml zeocin. The antibiotics zeocin and blasticidin were added for selection of the Flp recombination sites (FRT) and the doxycycline repressor sequence respectively. Flp-IN TRex U2OS cells grown in 10-cm dishes were transfected with 1 μg pcDNA5-Frt/TO vector encoding PAWS1-GFP or GFP only and 9μg pOG44 Flp recombinase encoding vector, diluted in 1 ml OPTIMEM and 20 μl of 1 mg/ml PEI. 24 h post-transfection, cells were cultured in medium containing 15 μg/ml blasticidin and 50 μg/ml hygromycin-B for 2-3 weeks (by replacing fresh medium every two days) until positive clones were selected, verified and expanded. Hygromycin B was added to ensure integration of the cDNA sequence of interest. Protein expression was induced with 20 ng/ml doxycycline for 16 hours prior to lysis and monitored by Western blotting and fluorescence microscopy.

2.2.1.6 Generation of PAWS1-GFP and PAWS1-luciferase reporter knock-in cell lines using the CRISPR/Cas9 system

Genome editing was performed using the CRISPR/Cas9 technology (Cong et al., 2013). The guide RNAs (gRNAs) used in this thesis are listed in Table 2-7. Cell transfections were carried out at ~60% confluence. For one 10 cm culture dish, 20 μl PEI was combined with 1 μg of the plasmid carrying sense gRNA and puromycin and 1 μg of plasmid carrying antisense gRNA and Cas9 D10A nickase and 3 μg of the donor vector in 1 ml Opti-MEM. The nickase cleaves one strand of the DNA complementary to gRNA; therefore, the generation of a double stranded break requires target-specific nicks on individual strands recognised by both sense and antisense gRNAs thereby reducing the potential off-target double stranded breaks. The DNA/PEI mixture was immediately vortexed for 10 sec and incubated for 20 min at room temperature, before being added

drop-wise to the cells. 24 and 48 h post-transfection, cells were cultured in medium containing 2 μg/ml puromycin for selection of transfected cells. Cells were then cultured in normal medium and the transfection was repeated, which was then followed by 2 days of puromycin selection. GFP-positive cells were then sorted by flow cytometry and single GFP-positive cells were plated on individual wells of two 96-well plates. Viable clones were expanded and the knock-in efficiency was analysed by immunoblotting cell extracts and DNA sequencing (Sections 2.2.3.7, 2.2.2.7).

2.2.1.6 Generation of Wnt3A-conditioned medium

L (control) and L3 (Wnt3A producing) cells were grown in 10 cm dishes to confluency and the culture medium was collected and sterile-filtered through 0.2 μm filters. 10 ml of fresh medium was added to cells for an additional 3 days. Then, the medium was collected, filtered, combined with the first batch of the collected conditioned medium and stored at 4 ºC. At this stage, cells were discarded.

2.2.1.7 Stimulation of cells with small molecules inhibitors and ligands

The small molecule inhibitors used in this thesis are included in Table 2-1. 10 mM stocks of small molecule inhibitors dissolved in DMSO was provided by the DSTT (University of Dundee), and stored in aliquots at -20 ºC. The commercial small molecule inhibitors were also dissolved in DMSO unless stated otherwise. The small molecule inhibitors were added directly into the cell culture medium and incubated for the desired time (indicated in the figure legends) at 37 ºC. An equivalent volume of DMSO was used as a control.

For ligands, typically a 1000-fold stock of the desired concentration was prepared in PBS and stored at -20 ºC. The solutions were added directly into the culture medium at the indicated concentrations. For Wnt3A stimulation, 100% of the conditioned medium was added directly to the cells for the time points indicated in the figure legends. For TGFβ and BMP ligands, cells were serum starved for 16 h at 37 ºC prior to treatment.

2.2.1.8 Luciferase reporter assays

PAWS1-luciferase reporter U2OS cells were seeded in 12-well plates and grown to 60-70% confluence, ensuring three replicates for each condition. Then, they were treated with the ligands as indicated in the figure legends for 1 h and were lysed with passive lysis buffer (Promega) after being washed twice with PBS. The lysis was allowed on a rocking platform for 15 min at room temperature. Extracts were collected and centrifuged at 14000 rpm for 5 min. To assay the luciferase reporter activity, the lysates

(20 µl) were transferred into each well of a 96-well plate (#655083, Greiner Bio-one) containing equal volume of 2 x Luciferase assay buffer. Data were obtained using Envision 2104 plate reader (PerkinElmer). The luciferase counts were normalised to the protein concentration and averaged. Plots and statistical analysis were performed using Prism6 software, as indicated in the figure legends.

2.2.1.8 Dual luciferase reporter assays

Cells (2 x 10^5) were plated in 6-well plates, ensuring three replicates for each condition. 24 h later, 500 ng of Super TOPflash or Super FOPflash and 10 ng of Renilla-luciferase plasmids were co-transfected using 4 µl PEI and 200 µl OPTI-MEM. For transient PAWS1 expression, 500 ng of pBabe PAWS1 was included to the transfection mix. 24 h later, cells were treated with L-conditioned medium or L-Wnt3A-conditioned medium or 20 mM LiCl for 16 h, washed twice with PBS and lysed in passive lysis. Firefly luciferase activity was measured as described in 2.2.1.7. Immediately after the measurement of the Firefly luciferase activity, 20 µl of Renilla assay buffer was added to each well of the 96-well plate and mixed by pipetting. Renilla luciferase activity was then measured using Envision 2104 plate reader. Firefly luciferase counts were normalized to Renilla luciferase counts, which represented a measure of transfection efficiency in each sample. Plots and statistical analysis were performed using Prism6 software, as indicated in the figure legends.

2.2.1.9 Cell lysis

Unless indicated otherwise, for general cell lysis, cells were washed twice with ice-cold PBS and scraped on ice in lysis buffer, supplemented with protease inhibitor cocktail as described (Table 2-2). Extracts were transferred to Eppendorf tubes and incubated on ice for 10 min before clarification by centrifugation at 14000 rpm for 20 min at 4 ºC.

When the chemical cross-linking reagent DSP was used, cells were lysed in lysis buffer with DSP (Table 2-2). Extracts were incubated at 4 ºC for 30 min before cross-linking reaction was quenched with Tris/HCl pH 7.5 at a final concentration of 0.2 M. Cell extracts were further incubated at 4 ºC for 30 min with vortexing every 5 min. Extracts were then centrifuged 14000 rpm for 20 min at 4 ºC and processed immediately or snap-frozen in liquid nitrogen and stored at -80 ºC.

For DNA and mRNA isolation, cells were processed using an RNA extraction kit according to the manufacturer's instructions (Qiagen DNeasy blood and tissue, and RNeasy kits respectively).

2.2.1.10 Cell proliferation assay

Cells were seeded in a 96-well plate in four different densities (10^3, 2 x 10^3, 3 x 10^3 and 4 x 10^3) and were left for 16 h at 37 ºC. Cell proliferation assay was carried out using the CellTiter 96® AQueous One Solution Cell Proliferation Assay, according to the manufacturer's instructions (Promega). Plots and statistical analysis were performed using Prism6 software with 2way ANOVA and post-hoc Bonferroni correction for multiple comparisons (Bland and Altman 1995).

2.2.1.11 Cell migration assay

U2OS cells (4-6 x 10^4) were plated into migration chambers (Ibidi) and grown to confluency (typically 18 hours), before being subjected to 2-dimensional migration assays by removing the silicone insert. Images were taken every 4 h by a Photometrics Cascade II CCD camera with Nikon NIS elements software. Wound closure was measured by Image J and reported as a percentage of closure relative to the starting wound size. Plots and statistical analysis were performed using Prism6 software with 2way ANOVA and post-hoc Bonferroni correction for multiple comparisons.

2.2.1.12 β-catenin stabilisation assay

Cells were stimulated with Wnt3A-conditioned medium or control-conditioned medium, as indicated. Cells were washed and collected in ice-cold PBS. Cell pellets were then resuspended in hypotonic lysis buffer (Table 2-2). Cell suspensions were incubated on ice for 30 min and passed multiple times through a 28G needle. Lysis of cells was controlled by checking under the microscope. Nuclear proteins, including the unlysed cells, were pelleted by centrifugation at 2000 rpm for 2 min at 4°C. The supernatant, that contained both cytoplasm and membrane proteins. was then centrifuged at 14000 rpm for 30 min at 4°C. The supernatant was collected and analysed further by SDS-PAGE followed by Western blotting (sections 2.2.3.5-7).

2.2.1.13 Xenopus laevis embryo manipulations

Xenopus laevis embryos were obtained by in vitro fertilization and staged according to Nieuwkoop and Faber (Nieuwkoop and Faber, 1994). Microinjections were carried out in 4% Ficoll in 75% Normal Amphibian Medium, and when they reached stage 8, they were transferred to 10% NAM. Embryos were injected with capped RNA

synthesized using SP6 mMessagemMachine kit (Thermo Fisher Scientific). For axis duplication assays, mRNA was injected into a single ventral blastomere at the 4- cell stage. Secondary axes were scored at stage 32 and were classed as complete if the second axis had eyes and a cement gland. Animal caps assays were performed as described previously (Jones et al., 1993). Dissociated animal caps were plated onto μ-Slide 8 well glass bottom chamber slides (#80827, Ibidi) or 12 well μChamber slides (#81201) coated with 3 μg/ml recombinant human E-cadherin protein (#8505-EC-050; R&D Systems) in 0.7 x Marc's Modified Ringers solution (MMR; 0.1 M NaCl, 2 mM KCl, 1 mM $MgSO_4$, 2 mM $CaCl_2$, 5 mM HEPES pH7.8, 0.1 mM EDTA). All experiments on *Xenopus* were performed by Kevin Dingwell (The Francis Crick Institute, London).

2.2.2 General molecular biology

2.2.2.1 Plasmid transformation, amplification and isolation

Competent *E. coli* DH5α (plasmid isolation) or BL21 (protein expression) cells, expanded and maintained by the DSTT, (University of Dundee), were thawed on ice and 1 μl of plasmid DNA (~10 ng) was added to the cells, followed by incubation for 30 min on ice. Cells were then heat-shocked at 42 ºC for 1 min to facilitate DNA uptake and placed on ice for 5 min. 500 μl of LB medium was added to the cells and they were placed in a 37 ºC thermomixer for 30 min to recover. Subsequently 50 μl was transferred onto an LB agar plate containing 100 μg/ml ampicillin or 50 μg/ml kanamycin as appropriate and left overnight in a 37 ºC incubator. To amplify the plasmids, one transformed colony was used to inoculate 200 ml LB medium containing 100 μg/ml ampicillin or 50 μg/ml kanamycin as appropriate for 16 h on a shaking incubator at 37 ºC. The cells were pelleted by centrifugation (3000 rpm, 20 min, 4 ºC) and the plasmid DNA was extracted using the Qiagen DNA Midi or Maxi kit according to the manufacturer's instructions.

2.2.2.2 Measurement of DNA and RNA concentration

Using a NanoDrop® spectrophotometer (Thermo Scientific) the absorbance of isolated DNA or RNA in aqueous solution was measured at 260 nm, after previous calibration with nuclease-free water**.**

2.2.2.3 Agarose gel electrophoresis

The size and the purity of DNA products were assessed by electrophoresis on 1% agarose gels. Each gel contained a 1:10000 dilution of SYBR Safe nucleotide gel stain. Gels were submerged in 1 x TAE running buffer. DNA (0.5 μg) was loaded onto the gel together with 1 x DNA loading dye. 0.5 μg of a 1 kbp DNA ladder was used as a marker.

Gels were run at 100 V for 30 min. The stained nucleotide complexes were visualised using a UV transilluminator.

2.2.2.4 Real time quantitative reverse transcription PCR (qRT-PCR; qPCR)

Total RNA was isolated from cells using the QIAGEN RNeasy kit. cDNA was made from 1 µg of isolated RNA using the SuperScript cDNA kit (BioRad) according to the manufacturer's protocol. qPCR reactions were performed in triplicates in 12 µl reaction final volume for 96-well plates or in quadruplicates in 10 µl reaction final volume for 384-well plates (Biorad). Each reaction included 0.5 µM forward primer, 0.5 µM reverse primer, 50% SsoFast EvaGreen Supermix (BioRad), and cDNA equivalent to 1 ng/µl of RNA in a CFX96 or CFX384 real-time system qPCR machine (BioRad). All primers were designed using PerlPrimer and purchased from Thermo Fisher Scientific. The data were normalized to the geometrical mean of the house-keeping gene GAPDH or β-actin and analysed with the $2^{-\Delta\Delta Ct}$ method for comparing relative gene expression results in Microsoft Excel (Livak and Schmittgen 2001). Plots and statistical analysis were performed using Prism6 software with 2way ANOVA and post-hoc Bonferroni correction for multiple comparisons.

2.2.2.5 PCR

DNA was isolated from cells using a DNeasy Blood and Tisssue Kit (Qiagen) according to the manufacturer's instructions. PCR was performed on a PCR Thermal Cycler (PT-200; MJ Research) using the KOD Hot Start DNA Polymerase kit (Toyobo) as per the manufacturers protocol. Each 50 µl reaction included 25 mM $MgSO_4$, dNTPs (2 mM each), 10 µM each of forward and reverse primers, 200 ng template DNA, 1 U KOD Hot Start DNA Polymerase, 3 µl DMSO and 1 X buffer for KOD Hot Start DNA Polymerase. The PCR products were assessed by electrophoresis on 1% agarose gels.

2.2.2.6 Subcloning of PCR products

PCR products were cloned into a pSC-B vector using the StrataClone Blunt PCR Cloning Kit (Agilent) as per the manufacturer's instructions. Each reaction contained 3 µl StrataClone Cloning Buffer, 2 µl of a 1:10 dilution of the PCR product and 1 µl StrataClone Vector Mix. StrataClone SoloPack Competent Cells (Agilent) were then transformed with the vector as per the manufacturer's instructions. Following transformation, 10 µl culture samples were plated on LB plates containing 2% X-Gal. Plates were inverted and incubated for 16 h at 37°C. White colonies were subsequently picked and used to inoculate a 4-ml culture of LB medium which was grown for 16 h at

37°C. Plasmid DNA was then purified using a Plasmid Mini Kit as per the manufacturer's instructions.

2.2.2.7 DNA sequencing

DNA plasmid sequencing was performed by the DNA Sequencing Service (University of Dundee) using Applied Biosystems Big-Dye v 3.1 chemistry on an Applied Biosystems model 3730 automated capillary DNA sequencer, using appropriate sequencing primers (Table 2-6).

2.2.2.8 DNA mutagenesis

DNA mutagenesis of all plasmids (Table 2-7) was performed by the DSTT (University of Dundee) cloning team using the QuikChange site directed mutagenesis method (Stratagene) with KOD polymerase (Novagen). All mutations were verified by DNA sequencing**.**

2.2.3 General biochemistry

2.2.3.1 Measurement of protein concentration

Protein concentration was determined by the Bradford method (Bradford, 1976). In principle, this is a colourimetric protein assay based on an absorbance shift from 465 nm to 595 nm once Coomassie dye binds to proteins in acidic medium. A standard curve was generated by plotting absorbance against a serial dilution of BSA standards (0.0625 mg/ml – 1 mg/ml). Samples were diluted in water by a factor of 10 and were added to a 96-well plate in triplicates (5 µl) along with 200 µl of Bradford reagent and a blank probe. After incubation for 5 min at room temperature, absorbance at 595 nm was measured with a VersaMax microplate reader and SoftMax Pro v4.8 software (Molecular Devices). The protein concentration of each sample was calculated from the average absorbance by reference to the standard curve. Because the colour response of the Coomassie reagent is non-stoichiometric with increasing protein concentration, a standard curve was run with each assay.

2.2.3.2 Immunoprecipitation (IP)

Cleared cell extracts were further pre-cleared to minimise unspecific binding of proteins to the solid phase resins by incubating with agarose or protein-G Sepharose beads for 1 hour at 4 °C prior to immunoprecipitation (IP). The pre-cleared extracts (0.5-1 mg protein for Western blot applications or 10 mg protein for mass spectrometry applications) were then mixed with FLAG- or HA-agarose beads (Sigma-Aldrich), GFP-Trap agarose beads (Chromotek) or antibody/IgG-coupled to protein G-Sepharose

or Agarose beads for up to 4 h at 4 ºC on a rotating platform. The flow-through was retained for Western blot analysis to assess IP efficiency and the beads were washed twice in lysis buffer containing 250 mM NaCl, and once in buffer A. For Western blot analysis, beads were resuspended in 1 x SDS sample buffer (typically in a final volume of 40 µl). IP samples, as well as equal amounts of flow-through and input samples reduced in SDS sample buffer were heated at 95 ºC for 5 min prior to SDS-PAGE.

2.2.3.3 Covalent coupling of antibodies to protein G-Sepharose

1 µl of Protein G-Sepharose beads per µg of antibody were incubated for 1 h at 4°C with gentle agitation. The beads were then washed five times with 10 volumes of 0.1 M sodium borate, pH 9. Beads were resuspended in 20 mM dimethyl pimelimidate dihydrochloride (DMP) in 0.1 M sodium borate, followed by gentle agitation for 30 min at room temperature. After repeating the final step one more time, beads were washed four times with 10 volumes of 50 mM glycine pH 2.5 to strip the beads of any antibody that had not been coupled covalently. Next, beads were neutralized by washing twice for 30 min at room temperature with 0.2 M Tris-HCl pH 8. Beads were resuspended in PBS containing 0.01% (v/v) NaN_3 and stored at 4 °C.

2.2.3.4 Subcellular fractionation

For nuclear and cytoplasmic extraction, a NE-PER kit from Thermo Scientific (#78833) was used in accordance with the manufactures' instructions. For membrane and cytoskeletal protein extraction a compartment protein extraction kit from Merck (#2145) was used according to the manufactures' instructions. The lysis buffers were supplemented with protease inhibitors (Roche). Fractions were reduced in SDS sample buffer as stated above.

2.2.3.5 Separation of proteins by SDS-PAGE

SDS-PAGE was carried out using either the NuPAGE Bis-Tris Electrophoresis System (Thermo Fisher Scientific) or the ATTO vertical polyacrylamide slab gel electrophoresis system (ATTO Corporation, Tokyo, Japan). Protein samples were prepared by adding 1 x Sample buffer and denatured by heating at 95°C for 5 min. Samples were loaded onto the pre-cast NuPAGE Novex gel using a micropipette equipped with gel-loading tips. Pre-Stained Standards with apparent molecular weights of 250, 150, 100, 75, 50, 37, 25, 20, 15 and 10 kDa were used as markers. Electrophoresis was carried out in an XCell SureLock Mini-Cell filled with 1 x MOPS Running Buffer. Electrophoresis was performed at constant voltage of 200 V for 50 min.

The ATTO system did not use pre-cast gels and therefore, it was necessary to prepare the minigels prior to electrophoresis. Slab minigels (90 mm x 80 mm x 1 mm) were poured between glass plates. The separating (resolving) gel was typically prepared at an acrylamide concentration of 10% and thus contained 375 mM Tris-HCl pH 8.6, 10% (w/v) acrylamide mix (1:29 molar ratio of bisacrylamide:acrylamide) and 0.1% (w/v) SDS. Polymerisation was initiated by addition of 0.075% (w/v) APS and 0.1% (v/v) TEMED and pouring the mix onto the gel assembly unit. 100% isopropanol was gently pipetted on top of the gel to level the surface and extract out bubbles. The separating gel was allowed to polymerise for at least 20 min at room temperature. After polymerisation was complete, the isopropanol was poured off completely and the stacking gel was prepared and poured directly onto the surface of the polymerised resolving gel. A clean Teflon comb was immediately inserted and the stacking gel was allowed to polymerise for around 30 minutes at room temperature. Gels were introduced into the ATTO electrophoresis chamber, in which both the upper and lower buffer tanks were filled with SDS-PAGE running buffer. 5 µl of Precision Plus Protein Standards (BioRad) and 20 µg (unless stated otherwise) of protein extracts in SDS sample buffer were loaded in a similar manner to that described for the NuPAGE system. Electrophoresis was performed at constant voltage of 150 V for 90 min.

2.2.3.6 Coomassie Blue Staining

After SDS-PAGE gels were washed in deionised waster and incubated in 20 ml of InstantBlue (Expedeon) on a rocking platform for 10 min – 16 h. Following this the gel was repeatedly washed in deionised water to de-stain.

2.2.3.7 Immunoblotting (Western blotting)

Following their resolution by SDS-PAGE, protein samples were transferred onto PVDF membranes, which had been activated in 100% methanol immediately prior to transfer assembly. The transfer was set at 80 V for 80 min in BioRad transfer apparatus filled with transfer buffer and a cooling block.

To visualise protein transfer efficiency in a reversible manner, PVDF membranes were immersed in Ponceau S staining solution for 2 min. The membranes were rinsed with dH_2O to remove background staining and the bands were visualised. The membranes were cut with a scalpel into smaller strips, so that proteins of different molecular weights could be probed at the same time, if necessary. Membranes were further washed with dH_2O until Ponceau S staining disappeared completely.

Membranes were then incubated in blocking solution (Table 2-2) for 30 min at room temperature on a rocking platform or orbital shaker. Blots were then incubated with primary antibody solution (Table 2-2) for 1 h at room temperature or 16 h at 4 ºC. Membranes were washed three times for 10 min in TBS-T before being incubated with the HRP-conjugated secondary antibodies (typically 0.2 μg/ml) in blocking solution for 1 h at room temperature. After washing as before in TBS-T, membranes were incubated with enhanced chemiluminescence (ECL) reagent for 1 min, placed in an X-ray cassette and exposed to X-ray films under safelight conditions. X-ray films were developed using a Konica automatic developer.

2.2.3.8 Immunofluorescence microscopy

U2OS cells were seeded onto 22 x 22 mm sterile coverslips in 6-well culture plates. Cells were washed in PBS before fixation with 4% paraformaldehyde for 10 min at room temperature. Paraformaldehyde was removed and the cross-linking reaction was quenched by washing twice with IF quenching buffer (10 min each wash). Coverslips were then washed with PBS and permeabilised with 0.5% Triton X-100 in PBS for 5 min. Subsequently, coverslips were washed with IF blocking solution (Table 2-2) and incubated in IF blocking solution for 30 min, to reduce non-specific epitope binding. Primary antibodies were prepared in IF blocking solution (1:250 for anti-PAWS1 Abcam, ab121750 and 1:100 for anti-CK1α, Santa Cruz, sc6477) and added directly into coverslips for 1 h. Cells were washed with 0.1% Triton X-100 in PBS, and incubated in the dark, with Alexa Fluor conjugated secondary antibodies (ThermoFisher Scientific), at a dilution of 1:500 in IF blocking solution, for 30 min at room temperature. Coverslips were then subjected to three 10 min washes in IF blocking solution and in the final wash, DAPI (1 μg/ml) was added onto the coverslips. Then, coverslips were dipped into sterile ddH_2O and mounted onto glass slides with Vectashield mounting medium. Once coverslips were completely dry, they were imaged using a DeltaVision system (Applied Precision) with an immerse-oil x63 objective lens. Z-series were collected at 0.2 μm intervals, and deconvolved using SoftWoRx (Applied Precision). Images were processed using ImageJ and OMERO software. The images presented correspond to one stack from the de-convolved three-dimensional images.

For the analysis of SMAD signalling in *Xenopus*, by Dr Kevin Dingwell, dissociated animal cap cells were fixed in MEMFA (0.1M MOPS pH 7.4, 2 mM EGTA, 1 mM MgSO4, 3.7% formaldehyde) for 10 min at room temperature, followed by three 5 min washes in PBS. Cells were permeabilised with 0.5% Triton X-100 for 5 min followed

by three 5 min washes with PBS and then blocked in *Xenopus* IF blocking solution (PBS, 0.1% Tween 20, 1% BSA, 10% goat serum) for 1 h at room temperature. Primary (anti-P-Smad1, CST #9511), and secondary antibodies (anti-rabbit Alexa568, Invitrogen #A11031) were used at 1:1000 in *Xenopus* IF blocking solution, each for 1 h, and then washed three times of 5 min each with PBS/0.1% Tween 20. Cells were mounted using Prolong Gold Antifade Mountant with DAPI (Thermo Fisher Scientific, #P36935). Images were captured on Zeiss LSM710 confocal microscope controlled by ZEN Black 2012software. Post-acquisition analysis was performed using ZEN Black, Zen Blue 2012 and ImageJ software packages.

2.2.3.9 NFAT assay

Cells were seeded om coverslips on 6-well plates and transfected with 500 ng of the plasmid encoding for NFAT with a C-terminal mCherry tag. 24 h later, cells were treated with 250 nM of the calcium ionophore A23187 or the equivalent volume of DMSO as a control. Cells were fixed and analysed by fluorescence microscopy for NFAT localisation as described in 2.2.38.

2.2.3.10 Protein expression and purification from E. coli

The GST-PAWS1-6xHis was expressed in *E. coli BL21* cells. A single bacterial colony transformed with pGex6T vector encoding GST-PAWS1-6xHis was inoculated in 3 ml LB medium (supplemented with 100 μg/ml ampicillin) for 8 hours at 37 °C with shaking at 220 rpm. 200 μl of the starter culture was used to inoculate 100 ml LB medium containing 100 μg/ml ampicillin and grown overnight at 37 °C at 220 rpm. The following day, 50 ml of the overnight culture was used to inoculate 1 L of LB medium containing 100 μg/ml ampicillin in a 2-litre flask. The cell suspension was incubated at 37 °C with shaking at 200 rpm until OD_{600} reached 0.6. Protein expression was induced with IPTG to a final concentration of 50 μM. The cell culture was incubated overnight at 16 °C with shaking at 200 rpm. Cells were harvested by centrifugation at 4000 x g for 20 min at 4 °C. The cell pellet was resuspended in bacterial lysis buffer (10 ml per gram of pellet) (Table 2-2). Cells were lysed by sonication and lysates were clarified by centrifugation at 30000 x g (JA-30.50 Ti rotor) for 30 min at 4 °C. The supernatant was filtered through a 0.2 micron filter and incubated with pre-equilibrated Ni-NTA resin (1ml per litre of culture) at 4 °C for 1 h with gentle agitation. The beads were then transferred to a 20 ml BioRad column and washed with His-tag protein binding buffer (~10 column volumes). Protein was eluted with His-tag protein elution buffer (Table 2-2) and collected in 1 ml

fractions. Peak protein concentration was determined by Bradford. Peak fractions were pooled and, dialyzed overnight at 4 ºC in His-tag protein dialysis buffer.

The recovered sample was further purified using Glutathione (GSH)-Sepharose resin (1ml per litre of culture) at 4 °C for 1 h with gentle agitation. The beads were then transferred to a 20 ml BioRad column and washed with GST-tag protein wash buffer (Table 2-2). Beads were washed until OD_{595} was at or near zero. Protein was eluted with GST-tag protein elution buffer (Table 2-2). 1 ml fractions were collected and the fractions for which OD_{595} was greater than 0.2 were pooled together. The purified product was analysed on a 10% SDS gel followed by Coomassie staining. Purified proteins were stored at -80 ºC. For proteins expressed as GST-tagged only, the GST purification procedure was performed as described here.

2.2.3.11 Removal of the GST tag from bacterially-expressed protein

The purified GST-tagged protein was mixed with GSH-Sepharose resin (1 ml packed beads per 500 µg of protein) for 3 h at 4 ºC with gentle agitation. After centrifugation at 1000 rpm for 1 min at 4 ºC, the beads were washed in 10 ml of binding assay buffer (Table 2-2). Beads were then re-suspended in 2 ml of binding assay buffer containing 500 µg of PreScission GST-tagged Protease for 16 h at 4 ºC. PreScission Protease is a fusion protein of the GST and human rhinovirus 3C protease (Walker, Leong et al. 1994) which specifically recognises the amino acid sequence Leu-Glu-Val-Leu-Phe-Gln/Gly-Pro, cleaving between the Gln and Gly residues (Cordingley, Callahan et al. 1990). Samples were filtered through a Spin-X column by centrifugation at 14000 rpm for 5 min to remove both the GST moiety of the fusion protein and the GST-tagged PreScission Protease, which both remained bound to the column while the protein of interest eluted in the column flow-through. The flow-throughs were then analysed by SDS-PAGE and Coomassie staining.

2.2.4 In vitro assays

2.2.4.1 In vitro kinase assays

25 µl reactions were set up using 200 ng of the kinase and 2 µg of substrate in the kinase assay buffer (Table 2-2) containing 0.1 mM $^{\gamma 32}$P-ATP (~500 cpm/pmol). Reactions were performed at 30 °C for 30 min and stopped by adding 10 µl SDS sample buffer with 5% β-mercaptoethanol and heating at 95°C for 5 min. Samples were resolved by SDS-PAGE and gels were stained with InstantBlue Coomassie reagent and dried. Radioactivity was analysed by autoradiography by exposing the dried gel on Hyperfilm

for different lengths of time. For long exposures, the cassette was placed in -80 ºC to enhance the autoradiographic signal. Films were developed using a Konica automatic developer.

For kinase assays against a substrate peptide (CK1tide, DSTT EP5630), reactions were set up in triplicates, in a final volume of 50 µl and they were stopped by spotting 40 µl of sample onto p81 phosphocellulose papers (2x2 cm; Whatman), which were immediately immersed in 75 mM phosphoric acid (5 ml of orthophosphoric acid per assay sample), being stirred continuously with a magnetic stirrer. The p81 papers were washed 3 times (5 min each wash) with 75 mM phosphoric acid until the $^{\gamma 32}$P-ATP that was not incorporated into the peptide was washed off. After the final wash, papers were rinsed briefly in acetone to remove the phosphoric acid and then dried with a hair dryer. Papers were then transferred into an Eppendorf tube and radioactivity was measured in a scintillation counter (PerkinElmer). In parallel, radioactivity of 1 µl aliquots of the stock 1 mM $^{\gamma 32}$P-ATP was measured to determine the specific radioactivity (cpm/pmol) of the $^{\gamma 32}$P -ATP so that the stoichiometry of the reaction could be determined.

2.2.4.2 In vitro protein binding assay

Purified GST-PAWS1-6xHis and GST-PAWS1$^{F296A/F300A}$ were mixed with GSH-Sepharose beads (20 µg of recombinant protein per ml of packed beads) for 3 h at 4 ºC with gentle agitation. Samples were washed twice in binding assay buffer (Table 2-2). Then, 200 ng of recombinant GST-cleaved CK1α was added to the beads followed by incubation for 1 h at room temperature. The assay samples were washed three times with binding assay buffer (Table 2-2) before being analysed by SDS-PAGE and Coomassie staining.

2.2.5 Mass spectrometry

2.2.5.1 Preparation of samples for mass spectrometry

For mass spectrometry analysis, U2OS cells expressing the protein of interest, were lysed in lysis buffer with DSP as described in 2.2.1.9. Extracts were incubated with Protein A-agarose beads for 1h on a rotating platform at 4 ºC to pre-clear non-specific proteins binding to the solid phase. Pre-cleared extracts were then filtered through a 0.45 micron filter and then extracts (10 mg of protein) were incubated with 10 µl GFP-Trap packed beads for 16 h at 4 ºC. The beads were washed twice in lysis buffer supplemented with 500 mM NaCl and once with Buffer A. IPs were denatured in LDS sample buffer supplemented with 0.1 M DTT, incubated for 1 h at 37 ºC to reverse the cross-linking

reaction and heated at 95 ºC for 5 min. The samples were filtered through a Spin-X column by centrifugation at 14000 rpm for 5 min, and the supernatant loaded onto 4-12% gradient precast SDS gels and separated by gel electrophoresis. Gels were stained with InstantBlue Coomassie reagent for 15 min, followed by destaining with dH_2O until the background stain was invisible.

2.2.5.2 In-gel digestion of proteins for mass spectrometry

To minimise contamination, all steps from this point onwards were carried out under a laminar flow hood (Model A3VB, Bassaire Limited). Disposable scalpels were used to excise the protein bands of interest from Coomassie-stained SDS-PAGE gels. Gel pieces were cut into 1 mm cubes and transferred into LoBind 1.5 ml Eppendorf tubes. After washing once in water, gel pieces were shrunk in acetonitrile (ACN), re-swollen in 50 mM Tris-HCl pH 8 and shrunk again in ACN (5min). The shrinking-swelling steps were repeated once more followed by reduction of the samples in 5 mM DTT/50 mM Tris-HCl pH 8 for 20 min at 65 °C. The proteins were then "in gel" alkylated with 50 mM iodoacetamide/50 mM Tris-HCl pH 8 for 20 min at room temperature. The gel pieces were then shrunk in ACN for 5 min, re-swollen in 50 mM Triethylammonium bicarbonate and shrunk again in ACN. Then the proteins were digested using 50 mM Triethylammonium bicarbonate containing 5 µg/ml Trypsin for 30 min at 30 °C followed by 3 h incubation at 37 °C. Then an equivalent volume of ACN was added to the digest for 15 min and the supernatants were collected. Gel pieces were re-swollen in 0.1% TFA and peptides were extracted twice with ACN until gel pieces were completely white and had shrunk. The supernatants were dried using Speed-Vac, before being submitted for analysis by the mass spectrometry team.

2.2.5.3 Peptide analysis by liquid chromatography-tandem mass spectrometry

The digested peptides were reconstituted in HPLC grade 5% ACN and 0.1% formic acid and injected into a nano liquid chromatography system coupled to a Thermo LTQ Orbitrap mass spectrometer. Raw files were converted into a list of identified peptides coupled with information given by the precursor intensity of the identified peptides and submitted to the in-house Mascot server. Data was searched against the International Protein Index human database with variable modifications allowing for phosphorylation of Serine/Threonine or Tyrosine residues and for Methionine oxidation, dioxidation or carboxy modification. Liquid chromatography-tandem mass spectrometry (LC-MS-MS) analysis was performed by Dr David Campbell, Robert Gourlay and Joby

Varghese (University of Dundee). Data analysis was performed using Scaffold 4.3 (Proteome software).

2.2.5.4 Identification of phosphorylated PAWS1 residues

[γ^{32}P]-phosphorylated PAWS1 (see section 2.2.4.1) was digested as described above. The dried peptides were reconstituted to a final concentration of 5% ACN/0.1% TFA and injected into a C_{18} column equilibrated with 0.1% TFA with a linear ACN/0.1% gradient at a flow rate of 0.2 ml/min and 100 µl fractions were collected. The major eluted [γ^{32}P]-peptides were analysed on OrbiTrap Velos LCMS system. To determine the phosphorylated residue in each [γ^{32}P]-labelled peptide, the peptides were immobilised on a Sequelon-AA membrane and subjected to solid-phase Edman degradation as described previously (Campbell and Morrice 2002). HPLC, mass spectrometry and Edman degradation were performed by Robert Gourlay (University of Dundee).

2.2.5.5 Phosphoproteome sample preparation and MS analysis

2.2.5.5.1 Protein extraction and digestion

Cells were stimulated with Wnt3A-conditioned medium or control-conditioned medium when they reached ~90% confluence, for 3 h. Before lysis, cells were washed once in ice-cold PBS and once in ice-cold PBS supplemented with the phosphatase inhibitors PhosSTOP (Roche), 2 mM Sodium orthovanadate 10 mM Na B glycerophosphate, 5 mM Na pyrophosphate, 50 mM NaF. Each 15-cm dish was lysed by scraping in 500 µl of Urea lysis buffer. Extracts were collected in Eppendorf tubes and sonicated (40% amplitude, 25 intervals of 5 sec each) on ice. Protein concentration was determined by the BCA assay (Thermo Fisher Scientific). Cell extracts were prepared at a final concentration of 3 mg/ml and were then reduced with 5 mM TCEP. The reduced cysteine residues were alkylated in the dark with 14 mM iodoacetamide before trypsin-digestion for 3 h at 37 ºC. Digests were acidified with 0.1 % (v/v) trifluoracetic acid (TFA) pH 2 for 15 min at 37 ºC. The acidified digests were centrifuged at 10,000 g for 10 min. The supernatant were subjected to C18 solid-phase extraction (SPE) (Sep-Pak) for further cleaning.

2.2.5.5.2 Phosphopeptide enrichment

The desalted peptides were resuspended in 1 ml of 2 M lactic acid/50% acetonitrile (ACN) and centrifuged at 15000 x g for 20 min. Supernatants were transferred to an Eppendorf tube containing 18 mg of titanium dioxide (TiO_2) beads (GL sciences, Japan) and vortexed for 1 h at room temperature. Beads were washed three times (10 min

per wash) with 2 M lactic acid/50% ACN and subsequently dried using a vacuum concentrator with a cold trap. Phosphopeptides were eluted twice in 150 µl of 50 mM ammonia solution (NH_4OH) (pH 10). The combined eluates were dried using a vacuum concentrator with a cold trap and then cleaned up using a C18 StageTip desalting (3M Empore™).

2.2.5.5.3 Tandem Mass Tagging (TMT) Labelling

TMT labelling for the enriched phosphopeptides was performed using the 6-plex TMT reagent (Thermo Fisher Scientific) according to the manufacturer's protocol Briefly, dried peptides were resuspended in 100 µl of 200 mM HEPES pH 8, vortexed and centrifuged at 4000 rpm for 3 min. TMT reagents (0.8 mg) were dissolved in 41 µl ACN and added to the peptides (12 µl per sample). After 1 h incubation at room temperature, reactions were quenched by adding 8 µl of 5% hydroxylamine followed by a 30-min incubation at room temperature. Labelled peptides were combined, acidified with 20 µl of 20% formic acid (FA) pH 2 and concentrated with C_{18} SPE on Sep-Pak cartridges (Waters).

2.2.5.5.4 LC-MS/MS analysis

TMT labelled phoshopeptides were dissolved in 3% ACN/0.1% TFA and then loaded on C_{18} trap column with 3 % ACN/0.1%TFA at a flow rate of 5 µl/min. Peptide separations were performed over EASY-Spray column (C18, 2 µm, 75 mm × 50 cm) with an integrated nano electrospray emitter at a flow rate of 300 nl/min. The LC separations were performed with a Thermo Dionex Ultimate 3000 RSLC Nano liquid chromatography instrument. Peptides were separated with a 220-min segmented gradient as follows: 3%–25% buffer B in 175 min, 25%–35% buffer B for 30 min, 35%–99% buffer B for 5 min, followed by a 10 min 99% wash. Eluted peptides were analyzed on an Orbitrap Fusion Tribrid platform with instrument control software version 3.0. The mass spectrometer was operated in data-dependent most intense precursors Top20 mode. The survey scan was acquired from m/z 400 to 1600 with a resolution of 120,000 resolving power with AGC target 200,000. The maximum injection time for full scan was set to 100 ms. The MS/MS analyses were performed by 1.6 m/z isolation with the quadrupole, normalised HCD collision energy of 37.5% and analysis of fragment ions in the Orbitrap using 60,000 resolving power with auto normal range scan starting from m/z 110. Dynamic exclusion was set to 35 seconds. Monoisotopic precursor selection was set to peptide, maxium injection time was set to 110 msec. AGC target was set to 50,000. Charge states unknown

and 1 or higher than 7 were excluded. LC-MS/MS was performed by Dr Julien Peltier (previously University of Dundee; currently Newcastle).

2.2.5.5.5 Data processing and analysis

Proteome Discoverer was used for processing the collected MS raw data. The raw data were searched against Uniprot human database (70,947 entries, downloaded on March 10, 2017) using MaxQuant (Cox and Mann, 2008). The precursor and fragment mass tolerances were set to 10 ppm and 0.01 Da, respectively. A maximum missed cleavages for trypsin digestion was set to 2. The cysteine carbamidomethylation and TMT modified N-term and Lysine residue were set as fixed modification, while methionine oxidation, asparagine and glutamine deamidation were set as variable modifications. False discovery rate (FDR) of peptide spectrum matches and identified results were validated by the Percolator algorithm at 1% based on q-values. The phosphopeptides were quantified using the intensity of TMT reporter ions. Data were further analysed with Perseus software and figures were made using Prism6. Analysis was performed by Dr Julien Peltier (previously University of Dundee; currently Newcastle).

2.2.6 Statistical analysis

All experiments have a minimum of three biological replicates. Additionally, luciferase qPCR experiments have three or four technical repeats for each biological replicate, respectively unless stated otherwise. Data are presented as the mean with error bars indicating the standard error of the mean, unless stated otherwise in figure legends. For correlation analyses, Pearson's coefficient was used, as long as data were normally distributed. Statistical significance of differences between experimental groups was assessed with Student's t-test or ANOVA with post-hoc Bonferroni Correction, unless stated differently in figure legends, using Prism6 software. Differences in means were considered significant if $p<0.05$. All Western blots and IF images are shown as representatives. Quantification of the western blots was performed using ImageJ software.

3. PAWS1 controls Wnt signalling through association with CK1α

3.1 Introduction

At the beginning of this research project, the only information on the molecular function of PAWS1 was limited to its characterisation by the Sapkota lab as a novel mediator of the non-canonical BMP signalling pathway. BMP and Wnt signalling pathways play crucial roles in shaping the body axis during embryogenesis (De Robertis and Kuroda 2004). Because PAWS1 was established as a SMAD1 interactor and was shown to be phosphorylated by BMPR1 in response to BMP, its potential role during *Xenopus* embryonic development was investigated. Remarkably, microinjection of PAWS1 mRNA at the early blastula (4-cell) stage of the *Xenopus* embryos led to the formation of a complete secondary body axis at the tadpole stage (Fig 3-1), whereas PAWS1 depletion with PAWS1 morpholinos caused embryonic lethality. Such phenotypes are mainly associated with either inhibition of BMP signalling or activation of the Wnt signalling pathway (see 1.4). The observations that PAWS1 played a significant role in dorsoventral patterning during embryogenesis prompted the investigation into the molecular role of PAWS1 in BMP and Wnt signalling.

The activation of BMP signalling results in changes in gene transcription via a signalling cascade, which involves the phosphorylation of SMAD1/5/8 proteins. As mentioned in the Introduction, PAWS1 did not appear to influence the canonical BMP signalling pathway, as the BMP-induced phosphorylation of SMAD1 and most of the BMP-target gene transcription was unaffected by knock-down or overexpression of PAWS1 (Vogt, Dingwell et al. 2014). However, since the previous research relied on PAWS1 overexpression or siRNA technologies, one of the aims of this chapter is to validate these findings in PAWS1 knockout cells.

Wnt signalling, which encompasses a complex network of many components and modulators, plays a fundamental role in regulation of embryogenesis, organogenesis and adult tissue homeostasis. Perturbation of different components leading to imbalances in the Wnt signalling cascade result in tumorigenesis (see 1.5.3.5). A hallmark of the Wnt signalling activation is the accumulation of non-phosphorylated β-catenin in the cytosol and its translocation in the nucleus, where it regulates the transcription of several Wnt-target genes, such as *AXIN2* (Polakis 2012). Therefore, two methods to monitor Wnt

signalling activation are by detecting the non-phosphorylated β-catenin at S45 and T41 using the so-called active β-catenin monoclonal antibody (van Noort et al., 2002) and by quantifying the relative expression of the *AXIN2* mRNA. However, the mechanisms that govern the nuclear/cytosolic shuttling of β-catenin are poorly characterised.

Although Wnt signalling has been studied for over 50 years, and many of the core components have been established, many of the regulatory mechanisms remain undefined. The main aim of this chapter is to elucidate whether and, if so, how PAWS1 regulates Wnt signalling. Addressing this aim could not only provide insights into the biological function of PAWS1 and the FAM83 proteins but also contribute to a novel regulatory node in the regulation of Wnt signalling.

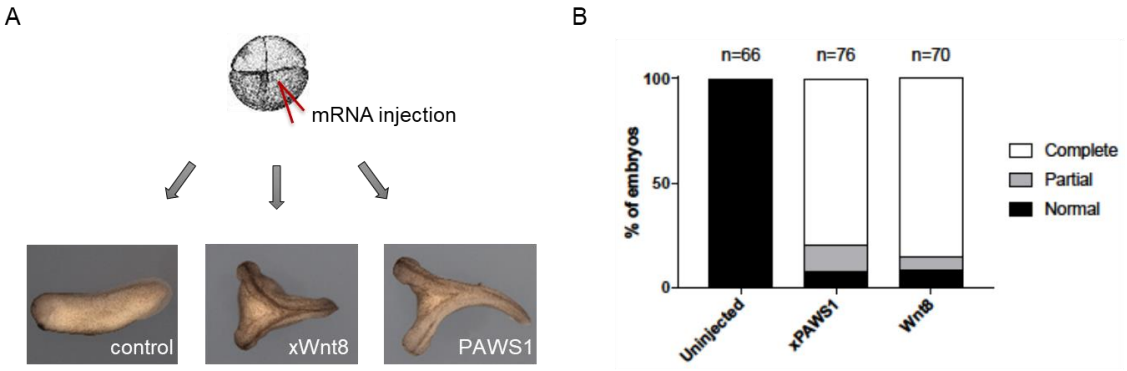

Figure 3- 1 PAWS1 causes axis duplication in *Xenopus* embryos.

A. Representative images of an uninjected embryo, and embryos injected with 5 pg xWnt8 mRNA or 250 pg xPAWS1 mRNA or at the ventral blastomeres of the 4-cell stage embryos. Representative images were taken at the tadpole stage (x= *Xenopus*). (Performed by K. Dingwell, The Francis Crick Institute, London).

B. Quantification of (A). Complete axis denotes embryos with a secondary axis with a cement gland, while a partial axis does not. (Performed by K. Dingwell, The Francis Crick Institute, London).

3.2 Results

3.2.1 PAWS1 does not inhibit canonical BMP signalling

To investigate if PAWS1 exerts its effect on inducing a secondary axis in *Xenopus* embryos by inhibiting BMP signalling, a series of experiments in dissociated animal caps were performed (Fig 3-2; K. Dingwell). It was found that over-expression of xPAWS1 did not inhibit BMP-induced nuclear translocation of SMAD1, nor did it affect the expression of the BMP-target genes *Msx-1* and *Vent1* (Fig 3-2A, B; K. Dingwell). These results indicated that the ability of PAWS1 to induce secondary axes in *Xenopus* embryos does not occur through inhibition of canonical BMP pathway.

To further explore if PAWS1 impacts BMP signalling in cells, CRISPR/Cas9 (clustered regularly interspaced short palindromic repeat (CRISPR) associated protein 9 (Cas9)) technology was employed for knocking out the endogenous PAWS1 gene. CRISPR/Cas9 has been widely applied to successfully knock out genes of interest in cultured cells and in mice (Cong, Ran et al. 2013, Mali, Yang et al. 2013). Briefly, this method employs a guide RNA (gRNA), designed to specifically target the gene of interest, which directs the Cas9 endonuclease at the target site to create a double-stranded DNA break (DSB), thereby disrupting the gene sequence. The two strands are then re-ligated via the non-homologous end-joining repair pathway, which results in repair by random insertion or deletion events at the DSB. This results in frameshifts and potentially creates both alleles displaying premature stop codons so that the target gene is knocked out. Dr T. Cummins employed this technology to knock out PAWS1 (Cummins, Wu et al. 2018) from U2OS cells that stably express Cas9 after induction with doxycycline (Munoz, Szyniarowski et al. 2014). CRISPR/Cas9 targeting of exon 2 of the PAWS1 gene (Fig 3-3A) resulted in PAWS1 loss from both alleles, which was verified by Western blotting and genomic sequencing.

Consistent with the data generated from *Xenopus*, PAWS1 loss had no significant effect on BMP-induced phosphorylation of SMAD1 at S463/S465 (Fig 3-3B). Similarly, stable PAWS1 introduction in PAWS1$^{-/-}$ cells, which resulted in higher PAWS1 protein expression compared to the wild type U2OS controls, did not alter the BMP-induced phosphorylation of SMAD1 (Fig 3-3B) nor the TGFβ-induced phosphorylation of SMAD2 and SMAD3 at S465/467 and S423/425, respectively (Fig 3-3B). Furthermore, BMP stimulation induced the transcription of the endogenous BMP-target gene ID1 in both wild type and PAWS1$^{-/-}$ cells, confirming that PAWS1 does not significantly regulate canonical BMP signalling (Fig 3-3C).

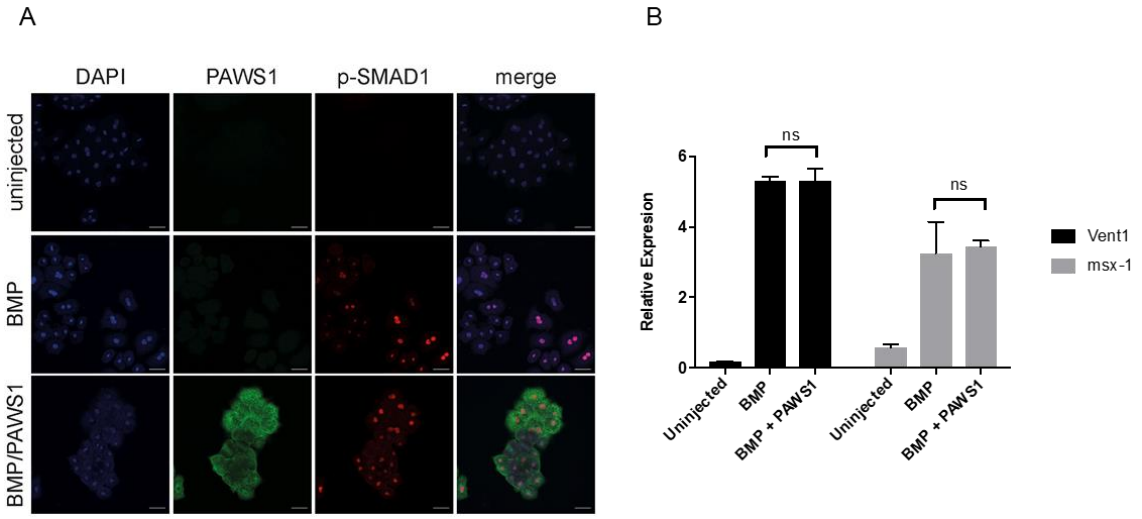

Figure 3- 2 PAWS1 does not affect BMP signalling pathway in *Xenopus* embryos

A. Embryos were injected into the animal pole of both blastomeres at the 2-cell stage with a total of either 1 ng of BMP_4 or 1 ng BMP_4 and 500 pg of Myc-tagged (MT) xPAWS1 mRNAs. Dissociated animal cap cells were stained with antibodies against MYC-tag (xPAWS1, green) and for phospho-SMAD1 (p-SMAD1, red). (by K. Dingwell, The Francis Crick Institute, London).

B. Animal cap cells injected at the 2-cell stage with a total of either 1 ng of BMP4 or 1ng BMP4 and 500 pg of MTxPAWS1 mRNA and the expression of the ventral genes *Vent1* (black bars) and *msx-1* (grey bars) was quantified by RT-PCR (n=3; Error bars represent ±SD, ns: not significant, t-test, unpaired, two-tailed with unequal variance). (by K. Dingwell, The Francis Crick Institute, London).

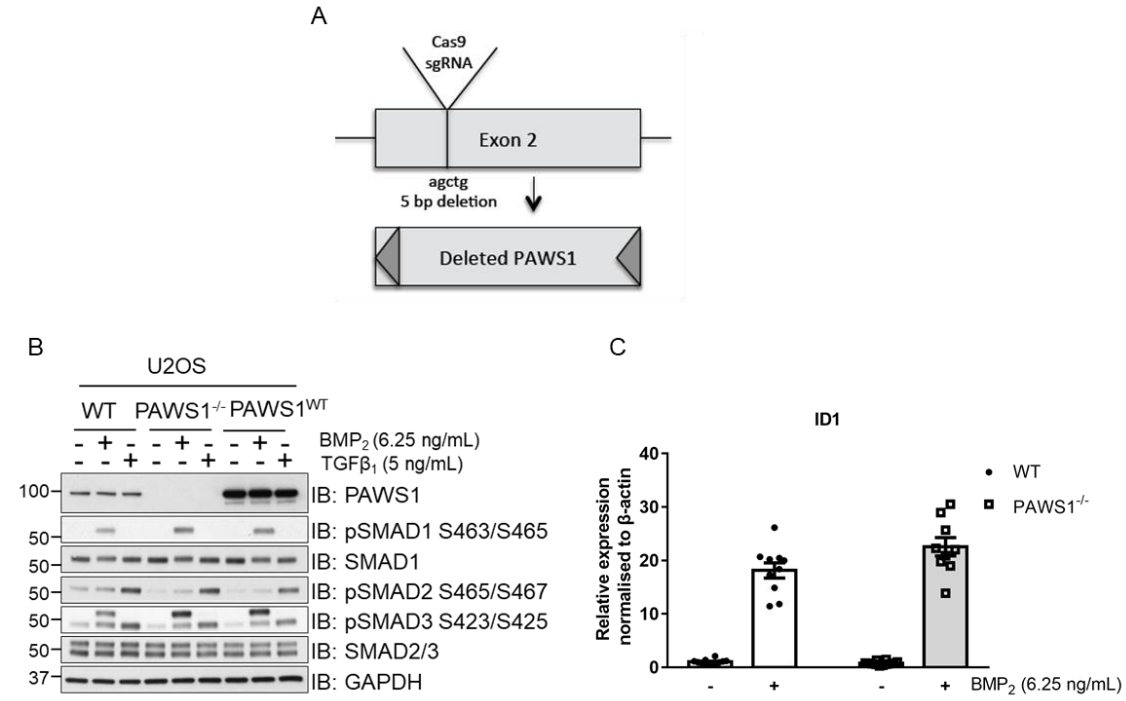

Figure 3- 3 BMP signalling is not compromised in U2OS PAWS1$^{-/-}$ cells

A. Schematic illustration of the strategy used for the generation PAWS1$^{-/-}$ cells by CRISPR/Cas9 genome editing. (sgRNA: single guide RNA)

B. U2OS wild type (WT), PAWS1$^{-/-}$ and PAWS1^{WT} rescue cells were serum-deprived for 16 hours. Cells were subsequently stimulated with either 6.25 ng/mL BMP_2 or 50 pM TGFβ1 for 1 hour prior to lysis. Cell extracts (15 μg) were resolved by SDS-PAGE and immunoblotted with the indicated antibodies. Note that the upper band in the pSMAD3 blot is a result of the antibody cross-reacting with pSMAD1. (by L. Hutchinson).

C. U2OS wild type (WT) and PAWS1$^{-/-}$ cells were serum-deprived for 16 hours. Subsequently, cells were either stimulated with 6.25 ng/mL for 6 h or left untreated prior to lysis. ID1 gene transcription was examined by qPCR. Transcript expression data are represented as fold induction over unstimulated control and are internally normalized to β-actin mRNA control. (n=3; Dots represent technical replicates; Error bars represent ±SEM of the 3 biological replicates).

3.2.2 PAWS1 enhances canonical Wnt signalling

Since PAWS1 had no inhibitory effect on canonical BMP signalling that could account for the axis duplication phenotype it caused in *Xenopus* embryos, its role in activating canonical Wnt signalling in human cells and in embryos was investigated. First, the ability of PAWS1 to impact Wnt/β-catenin reporter activity (see 1.5.3.4) was examined in human cells (Fig 3-4A). Control plasmids or those encoding for PAWS1 were overexpressed in U2OS osteosarcoma and HEK293 embryonic kidney cells, together with the TOPflash reporter plasmid, encoding for Firefly luciferase, and a plasmid encoding for Renilla luciferase as an internal control for transfection efficiency. Because the Firefly requires luciferin as a substrate while Renilla requires coelenterazine, the two enzymes can be used together in dual-reporter assays, while the normalised ratio of the two luciferase activities represents the relative Wnt/β-catenin reporter activity (Inouye and Shimomura 1997, Grentzmann, Ingram et al. 1998). The cells were then stimulated with Wnt3A or control-conditioned medium for 12 h prior to lysis and measurement of luciferase activities. As expected, in both cell lines transfected with control plasmids, Wnt3A induced TOPflash reporter activity compared to the untreated controls. LiCl, which potently inhibits GSK3 activity thereby stabilising β-catenin (Klein and Melton 1996), induced maximal reporter activity (Fig 3-4B). Overexpression of PAWS1 in both cell lines enhanced both basal and Wnt-induced luciferase reporter activity (Fig 3-4B), suggesting that PAWS1 overexpression activates Wnt signalling in human cells. PAWS1 overexpression had no additive effect on LiCl-induced luciferase activity, most likely because LiCl alone achieves maximal activation of the Wnt pathway.

In agreement with the results obtained from human culture cells, overexpression of xPAWS1 in isolated *Xenopus* animal cap cells resulted in increased stabilisation of the co-expressed GFP-β-catenin compared to the stabilised GFP-β-catenin in the absence of xPAWS1 (Fig 3-5A, B; K. Dingwell). Likewise, animal caps injected with xPAWS1 alone activated the mRNA expression of the Wnt target *Siamois* and the dorsalising factor *Chordin*, demonstrating that PAWS1 can ectopically activate the canonical Wnt pathway (Fig 3-5C; K. Dingwell).

To identify the domain of PAWS1 that is required for Wnt activation, different xPAWS1 fragments (Fig 3-6A) were tested for their ability to induce *Siamois* expression in naïve animal caps and form a secondary axis when injected into a ventral blastomere. The deletion of the PAWS1 c-terminal domain (722, 710), which lacks the BMPRI phosphorylation sites S711/S714/S715 (equivalent to human PAWS1 S610/S613/S614)

had no effect on its activity (Fig 3-6B, C), suggesting that the BMPRI phosphorylation sites of PAWS1 are not required for PAWS1 activity. Deletion or partial deletion of the DUF1669 domain (291 and 151 respectively) eliminated the axis-inducing activity suggesting that the DUF1669 domain is essential. However, expression of the DUF1669 domain fragments (DUF, 351) were unable to induce a secondary axis. Only a PAWS1 fragment spanning residues 1-583, which includes ~200 C-terminal residues after the conserved DUF1669 domain displayed axis-inducing activity and *Siamois* expression, indicating that the DUF1669 domain is necessary but not sufficient to activate Wnt signalling (Fig 3-6).

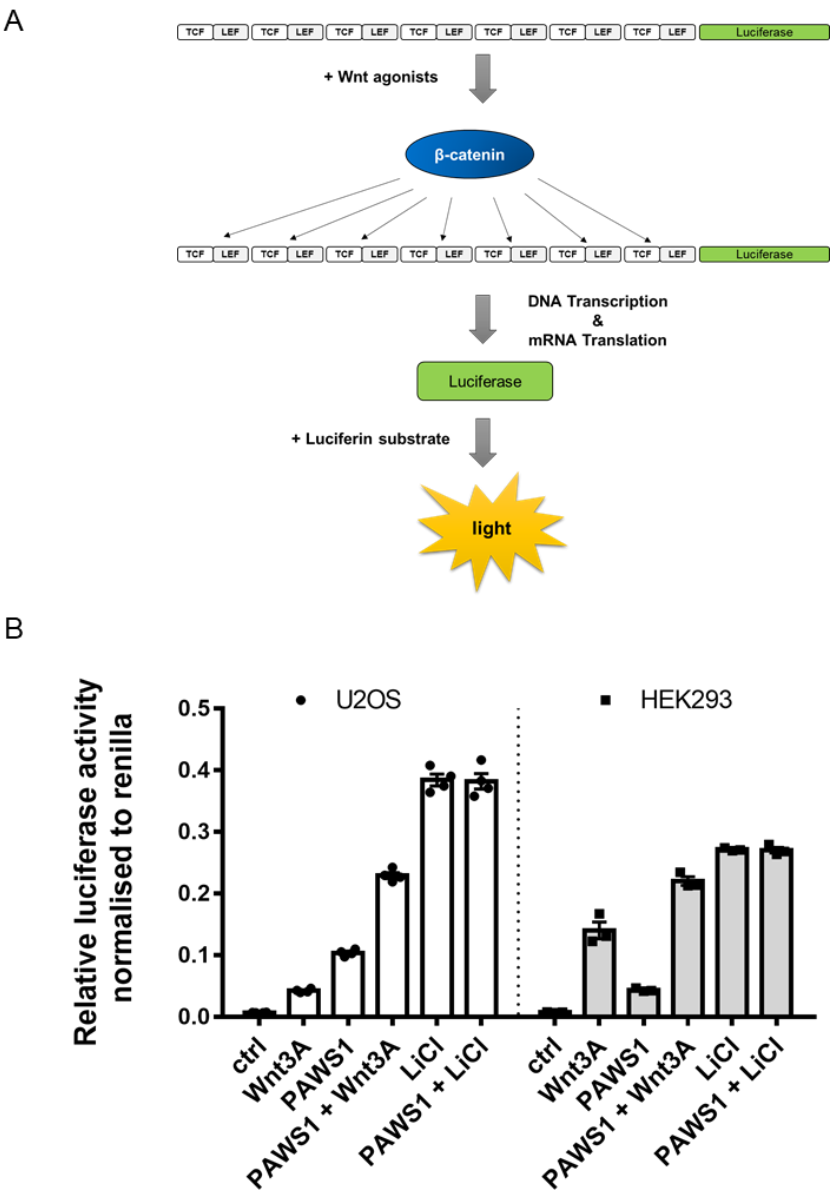

Figure 3- 4 PAWS1 overexpression enhances canonical Wnt signalling in human U2OS and HEK293 cells.

A. Schematic representation of TOPflash luciferase assay used to measure Wnt signalling activity. Cells are transfected with a plasmid that encodes a sequence with 7 TCF/LEF elements upstream of a firefly luciferase reporter. Treatment with agonists of the canonical Wnt signalling such as Wnt3A-conditioned medium or GSK3 inhibitors, results in the binding of β-catenin to the TCF/LEF repeats and the promotion of luciferase expression. Incubation of cell extracts with Luciferin results in light emission which is measured with a luminometer. FOPflash vector with mutated the TCF/LEF sites is used as a negative control.

B. HEK293 and U2OS cells were transfected with cDNA plasmids encoding PAWS1 or an empty vector as a control together with plasmids encoding TOPflash luciferase and Renilla luciferase (used as transfection control). The luciferase activities were measured after treatment with either control conditioned medium (L-CM), Wnt3A conditioned medium (L3-CM) or 20 mM LiCl for 12 h. Data are normalised to Renilla luciferase internal control. (n=4; Error bars represent ±SEM).

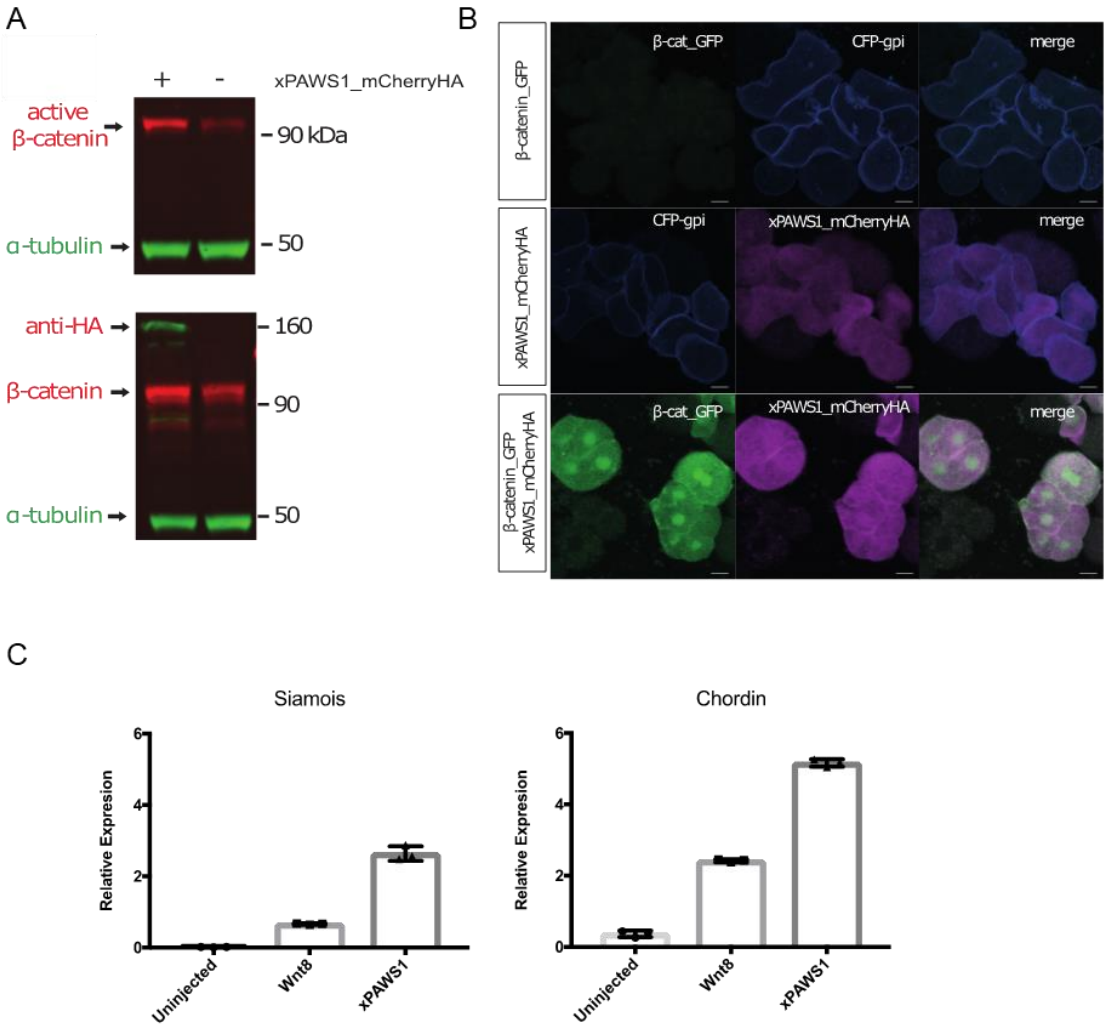

Figure 3- 5 PAWS1 activates canonical Wnt signaling in dissociated *Xenopus* animal caps.

A. *Xenopus* embryos were left uninjected or injected at the 1-cell stage with 250 pg of xPAWS1_mCherryHA mRNA. At stage 8.5 animal caps were collected from injected and uninjected embryos and cultured until control embryos reached stage 10. Extracts were immunoblotted with the indicated antibodies. (by K. Dingwell, The Francis Crick Institute, London).

B. Dissociated animal cap cells injected with either 50 pg of β-catenin_GFP or with 50 pg β-catenin_GFP and 250 pg xPAWS1_mCherryHA mRNAs were plated on coverslips and imaged by confocal microscopy. Only β-catenin_GFP cells co-injected with xPAWS1_mCherryHA mRNA accumulated robust levels of β-catenin in the nucleus. (by K. Dingwell, The Francis Crick Institute, London).

C. Embryos were injected at the 1-cell stage with 250 pg of xPAWS1 mRNA and then at stage 8.5, animal caps were collected from injected and uninjected embryos and assessed for Chordin and Siamois expression by qPCR. (n=3; Error bars represent ±SD). (by K. Dingwell, The Francis Crick Institute, London).

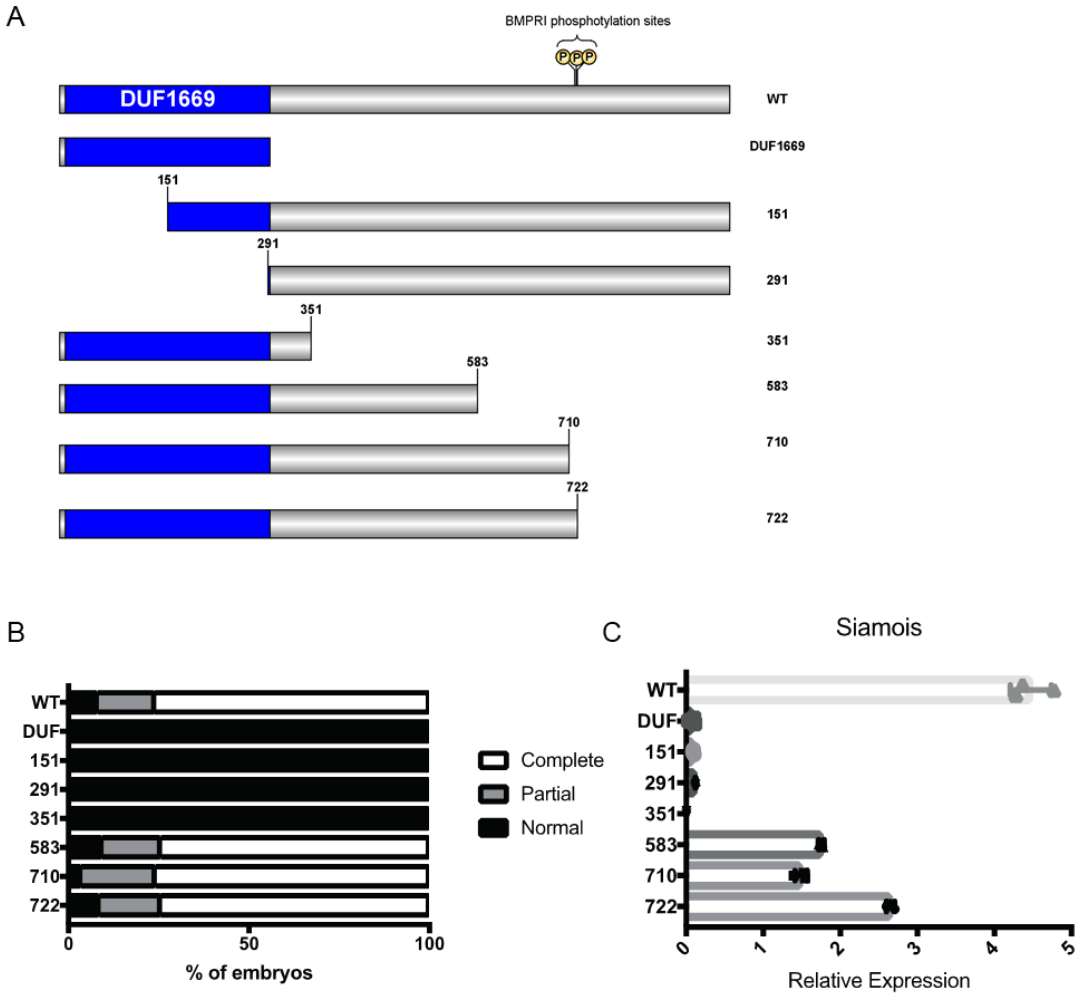

Figure 3- 6 The DUF1669 domain is necessary but not sufficient to induce a secondary axis and activate *Siamois* expression in *Xenopus* embryos

A. Schematic representation of the xPAWS1 fragments used in B and C.

B. 250 pg of xPAWS1 mRNAs encoding N, and C-terminal truncation fragments were injected into one ventral blastomere at the 4-cell stage. Axis induction was assessed at stage 28. (by K. Dingwell, The Francis Crick Institute, London).

C. Embryos were injected at the 1 cell stage with 250pg of Myc-tagged (MT)_xPAWS1 mRNAs encoding N- and C-terminal mutants and then at stage 8.5 animal caps were collected and assessed for *Siamois* expression by qPCR (n=3; Error bars represent ± SD). (by K. Dingwell, The Francis Crick Institute, London).

3.2.3 PAWS1 deficiency attenuates Wnt signalling

After demonstrating the impact of PAWS1 overexpression on Wnt activation in human cells and *Xenopus* embryos, the next aim was to study how loss of PAWS1 expression influences Wnt signalling. In comparison to wild type U2OS cells, Wnt-induced TOPflash luciferase activity in PAWS1$^{-/-}$ cells was substantially reduced (Fig 3-7A). As expected, the FOPflash luciferase reporter activity, which was employed as a negative control, was not enhanced by Wnt stimulation (Fig 3-7A).

Next, the expression of the endogenous Wnt-target genes *AXIN2* and *CYCLIN D1* in wild type and PAWS1$^{-/-}$ U2OS cells was examined by qPCR. In wild type U2OS cells, the expression of *AXIN2* and *CYCLIN D1* transcripts was significantly enhanced over a time course of Wnt stimulation (Fig 3-7B). In contrast, under these conditions, the Wnt-induced expression of these transcripts was significantly inhibited in PAWS1$^{-/-}$ U2OS cells (Fig 3-7B). The previous observation that PAWS1$^{-/-}$ U2OS cells activated the mRNA transcription of *ID1* in response to BMP stimulation (Fig 3-3C), excluded the possibility of PAWS1 being a general activator of transcription, validating that loss of PAWS1 does not affect global gene transcription.

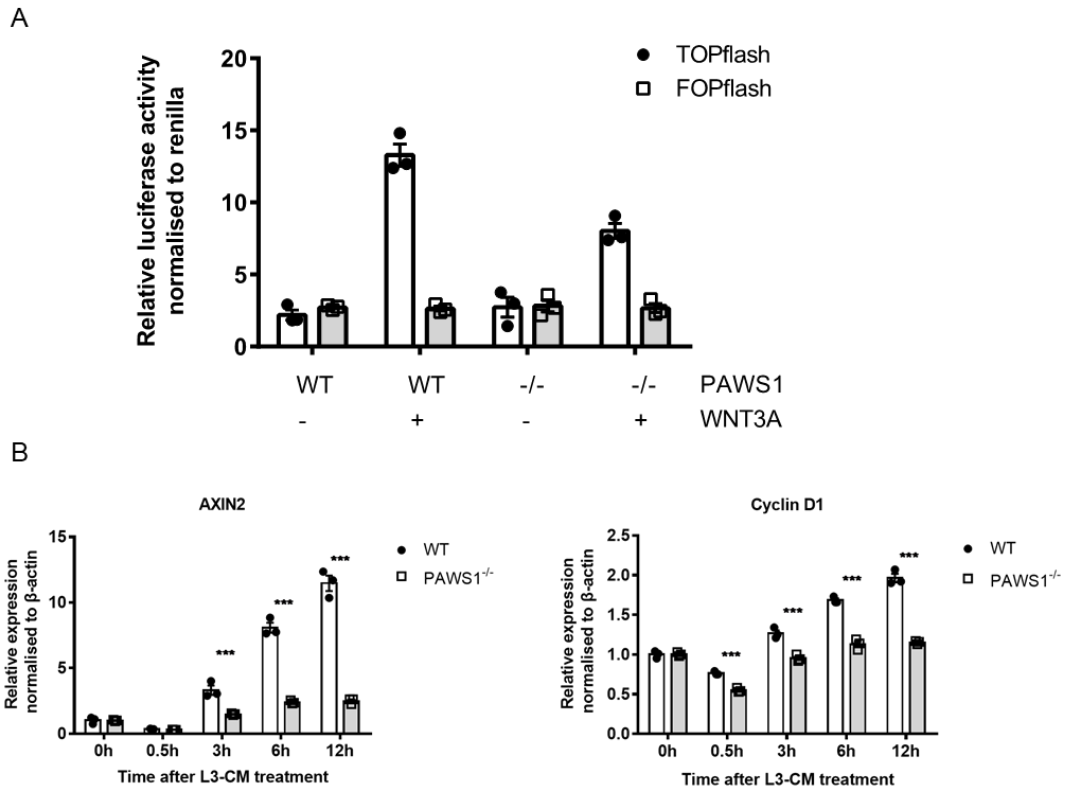

Figure 3- 7: Loss of PAWS1 expression attenuates cell responses to Wnt signalling

A. As in Fig 3-4B, except PAWS1^{WT} and PAWS1$^{-/-}$ U2OS cells were used. Relative TOPflash luciferase activity of PAWS1WT and PAWS1$^{-/-}$ U2OS cells after treatment with conditioned media (L-CM) or Wnt3A conditioned media (L3-CM) are plotted.

B. Wnt3A-induced activation of the endogenous target genes AXIN2 and Cyclin D1 was examined by qPCR at the indicated time points in PAWS1^{WT} and PAWS1$^{-/-}$ U2OS cells. Transcript expression data are represented as fold induction over unstimulated control and are internally normalized to β-actin control. (n=3; Error bars represent ±SEM; ***: $p<0.0001$).

3.2.4 PAWS1 functions downstream of the β-catenin destruction complex

To assess whether the loss of PAWS1 had an impact on the known components of the Wnt signalling cascade, the levels of the endogenous proteins were analysed by Western blotting in a time course experiment using control or Wnt3A conditioned medium (Fig 3-8). To exclude the potential off-target effects of using conditioned medium, cells that had been grown in regular growth medium and conditioned medium for the longest time point of the experiment were used as controls. As discussed in the Introduction, Wnt binding to LRP6 causes its phosphorylation at Ser1490, which then triggers a cascade of events leading to the stabilisation and accumulation of β-catenin. No significant differences in the Wnt-induced levels of phospho-LRP6 or in its phosphorylation kinetics were observed between wild type and PAWS1$^{-/-}$ cells (Fig 3-8). This indicated that the loss of PAWS1 does not affect the phosphorylation or activation of the Wnt receptor. Hence, the decreased responses to Wnt signals observed in PAWS1$^{-/-}$ cells must be due to downstream events. Next, the post-translational modification of β-catenin was examined since elevated phosphorylation levels can lead to enhanced proteasomal degradation and inhibition of Wnt-target genes activation. Wnt stimulation induced an acute loss of both CK1 (pS45) and GSK3 (pS33/pS37/pT41) phospho-residues on β-catenin within 30 min in both wild type and PAWS1$^{-/-}$ cells, while the levels then slowly recovered in a time-dependent manner (Fig 3-8).

To confirm that there was no effect of PAWS1 on the Wnt-induced cytosolic accumulation of β-catenin, β-catenin stabilisation assay was performed. As shown in Fig 3-9, no difference in total β-catenin protein levels were observed between wild type and PAWS1$^{-/-}$ cells after 6h of stimulation with control- or Wnt3A-conditioned medium. Similarly, PAWS1 loss had no substantial impact on the phosphorylation of β-catenin at CK1 and GSK3 sites (Fig 3-9). Wnt stimulation resulted in a slight decrease of the GSK3 phospho-sites (S33/S37/T41) on β-catenin in both wild type and PAWS1$^{-/-}$ cells, with no substantial differences between the cell lines. The CK1 phospho-site (S45) on β-catenin was also not substantially altered under the conditions tested. In addition to β-catenin, the protein levels of the destruction complex GSK3, Axin2 and CK1α were also examined. No differences between wild type and PAWS1$^{-/-}$ cells were observed under basal conditions in regard to GSK3 protein levels and, Wnt stimulation had no effect either (Fig 3-9). Interestingly, the Wnt-induced elevation of the protein levels of Axin2 was less pronounced in PAWS1$^{-/-}$ cells compared to the wild type cells (Fig 3-9). The most striking result to emerge from this data was that the protein levels of CK1α in PAWS1$^{-/-}$ cells were

substantially lower compared to wild type cells under both basal and Wnt-stimulated conditions (Fig 3-9). However, the lower CK1α levels in PAWS1$^{-/-}$ cells did not result in lower phosphorylation levels of its reported physiological substrate pS45-β-catenin (Liu et al., 2002). This could suggest either that the lower CK1α levels do not mean lower levels of its enzymatic activity or that other CK1 isoforms might mediate, or compensate CK1α for the phosphorylation of β-catenin at S45. Nevertheless, the data indicated that CK1α might be a promising factor that could account for the role of PAWS1 in Wnt signalling. Overall, these results support the hypothesis that PAWS1 functions at the level of the β-catenin destruction complex or downstream of it and that there is an association between PAWS1 loss and a decrease in the protein levels of CK1α.

To further elucidate where within the Wnt signalling cascade that PAWS1 acts at, epistasis experiments were performed in *Xenopus* embryos. First, naïve animal caps were injected with xWnt8 or xPAWS1 mRNA with or without co-injection of the dominant-negative Wnt receptor Lrp6m5 and the induction of the direct Wnt-target gene *Siamois* was tested. Injection of either xWnt8 or xPAWS1 induced *Siamois* expression whereas injection of Lrp6m5 alone or in the presence of xWnt8 completely inhibited *Siamois* expression in animal caps. Notably, Lrp6m5 was unable to inhibit *Siamois* expression injected with xPAWS1 suggesting again that PAWS1 acts downstream of the Wnt receptor (Fig3-10A).

Next, the impact of the selective GSK3 inhibitor CHIR99021 on Wnt activity in wild type and PAWS1$^{-/-}$ U2OS cells using TOPflash assay, was employed. Inhibition of GSK3 activity results in accumulation of β-catenin by preventing its phosphorylation and subsequent proteasomal degradation. GSK3 inhibition yielded maximal induction of Wnt reporter activity in wild type cells but failed to activate the reporter activity to the same extent in PAWS1$^{-/-}$ cells (Fig 3-10B). Collectively these data supported the observation that PAWS1 acts downstream of both the Wnt receptor and the destruction complex.

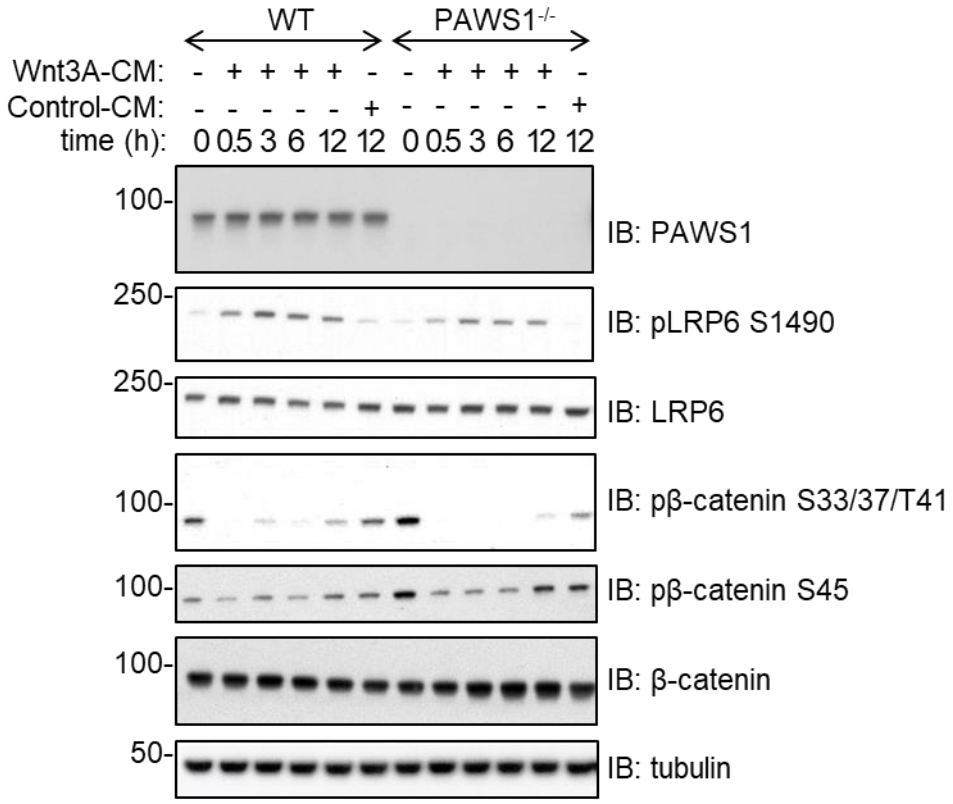

Figure 3- 8 PAWS1 loss does not affect the phosphorylation and protein levels of the major Wnt components.

U2OS wild type (WT) and PAWS1$^{-/-}$ cells were grown in either Wnt3a or control conditioned medium (CM) for the indicated time points prior to lysis. Cell extracts (15 µg of protein) were subjected to SDS-PAGE followed by Western blot analysis with the indicated antibodies.

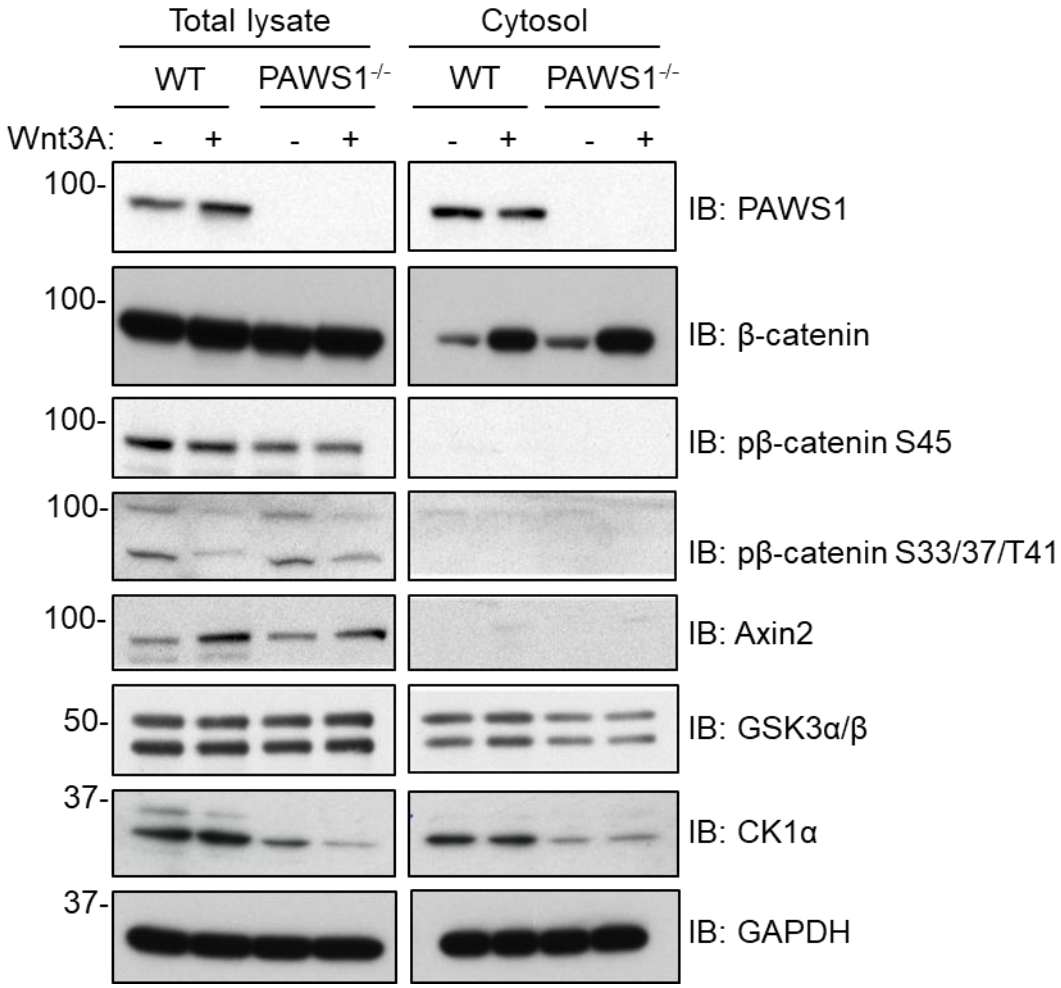

Figure 3- 9 Loss of PAWS1 does not affect the Wnt-induced cytosolic accumulation of total β-catenin protein.

U2OS wild type (WT) and PAWS1$^{-/-}$ cells were grown in control- or Wnt3A-conditioned medium for 6 hours and lysed in lysis buffer with or without detergent to get the total lysate and the cytosolic fraction only respectively. Cell extracts (20 μg of protein) were resolved by SDS-PAGE followed by immunoblotting with the indicated antibodies.

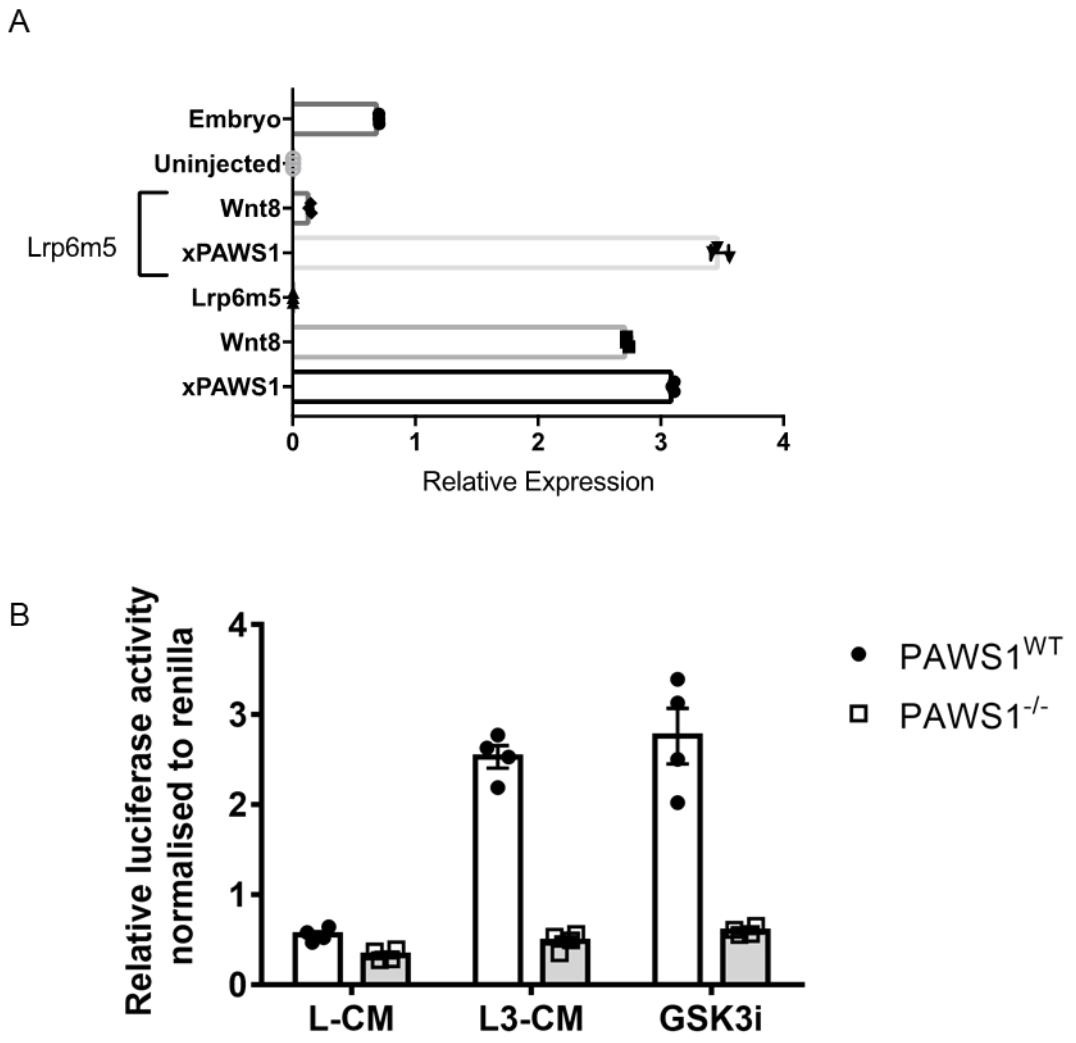

Figure 3- 10 PAWS1 appears to function at the level of the destruction complex.

A. *Xenopus* embryos were injected at the 1-cell stage with the indicated mRNAs and then at stage 10 animal caps were assessed by qPCR for the expression of *Siamois*. (n=3; Error bars represent ±SD).

B. Relative TOPflash luciferase activity of $PAWS1^{WT}$ and $PAWS1^{-/-}$ U2OS cells after treatment with either conditioned medium (L-CM), WNT3A conditioned medium (L3-CM) or 5μM of the GSK3 inhibitor CHIR99021 for 6 h. Data were normalized to Renilla internal control (n=4; Error bars represent ±SEM).

3.2.5 PAWS1 interacts with CK1α

To uncover the mechanisms by which PAWS1 activates the Wnt signalling, a proteomic approach was employed to identify potential interactors of endogenous PAWS1 was employed. First, U2OS cells were introduced with a GFP tag at the C-terminus of the endogenous PAWS1 gene on both alleles using CRISPR/Cas9 genome editing. In *Xenopus laevis* embryos, both untagged C-terminally GFP-tagged PAWS1 caused axis duplication (personal communication with K. Dingwell), suggesting that adding the GFP tag on PAWS1 at the C-terminus still retained Wnt-inducing activity. To generate PAWS1-GFP knockin cells, a modified version of the CRISPR/Cas9 technology that was described earlier for the generation of PAWS1$^{-/-}$ cells (see 3.2.1) was followed. Briefly, a pair of guide (sense and anti-sense) RNAs (gRNAs) targeting a genomic sequence just upstream of PAWS1 stop codon and a GFP-donor guide to insert GFP in-frame to the C-terminus of PAWS1 were designed by T. Macartney (DSTT, MRC-PPU) (Fig 3-11A). In order to reduce potential off-target mutagenesis, Cas9 harbouring the D10A mutation was encoded in the same plasmid carrying the anti-sense gRNA plasmid. Cas9 D10A causes single-strand nicks at the target sites, which two nicks close to the target site ensuring target-specific double-strand breaks (Ran et al., 2013). The nicks are repaired via homologous DNA recombination using the donor DNA as a repair template. Homozygous GFP-positive cells were verified by Western blotting and genomic sequencing which confirmed the GFP incorporation *in frame* with the PAWS1 gene (Fig 3-11B-F).

Anti-GFP immunoprecipitations (IP) were performed in the PAWS1$^{GFP/GFP}$ cell extracts to pull down endogenous PAWS1-GFP and its interacting partners. Endogenous PAWS1-GFP was visualized by Coomassie staining in the SDS-PAGE gel and its identity was verified by mass-spectrometry (MS) (Fig 3-12A) Among the interacting partners detected (Fig 3-12C), casein kinase 1α isoform (CK1α), which is also visible by Coomassie staining, was identified as the major interactor of PAWS1 by mass-spectrometry (Fig 3-12A-D). Some of the peptides that were identified by MS and were assigned to CK1α are shared with another CK1 isoform, CK1αL (Fig 3-12E). Since no peptides exclusive to CK1αL were detected (Fig 3-12D, E), it is unclear if this isoform is expressed in U2OS cells. With the lack of antibodies that specifically recognise CK1αL the focus of this research was shifted towards CK1α.

The interaction was verified by Western blotting in which endogenous CK1α was detected in anti-GFP IPs from PAWS1$^{GFP/GFP}$ knockin cells but not from PAWS1$^{-/-}$ U2OS

cells (Fig 3-13A). Similarly, endogenous PAWS1 was detected in IPs of endogenous CK1α from wild type but not PAWS1$^{-/-}$ U2OS cells (Fig 3-13B). As expected, control IgG IPs from either cell line did not pull down either PAWS1 or CK1α (Fig 3-13B). Stimulating cells with Wnt3A did not affect the ability of PAWS1 to interact with endogenous CK1α (Fig 3-13C), suggesting that the interaction between PAWS1 and CK1α is constitutive and does not depend on Wnt stimulation.

The CK1 branch of the human protein kinases also includes CK1 γ1, γ2, and γ3 isoforms, tau tubulin kinases (TTBK) 1 & 2 and vaccinia related kinases (VRK) 1-3 (Manning, Whyte et al. 2002). In cell extracts, under co-expression conditions in which PAWS1 interacted with CK1α, no interaction between PAWS1 and either TTBK2 or CK1γ were detected (Fig 3-13D). CK1δ isoform was found to interact with PAWS1 under overexpression conditions (Fig 3-13D) but since it was not detected in endogenous PAWS1 IPs (Fig 3-12C), this result should be considered with caution.

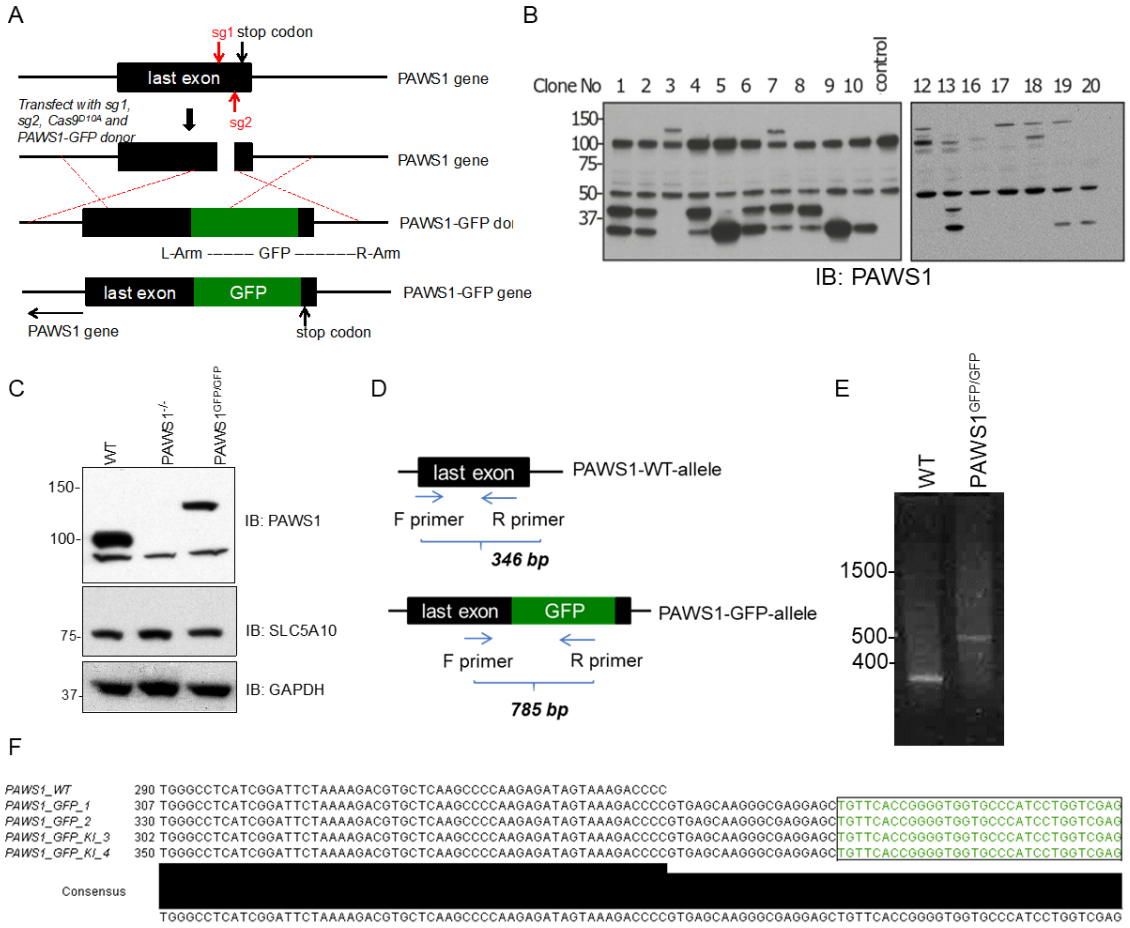

Figure 3- 11 Generation of PAWS1-GFP expressing cells under the endogenous promoter

A. Schematic illustration of the CRISPR/Cas9 genome editing strategy followed to generate PAWS1-GFP knock-ins in U2OS cells. A pair of guide RNAs, which recognise a genomic sequence upstream of the stop codon of PAWS1 gene, was used in combination with a donor vector, which inserts GFP in frame at the C-terminus of PAWS1.

B. Western blot screen of PAWS1-GFP knock-in clones. A homozygous GFP-knockin would shift the apparent molecular weight of endogenous PAWS1-GFP equivalent to that of both proteins, as recognized by the anti-PAWS1 antibody.

C. Cell extract from clone 17 from (B) ($PAWS1^{GFP/GFP}$) was compared with the wild type and $PAWS1^{-/-}$ cell extract, confirming that the gene in the reverse strand of PAWS1, SLC5A10 is not disturbed.

D. Schematic representation of the predicted genomic PCR products that were amplified with a pair of primers targeting the indicated regions.

E. DNA was extracted from U2OS wild type (WT) and PAWS1-GFP knock-in cells (clone 17) a pair of primers was used to amplify the genomic region by PCR, as shown in (D), followed by agarose gel electrophoresis.

F. Sequence alignment of four independent PCR products from (E), showing that the GFP gene (in green) was integrated in frame with PAWS1. Alignment was performed in Jalview 2.10.3 with ClustalO.

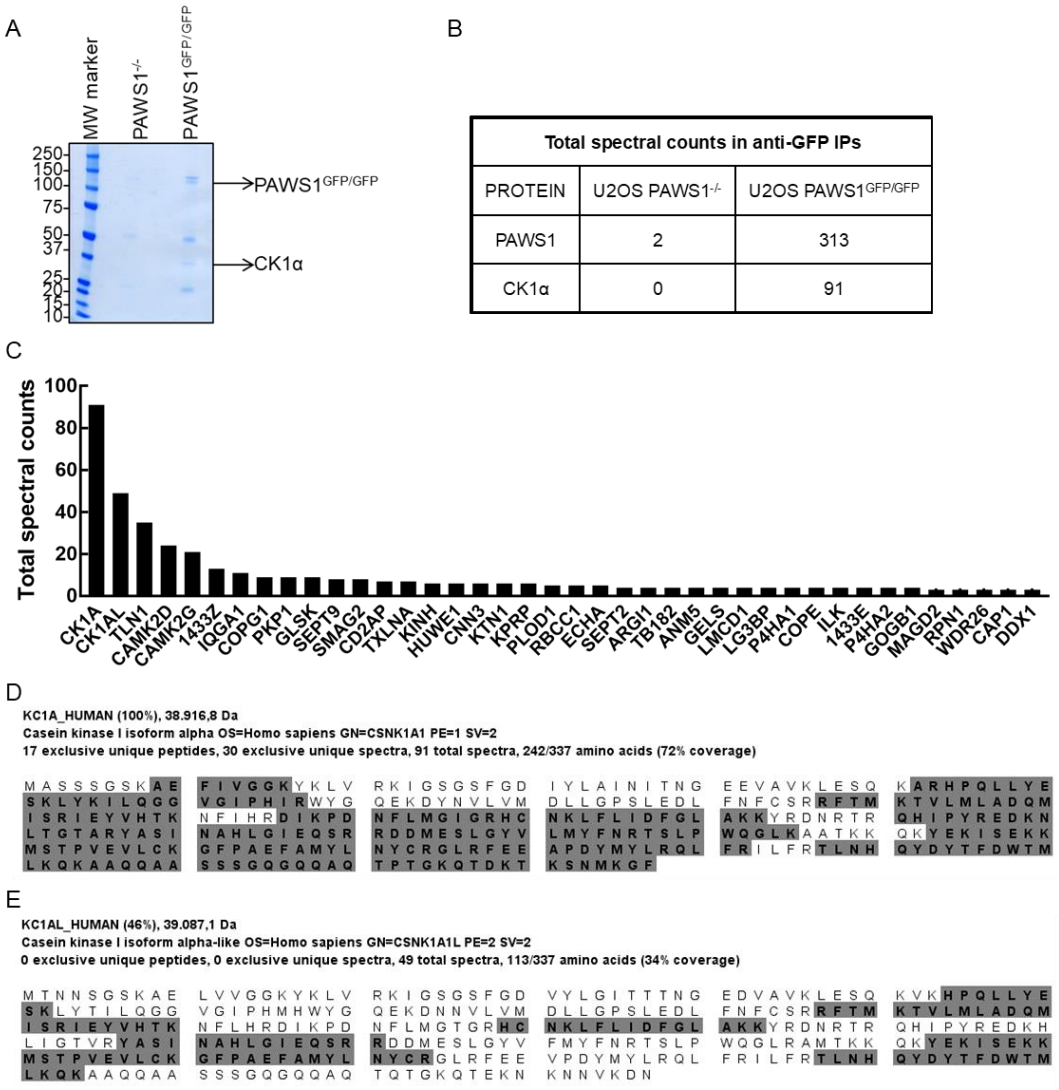

Total spectral counts in anti-GFP IPs		
PROTEIN	U2OS PAWS1$^{-/-}$	U2OS PAWS1$^{GFP/GFP}$
PAWS1	2	313
CK1α	0	91

Figure 3- 12 PAWS1 interacts with CK1α at the endogenous level.

A. GFP pull downs from U2OS PAWS1$^{-/-}$ and PAWS1$^{GFP/GFP}$ cells were resolved by SDS-PAGE and the gel was stained with Coomassie. Each lane was cut in 6 pieces, which were subsequently processed for protein identification by mass-spectrometry.

B. Mass fingerprinting analysis of PAWS1-GFP interactors from (A) identified CK1α as a major interactor. The table shows total spectral counts for PAWS1 and CK1α tryptic peptides identified in anti-GFP IPs.

C. PAWS1-GFP interacting proteins were plotted using total spectral counts for selected individual protein. Total spectral counts are defined as the sum of all the spectra associated with a specific protein within a sample, which includes also those spectra that are shared with other proteins. A spectral count of 3 or more in PAWS1-GFP IPs and no spectral counts in GFP control IPs were set as threshold for inclusion. The spectral counts for PAWS1 were excluded from the graph.

D. The highlighted tryptic peptides identified by mass-spectrometry on CK1α (top panel) and on CK1α (bottom panel) indicate the overall protein coverage. The images were obtained using Scaffold V4.3 analysis of the LC-MS/MS data.

E. Same as (D) but for CK1αL.

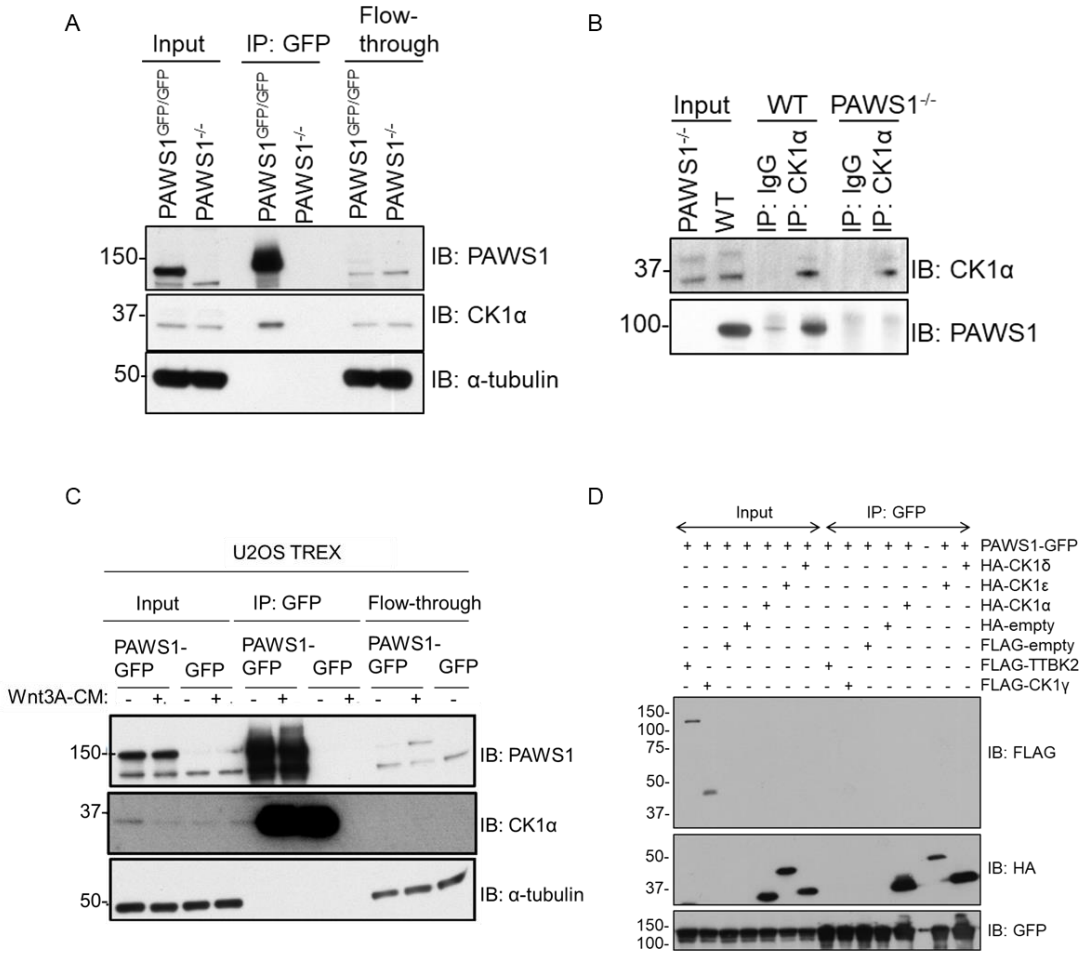

Figure 3- 13 Validation of the PAWS1:CK1α interaction

A. GFP pull downs from U2OS PAWS1$^{-/-}$ and PAWS1$^{GFP/GFP}$ cells were resolved by SDS-PAGE and analysed by Western blot using the indicated antibodies.

B. Anti-CK1α IPs from U2OS PAWS1^{WT} and PAWS1$^{-/-}$ cells were resolved by SDS-PAGE and analysed by Western blot using the indicated antibodies.

C. PAWS1 interacts with CK1α independent of Wnt stimulation. Stable U2OS Flp-In Trex cells were subjected to 20 ng/ml doxycycline for inducing PAWS1-GFP expression or GFP expression alone for 24 h. Wnt3A or control medium was added to the cells for 6 h before lysis. 20 mg of cell extract was subjected to GFP-trap IP. Input (20µg of protein), 5% of the pull down and flow-through extract (20 µg of protein) were subjected to SDS-PAGE followed by Western blot analysis with the indicated antibodies.

D. The indicated FLAG or HA-tagged CK1 family members were co-expressed with PAWS1-GFP in U2OS cells. Input extracts and GFP-IPs were resolved by SDS-PAGE followed by Western blot analysis with the indicated antibodies.

3.2.6 Mapping the interaction sites between PAWS1 and CK1α

Having verified the interaction between PAWS1 and CK1α, the next aim was to identify the sites on the PAWS1 protein sequence that bind to CK1α. First, the minimal domain within PAWS1 that mediates the interaction with CK1α was determined. For this, truncated fragments of Myc-tagged xPAWS1 were co-expressed with full-length HA-tagged CK1α in U2OS PAWS1$^{-/-}$ cells, followed by HA-IPs (Fig 3-14). HA-CK1α was able to co-precipitate only those PAWS1 fragments that contained residues 151-291 within the DUF1669 domain (Fig 3-14), which are equivalent to the human residues 165-307.

Interestingly, within this mapped region, PAWS1 contains an F-x-x-x-F sequence motif which, as mentioned in the Introduction, has been reported to be a CK1 docking motif in NFAT and PER1/2 proteins (Okamura et al., 2004). To determine if the F^{296}-x-x-x-F^{300} motif within PAWS1 indeed mediates its interaction with CK1α these phenylalanine residues were targeted for mutagenesis. Single FLAG-tagged F296A, F300A and double F296A/F300A mutants were generated and overexpressed in U2OS cells and extracts subjected to IPs using anti-FLAG beads. The locations of the mutated residues are indicated in a schematic representation of PAWS1 (Fig 3-15A). As expected, endogenous CK1α was detected in anti-FLAG IPs from wild type FLAG-PAWS1 expressing extracts resulting in an almost complete immuno-depletion of CK1α from the flow-through extracts. Endogenous CK1α was also detected in FLAG-IPs from FLAG-PAWS1^{F300A} but not from FLAG-PAWS1^{F296A} and FLAG-PAWS1$^{F296A/F300A}$ extracts (Fig 3-15B), suggesting F296 in PAWS1 contributed to the association with CK1α. For PER1/2, it had previously been shown that both Phe residues within the F-x-x-x-F motif were essential for interaction with CK1, as mutating either contributed to the loss of interaction with CK1 (Okamura, Garcia-Rodriguez et al. 2004). However, for PAWS1, the fact that PAWS1^{F300A} was still able to interact with CK1α suggested that perhaps the mode of interaction between PAWS1 and CK1α is mediated through a unique mechanism.

In the light of the resolved structure of the DUF1669 domain of FAM83A, it was observed that an Aspartic residue lies very close to the corresponding F300 residue in FAM83A and it was hypothesised that it could impact the interaction with CK1α. Indeed, mutating the Asp262 to Ala (PAWS1^{D262A}) also abolished the association with CK1α (Fig 3-15A, B). Collectively, these data demonstrate that PAWS1 interacts with CK1α at the

endogenous level and two residues within the DUF1669 domain of PAWS1, D262 and F296, individually contribute to the association with CK1α.

To test if the interaction between PAWS1 and CK1α was direct, an *in vitro* binding assay was performed. For this GST-PAWS1^{WT}-6xHis and GST-PAWS1$^{F296A/F300A}$ were expressed and purified from *E.coli*. Recombinant GST-CK1α had been previously purified by the Protein Production team in DSTT and the GST tag was cleaved with PreScission protease. As seen in Fig 3-15C, a robust interaction between PAWS1^{WT} and CK1α was observed but not with GST alone. In concurrence with the co-IP experiment from U2OS cell extracts (Fig 3-15B), no CK1α was found to bind to PAWS1$^{F296A/F300A}$. These results indicate that PAWS1 and CK1α bind to each other in a direct manner.

Next, whether restoration of PAWS1 expression in U2OS PAWS1$^{-/-}$ cells could rescue the PAWS1 interaction with CK1α was assessed. To address this, retroviruses encoding the PAWS1^{WT}, PAWS1^{F296A}, PAWS1^{D262A} or GFP control were produced in HEK293-FT cells and used at different dilutions to infect PAWS1$^{-/-}$ cells. The expression of the infected PAWS1 constructs in PAWS1$^{-/-}$ cell extracts was confirmed by Western blotting (Fig 3-16A). Dilution of retroviral titre was performed in order to achieve stable PAWS1 expression levels in PAWS1$^{-/-}$ cells as close to the endogenous levels seen in wild type U2OS cells. However, as seen in Fig 3-16A, PAWS1 is substantially over-expressed in the PAWS1$^{-/-}$ cells rescued with dilutions of retroviral infections compared to the wild type cells. With the lack of a better method of restoring PAWS1 expression in PAWS1$^{-/-}$ cells to the endogenous levels, the cell lines which were generated using 1:5 dilution of the retroviral titre were selected for all the experiments described in this thesis. Fig 3-16B shows that IPs of endogenous CK1α from rescue cell extracts pulled down PAWS1 only from PAWS1^{WT} rescue cells but not from the others. No PAWS1 was detected in IgG IPs, that were employed as controls (Fig 3-16B). Furthermore, immunofluorescence microscopy of the rescue cells showed overlapping cytoplasmic staining of PAWS1^{WT} and CK1α, while no overlapping staining was detected between PAWS1^{F296A} and CK1α (Fig 3-17; K. Wu). Predictably, no immunofluorescence signal for PAWS1 was observed in the PAWS1$^{-/-}$ cells, while CK1α staining in these cells and PAWS1^{F296A} rescue was diminished compared to PAWS1^{WT} rescue cells (Fig 3-17; K. Wu).

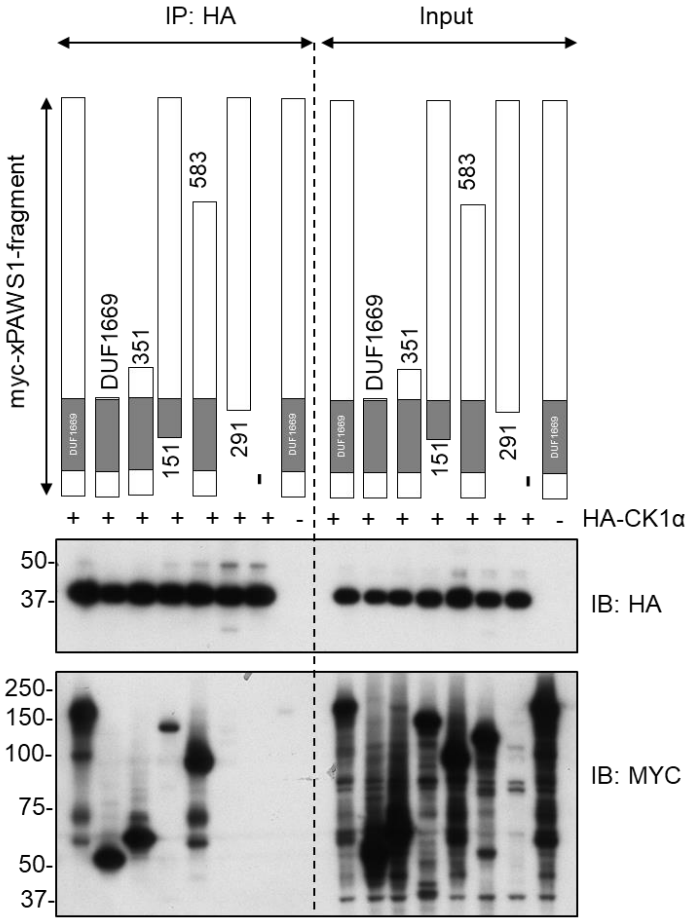

Figure 3- 14 The DUF1669 domain of PAWS1 is sufficient in mediating the interaction with CK1α.

The indicated fragments of Myc-tagged PAWS1 (see Fig 3-3A) were co-expressed with HA-CK1α in U2OS PAWS1$^{-/-}$ cells for 48 h. Inputs and Anti-HA IPs were subjected SDS-PAGE followed by Western blot analysis with the indicated antibodies.

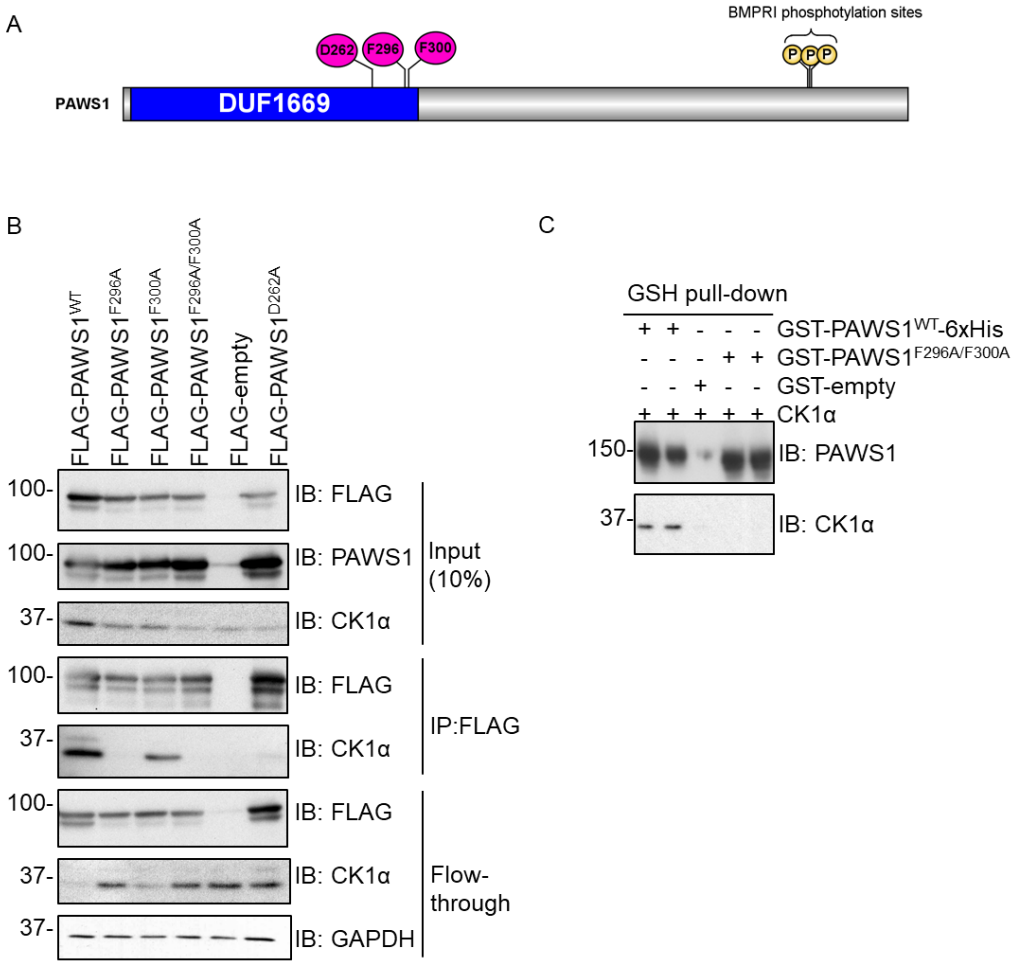

Figure 3- 15 Identification of the residues on PAWS1 that are required for CK1α interaction

A. Schematic representation of PAWS1 indicating the position of key residues that were mutated for the following experiments.

B. U2OS cells were transiently transfected with cDNA encoding FLAG-tagged PAWS1^{WT}, PAWS1^{F296A}, PAWS1^{F300A}, PAWS1$^{F296A/F300A}$, PAWS1^{D262A} and FLAG-empty vector. Anti-FLAG IPs were immunoblotted with the indicated antibodies.

C. PAWS1 forms a direct interaction with CK1α. Glutathione-sepharose raisin was loaded with GST-PAWS1^{WT}-6xHis or GST-PAWS1$^{F296A/F300A}$ and used to pull down CK1α. GST-empty was used as a negative control. The pull-down products were analysed by Western blot using the indicated antibodies.

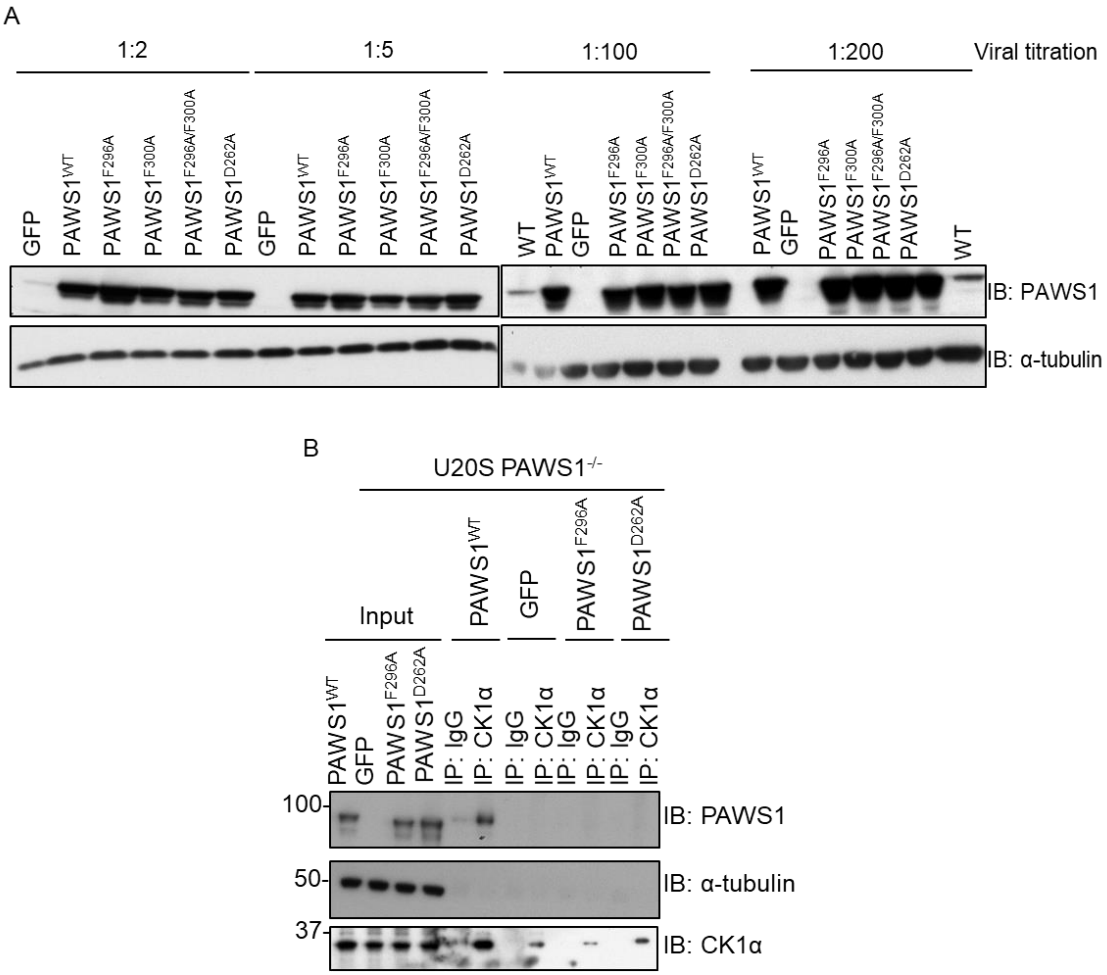

Figure 3- 16 Restoration of PAWS1 expression in PAWS1$^{-/-}$ cells.

A. U2OS PAWS1$^{-/-}$ cells were infected with retroviruses in order to stably rescue cells with GFP-control, PAWS1^{WT}, PAWS1^{F296A}, PAWS1^{F300A}, PAWS1$^{F296A/F300A}$ or PAWS1^{D2626A} at the indicated dilutions from retroviral medium collected from 293-FT cells. For example, a 1:5 dilution means that the infection medium applied to cells contained one portion of retroviral medium mixed with four portions of the fresh medium. Puromycin-selected cells were lysed and extracts were resolved by SDS-PAGE and analysed by Western blotting using the indicated antibodies. Expression levels were compared to endogenous PAWS1 levels from wild type U2OS extracts.

B. Anti-CK1α IPs and IgG-IPs (from 500 µg of protein) from stable U2OS PAWS1^{WT}, GFP, PAWS1^{F296A} and PAWS1^{D262A} rescue cells were resolved by SDS-PAGE and analysed by Western blotting using the indicated antibodies.

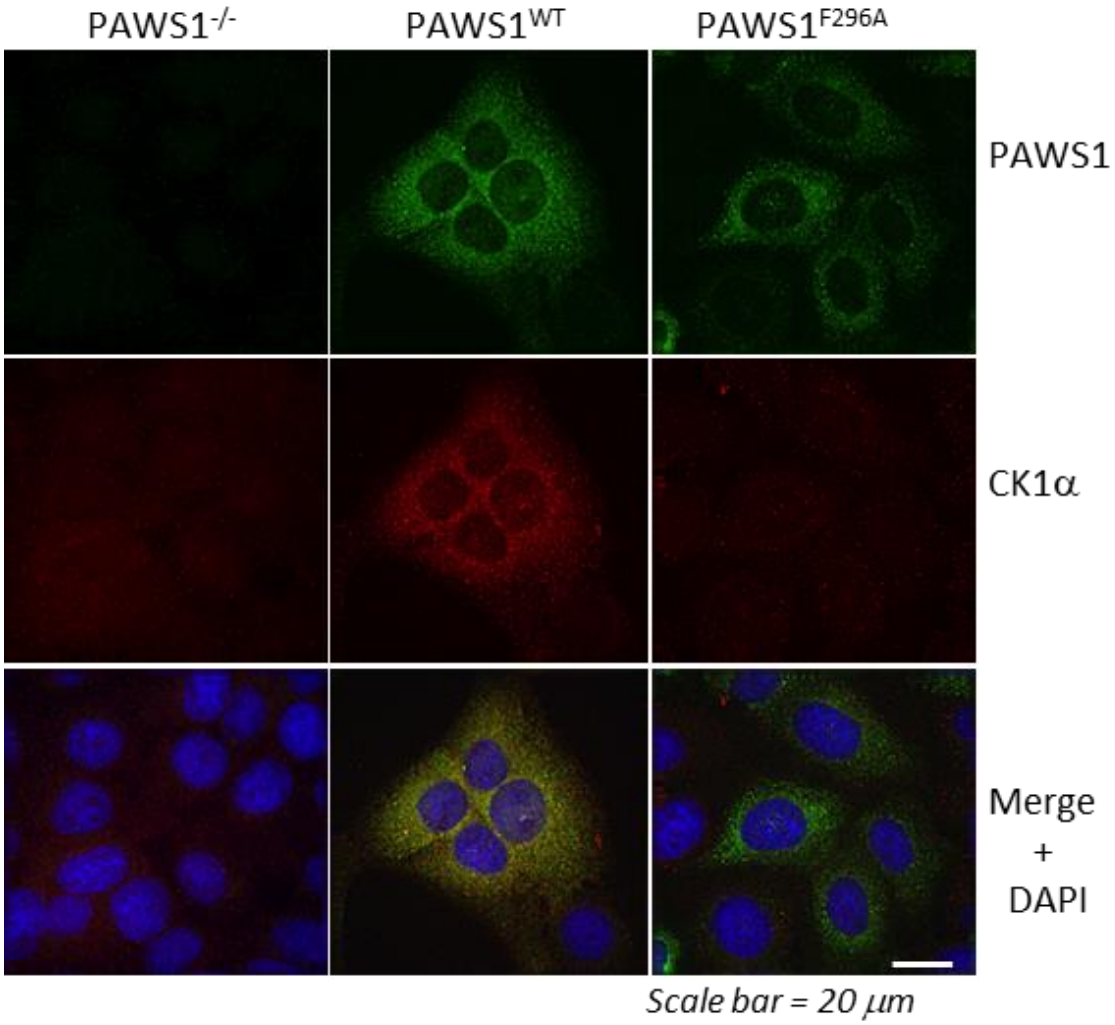

Figure 3- 17 PAWS1 interacts and co-localises with CK1α in U2OS cells.

PAWS1$^{-/-}$ cells in which PAWS1^{WT} or PAWS1^{F296A} expression was restored, were fixed for immunofluorescence using antibodies against PAWS1 and CK1α. Scale bar is 20 μm. (by K. Wu).

3.2.7 Interaction between PAWS1 and CK1α is essential for PAWS1-dependent axis duplication and the activation of Wnt signalling.

After establishing that PAWS1 interacts and co-localise with CK1α constitutively, the role, if any, of the PAWS1:CK1α complex in the activation of Wnt signalling was assessed using *Xenopus* embryos and U2OS cells. First, the role of the association between PAWS1 and CK1α in PAWS1-induced axis duplication in *Xenopus* embryos was investigated. PAWS1-induced axis duplication ability was scored at the tadpole stage, following microinjection of *Xenopus* embryos with wild type PAWS1, three separate CK1α-interaction deficient PAWS1 mutants ($PAWS1^{D262A}$, $PAWS1^{F296A}$, and $PAWS1^{F296A/F300A}$) as well as the $PAWS1^{F300A}$ mutant that still interacts with CK1α (Fig 3-18A, B). Both $PAWS1^{WT}$ and the $PAWS1^{F300A}$ mutant that interact with CK1α induced partial or complete axis duplication in ~80% of embryos. In contrast, the CK1α-interaction deficient PAWS1 mutants, $PAWS1^{D262A}$, $PAWS1^{F296A}$, and $PAWS1^{F296A/F300A}$ failed to induce secondary axes in the embryos (Fig 3-18B). These results demonstrate that the interaction between PAWS1 and CK1α is essential for PAWS1-mediated axis duplication in *Xenopus* embryos.

Second, whether the induction of the Wnt reporter activity in U2OS cells also required interaction between PAWS1 and CK1α was investigated. For this, Wnt-reporter activity was assessed in wild type, $PAWS1^{-/-}$ as well as $PAWS1^{-/-}$ cells rescued with either $PAWS1^{WT}$ or the CK1α-interaction deficient $PAWS1^{F296A}$ mutant. Stimulation of wild type cells with Wnt3A substantially enhanced the luciferase reporter activity over unstimulated controls, while in $PAWS1^{-/-}$ cells it did not (Fig 3-18C). In $PAWS1^{-/-}$ cells rescued with wild type PAWS1, the Wnt3A-induced luciferase reporter activity was restored to levels similar to those seen in wild type cells. In contrast, in $PAWS1^{-/-}$ cells rescued with the $PAWS1^{F296A}$ mutant, the Wnt3A-induced luciferase reporter activity was not restored (Fig 3-18C), suggesting that PAWS1-mediated activation of Wnt signaling necessitates its ability to interact with CK1α.

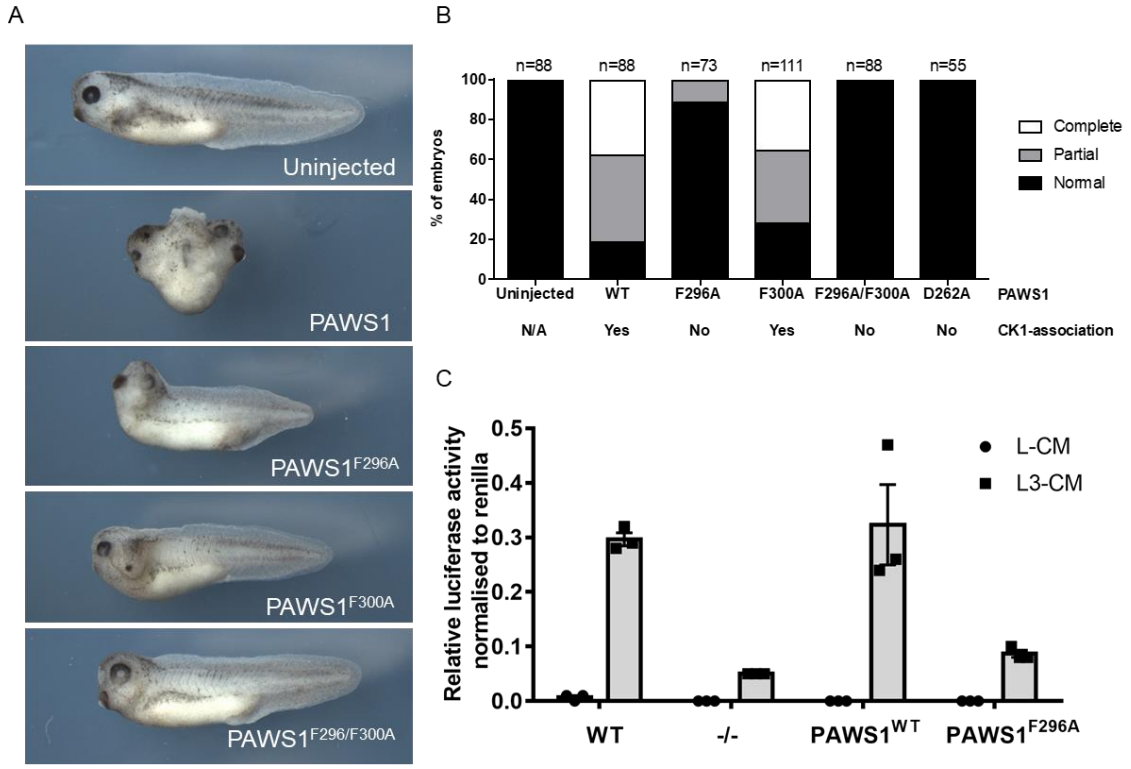

Figure 3- 18 PAWS1:CK1*α* interaction is critical for the activation of Wnt signalling in *Xenopus* embryos and in human cells.

A. Representative images of an uninjected *Xenopus* embryo and embryos injected with the indicated mRNAs. PAWS1^{F296A} and PAWS1$^{F296A/F300A}$ mutants that do not interact with CK1α fail to induce a secondary axis in *Xenopus* embryos. (by K. Dingwell, The Francis Crick Institute, London).

B. Quantification of (A) with the inclusion of embryos injected with PAWS1^{D262A}. Complete axis denotes embryos with a secondary axis with a cement gland, while a partial axis does not.

C. Relative TOPflash luciferase activity of U2OS WT, PAWS1$^{-/-}$, PAWS1^{WT} and PAWS1^{F296A} rescue cells after treatment with control-conditioned media (L-CM), Wnt3A-conditioned media (L3-CM) for 16h. (n=3; Error bars Data were normalized to Renilla internal control (n=3; Error bars represent ±SEM).

3.2.8 PAWS1 does not affect the composition of the destruction complex

As mentioned in the Introduction, CK1 isoforms are known to phosphorylate many Wnt components, including β-catenin. Although the loss of PAWS1 did not cause any apparent changes in the phosphorylation levels of β-catenin (Fig 3-8, 3-9), Wnt signalling was clearly attenuated in PAWS1$^{-/-}$ cells after stimulation with Wnt3A-conditioned medium or GSK3 inhibition (Fig 3-6, 3-10). Since PAWS1 was shown to function at the level of the destruction complex or downstream of it (Fig 3-10), co-immunoprecipitation (IP) assays were performed to assess the potential impact of the PAWS1:CK1α interaction on the composition of the destruction complex. Initially, endogenous CK1α-IPs were performed at an early stage of the Wnt signalling response, namely after 30 min and 1 h of Wnt stimulation (Fig 3-19). No significant levels of β-catenin were detected in CK1α-IPs with or without Wnt stimulation and no differences were observed in WT and PAWS1$^{-/-}$ cells. This result indicated that PAWS1 does not affect the interaction between CK1α and β-catenin. This observation is consistent with the findings that phosphorylation of β-catenin on CK1 sites remain largely unaltered in PAWS1$^{-/-}$ cells compared to wild type cells (Fig 3-8, 3-9).

Next, endogenous CK1α, Axin1 and β-catenin were immunoprecipitated from WT and PAWS1$^{-/-}$ U2OS cell extracts, following 3h treatment with either control or Wnt3A-conditioned medium, and their abilities to interact with components of the destruction complex were probed by Western blotting. In endogenous CK1α IPs from both WT and PAWS1$^{-/-}$ cells, Axin1, GSK3α/β and β-catenin were not detectable, regardless of Wnt3A stimulation, while as expected PAWS1 was identified in CK1α IPs from WT cells but not PAWS1$^{-/-}$ cells (Fig 3-20). In Axin1 IPs, GSK3α/β were detected robustly, while very low levels of β-catenin were also detected, although neither Wnt3A treatment nor the PAWS1-status had any effect on these Axin1 complexes (Fig. 3-19). Similarly, in β-catenin IPs, low levels of GSK3β, as well as CK1δ and CK1ε but not CK1α were detected (Fig 3-21). This might suggest that either the immunoprecipitation conditions used here did not favour the stability of the CK1α-binding to the β-catenin destruction complex or that CK1δ and CK1ε may be the kinases that mediate β-catenin phosphorylation at Ser45 and not CK1α.

In an effort to elucidate the mechanisms of function of the PAWS1:CK1α complex in the Wnt signalling pathway, an unbiased proteomic approach was employed. For this, U2OS cells that stably express PAWS1-GFP or GFP control upon doxycycline induction were stimulated with control or Wnt3A-conditioned medium for 3 h, lysed and extracts

subjected to GFP-IPs. Following resolution by SDS-PAGE, the interacting proteins were excised, trypsin-digested and identified by mass spectrometry. Other than CK1α and CK1αL, no major known components of the Wnt pathway, especially those of the destruction complex, were identified under control or Wnt3A-stimulated conditions (Fig 3-21). Interestingly, some PAWS1 interactors were enriched in Wnt3A-stimulated conditions but with much lower abundance than CK1α and CK1αL. However, these interactors are not yet known to play roles in the Wnt signalling pathway and still need to be validated as PAWS1 interactors at the endogenous level.

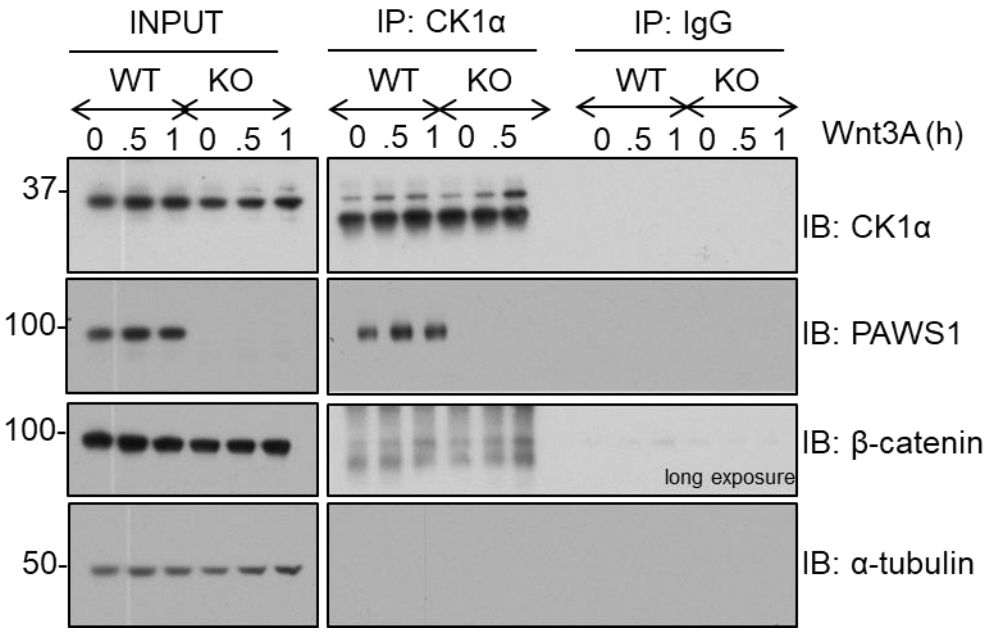

Figure 3- 19 PAWS1 has no effect the interaction between CK1α and β-catenin.

U2OS wild type (WT) and PAWS1$^{-/-}$ (KO) cells were treated with control conditioned medium or Wnt3A-conditioned medium and lysed after the indicated time points. Extracts (0.5 mg protein) were subjected to IPs using anti-CK1α or pre-immune IgG control (10 µg antibodies coupled to 10 µl packed protein-G sepharose beads). IPs were resolved by SDS-PAGE and immunoblotted with the indicated antibodies.

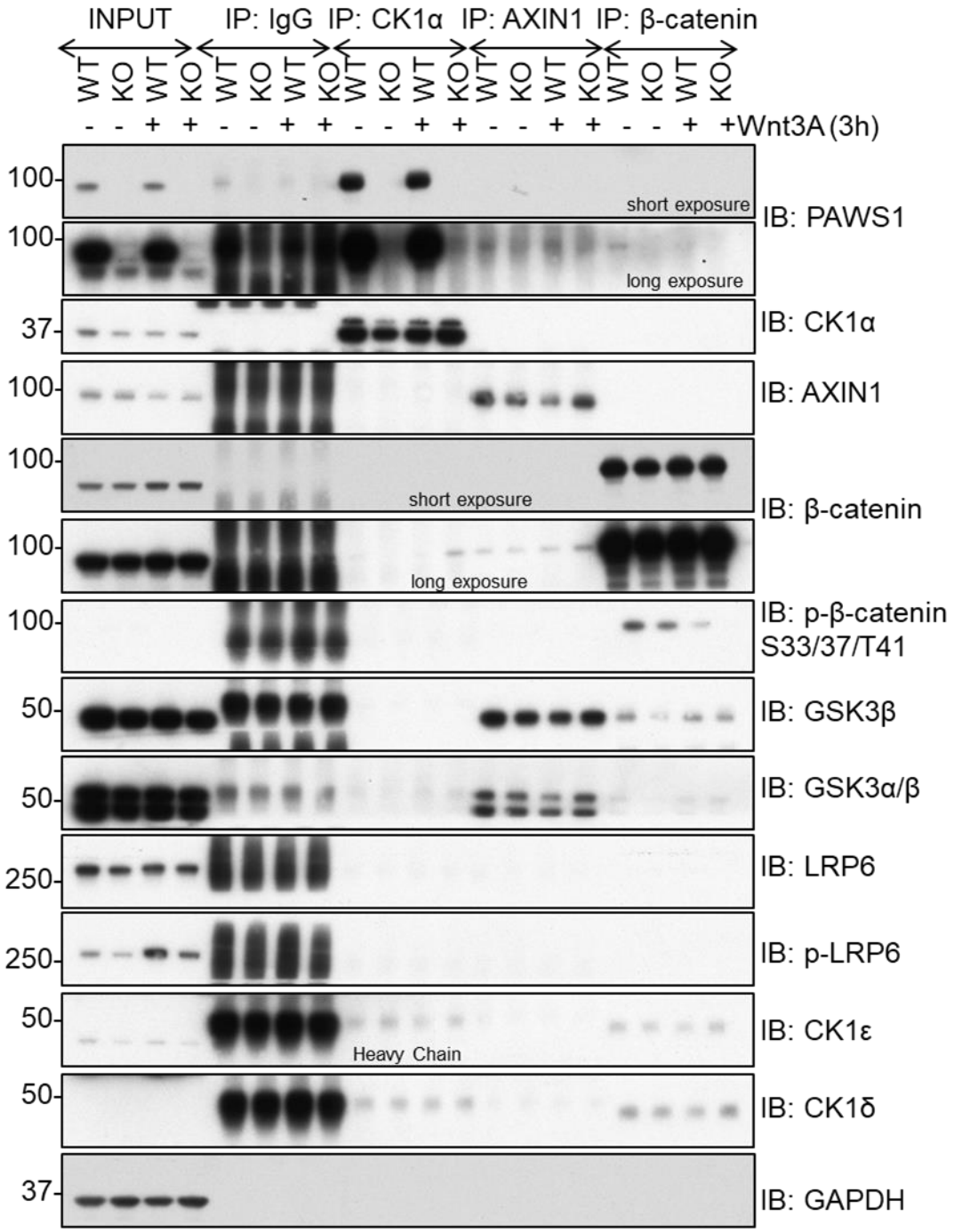

Figure 3- 20 PAWS1 does not appear to affect the composition of the destruction complex upon Wnt signalling activation.

U2OS wild type (WT) and PAWS1$^{-/-}$ (KO) cells were treated with control conditioned medium or Wnt3A-conditioned medium and the extracts (0.5 mg protein) were subjected to immunoprecipitation using antibodies against the endogenous CK1α, AXIN1 and β-catenin antibodies or anti-rabbit pre-immune IgG as a control (10 µg antibodies coupled to 10 µl packed protein-G sepharose beads). IPs were resolved by SDS-PAGE and immunoblotted with the indicated antibodies.

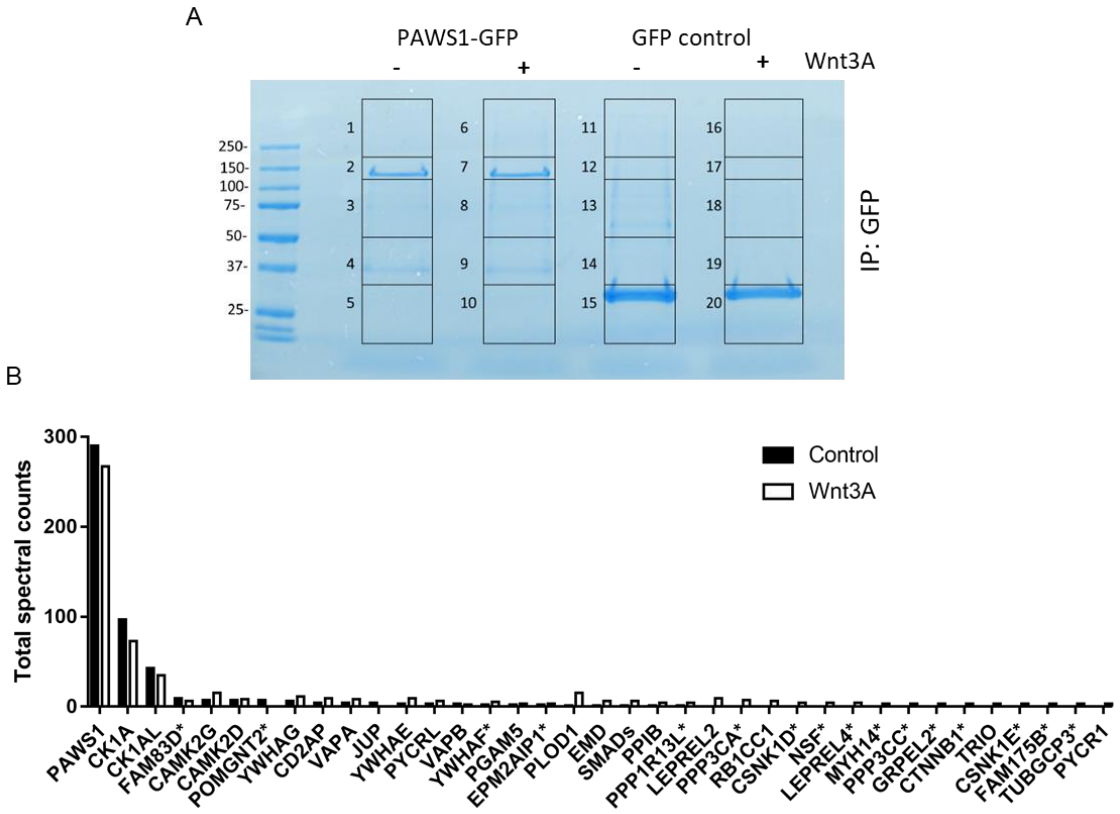

Figure 3- 21 PAWS1 interactome before and after Wnt3A stimulation

A. Stable U2OS Flp-In TRex cells were treated with 20 ng/ml doxycycline for 16 hours, for induction of PAWS1-GFP or GFP-control protein expression for 24 hours, and with Wnt3A conditioned medium or control medium for 3 hours prior to lysis. GFP pull downs were resolved by SDS-PAGE and the gel was stained with Coomassie. Each lane was cut in 5 pieces, which were subsequently processed for protein identification by Mass fingerprinting analysis.

B. PAWS1-GFP interacting proteins were plotted using total spectral counts for selected individual protein for both control (filled) and Wnt3A (open) conditions. Total spectral counts are defined as the sum of all the spectra associated with a specific protein within a sample, which includes also those spectra that are shared with other proteins. A spectral count of 3 or more in either control or Wnt3A condition in PAWS1-GFP IPs and no spectral counts in GFP control IPs were set as threshold for inclusion. All proteins, except those indicated with asterisks, were identified as endogenous PAWS1$^{GFP/GFP}$ interactors as well (Fig 3-12).

3.2.9 The PAWS1:CK1α complex facilitates the nuclear translocation of β-catenin upon Wnt stimulation

Wnt stimulation results in the accumulation of non-phosphorylated β-catenin, which translocates into the nucleus in order to activate the transcription of Wnt-target genes. Since the Wnt-induced phospho- and total β-catenin levels in U2OS cell extracts did not appear to change substantially to account for the inhibition of Wnt signalling caused by the loss of PAWS1, the cytoplasmic and nuclear distribution of β-catenin was analysed in wild type, PAWS1$^{-/-}$, and PAWS1^{WT} and PAWS1^{F296A} rescue U2OS cells after 3h of Wnt-stimulation (Fig 3-22A). The levels of the GSK3 and CK1 phospho-residues on β-catenin, the total levels and the non-phosphorylated - active β-catenin were monitored by Western blotting. Compared to wild type and PAWS1^{WT} rescue cells, both basal and Wnt-induced levels of β-catenin-pSer45, β-catenin-p/Ser33/Ser37/Thr41, active β-catenin and to some extent total β-catenin in nuclear, but not cytoplasmic, fractions were markedly lower in PAWS1$^{-/-}$ and PAWS1^{F296A} rescue cells (Fig 3-22A). This was particularly evident after quantification of the levels of active β-catenin in each fraction relative to that present in the cytoplasmic fraction of WT U2OS cells (Fig 3-22B), suggesting that PAWS1 promotes nuclear accumulation of β-catenin.

Because most of the β-catenin protein has been reported to be associated with the plasma membrane, the potential effect of PAWS1-loss on membrane associated pool of β-catenin was assessed. Indeed, β-catenin was enriched in the plasma membrane fractions and quite substantial amounts were observed in the cytoskeletal fractions, when compared to cytoplasmic and nuclear fractions (Fig 3-23). However, neither the loss of PAWS1 nor Wnt3A stimulation changed the protein levels of β-catenin in the membrane and cytoskeletal fractions (Fig 3-23). Under these conditions, very low levels of PAWS1 and CK1α were detected in the membrane and cytoskeletal fractions (Fig 3-23).

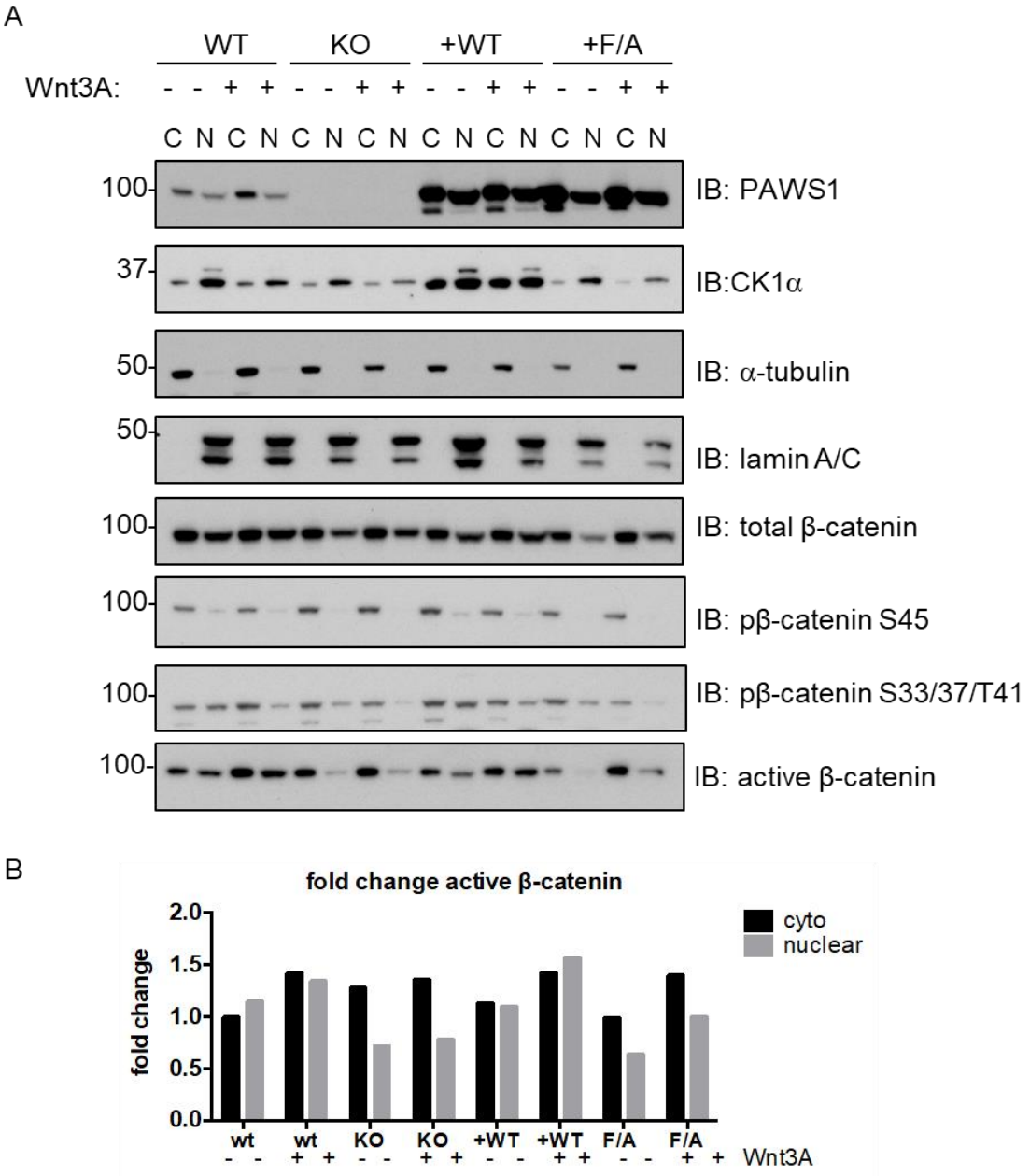

Figure 3- 22 PAWS1 promotes Wnt signaling through increased accumulation of nuclear active β-catenin.

A. U2OS wild type (WT), PAWS1$^{-/-}$ (KO), PAWS1^{WT} (+WT) and PAWS1^{F296A} (F/A) rescue cells were exposed to either Wnt3A or control medium for 3h followed by separation and preparation of cytoplasmic and nuclear fractions. The extracts were subjected to SDS-PAGE followed by western blot analysis with the indicated antibodies.

B. The fold changes in active β-catenin intensities in each fraction relative to those seen in the cytoplasmic fraction of control WT U2OS cells. The intensities of the active β-catenin bands in each fraction were quantified by using the ImageJ software.

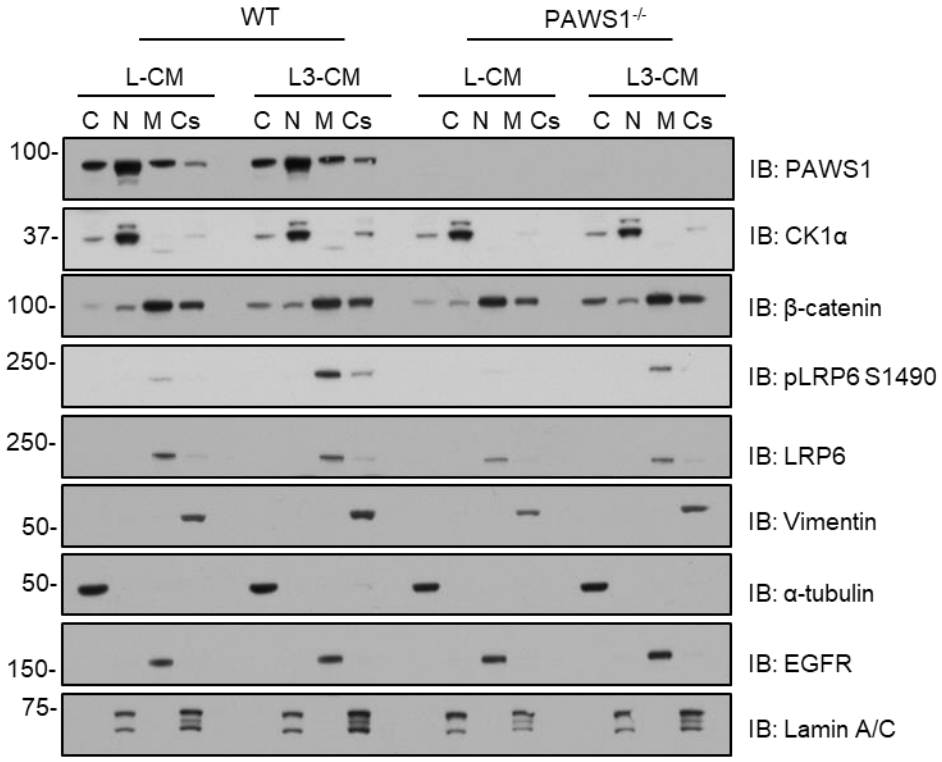

Figure 3- 23 PAWS1 does not affect the membrane-associated pool of β-catenin

U2OS wild type (WT) and PAWS1$^{-/-}$ cells were treated with control (L-CM) or Wnt3A conditioned medium (L3-CM) for 3 h and fractionated into cytoplasmic (C), nuclear (N), membrane (M) and cytoskeletal (Cs) fractions. Equal volumes of each fraction were resolved by SDS-PAGE followed by Western blotting with the indicated antibodies. α-tubulin was used as a cytosolic marker, Lamin A/C as a nuclear, LRP6 and EGFR were used as membrane markers and Vimentin was used as a cytoskeletal marker.

3.3 Discussion

In this chapter, a novel role for the poorly characterised protein PAWS1 in the activation of the canonical/β-catenin-dependent Wnt signalling has been presented. Canonical Wnt signalling plays critical roles during embryogenesis where together with the BMP signalling it shapes the formation of the body axis. PAWS1 was previously identified as an interactor of the transcription factor SMAD1 in the BMP signalling pathway (Vogt, Dingwell et al. 2014). It was shown to mediate the transcription of a subset of non-canonical (SMAD4-independent) BMP-target genes but without affecting the activation of the canonical BMP signalling cascade. One of the most striking finding about PAWS1 was its ability upon overexpression to induce the formation of a complete secondary axis in *Xenopus laevis* embryos. Similar phenotypes can be explained by either inhibition of BMP signalling or activation of the Wnt signalling pathway. Since PAWS1 was shown to associate with SMAD1, initially it was thought that this phenotype could be exerted due to potential inhibition of BMP signalling by PAWS1. However, it has been shown here that PAWS1 had no effect on canonical BMP signalling in both *Xenopus* embryos and in human cells.

Furthermore, PAWS1 was reported to be the first non-SMAD protein to be phosphorylated by the BMPR1 receptor in human cells in response to BMP stimulation. However, here it is shown that the mutation of the BMP-induced phosphorylation residues on PAWS1 did not impact its ability to induce a secondary axis in *Xenopus*. In line with this, the minimum PAWS1 fragment that was sufficient for axis duplication to occur lacks the BMPR1 phosphorylation sites. Taken all the above into account, PAWS1 appears to have no significant role in the regulation of the canonical BMP signalling pathway. Therefore, its ability to induce axis duplication cannot be attributed to inhibition of the BMP signalling, suggesting that it is likely to be mediated through the activation of Wnt signalling.

Indeed, the data presented in this chapter, clearly demonstrates a significant role of PAWS1 in regulating Wnt signalling in both *Xenopus* embryos and human cells. PAWS1 overexpression activated Wnt-transcriptional reporter activity in U2OS and HEK293 cells, even in the absence of Wnt stimulation. Similarly, PAWS1 microinjection in *Xenopus* embryos resulted in enhanced stabilisation of the co-injected β-catenin and subsequent activation of the Wnt-target genes *Siamois* and *Chordin* in the animal caps.

Moreover, knocking out PAWS1 gene from U2OS cells resulted in the attenuation of the Wnt-reporter activity as well as the transcription of the Wnt-target genes *AXIN2* and *CYCLIND1* in response to Wnt3A stimulation, compared to wild type cells. Collectively, these results have established that PAWS1 is a novel regulator of the Wnt signalling pathway.

The activation of Wnt signalling involves the binding of Wnt to its receptors FZD and LRP5/6, which then initiates a cascade of signalling events, including the phosphorylation of the cytoplasmic part of LRP6 and the formation of the Wnt signalosome close to the plasma membrane. This results in the stabilisation and the accumulation of β-catenin which then translocates to the nucleus to activate the transcription of the Wnt-target genes. Any alterations in the signalling cascade that inhibit the Wnt responses can be monitored by the reduced transcriptional activity of β-catenin. In *Xenopus* animal cap cells, expression of a dominant negative form of LRP6 (Lrp6m5) did not inhibit the PAWS1-induced *Siamois* expression, suggesting that PAWS1 activates Wnt signalling downstream of the Wnt receptor. Rather surprisingly, the loss of PAWS1 did not result in any substantial changes in either the levels or the phosphorylation of the major components of the destruction complex downstream of the LRP6, despite inhibition of the transcriptional Wnt/β-catenin activity. Hence, it could be hypothesised that PAWS1 probably functions downstream of the destruction complex, where it does not affect the phosphorylation status/or the stabilisation of β-catenin. Indeed, the data from this study support the notion that PAWS1 acts downstream of the destruction complex, as inhibition of β-catenin phosphorylation and its subsequent degradation by the GSK3 inhibitor could not restore Wnt-reporter activity in PAWS1$^{-/-}$ cells to the extent it did in the wild type cells.

The generation of a U2OS cell line which expresses PAWS1 with a C-terminal GFP tag under the endogenous promotor has allowed the identification of endogenous PAWS1 interactors that could potentially explain its role in the Wnt signalling pathway. Interestingly, the major interactor of PAWS1 was found to be CK1α, which is a central component of the Wnt signalling pathway. PAWS1 was shown to interact with CK1α independent of Wnt stimulation which might suggest that PAWS1 could be a novel global regulator of CK1α in cells, a hypothesis that is going to be discussed in the next chapter.

Remarkably, the association of PAWS1 with CK1α was proven to be critical for the activation of Wnt signalling both in *Xenopus* embryos and in human cells (Fig 3-24). Two residues, D^{262} and F^{296}, within the conserved domain of unknown function,

DUF1669, at the N-terminus of PAWS1 were mapped as key for mediating interaction with CK1α. Mutation of either CK1 binding residues on PAWS1 resulted in complete loss of the ability of PAWS1 to induce secondary axis in *Xenopus* embryos an activate Wnt signalling. In PAWS1$^{-/-}$ cells, PAWS1^{F296A} failed to rescue Wnt transcriptional reporter activity. One obvious explanation of these phenotypes would be that the interaction of PAWS1 with CK1α could regulate the sequestration of CK1α from the destruction complex resulting in reduced phosphorylation of β-catenin which would lead to increased β-catenin stabilisation. If this was true, PAWS1 depletion would result in enhanced association of CK1α with the components of the destruction complex and increased phosphorylation and degradation of β-catenin which would explain the compromised responses of the PAWS1$^{-/-}$ cells to Wnt signals. However, the data presented here does not favour this hypothesis, as neither the components of the destruction complex nor the CK1-mediated phosphorylation of β-catenin changed in PAWS1$^{-/-}$ cells compared to the wild type cells. A possible explanation for this could be that the interaction of PAWS1:CK1α occurs away from the destruction complex. This is supported by the observation that no other components of the destruction complex were identified in the mass spectrometric analysis of the PAWS1-GFP IPs with or without Wnt stimulation.

The event that follows the cytosolic accumulation of β-catenin in the Wnt signalling cascade is its translocation into the nucleus, which is crucial for it to activate the transcription of Wnt-target genes. However, the mechanisms that mediate the entry of β-catenin into the nucleus in response to Wnt signals are not fully understood. Here, it has been demonstrated that the loss of PAWS1 or interference of the PAWS1:CK1α interaction results in reduced accumulation of β-catenin in the nucleus and reduced transcription of the Wnt-target genes. To date, there are no references associating the CK1 isoforms with the nuclear/cytosolic shuttling of β-catenin. Both PAWS1 and CK1α were shown to localise both in the cytosol and the nucleus. Hence, binding of PAWS1 to CK1α could regulate the activity of CK1α towards different subsets of substrates, either in the cytosol or in the nucleus, that might be involved in the transport of β-catenin. Identifying the potential CK1 substrates that are regulated by its interaction with PAWS1 might help to elucidate the mechanisms that regulate the nuclear/cytosolic shuttling of β-catenin in the Wnt signaling pathway.

PAWS1 belongs to the FAM83 family of proteins, which all share the DUF1669 domain of unknown function. It is yet unknown if there is redundancy among the FAM83

proteins, which could potentially account for the observations that PAWS1$^{-/-}$ cells were not found to be completely unresponsive to Wnt stimulation. The possibility of other FAM83 members being involved in Wnt signalling as well as being binding partners of CK1 isoforms will be discussed in the following Chapter.

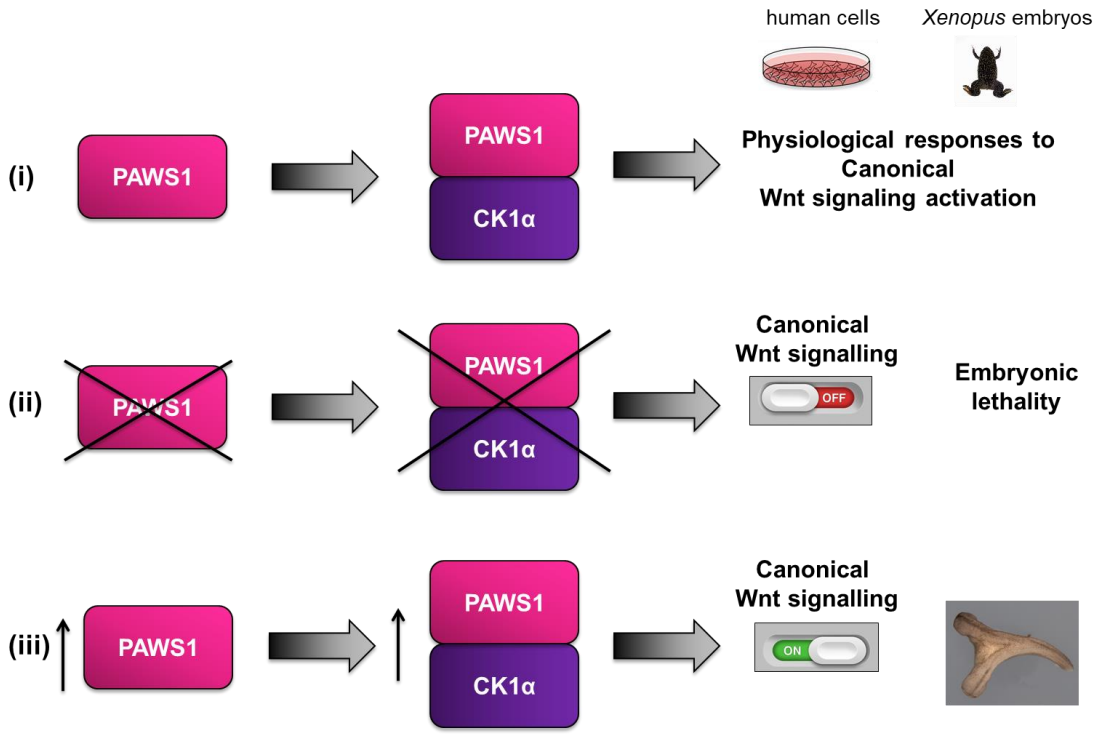

Figure 3- 24 Summary of the biological outcomes from the PAWS1:CK1α interaction in human cells and in *Xenopus* embryos

(i) Endogenous PAWS1 associates with CK1α and the complex formed mediates physiological responses to Wnt signals in cells and normal embryonic development in *Xenopus*. **(ii)** Depletion of PAWS1 by knocking out PAWS1 gene in human cells or by morpholinos in *Xenopus* embryos results in inhibition of Wnt signalling activation and lethality in cells and *Xenopus* respectively. Similarly, inhibition of PAWS1:CK1α interaction abrogates Wnt signalling activation. **(iii)** Overexpression of PAWS1 results in enhanced PAWS1:CK1α complex formation which leads to Wnt activation and axis duplication.

4. PAWS1 is a regulator of CK1α in cells

4.1 Introduction

CK1 isoforms play central roles in many cellular processes and their mis-regulation has been associated with human diseases including cancer and neurodegeneration (see 1.6.5). CK1 proteins are evolutionarily conserved, from prokaryotic organisms, such as bacteria, to all eukaryotic organisms. The conservation of the CK1 genes throughout evolution suggests key biological roles for these enzymes. Indeed, mice with homozygous deletion of CK1α or CK1δ exhibit early embryonic lethality (Etchegaray, Machida et al. 2009, Elyada, Pribluda et al. 2011). Despite advances made in establishing many biological roles for different CK1 isoforms, the precise mechanisms of their regulation in cells remain poorly defined. To date, our understanding about how these pleiotropic kinases achieve substrate specificity is limited to substrates that appear to interact with CK1 isoforms and primed substrates that conform to the CK1 consensus phosphorylation motif (see 1.6.3). Therefore, establishing how specific CK1 isoforms recognise and phosphorylate their substrates in specific subcellular compartments in response to specific signaling cues may provide opportunities for drug discovery against these enzymes.

In the previous Chapter, it was demonstrated that the PAWS1:CK1α complex plays a crucial role in the transduction of the Wnt signaling pathway. CK1α has been reported to play both positive and negative roes in the Wnt signaling pathway (Cruciat 2014). Overexpression of CK1α in *Xenopus* embryos has been shown to induce the formation of a secondary body axis via activation of Wnt signaling (Peters, McKay et al. 1999). However, ablation of CK1α from the gut epithelium has been linked to Wnt activation in that tissue (Elyada, Pribluda et al. 2011). This apparent discrepancy in CK1α function might be attributed to intricate spatiotemporal regulation of CK1α, a mode of regulation that would allow it to target unique subsets of substrates, in different cellular compartments. Given its robust interaction with CK1α, PAWS1 is a promising candidate that might act as key regulatory factor for CK1α in cells.

In this Chapter, the studies on the PAWS1:CK1α complex have been expanded, with the aim of understanding whether and how PAWS1 impacts CK1α function in cells. To address this, the following questions were formulated:

a) Does PAWS1 regulate the protein levels and/or the stability of CK1α?
b) Is PAWS1 a substrate of CK1α? If so, is PAWS1 function reliant on this phosphorylation event?
c) Does PAWS1 regulate the kinase activity of CK1α?
d) Does PAWS1 regulate a subset of CK1α substrates in cells?

4.2 Results

4.2.1 PAWS1 regulates the protein levels of CK1α

Driven by the previous observations that the protein levels of CK1α are significantly lower in the PAWS1$^{-/-}$ U2OS cells compared to the wild type controls (Fig 3-9), the expression of CK1α was analysed thoroughly, after restoration of PAWS1 protein levels in PAWS1$^{-/-}$ cells with wild type (PAWS1^{WT}) or various PAWS1 mutants (PAWS1^{F296A}, PAWS1F^{300A}, PAWS1$^{F296A/F300A}$ and PAWS1^{D262A}) (Fig 4-1). Restoring PAWS1^{WT} expression in PAWS1$^{-/-}$ cells resulted in restoration of endogenous CK1α levels, to those seen in wild type U2OS cells. Strikingly, restoration of the CK1α-interaction deficient mutants PAWS1^{F296A}, PAWS1$^{F296A/F300A}$ and PAWS1^{D262A}, did not elevate the endogenous CK1α protein levels to those seen in wild type cells, suggesting that the levels of endogenous CK1α protein are controlled by its interaction with PAWS1 (Fig 4-1). Consistent with these observations, the restoration of PAWS1^{F300A}, which interacts with CK1α, resulted in restoration of the endogenous CK1α levels to those seen in wild type U2OS cells (Fig 4-1). As expected, the expression of GFP control in PAWS1$^{-/-}$ cells, did not elevate the endogenous CK1α protein levels to those seen in wild type cells (Fig 4-1). These data suggest that PAWS1 controls the levels of endogenous CK1α protein levels, which could be mediated through enhanced stabilisation via reduced protein degradation, enhanced transcription or other mechanisms.

Proteins that are part of the same complex tend to be under co-ordinated expression so that their abundance is co-regulated (Ori, Iskar et al. 2016). Consistent with this notion, transient depletion of endogenous CK1α protein with siRNA duplexes led to a concomitant substantial reduction of PAWS1 protein levels, as well (Fig 4-2). These observations support the reciprocal nature of PAWS1 and CK1α in regulating the cellular protein levels of the other protein.

Next, the analysis of the correlation between endogenous PAWS1 and CK1α protein levels was expanded to a panel of mammalian cell lines (Fig 4-3). PAWS1 protein expression was absent in many human cancer cells, including SK-ES (bone), MCF-7 (breast), SK-N-MC (brain) and PC3 (prostate) cells while robust PAWS1 expression was observed in HCT116 (colorectal), HEPG2 (liver), PNTA1 (prostate) and HeLa (cervix) cells. Strikingly, the expression of PAWS1 correlated with the levels of CK1α protein in these cell lines (Fig 4-3A). Cells that lacked PAWS1 expression generally correlated with no detectable or low levels of CK1α protein, whereas cells that had relatively higher

PAWS1 levels also expressed higher levels of CK1α (Fig 4-3A). Interestingly introduction of $PAWS1^{WT}$ expression in PC3 cells using retroviral infection, also led to increased levels of CK1α (Fig 4-3A). No correlation in protein expression was evident between PAWS1 and CK1ε, which was not identified as a PAWS1-interactor. The immunoblots were analysed by densitometric quantification followed by statistical correlation analysis using the Pearson's correlation coefficient (Pearson 1992), which measured the linear relationship between PAWS1 and CK1α protein levels. Pearson's correlation coefficient (r) is constrained as $-1 \leq r \leq 1$, while positive values denote positive correlation, negative values denote negative correlation and a value of 0 denoted no correlation. The magnitude of the Pearson's r coefficient determines the strength of the correlation, while the p-value denotes the significance of the correlation (Evans 1996). Thus, when $p<0.05$, the correlation is significant whereas when $p>0.05$ there is no significant correlation. Positive correlation was found between PAWS1 and CK1α protein levels, ($r = 0.4128$, $p = 0.0281$) which confirmed that there is a correlation between the variance of PAWS1 and the variance of CK1α protein levels in the panel of the cell lines tested. No significant correlation was found between PAWS1 and CK1ε protein levels ($r= 0.2279$, $p = 0.1538$) (Fig 4-3B, C).

In order to test whether the correlation in PAWS1 and CK1α protein levels was due to a similar correlation in their mRNA expression, PAWS1 and CK1α mRNA levels were assessed in six of the above mammalian cell lines (Fig 4-4). The Pearson's correlation coefficient, which was used to determine the relationship between the PAWS1 and CK1α mRNA levels, showed that there is no significant correlation at the mRNA level ($r = 0.2254$, $p = 0.0508$), indicating that at least in the cell lines tested, the interrelationship between PAWS1 and CK1α protein levels occurs post-translationally.

To investigate if PAWS1 regulates the turnover of CK1α protein in cells, proteasomal and lysosomal inhibitors of protein degradation were used. Poly-K48-linked-ubiquitinated proteins are targeted for proteasomal degradation, which can be blocked with Bortezomib, a selective and potent inhibitor of the proteasome (Adams, 2003). Proteasomal inhibition did not rescue the reduced CK1α levels caused by PAWS1 depletion to those seen in wild type cells (Fig 4-5A). Blocking the autophagic-lysosomal degradation pathway with Bafilomycin A1, which inhibits lysosomal acidification through blocking the action the vacuolar-type H^+-ATPase (Yoshimori et al., 1991), did not enhance the stability of CK1α protein either (Fig 4-5B). Therefore, the lower levels of CK1α protein observed in $PAWS1^{-/-}$ cells compared to the wild type cells are unlikely

to be due to increased CK1α protein degradation via the proteasomal or lysosomal pathways. Similarly, the mRNA levels of CK1α were comparable in PAWS1^{WT}, PAWS1$^{-/-}$ and PAWS1^{F296A} rescue cells (Fig 4-5C), suggesting that the PAWS1 regulation of CK1α protein levels is unlikely to be through its transcriptional regulation. Collectively, these results suggest that the PAWS1 regulation of CK1α protein levels is unlikely to be due to the regulation of CK1α turnover through proteasomal or lysosomal pathways, nor through transcriptional modulation.

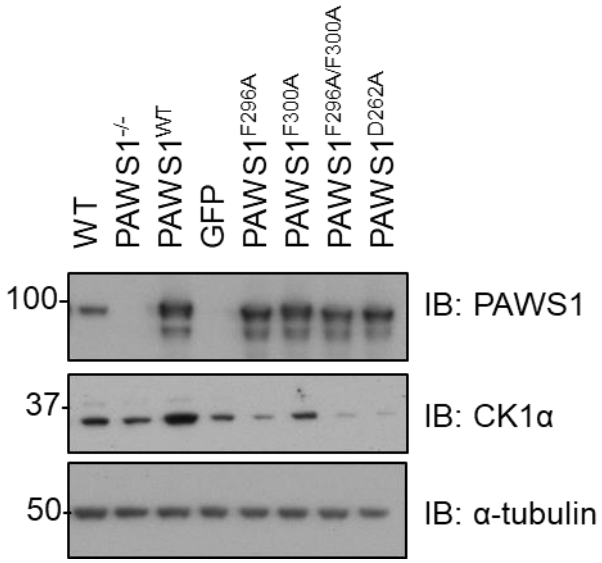

Figure 4- 1 PAWS1 regulates the protein levels of CK1α in cells.

Cell extracts (20 μg of protein) from U2OS wild type, PAWS1$^{-/-}$ and PAWS1$^{-/-}$ cells in which PAWS1^{WT}, GFP control, PAWS1^{F296A}, PAWS1^{F300A}, PAWS1$^{F296A/F300A}$ or PAWS1^{D262A} was stably restored, were resolved by SDS-PAGE and immunoblotted with the indicated antibodies.

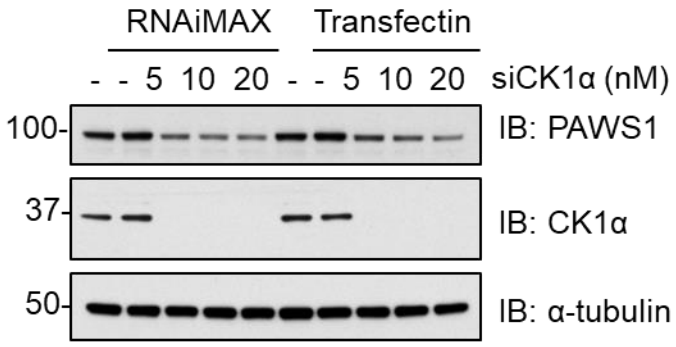

Figure 4- 2 RNAi-mediated silencing of CK1α downregulates PAWS1 protein levels

CK1α expression was silenced in U2OS cells with indicated amounts of siRNA targeted against CK1αusing two different transfection methods (RNAi-Max or TransFectin). Cells

were lysed after 48 h and cell extracts (20 µg of protein) were resolved by SDS-PAGE and immunoblotted with the indicated antibodies.

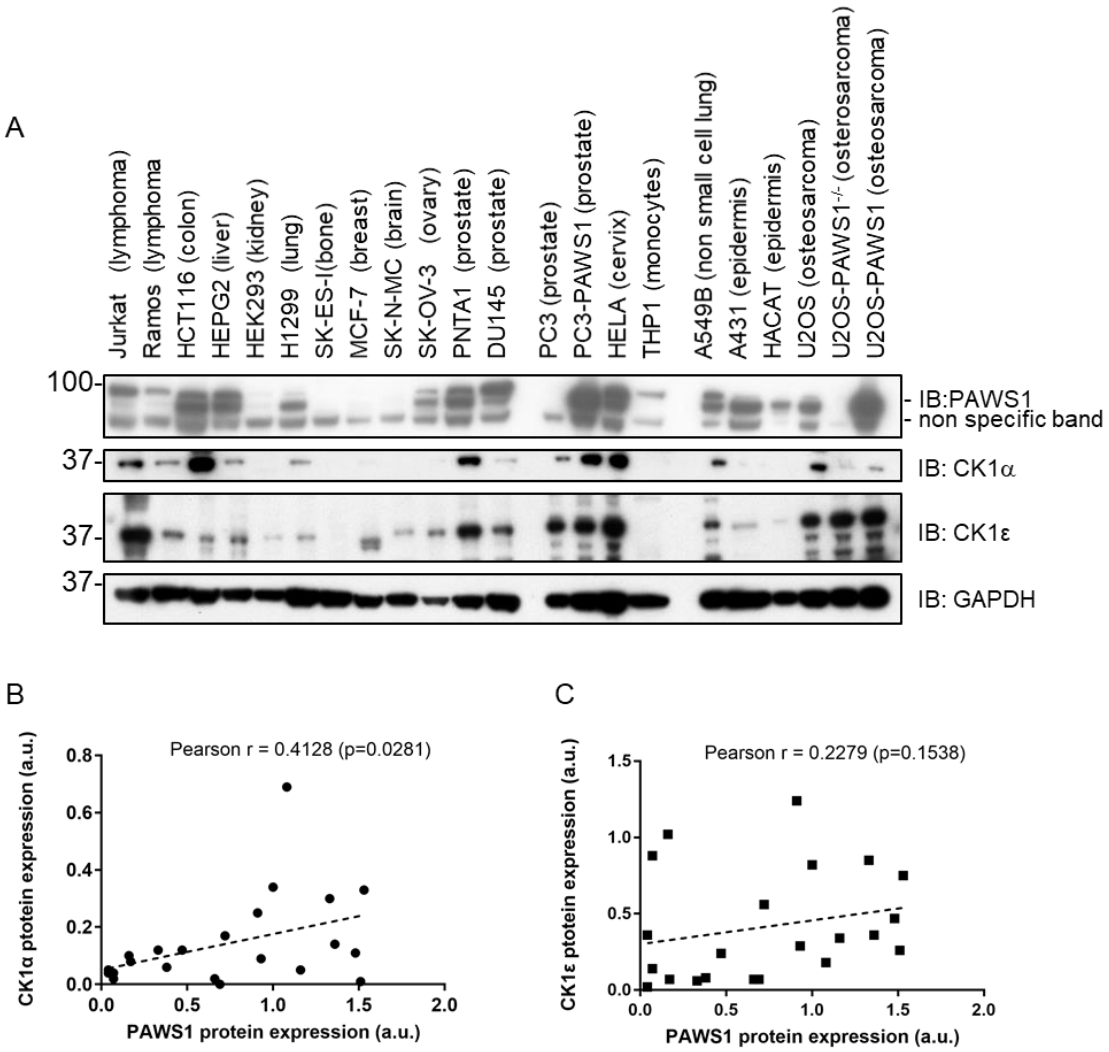

Figure 4- 3 The protein levels of CK1α correlate with the protein levels of PAWS1 in mammalian cell lines

A. Expression of PAWS1 and CK1α protein in the indicated cell line extracts (10 µg of protein) was monitored by Western blotting. Cell extracts were kindly provided by Dr Christophe Lachaud.

B. Pearson's correlation plots of PAWS1 and CK1α protein expression (normalized to GAPDH) based on densitometric quantification of immunoblots from (A); a.u.= arbitrary units. Pearson r coefficient and one-tailed p-values were calculated with Prism6 software.

C. Same as (B) except that PAWS1 and CK1ε protein levels were quantified and plotted.

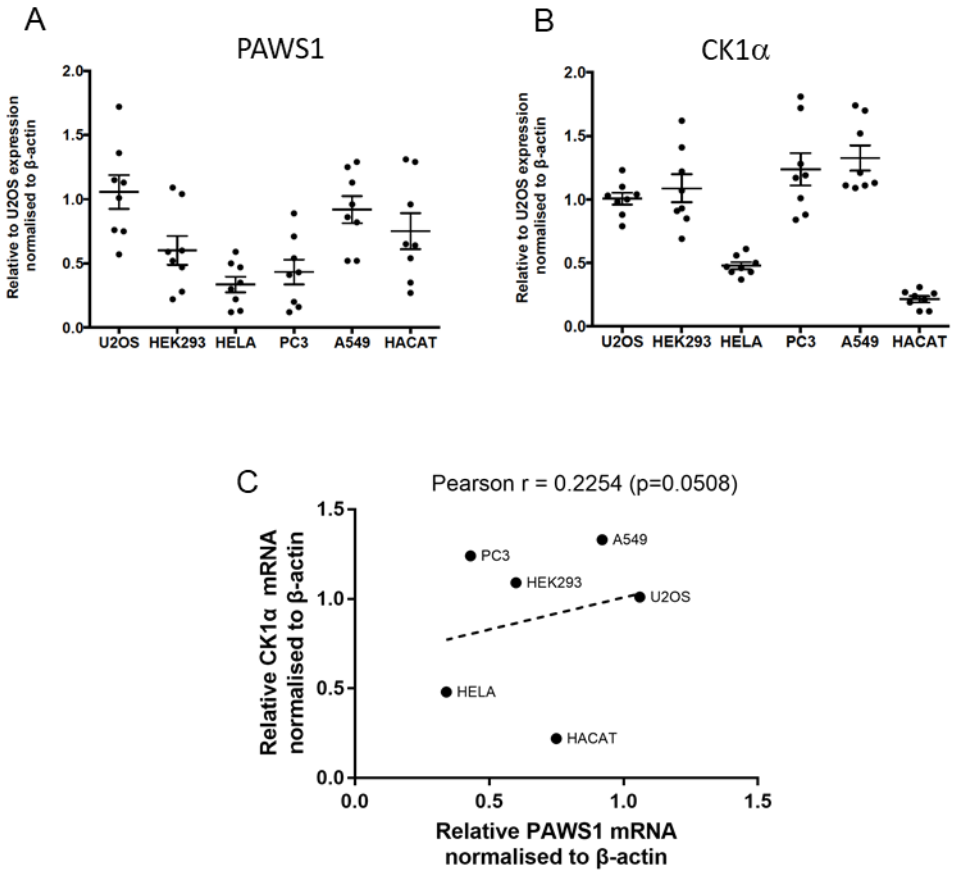

Figure 4- 4 The mRNA levels of PAWS1 do not correlate with the mRNA levels of CK1α in mammalian cell lines

A. Relative expression of PAWS1 mRNA in the indicated cancer cell lines was measured by qPCR and plotted relative to expression in U2OS cells (n=3; Error bars represents ±SEM, dots represent technical replicates).

B. Relative expression of CK1α mRNA in the indicated cancer cell lines was measured by qPCR and plotted relative to expression in U2OS cells (n=3; Error bars represents ±SEM).

C. Correlation plot of relative PAWS1 and CK1α mRNA expression (normalized to β-actin) in the indicated cancer cell lines. Pearson r coefficient and one-tailed p-values were calculated with Prism6 software.

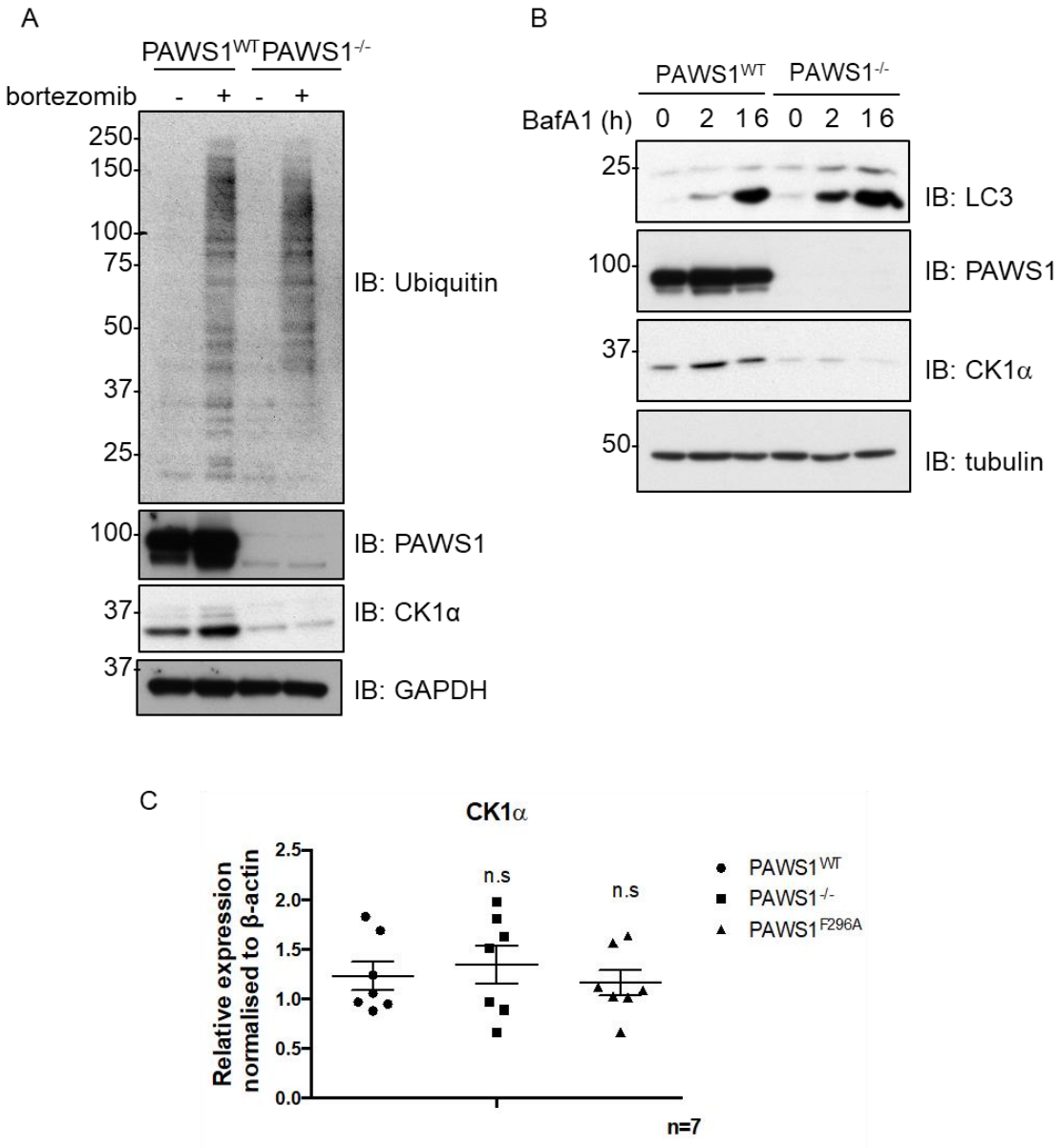

Figure 4- 5 PAWS1 regulates the CK1α protein but not mRNA levels in cells

A. PAWS1^{WT} and PAWS1$^{-/-}$ U2OS cells were treated with 10 μM of the proteasome inhibitor Bortezomib for 6 h before lysis and extracts (20 μg of protein) were resolved by SDS-PAGE and immunoblotted with the indicated antibodies.

B. PAWS1^{WT} and PAWS1$^{-/-}$ U2OS cells were treated with 50 μM Bafilomycin A1 (BafA1) for 2 or 16 h before lysis and extracts (20 μg of protein) were resolved by SDS-PAGE and immunoblotted with the indicated antibodies.

C. CK1α mRNA in PAWS1$^{-/-}$ cells rescued with PAWS1^{WT} or GFP control was analysed by qPCR. Data are represented as fold changes over controls and normalized internally to β-actin control. (n.s.: no statistical significance; n=3; Error bars represent ±SEM, dots represent technical replicates).

4.2.2 PAWS1 is phosphorylated by CK1α in vitro

CK1 isoforms phosphorylate numerous proteins in cells. Armed with this knoweldge, the next aim was to determine whether PAWS1 could be a *bona fide* substrate of CK1α. For this, an *in vitro* kinase assay was set up using recombinant GST-CK1α protein and full-length GST-PAWS1-6xHis, both purified from *E. coli.* As seen in Fig 4-6A, PAWS1 was phosphorylated robustly by CK1α, while no signal was observed in the absence of PAWS1. To eliminate the possibility that a contaminating bacterial kinase might be responsible for this phosphorylation, the DUF1669 domain of FAM83A was expressed with a GST-tag and purified at the same time as PAWS1, and included as a control. β-catenin is one of the many CK1 substrates (Liu, Li et al. 2002) and therefore GST-β-catenin was used as a positive control for the kinase assay. The extent of PAWS1 phosphorylation by CK1α was similar to that of β-catenin, although comparatively more β-catenin than PAWS1 was used in the assay. No signal was observed in the absence of CK1α, eliminating the possibility that PAWS1 was phosphorylated by a contaminating bacterial kinase. Under the conditions employed, DUF1669-FAM83A-GST was not phosphorylated by CK1α (Fig 4-6B). Furthermore, the use of the CK1 inhibitor D4476 (Rena, Bain et al. 2004) at 10 μM blocked the phosphorylation of PAWS1 by CK1α *in vitro* (Fig 4-6C).

Having established that CK1α phosphorylates PAWS1 *in vitro*, the CK1α phosphorylation sites on PAWS1 were determined by Edman sequencing and mass-spectrometry (Fig 4-7). PAWS1 was phosphorylated by CK1α using γ^{32}P-ATP *in vitro* and the reaction sample was resolved by SDS-PAGE. The γ^{32}P-PAWS1 band was excised, digested with trypsin and the resulting peptides were separated by chromatography on a C_{18} column, using an increasing acetonitrile gradient. Three peaks of ^{32}P release were observed, with the major peak appearing after 54 min. Analysis of this eluted phospho-peptide by mass spectrometry revealed the PAWS1 tryptic peptide RPSVASSVSEEYFEVR with an additional single phospho-modification. To determine the precise phosphorylated residue in the ^{32}P-labelled peptide, solid-phase Edman degradation was employed (Performed by R. Gourlay). ^{32}P radioactivity was released after the seventh cycle of Edman degradation, suggesting that CK1α phosphorylates PAWS1 on S614 (Fig 4-7B). Analysis of the two minor peaks revealed indiscernible phospho-sites, potentially T509/S610/T145 and S614/S781 (Fig 4-7C).

To confirm the major phosphorylation site identified by mass spectrometry and Edman degradation, an *in vitro* kinase assay was set up. In this assay, wild type PAWS1,

as well as the PAWS1-S614A mutant expressed in bacteria, were used as substrates with wild type or catalytically inactive (kinase dead; KD) CK1α. Wild type CK1α phosphorylated PAWS1 but not the PAWS1-S614A mutant, confirming that S614 is the main residue on PAWS1 that is phosphorylated by CK1α *in vitro* (Fig 4-7D). CK1α KD did not phosphorylate PAWS1 or the PAWS1-S614A mutant (Fig 4-7D). Due to the limitations of the pSer^{614} PAWS1 antibody, it has not been possible to validate whether endogenous PAWS1 is phosphorylated at S614 in cells. Therefore, future research will reveal if PAWS1 is indeed a *bona fide* substrate of CK1α *in vivo*.

It was previously demonstrated that the minimum PAWS1 protein fragment that is able to induce axis duplication in *Xenopus* embryos does not include the S614 residue. In line with this, mRNA injection of PAWS1^{S614A} phospho-mutant did not inhibit the PAWS1-induced axis duplication phenotype (Fig 4-8A). Additionally, FLAG-PAWS1^{S614A} could still interact with endogenous CK1α in U2OS cells to a similar extent as PAWS1^{WT} did. These results suggest that phosphorylation of PAWS1 is not required for its function in Wnt signalling, or its interaction with CK1α.

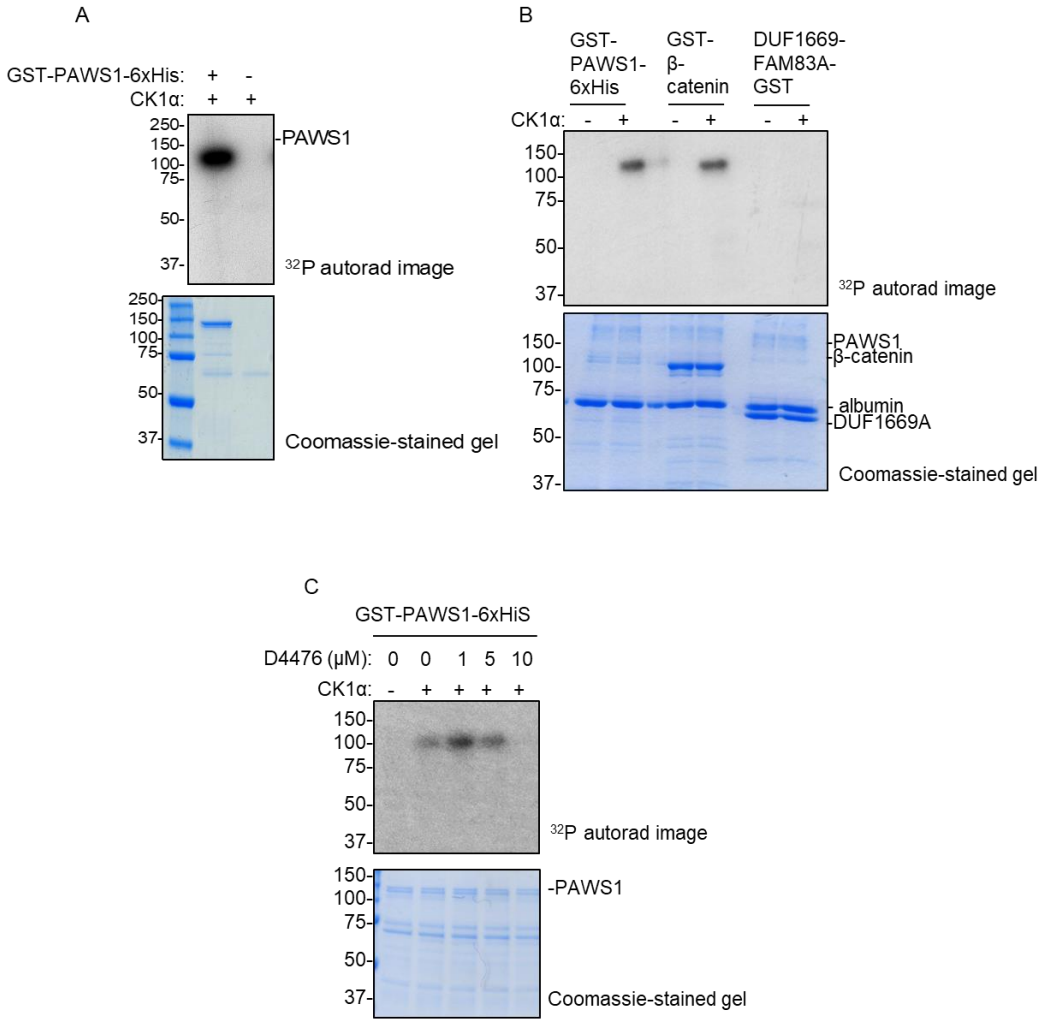

Figure 4- 6 PAWS1 is phosphorylated by CK1α *in vitro*

A. *In vitro* kinase assay with GST-CK1α and GST-PAWS1-6xHis in the presence of ^{32}P-ATP (500 cpm/pmol). The reaction was stopped after 30 min at 30 °C and the samples were resolved by SDS-PAGE. The gel was Coomassie stained and radioactivity was analysed by autoradiography.

B. Same as A except that GST-β-catenin and FAM83A (DUF1669)-GST were used as substrates, too.

C. Same as A except that the assays were performed in the presence of the indicated concentrations of the CK1α inhibitor D4476.

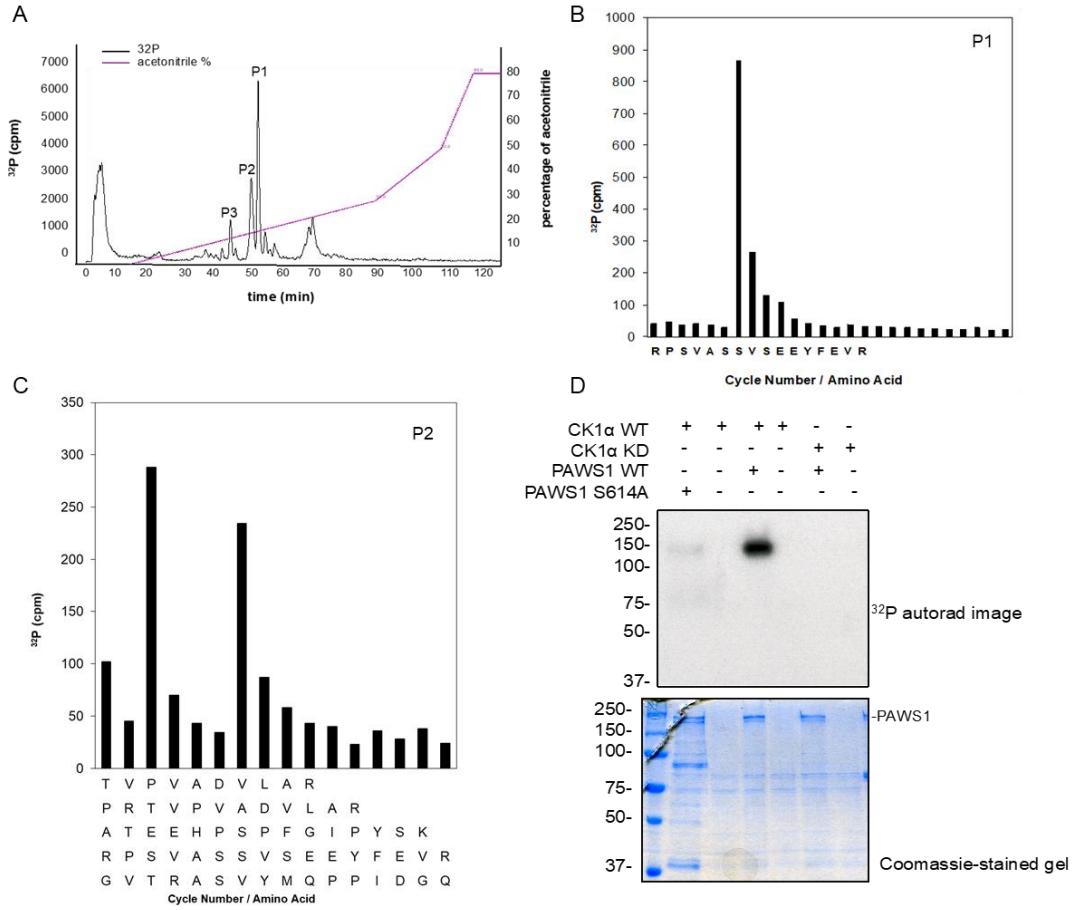

Figure 4- 7 CK1α phosphorylates PAWS1 at S614 *in vitro*

A. GST-PAWS1-6xHis was phosphorylated by CK1α in vitro as in 4-6A, excised, trypsin-digested and resolved by HPLC on a C_{18} column on an increasing acetonitrile gradient as indicated. Three peaks of ^{32}P release were observed (P1-3). Analysis of the P1 by mass spectrometry revealed the presence of RPSVASSVSEEYFEVR peptide with an additional single phosphor-moiety.

B. Solid-phase sequencing of peak P1 revealed the release of ^{32}P after the seventh cycle of Edman degradation corresponding to RPSVASS*VSEEYFEVR phospho-peptide, where S* denotes pS614. (Performed by R. Gourlay).

C. Solid-phase sequencing of peak P2 revealed the release of ^{32}P after the third and the seventh cycles of Edman degradation. All possible phospho-peptides are indicated but none were detected by mass spectrometry. (performed by R. Gourlay).

D. *In vitro* kinase assay with GST-CK1α or GST-CK1α KD (kinase dead) and PAWS1 WT (GST-PAWS1-6xHis) or PAWS1 S614A (GST-PAWS1 S614A) in the presence of ^{32}P-ATP (500 cpm/pmol). The reaction was stopped after 30 min at 30 °C and the samples were resolved by SDS-PAGE. The gel was Coomassie stained and radioactivity was analysed by autoradiography.

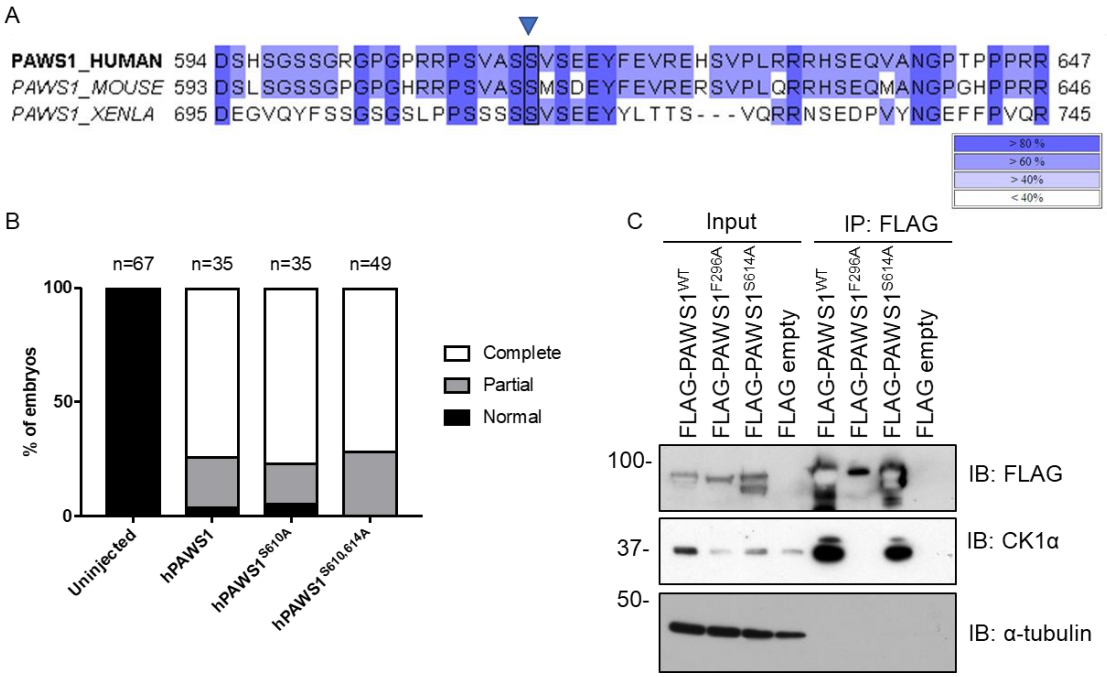

Figure 4- 8 The PAWS1 S614A mutant still binds to CK1α and induces axis duplication in *Xenopus* embryos

A. Sequence alignment of human, mouse and *Xenopus laevis* (XNLA) PAWS1 around the conserved S614 phosphorylation residue, indicated by the blue arrow. Alignment was performed with ClustalO in Jalview 2.10.3 and colouring indicates the % of sequence identity as shown in the box.

B. Human PAWS1^{WT}, hPAWS1^{S610A} and hPAWS1$^{S610A/S614A}$ induce axis duplication in *Xenopus* embryos.

C. PAWS1$^{-/-}$ U2OS cells were transfected with FLAG-PAWS1^{WT}, FLAG-PAWS1^{F296A}, FLAG-PAWS1^{S614A} or FLAG-empty. 48h later, cells were lysed and cell extracts (20 µg of protein) were subjected to FLAG-IPs and were resolved by SDS-PAGE, followed by immunoblotting with the indicated antibodies.

4.2.3 PAWS1 does not affect the kinase activity of CK1α in vitro or in cells

To assess whether PAWS1 regulates the kinase activity of CK1α, a kinase assay was performed on the PAWS1-associated CK1α, immunoprecipitated from cell extracts, against an optimised CK1 peptide substrate (CK1tide). For this assay, endogenous PAWS1 was immunoprecipitated from U2OS wild type and PAWS1$^{-/-}$cell extracts and subjected to an *in vitro* kinase assay using ^{32}P-ATP and the CK1tide peptide substrate. Robust CK1α kinase activity was detected in PAWS1 IPs from wild type but not from PAWS1$^{-/-}$ cell extracts (Fig 4-9A). The detection of endogenous CK1α in PAWS1 IPs from wild type but not from PAWS1$^{-/-}$ cell extracts by Western blotting, correlated with the observed *in vitro* kinase activities against CK1tide (Fig 4-9A). This result indicates that association of PAWS1 with CK1α, at the least, does not inhibit the intrinsic CK1α kinase activity.

Next, it was tested whether PAWS1 could potentiate the kinase activity of recombinant CK1α through association. *In vitro* kinase assays were performed with ^{32}P-ATP and the CK1tide peptide, using recombinant WT or KD CK1α, with or without recombinant PAWS1^{WT} or the CK1α-binding deficient PAWS1^{F296A} mutant. As expected, CK1α WT displayed *in vitro* kinase activity against the CK1tide, while CK1α KD did not (Fig 4-9B). The addition of either PAWS1^{WT} or PAWS1^{F296A} did not substantially affect the ability of CK1α to phosphorylate CK1tide (Fig 4-9B). Collectively, these data suggest that PAWS1 is unlikely to directly regulate the kinase activity of CK1α *in vitro* or in cells.

Next, the impact of CK1α kinase activity and the synergistic impact of PAWS1 were investigated in *Xenopus* embryos. As shown in Fig 4-10A, overexpression of either wild type PAWS1 or wild type CK1α in *Xenopus* embryos induced a secondary body axis. However, overexpression of catalytically inactive mutant CK1α (D136N; kinase dead; KD) alone did not induce axis duplication in *Xenopus* embryos. These results indicated that the kinase activity was necessary for CK1α to induce the axis duplication phenotype. Given the observations that PAWS1 mutants incapable of binding CK1α do not induce axis duplication (Fig 3-18A, B), the potential impact of CK1α activity on the ability of PAWS1 to induce axis duplication was investigated. First, to evaluate if PAWS1 could still interact with CK1α KD, co-expression/IP experiments were performed and showed that both CK1α WT and KD interact robustly with FLAG-PAWS1 (Fig 4-10B). Nevertheless, in *Xenopus* embryos, when PAWS1 and WT CK1α were co-expressed, the embryos exhibited normal phenotypes (Fig 4-10A). A possible explanation for this is that

PAWS1 inhibits CK1α activity, hence overexpression of CK1α counters the PAWS1 effects on axis duplication. However, as it has been shown above, PAWS1 does not impair CK1α activity *in vitro*. Therefore, these observations suggest that overexpression of either PAWS1 or CK1α alone in embryos potentially disrupt the endogenous PAWS1:CK1α complex homeostasis, resulting in concurrent disturbances in Wnt signalling that results in the axis duplication phenotypes observed. In contrast, when these proteins are co-expressed, this interference on the endogenous PAWS1:CK1α complex is minimized, resulting in normal phenotypes. If this were the case, then one would expect similar outcomes using a catalytically inactive mutant of CK1α that still interacts with PAWS1 with similar affinity to the wild type CK1α (Fig 4-10A). Indeed, co-expression of PAWS1 and the catalytically inactive CK1α mutant in *Xenopus* embryos also resulted in completely normal embryos (Fig 4-10A). Furthermore, CK1 δ and ε isoforms, which do not interact with PAWS1, also induced axis duplication when expressed on their own, whereas overexpression of CK1ε KD had no effect on the axis duplication (Fig 4-10A). Axis duplication caused by PAWS1 was not affected when co-expressed with CK1ε WT or KD, or CK1δ WT (Fig 4-10A).

The results so far show that PAWS1 and CK1α interact and co-localise in cells and this interaction is essential for the activation of the Wnt signalling pathway as well as the induction of axis duplication in *Xenopus* embryos. However, PAWS1 does not affect the intrinsic CK1α catalytic activity. Collectively, these data suggest that the PAWS1:CK1α complex potentially regulates the phosphorylation of key CK1α substrates within the Wnt signalling pathway. Therefore, a global phospho-proteomic approach was undertaken to establish PAWS1-dependent CK1α substrates in U2OS cells.

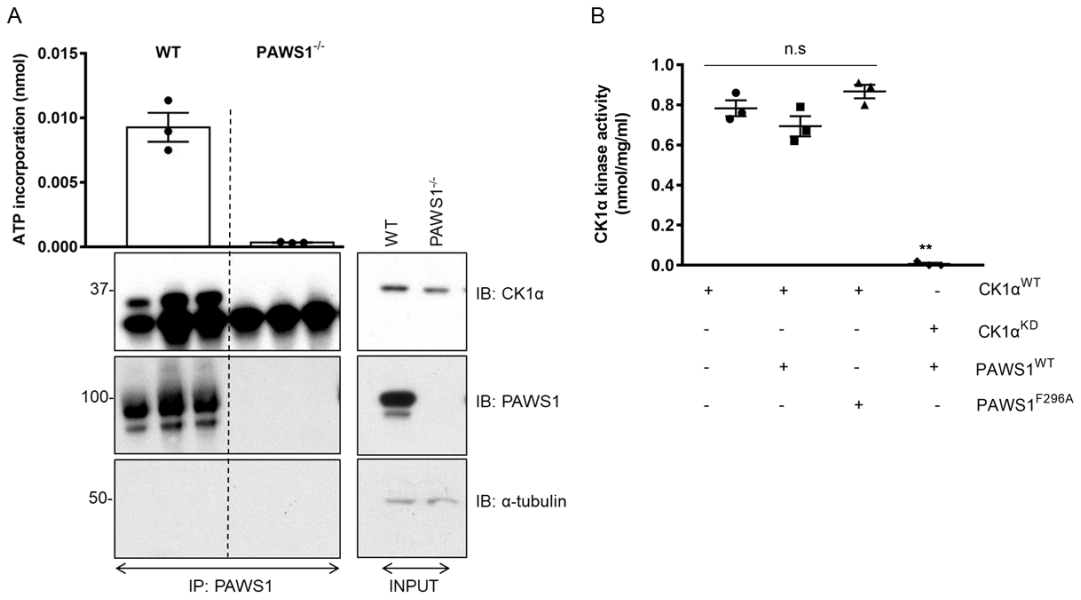

Figure 4- 9 PAWS1 does not affect the kinase activity of CK1α in cells or *in vitro*

A. Endogenous PAWS1 was immunoprecipitated from wild type and PAWS1$^{-/-}$ U2OS cells (n=3) and the associated CK1α kinase activity was measured following a kinase assay using ^{32}P-ATP and the CK1tide peptide substrate. One third of the PAWS1 IP samples were resolved by SDS-PAGE and immunoblotted with the indicated antibodies (bottom panel) (n=3, error bars represent ±SEM).

B. *In vitro* wild-type (WT) or catalytically inactive (KD) CK1α kinase assay using CK1tide as a substrate in the presence or absence of recombinant PAWS1^{WT} or PAWS1^{F296A}.

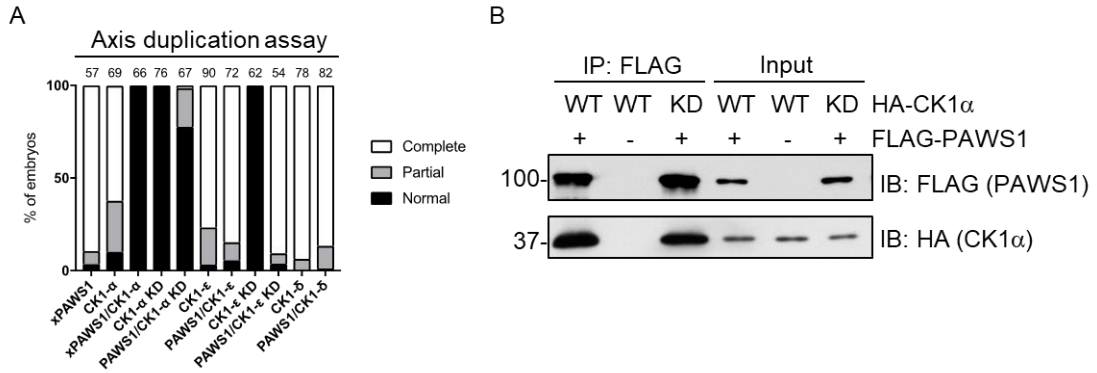

Figure 4- 10 CK1α kinase activity is required for PAWS1-induced axis duplication in *Xenopus* embryos

A. 250 pg of xPAWS1 and 300 pg of the indicated CK1 isoform mRNAs were injected into 1 ventral bastomere at the 4-cell stage. Axis induction was assessed at stage 28 (tadpole stage). (Performed by K. Dingwell, The Francis Crick Institute, London).

B. U2OS cells were co-transfected with HA-CK1α (WT or KD) and FLAG-PAWS1 and cells were lysed after 36 h. Cell extracts (20 μg of protein) were subjected to FLAG IP, followed by SDS-PAGE and immunoblotting with the indicated antibodies.

4.2.3 Global phospho-proteomics comparison of wild type versus PAWS1$^{-/-}$ U2OS cells

To identify potential CK1α substrates that are regulated by the PAWS1-CK1α interaction, a quantitative phospho-proteomics approach was undertaken. Specifically, U2OS wild type, PAWS1$^{-/-}$ and PAWS1$^{-/-}$ rescued with wild type PAWS1 (PAWS1^{WT}) cells were treated with control- or Wnt3A-conditioned medium for 3 h and cell extracts were processed for phospho-proteomics analysis as described in Fig 4-11. The data for each experimental condition is representative of four replicates. Overall, 5170 phospho-peptides were identified, for which the phosphorylation events could be mapped to specific residues. For the quantitative analysis of the phosphoproteins under different experimental conditions, the change of phospho-peptides have been paired against cell lines and in either control or Wnt3A treatments. Student t-tests were performed for measuring statistical significance between different comparisons.

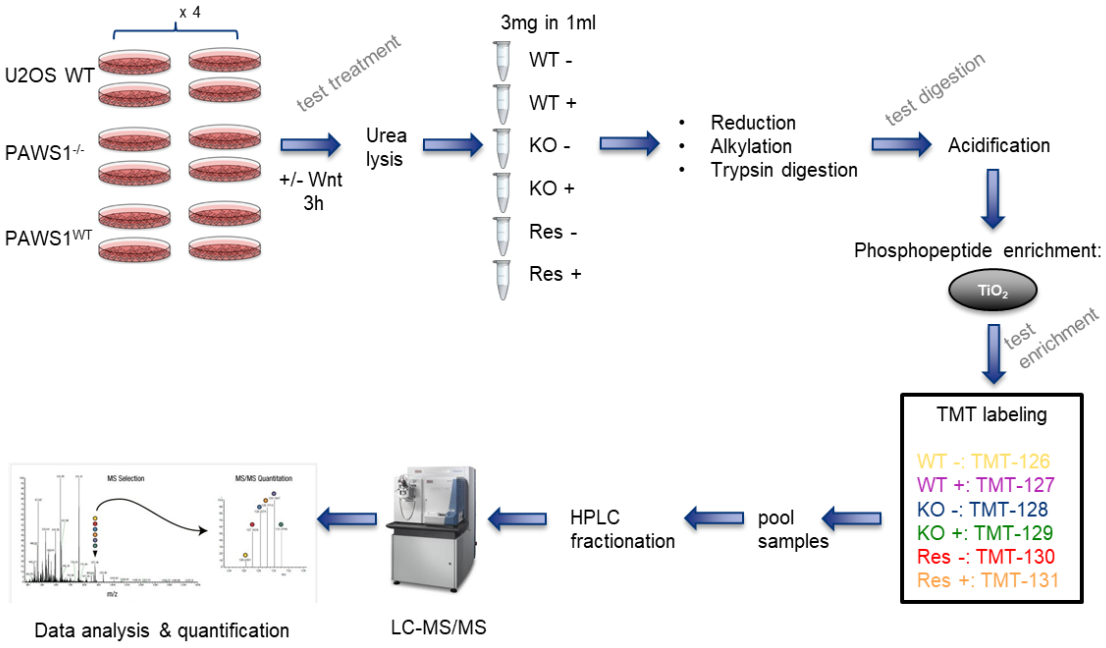

Figure 4- 11 Overview of the quantitative phosphoproteomics experiment

Schematic representation of the workflow. U2OS^{WT}, PAWS1$^{-/-}$ and PAWS1^{WT} rescue (Res) cells were seeded in 15-cm dishes in quadruplicates and treated with either control- or Wnt3A conditioned medium for 3 h prior to lysis in lysis buffer containing 8 M urea. Protein extracts (3 mg of protein) were reduced, alkylated, trypsin-digested and acidified. Phosphopeptides were enriched by TiO_2 and labelled with 6-plex TMT reagents. All the labelled phosphopeptides of each biological replicate were pooled together and subjected to HPLC fractionation followed by analysis by LC-MS/MS.

Statistical analysis of four replicate experiments revealed a set of 333 phosphorylation sites, that were significantly different between WT and PAWS1$^{-/-}$ cells and 495 sites that were significantly different between WT and PAWS1^{WT} under unstimulated conditions. 553 phosphorylation sites were significantly different between WT and PAWS1$^{-/-}$ cells and 535 sites between WT and PAWS1^{WT} cells in Wnt-stimulated conditions. In the WT cells, 213 phosphorylation sites were found to be regulated by Wnt stimulation. Of those sites, 92 were identified in the unstimulated cells and 121 in the Wnt-stimulated cells. Interestingly, none of the well characterised Wnt pathway components, such as β-catenin-pSer^{45}, were identified in any of the above sets, which suggests that the coverage of phospho-peptides here was not comprehensive but nonetheless the identification of novel Wnt-dependent phospho-events indicates that Wnt responses potentially extend vastly beyond the currently established protein networks. Of the phospho-peptides identified, a small number with significant changes across different conditions could not be clustered according to gene ontology databases (DAVID, PANTHER). Therefore, these results need to be interpreted with caution, as they do not represent an exhaustive survey of all possible phosphorylation changes using the conditions described. Of note, in similar phospho-proteomic approaches undertaken by others within the MRC Protein Phosphorylation and Ubiquitylation Unit, ~18,000 phospho-peptides have been identified.

To graphically represent the changes in phospho-peptides identified, volcano plots (Cui and Churchill 2003) were constructed (Fig 4-12 – 4-14). The log2 of the fold change values were plotted against the negative decadic logarithm of the p-value derived from the t-test. Proteins with a minimum of 2-fold change (indicated by the vertical dashed red lines) combined with a p-value smaller than 0.05 (indicated by the horizontal dashed red line) were considered significant.

As this experiment quantified the global phosphorylation changes in the cell proteome, a further refinement was carried out by filtering the dataset for the presence of the CK1 phosphorylation consensus motif, D/E-x-x-S*/T*, for phospho-peptides with a significant change higher than 2-fold. This refinement could potentially provide the initial step in the identification of CK1α-specific substrates that might be regulated by the presence or absence of PAWS1 in cells both in unstimulated and Wnt3A stimulated conditions (Appendix A-2 – A-4). Moreover, because CK1 can also target S/T residues that have a pS/pT-x-x-S*/T* motif (primed motif), the analysis was also refined further to consider phospho-peptides with priming phosphorylation (pS/pT) at the n-3 position.

Any other phospho-peptides could be considered either as non-canonical CK1 phosphorylation events or as indirect phosphorylation events mediated by other kinases downstream of CK1.

From the analyses above, one interesting phospho-protein that was specifically enriched in both control and Wnt3A treated wild type cells, while being absent from PAWS1$^{-/-}$ cells, was Bicaudal C homolog 1 (*A6NGY7*). The phosphorylated residue was mapped to Ser429. BICC1 is an RNA-binding protein that represses mRNA translation (Gamberi and Lasko 2012). It has been shown to co-precipitate with mRNAs that regulate Wnt signalling, vesicular trafficking and cytoskeletal organisation (Chicoine, Benoit et al. 2007). Notably, in *Xenopus* embryos, the maternal BICC1 protein was shown to form a gradient from the animal pole to vegetal pole, which mirrored the repression of the BICC1-mediated repression of mRNA translation. Additionally, BICC1 depletion from *Xenopus* oocytes was shown to result in Wnt signalling activation with an excess of dorsal-anterior structures (Park, Blaser et al. 2016). To date, it is not known how BICC1-mediated repression of mRNA translation is regulated spatiotemporally. An emerging hypothesis would be that this precise regulation is controlled through phosphorylation. Hence, in wild type cells BICC1 might be negatively regulated via its phosphorylation at Ser429, thereby, inhibiting its function as a translational repressor. In contrast, the absence of BICC1 phosphorylation in PAWS1$^{-/-}$ cells might mean that BICC1 is in an active state in which it is able to bind and inhibit mRNAs from being translated. This would not only explain why PAWS1$^{-/-}$ cells do not respond to Wnt signalling to the same extent as the wild type cells but it could also provide an indication of the lower expression levels of CK1α that follow PAWS1 loss.

Further research is required for the validation of the phospho-peptides that were identified as significantly (more than 2-fold) altered between the experimental conditions described above. *In vitro* validations could be performed with kinase assays using recombinant CK1α and the identified proteins, with or without PAWS1 co-administration. Furthermore, phosphorylation site-specific antibodies for the identified phospho-residues can also be exploited in immunoblotting experiments, monitoring cell extracts from U2OS wild type and PAWS1$^{-/-}$ cells that were stimulated with control or Wnt3A conditioned medium. If no specific phospho-antibodies are available, the Phos-tag SDS-PAGE methodology could be employed. This methodology has been exploited for visualising protein phosphorylation, as evidenced through a change in their electrophoretic mobility shift (Kinoshita, Kinoshita-Kikuta et al. 2006). Briefly,

Phos-tag (1,3-bis[bis(pyridin-2-ylmethyl) amino]propan-2-olato dizinc(II) complex) agent binds phosphate ions with high affinity and as a result it interacts with proteins and peptides with phosphorylated residues (Kinoshita, Yamada et al. 2005). Phos-tag acrylamide is added to SDS/polyacrylamide gels and retards the electrophoretic mobility of phosphorylated proteins, causing substantial mobility shifts, which can then be visualised by Western blotting, using an antibody against the total, unphosphorylated form of the protein of interest (Kinoshita, Kinoshita-Kikuta et al. 2006). Following the validation of CK1α targets, cell-based assays, including for example, Wnt transcriptional reporter activity and nuclear/cytosolic accumulation of β-catenin assays could be performed after overexpressing the phospho-deficient and phospho-mimetic mutants of each validated CK1α-target, in order to evaluate their impact on Wnt signalling. Additionally, the ability of the potential phospho-mimetic mutants of each CK1α target to restore Wnt signalling responses in PAWS1$^{-/-}$ cells, to the levels seen in the wild type cells, could be examined.

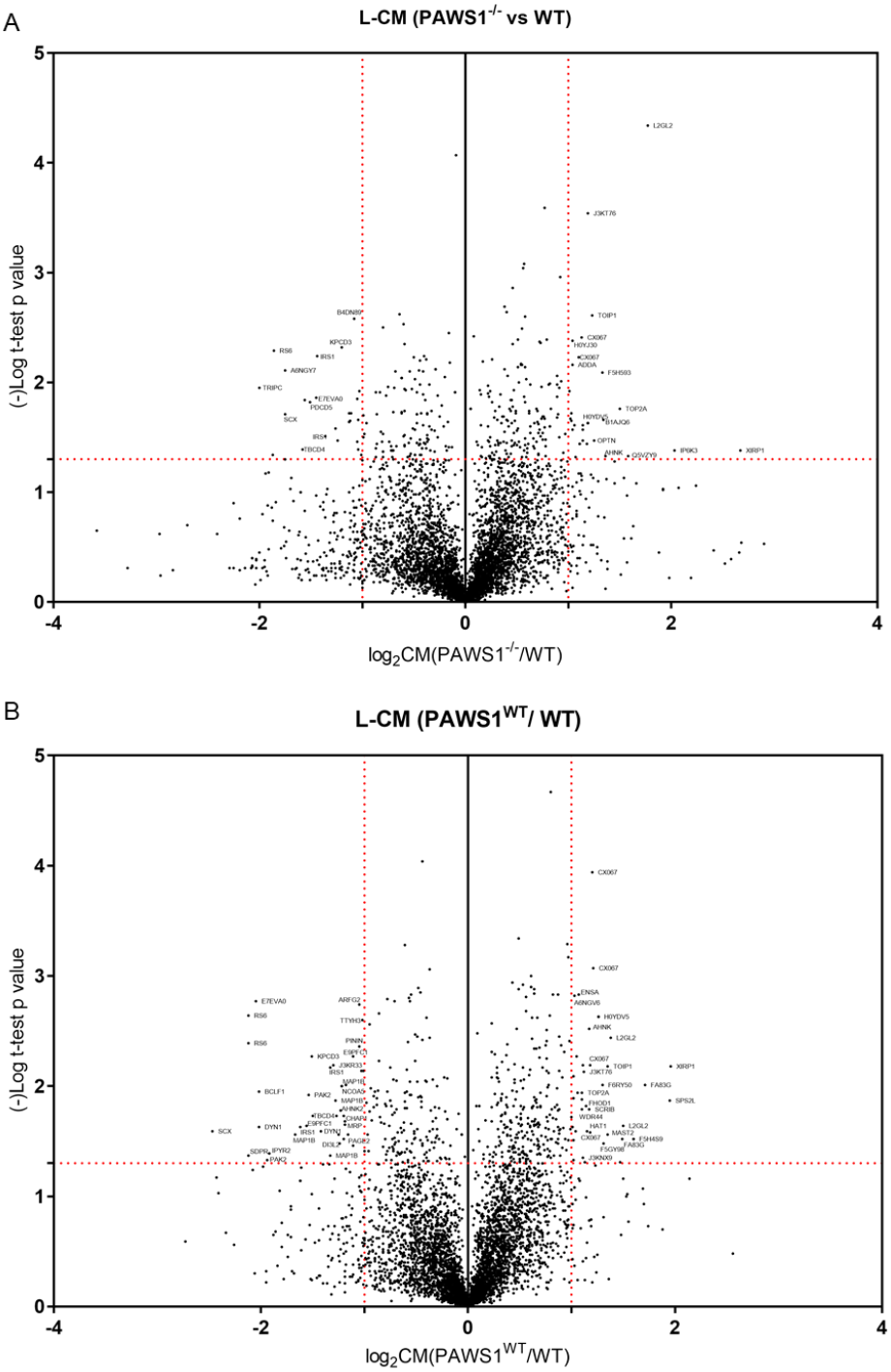

Figure 4- 12 Changes in global phosphoprotein abundance under control unstimulated conditions

A. Volcano plot of the phosphoproteins identified in the PAWS1$^{-/-}$ and wild type cells under basal unstimulated conditions. Each dot represents a phosphoprotein. The log2 of the average phospho-site ratios (n=4) of PAWS1$^{-/-}$ versus wild type (x-axis) are plotted against the negative decadic logarithm of the p-value derived from a t-test (y-axis). Proteins with a minimum of 2-fold change (indicated by the vertical dashed red lines) combined with a p-value smaller than 0.05 (indicated by the horizontal dashed red line) are considered significant and are labelled with their gene symbol.

B. Same as (A) but for PAWS1^{WT} and wild type phosphoproteins.

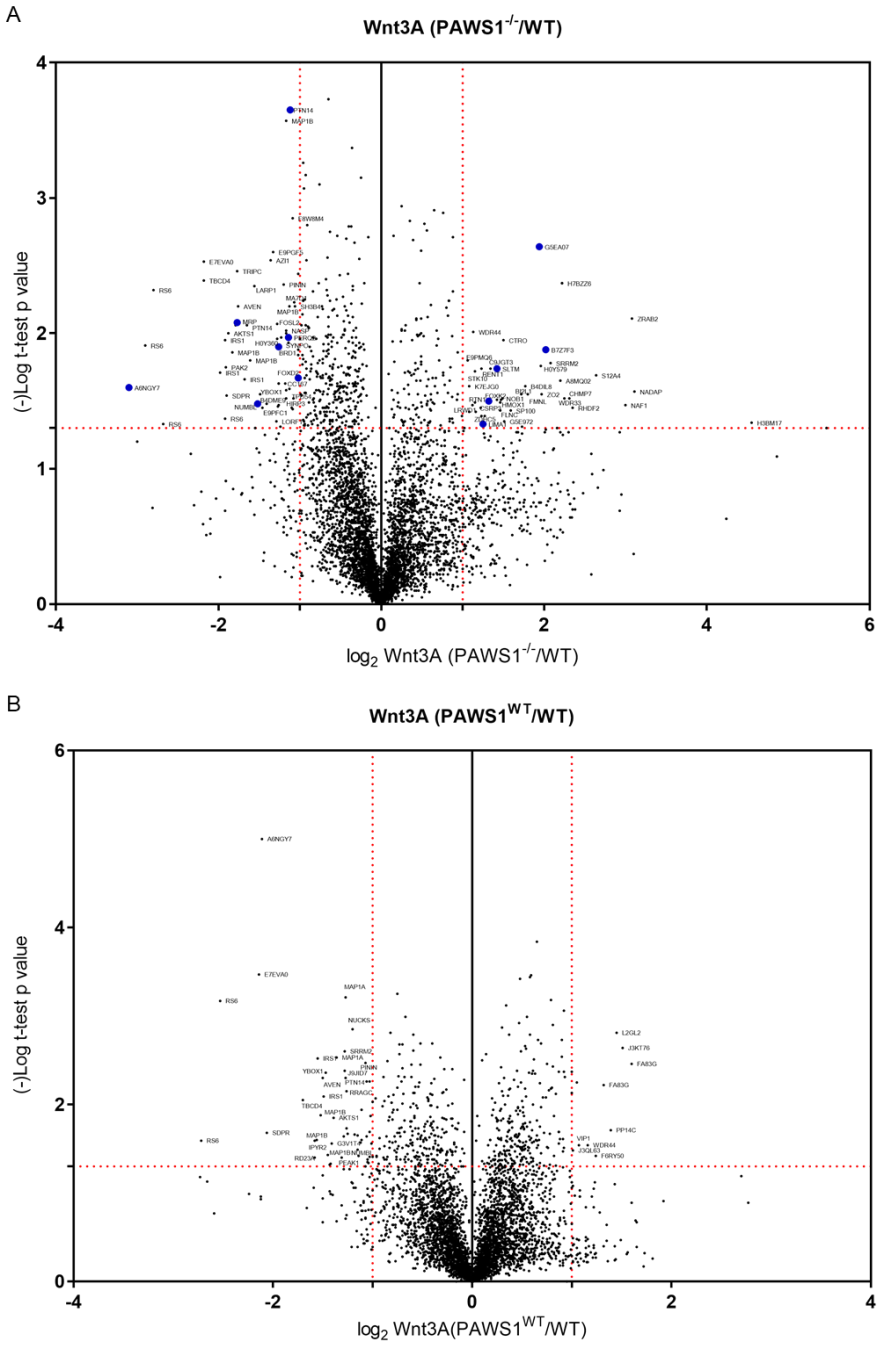

Figure 4- 13 Changes in global phosphoprotein abundance upon Wnt3A stimulation

A. Volcano plot of the phosphoproteins identified in the PAWS1$^{-/-}$ and wild type cells under Wnt3A stimulation (3h). Each dot represents a phosphoprotein. The log2 of the average phospho-site ratios (n=4) of PAWS1$^{-/-}$ versus wild type phosphoproteins (x-axis) are plotted against the negative decadic logarithm of the p-value derived from a t-test (y-axis). Proteins with a minimum of 2-fold change (indicated by the vertical dashed red lines) combined with a p-value smaller than 0.05 (indicated by the horizontal dashed red line) are considered significant and are labelled with their gene symbol. Proteins with a potential involvement in the Wnt signalling pathway are highlighted with a blue dot.

B. Same as (A) but for PAWS1^{WT} and wild type phosphoproteins.

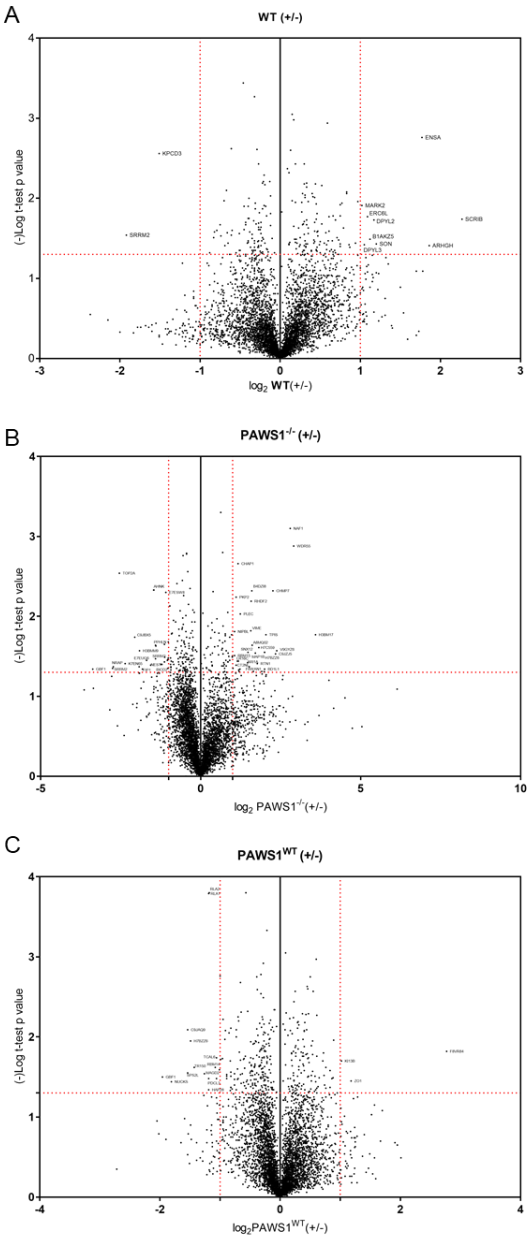

Figure 4- 14 Changes in global phosphoprotein abundance in control versus Wnt3A treated cells

A. Volcano plot of the phosphoproteins identified in the wild type cells treated with control conditioned medium versus Wnt3A-treated (3h) cells. Each dot represents a phosphoprotein. The log2 of the average phospho-site ratios (n=4) of untreated versus Wnt3A-treated phosphoproteins (x-axis) are plotted against the negative decadic logarithm of the p-value derived from a t-test (y-axis). Proteins with a minimum of 2-fold change (indicated by the vertical dashed red lines) combined with a p-value smaller than 0.05 (indicated by the horizontal dashed red line) are considered significant and are labelled with their gene symbol.

B. Same as (A) but for PAWS1$^{-/-}$ cells.

C. Same as (A) but for PAWS1^{WT} cells.

4.2.4 All FAM83 proteins interact with different CK1 isoforms

Following the discovery that endogenous PAWS1 interacts with CK1α robustly, and the demonstration that the interaction is mediated through two residues within the DUF1669 domain of PAWS1, namely D^{262} and F^{296}, both of which are conserved in all FAM83 members (Fig 4-15A), it was hypothesized that all FAM83 proteins might also interact with CK1 isoforms. Another PhD student in the lab (L. Fulcher) explored this hypothesis by expressing each FAM83 protein with a GFP-tag at the N-terminus in HEK293 cells and testing their ability to pull down endogenous CK1α, δ and ε isoforms. As shown in Fig 4-15B, CK1α was co-immunoprecipitated with every FAM83 protein but not with the GFP-only control. FAM83B, FAM83E, FAM83G (PAWS1) and FAM83H interacted with CK1α with apparently higher affinities compared to FAM83A, FAM83C, FAM83D and FAM83F (Fig 4-15B). Furthermore, endogenous CK1δ and CK1ε were detected only in FAM83B, FAM83E, and FAM83H IPs, and to a lower extent in FAM83A IPs (Fig 4-15B). In line with previously reported data (Dunsch, Hammond et al. 2012, Vogt, Dingwell et al. 2014), endogenous SMAD1 co-precipitated with only PAWS1, while endogenous HMMR and DYNLL1 co-precipitated exclusively with FAM83D (Fig 4-15B).

Having validated that $PAWS1^{F296A}$ and $PAWS1^{D262A}$ mutants abolish the interaction with CK1α, the equivalent conserved Phe and Asp residues were mutated to Ala in FAM83E (F^{277} and D^{243}), FAM83F (F^{284} and D^{250}) and FAM83H (F^{270} and D^{236}). Then, wild type GFP-FAM83E-H, GFP-FAM83E-$H^{F/A}$, or GFP-FAM83E-$H^{D/A}$ mutants were expressed in U2OS cells and immunoprecipitated to assess their abilities to co-precipitate endogenous CK1α or CK1ε isoforms (Fig 4-15C). In comparison to wild type FAM83E-H, both F/A and D/A mutations attenuated the interaction with CK1α and CK1ε (Fig 4-15C, by L. Fulcher). These observations suggest that the interaction between the DUF1669 domain and CK1 isoforms may be mediated through a conserved structural motif surrounding residues equivalent to PAWS1 D^{262} and F^{296}. Consistent with previous observations (Fig 4-15B), while FAM83E and FAM83H bound both CK1α and CK1ε, FAM83F and PAWS1 bound only CK1α (Fig 4-15C). These observations, with other ongoing studies in the Sapkota lab, have consolidated the hypothesis that FAM83 proteins serve as anchors for different CK1 isoforms in order to regulate their subcellular distribution, and potentially their substrate accessibility, in response to different signalling cues. Therefore, a whole new avenue has opened up for investigating the regulation of CK1 biology and their substrates, through distinct FAM83 proteins.

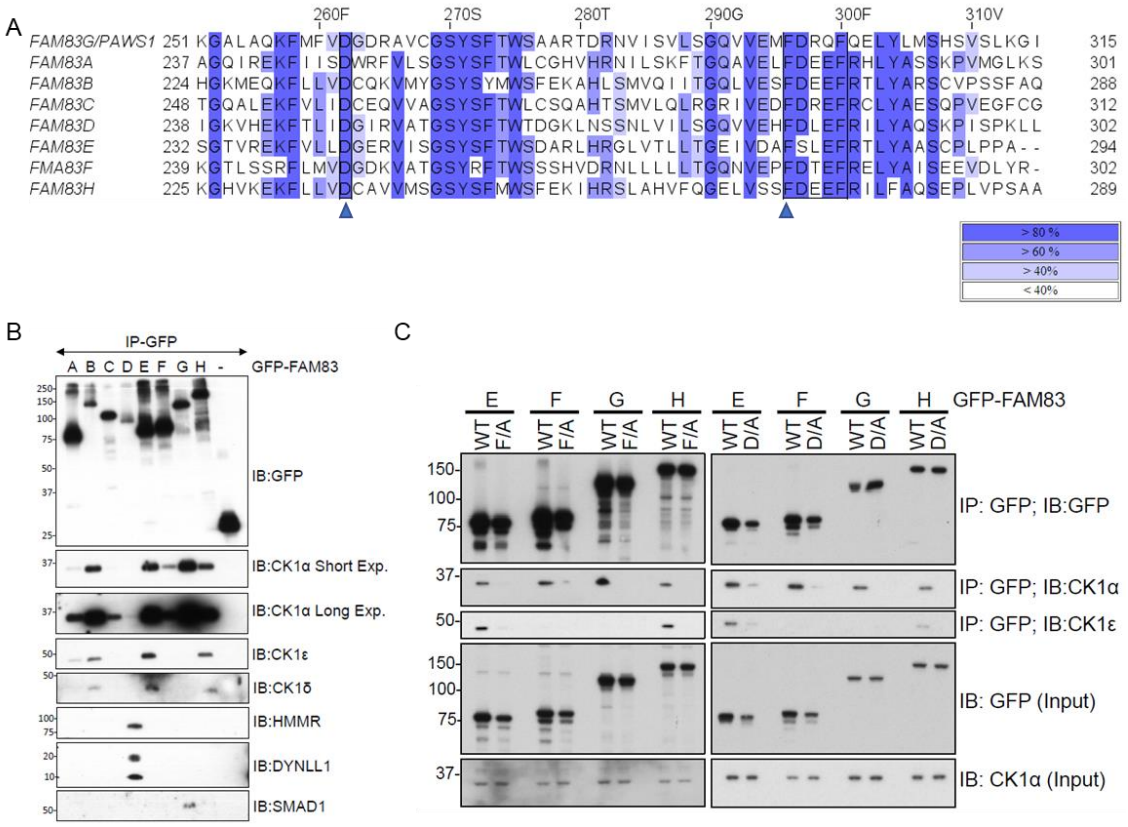

Figure 4- 15 The FAM83 proteins interact with CK1 isoforms

A. Sequence alignment of the FAM83 members around the CK1 binding sites. The blue arrows indicate the conserved residues (D^{262} and F^{296}) required for the PAWS1-CK1α interaction. Alignment was performed with ClustalO in Jalview 2.10.3 and colouring indicates the % of sequence identity as shown in the box.

B. A single copy of FAM83A-H gene each tagged with GFP at the N-terminus was stably inserted downstream of a tetracycline-inducible promoter in Flp-In T-Rex HEK293 cells. Cells were treated with 20 ng/ml doxycycline for 24 h before lysis. Extracts (1 mg of protein) were subjected to GFP-IPs, followed by SDS-PAGE and immunoblotting with the indicated antibodies. (Performed by L. Fulcher).

C. WT, conserved CK1-interaction residue (F/A and D/A) mutants of GFP-FAM83E-H from (A) were transiently expressed in U2OS cells. Input extracts (20 µg of protein) and GFP-IPs (from 1 mg protein extracts) were resolved by SDS-PAGE, followed by immunoblotting with the indicated antibodies (Performed by L. Fulcher).

4.2.5 Some FAM83 proteins can activate Wnt signaling

As discussed extensively in the Introduction, CK1 isoforms play critical roles in regulating Wnt signalling. After establishing all FAM83 members are capable of interacting with CK1α and half of them also interact with other CK1 isoforms, their ability to activate the canonical Wnt pathway was investigated. For this, the ability of FAM83 members to activate Wnt transcriptional reporter activity in U2OS cells was tested (Fig 4-16). Apart from PAWS1, overexpression of FAM83B, FAM83E and FAM83F significantly enhanced the Wnt transcriptional reporter activity upon treatment with Wnt3A-conditioned medium (Fig 4-16A). Notably, overexpression of FAM83F, which also selectively interacts with CK1α, activated the Wnt transcriptional reporter activity in cells substantially more than other FAM83 members and even in the absence of Wnt3A-conditioned medium (Fig 4-16A). Remarkably, FAM83F is the only other FAM83 member that induces axis duplication in *Xenopus* embryos (personal communication with K. Dingwell, The Francis Crick Institute, London). These findings suggest that there could be some synergistic or redundant action between FAM83F and PAWS1 in the regulation of CK1α action in the Wnt signalling cascade.

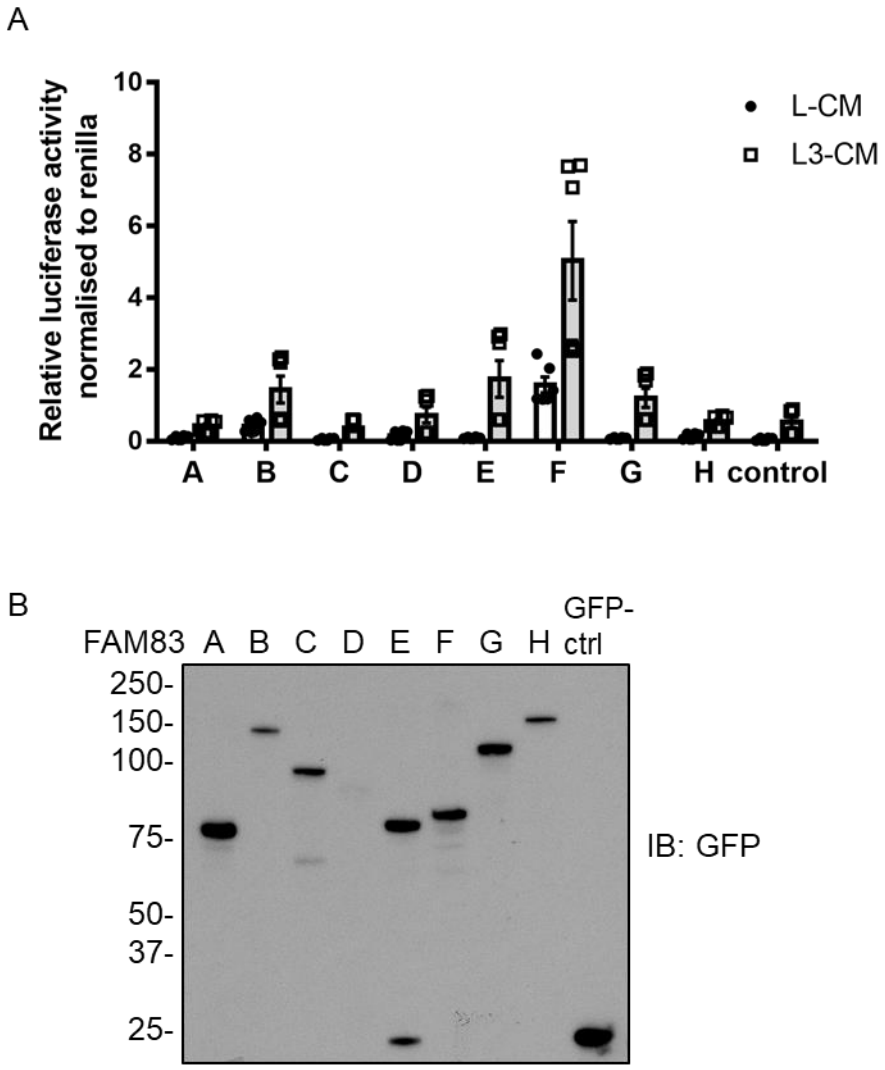

Figure 4- 16 Overexpression of FAM83B, FAM83E, FAM83F and FAM83G activates the Wnt-transcriptional luciferase reporter activity in U2OS cells

A. Plasmids encoding (FAM83A-H)-GFP and GFP control were transiently expressed in U2OS cells together with those encoding TOPflash luciferase and Renilla luciferase. TOPflash luciferase activity was measured after treatment with either conditioned medium (L-CM) or Wnt3A conditioned medium (L3-CM) for 12 h. Data are normalised to Renilla luciferase internal control. (n=4; Error bars represent ±SEM).

B. Cell extracts from (A) were resolved by SDS-PAGE and immunoblotted with anti-GFP to monitor the levels of FAM83-GFP expression.

4.2.6 Generation of an endogenously driven transcriptional reporter for PAWS1

Given the robust nature of the PAWS1:CK1α interaction in cells, understanding how PAWS1 is regulated transcriptionally and post-transcriptionally could inform the regulation of CK1α function in cells. Because CK1α protein levels are regulated by PAWS1, manipulating the expression of PAWS1 mRNA and protein levels could regulate CK1α activity via regulating protein levels. While post-translational regulation of PAWS1 is a focus in the Sapkota lab (and is covered briefly in Chapter 6), very little is known about its transcriptional regulation. Therefore, in order to investigate the transcriptional regulation of PAWS1, an endogenous transcriptional reporter for the PAWS1 gene was generated using CRISPR/Cas9 genome editing. This technology allowed for an integration of a polycistronic cassette containing non-fused firefly luciferase and GFP genes at the start codon of the PAWS1 gene locus in U2OS cells (Fig 4-16A). Directly downstream of the luciferase gene, an internal ribosome entry site (IRES) was incorporated to ensure separate expression of the GFP gene from the luciferase protein. A 2A self-cleaving peptide was also incorporated downstream of the GFP gene to ensure cleavage of the GFP protein from PAWS1, which was left in frame after 2A. A similar reporter system from the Sapkota lab, which introduced luciferase gene at the start codon of TGFβ-target gene PAI-1, has already verified the effectiveness of the system downstream of TGFβ signalling (Rojas-Fernandez, Herhaus et al. 2015).

GFP protein expression was used to ensure the detection of transgene delivery and rapid isolation of positive single cell clones. Eighteen GFP-positive clones were subjected to luciferase assay and half of them were found to be positive for luciferase activity under basal conditions (Fig 4-16B). PAWS1 protein expression in luciferase- and GFP-positive clones was monitored by Western blotting (Fig 4-16C). It appeared that PAWS1 expression was significantly reduced or lost in two GFP- and luciferase-positive cell clones. Loss of PAWS1 could be possibly attributed to mistakes during homologous recombination which resulted in incorporation of random mutations, base insertions or deletions that could lead to premature stop codon formation. To investigate if this was the case, genomic DNA from clones 3 and 4 was isolated and analysed by PCR and sequencing. First, the genomic region of PAWS1 gene was amplified with primers located outside of the homologous recombination arms from DNA that was isolated from U2OS wild type and the PAWS1-reporter cells using genomic DNA isolated from clone 3 and clone 4. Next, the PCR products were separated on an agarose gel (Fig 4-16D). The

DNA band at around 5000 bp indicated that both clones had integrated the reporter cassette in at least one allele. In clone 3 the second band that was visible close to the wild type length suggested that clone 3 was probably a heterozygote. To confirm this, the shorter fragments were amplified, cloned and sequenced. Two sets of primers were used; the first amplified the genomic region from the start codon of PAWS1 to the most upstream region of the luciferase gene and the second amplified the region from the last nucleotides of the GFP gene and the beginning of the PAWS1 coding region (Fig 4-18A, 4-19A). Genomic sequencing confirmed that clone 4 had inserted the reporter cassette in both alleles, while clone 3 was a heterozygote (Fig 4-18B, 4-19B).

Since this reporter system utilises intact endogenous chromatin architecture, it is ideal to identify signals and small molecules that regulate endogenous PAWS1 transcription in a high throughput format. Once identified, positive and negative regulators of PAWS1 transcription will be verified by qPCR. A pilot experiment was performed to test the effect of different ligands and growth factors on PAWS1 transcription. For this, the heterozygous clone 3 and the homozygous clone 4 were selected and treated with growth factors and ligands followed by measurement of their endogenous luciferase activity. As seen in Fig 4-20, EGF and FGF_4 activated luciferase activity in clone 3 but not in clone 4. Significant decrease in the luciferase activity was observed in clone 3 cells that had been treated with BMP_4, TGFβ and Wnt3A. A similar trend was obvious for clone 4 but the changes were not statistically significant. The incorporation of the luciferase cassette to just one of the two alleles might be a possible reason for the different degrees of sensitivity to the stimuli.

Further work is required to validate the observed differences on PAWS1 transcript levels with qPCR and also to evaluate if there are changes at the protein levels of both PAWS1 and CK1α, too. Moreover, the screening of regulators of PAWS1 transcription can be expanded to panels of kinase inhibitors and small molecules that are available and can be easily administered to cell lines (Elkins, Fedele et al. 2016, Williams, Gray et al. 2017).

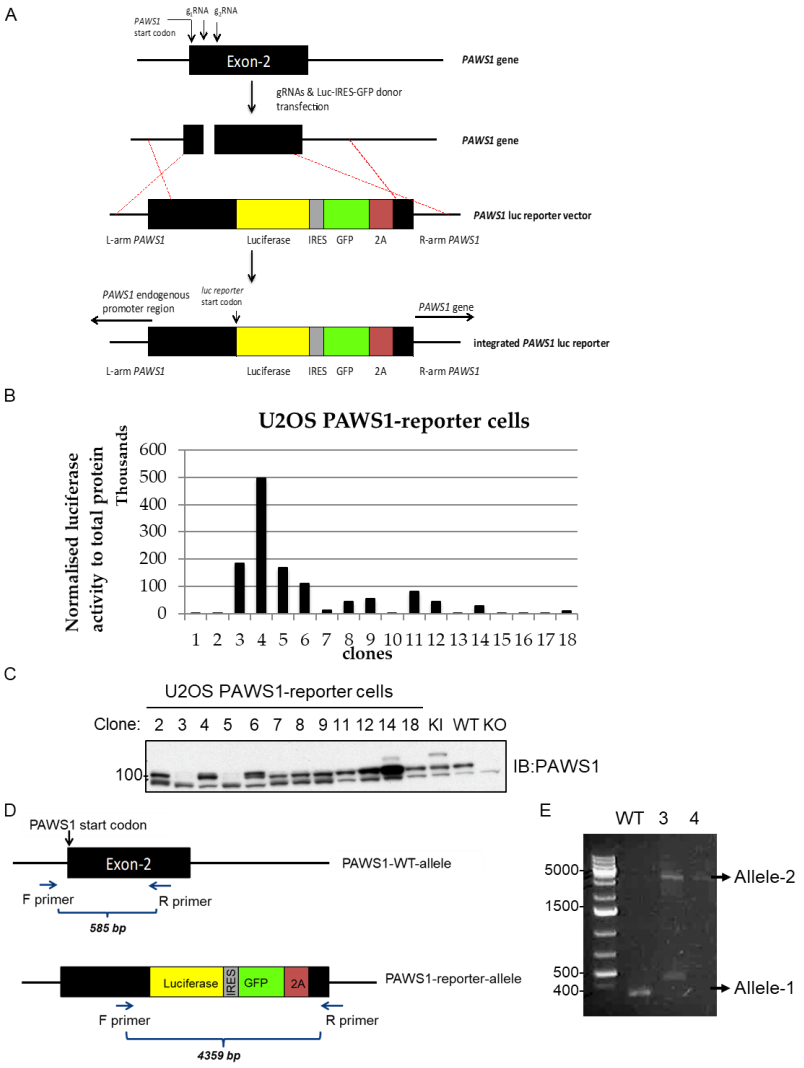

Figure 4- 17 Generation of endogenous PAWS1-transcriptional reporter U2OS cells by CRISPR Cas9 genome editing

A. Schematic representation of the strategy used to generate the PAWS1transcriptional reporter cells with CRISPR/Cas9. U2OS cells were co-transfected with a pair of guide RNAS (gRNAs) targeting the start codon region of the PAWS1 gene, together with the PAWS1 reporter donor vector containing two homology arms of the PAWS1 gene, one upstream (L-arm) and one downstream (R-arm) from the gRNA targeting sites with the luciferase-IRES-GFP-2A reporter cassette in the middle, to allow for homologous recombination.

B. Measurement of basal luciferase activity of GFP-positive single cell clones.

C. Cell extracts from clones from (B) that displayed luciferase activity were resolved by SDS-PAGE and immunoblotted with anti-PAWS1. Extracts from PAWS1$^{GFP/GFP}$ (KI), wild type (WT) and PAWS1$^{-/-}$ cells were used as controls.

D. Schematic representation of the predicted genomic PCR products of the PAWS1 gene and the reporter inserted allele.

E. SYBR-safe-stained agarose gel showing PCR products of genomic samples of U2OS wild type controls and PAWS1-reporter clones 3 and 4.

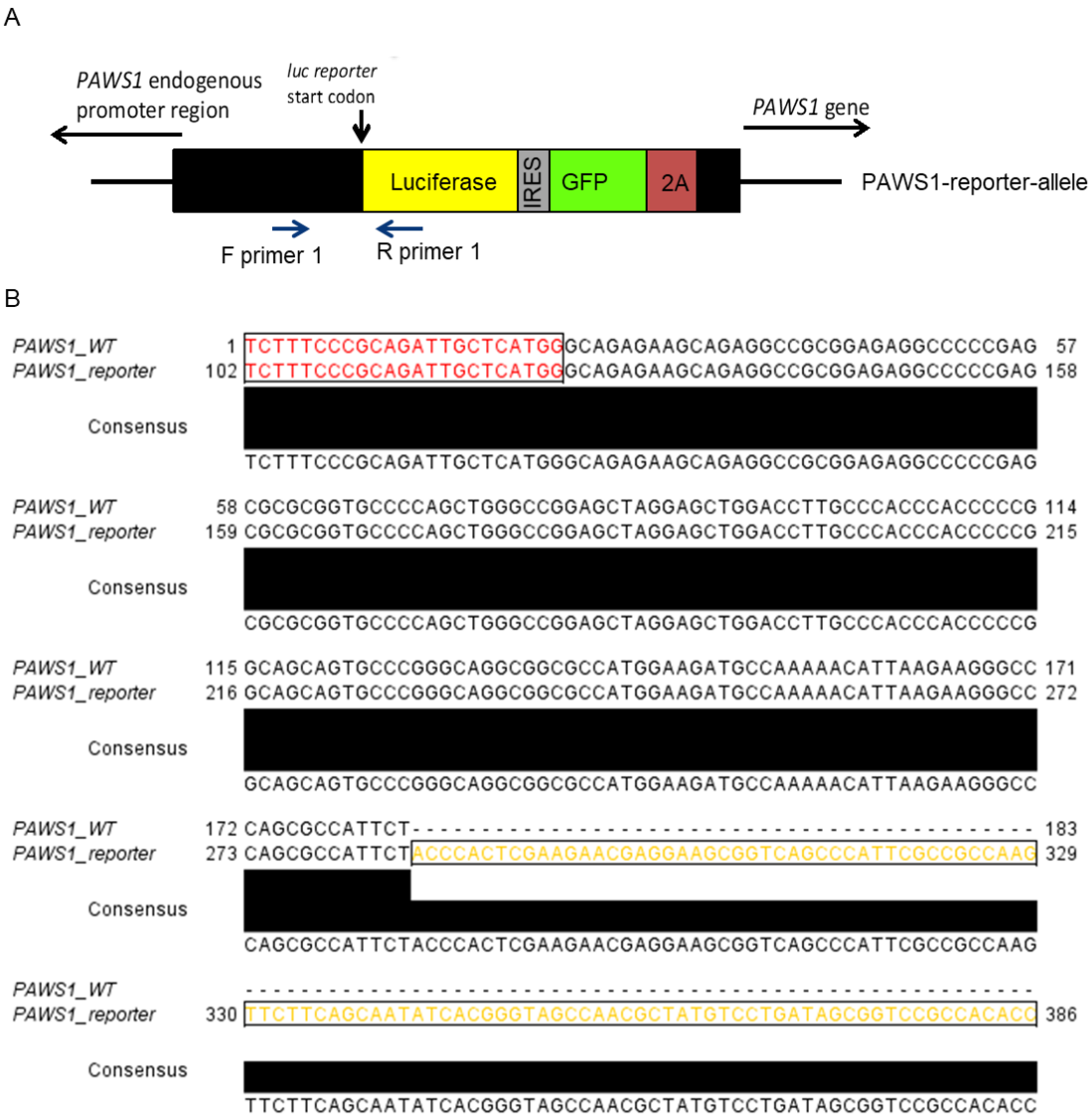

Figure 4- 18 Genomic sequence of the PAW1-transcriptional reporter for the luciferase gene

A. Schematic representation of the predicted genomic PCR products that were amplified with a pair of primers targeting the indicated regions.

B. Sequence alignment of the PCR products from (A), showing that the luciferase gene (in yellow) was integrated in frame with PAWS1. Alignment was performed in Jalview 2.10.3 with ClustalO.

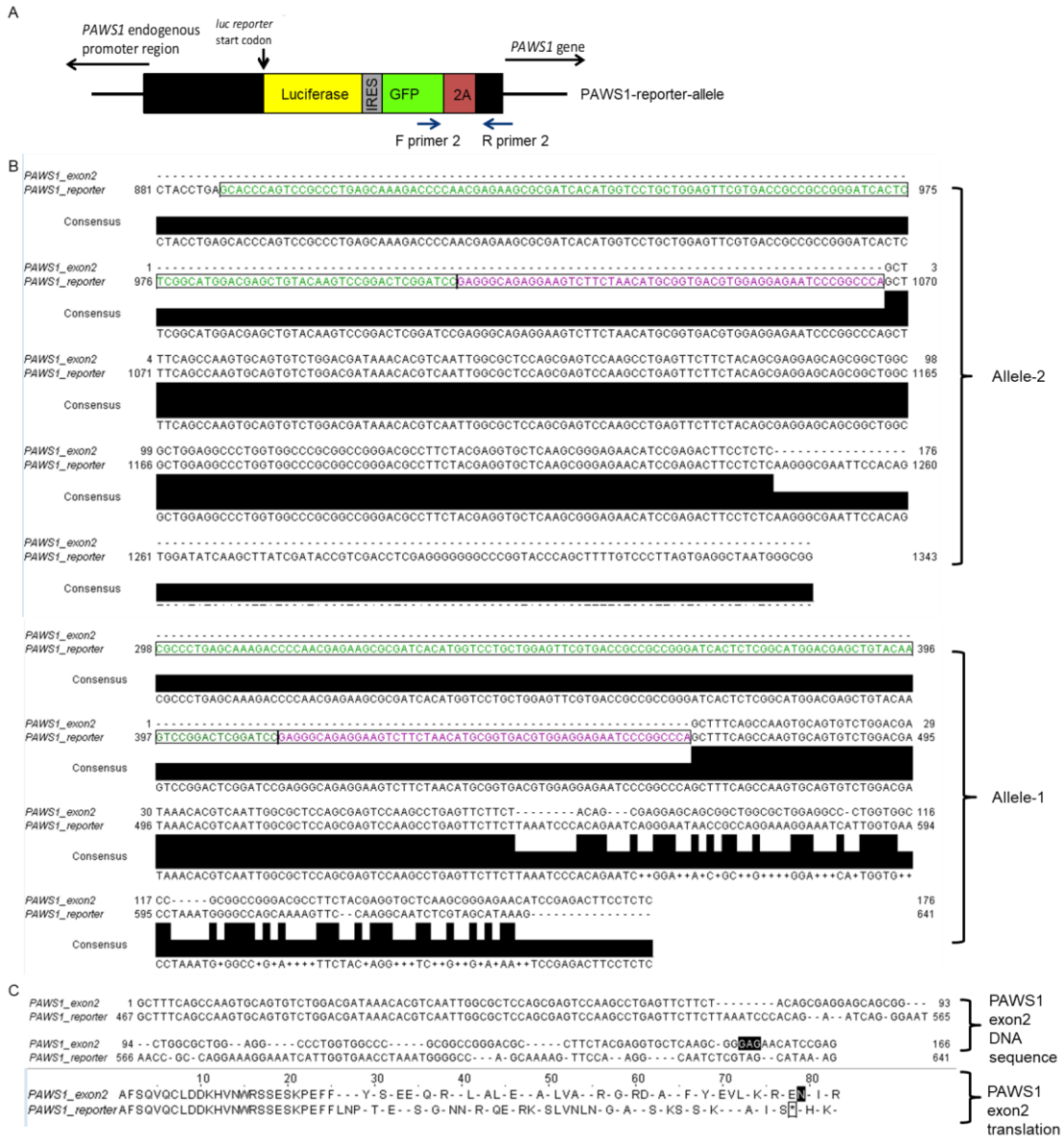

Figure 4- 19 Genomic sequence of the PAWS1-transcriptional reporter for the GFP gene

A. Schematic representation of the predicted genomic PCR products that were amplified with a pair of primers targeting the indicated regions.

B. Sequence alignment of the PCR products from (A), showing that the GFP gene (in green) and the 2A gene (in purple) were integrated in frame with PAWS1 in both alleles. In allele-1 of clone 3, an insertion of 7 nucleotides caused a frame-shift. Alignment was performed in Jalview 2.10.3 with ClustalO.

C. A zoom into the PAWS1 coding region of allele-1 from (B) (top panel) and the corresponding amino-acid sequence (bottom panel) showing a premature stop codon that was formed due to the frame-shift mutations. Alignments were performed in Jalview 2.10.3.

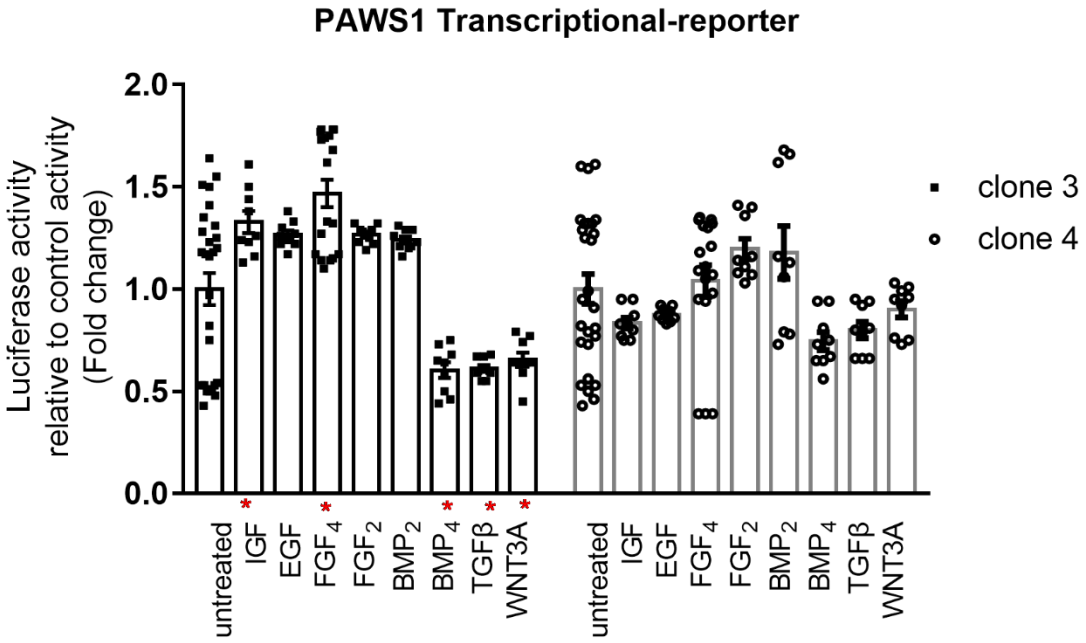

Figure 4- 20 Luciferase activation in the PAWS1-reporter cells upon ligands stimulation

PAWS1 reporter cells were stimulated with the indicated ligands and growth factors and luciferase activity was measured. Data were normalised to total protein concentration and to the basal activity of the untreated control cells for each clone. The red asterisks indicate statistically significant changes of $p<0.05$ (2way ANOVA with Bonferroni correction for multiple comparisons; n=3; Error bars represents ±SEM, dots represent technical replicates).

4.3 Discussion

In this Chapter, it has been demonstrated that PAWS1 and CK1α exist in a complex in cells and that they regulate each other's protein levels reciprocally. The correlation between their protein levels was observed in a panel of mammalian cell lines that are commonly used for cancer research. This correlation was confirmed to be regulated at the protein level while no correlation on the PAWS1 and CK1α mRNA levels was observed. Loss of PAWS1 expression resulted in a decrease in the CK1α protein levels, whereas PAWS1 overexpression increased CK1α protein levels in cells, without affecting CK1α mRNA levels. These findings suggest that PAWS1 might enhance the protein stability of CK1α by preventing its degradation. However, inhibition of the proteasomal and lysosomal protein degradation pathways did not rescue the attenuated CK1α levels in PAWS1$^{-/-}$ cells. A possible explanation for the above findings would be that PAWS1 and CK1α are co-translationally regulated. Alternatively, the PAWS1:CK1α complex might regulate mRNAs to aid the translation of both proteins. Such protein:mRNA interactions can control the rate and efficiency of protein translation (Standart and Jackson, 1994). None of the above possibilities have yet been tested for PAWS1 and CK1α.

PAWS1 was found to be phosphorylated at S614 by CK1α *in vitro*. The robust interaction between PAWS1 and CK1α is contrary to the notion that the association between a kinase and its substrate is transient and weak. However, the phosphorylation of PAWS1 by CK1α was only established *in vitro*. It was shown that CK1α phosphorylates PAWS1 at S614 independent of their interaction. CK1 isoforms have a preference towards acidic substrates and they usually phosphorylate S/T residues in a consensus motif D/E-x-x-S*/T* or pS/pT-x-x-S*/T*. S614 does not conform to either motif. Although it is not unusual for CK1 to phosphorylate a residue that does not fall into its consensus phosphorylation motif, it is still not known if PAWS1 is phosphorylated by CK1α at S614 *in vivo*.

Nevertheless, the phosphorylation of PAWS1 at S614 was not found to be involved in its role in Wnt signalling. First, the minimum PAWS1 sequence that was required for the induction of axis duplication in *Xenopus* embryos did not include S614 and second, the overexpression of the phospho-mutant PAWS1^{S614A} still induced a secondary axis formation to the same extent as the wild type. However, the phosphorylation of PAWS1 at S614 may be required for other PAWS1 functions that have yet to be discovered.

Like PAWS1, wild type CK1α, but not the kinase dead mutant, also caused axis duplication in *Xenopus* embryos. An interesting observation here was that the co-expression of PAWS1 with either wild type or catalytically inactive CK1α, which both interact with PAWS1, blocked the induction of a secondary axis caused by overexpression of PAWS1 or $CK1\alpha^{WT}$ alone. These phenotypes are not surprising if we consider that the signaling pathways that control developmental processes must be tightly regulated. Therefore, perturbations that disturb the homeostatic balance of the components of a complex may have detrimental outcomes. Here, it has been shown that when the levels of PAWS1 or CK1α are over-expressed or depleted, the protein levels of the other partner are affected. In contrast, co-expression of both PAWS1 and CK1α, potentially, restores the balance that is required for their proper function. It is thus proposed that the biological outcome that is observed with the axis duplication assays is more due to the perturbation of the homeostatic PAWS1:CK1α complex, perhaps leading to the mislocalisation of the PAWS1:CK1α complex, thereby resulting in abnormal phosphorylation patterns of key CK1α substrates, thus affecting Wnt signalling responses.

This proposal was further supported by the finding that the intrinsic kinase activity of CK1α was not inhibited by its interaction with PAWS1. Therefore, the axis duplication inhibition observed upon co-expression of PAWS1 and CK1α was not due to inhibition of intrinsic CK1α catalytic activity. Although PAWS1 was not found to influence the kinase activity of CK1α in cells, it regulates CK1α localisation (Fig 3-17) which could potentially affect its access to specific substrates in response to specific signals. Therefore, it is pertinent to understand the key PAWS1-dependent CK1α substrates in order to establish molecular mechanisms through which the PAWS1:CK1α complex regulates Wnt signalling.

An initial foray into global phospho-proteomics analysis in U2OS wild type, $PAWS1^{-/-}$ and $PAWS1^{WT}$-rescue cells, revealed hundreds of phospho-peptides that were differentially enriched or attenuated in the different cell lines under unstimulated or Wnt3A-stimulated conditions. The phospho-peptides that were enriched exclusively in the wild type cells, but were absent in the $PAWS1^{-/-}$ cells, might reveal CK1α substrates that are regulated by the PAWS1:CK1α interaction. Interestingly, one of phosphoproteins that was significantly altered between wild type and $PAWS1^{-/-}$ cells and was identified in both Wnt3A-stimulated and unstimulated wild type cells, was BICC1. BICC1 is an RNA-binding protein that may act as a translational repressor (Park, Blaser et al. 2016). In

Xenopus embryos, the maternal *bicc1* mRNA forms a gradient that regulates translational repression of signalling mRNAs, such as *Wnt11* and *ddx5* (Park, Blaser et al. 2016). Most of the BICC1 targets are modulators of Wnt signalling and it was suggested that it may act as a novel regulator of the Wnt signalling pathway (Maisonneuve, Guilleret et al. 2009, Park, Blaser et al. 2016). Due to its potential relevance to Wnt signaling, BICC1 should be considered in future studies focused on the role of the PAWS1:CK1α interaction in Wnt signalling. Additional phospho-proteins in the same category as BICC1 could be evaluated on the basis of their known roles in the Wnt signalling, as well as their abilities to cause axis duplication in *Xenopus* embryos.

Moreover, phospho-peptides that were enriched exclusively in the PAWS1$^{-/-}$ cells might shed light into the mechanisms that regulate the aberrant response of these cells to Wnt signaling. Under basal conditions most of the phospho-peptides enriched in PAWS1$^{-/-}$ cells were mapped to actin-binding proteins such as ADDA, XIRP1 and AHNK. Hence, it could be hypothesised that the phosphorylation of these proteins might regulate the actin cytoskeleton, which is known to be regulated by PAWS1 (Cummins, Wu et al. 2018) ;Chapter 5).

To validate the phosphorylation of the identified proteins at the relevant sites in cells, a number of experimental strategies could be employed. First of all, in order to establish whether the phosphorylation of the endogenous substrates is due to CK1α, treatment of cells with pharmacological inhibitors of CK1α, such as D4476, should demonstrate reduced phosphorylation of the relevant residues. Alternatively, validation could be accomplished by the depletion of the CK1α protein in cells by RNAi. Furthermore, it should be demonstrated that PAWS1$^{-/-}$ cells, which have substantially lower levels of CK1α compared to wild type cells, display reduced phosphorylation of the relevant residues. An additional benefit of this approach would be the validation of CK1α substrates that are regulated by the PAWS1:CK1α interaction. In all cases, changes in the phosphorylation levels may be monitored in cell extracts with phospho-specific antibodies or by the Phos-tag method. Additionally, validation of the PAWS1-dependent CK1α substrates under Wnt3A- stimulated conditions, should include experiments that assess the impact of phospho-deficient and phospho-mimetic mutants of the relevant targets, in Wnt signalling activation assays in cells and in axis duplication studies in *Xenopus* embryos.

One of the most important findings presented in this Chapter, prompted by the initial observations of the PAWS1:CK1α association was the demonstration that each

member of the FAM83 family is able to interact with different CK1 isoforms via their DUF1669 domain. While all FAM83 members interacted with CK1α, FAM83A, FAM83B, FAM83E, and FAM83H also interacted with CK1δ and CK1ε. Key conserved residues within the DUF1669 domain were identified as critical mediators of the CK1 interaction. The DUF1669 domain is evolutionarily conserved in vertebrates. The pleiotropic nature of CK1 isoforms probably necessitated additional regulatory mechanisms in the more evolutionary advanced organisms, which could have possibly resulted in, through an evolutionary pressure, the evolution of the DUF1669 domain as a CK1 interactor. In humans, the DUF1669 domain is present only in FAM83 proteins. Perhaps the DUF1669 domain of FAM83 proteins serves as an anchor for CK1 isoforms, tethering them to specific cellular organelles or membranes in proximity to their substrates, other enzymes or signalling molecules. This is not something new in the biology of cell signalling, as the A-Kinase Anchoring Proteins (AKAPs) regulate the local activation of Protein Kinase A by localising it to its substrates to streamline signal transduction (Esseltine and Scott 2013). However, it is yet to be defined whether FAM83 proteins interact with CK1 isoforms in a synergistic or competitive manner, to regulate CK1 enzymatic function in cells.

The robust interactions between FAM83 proteins and the CK1 isoforms provide unique opportunities to target specific CK1 isoforms in cells. Misregulation of CK1 isoforms has been linked with many human diseases, including cancer and neurodegeneration (see 1.6.5). However, poor understanding of CK1 functional regulation, together with the enzymatic pleiotropy, have limited the exploitation of CK1 isoforms as targets in therapeutics. The data presented here have demonstrated that FAM83 proteins, and in particular PAWS1, can regulate CK1α and that perturbations of PAWS1 levels have a direct influence on CK1α levels, as well. Although further research is required to address if alterations in CK1α protein levels are accompanied by perturbations in its kinase activity, the ability to modulate PAWS1 levels will be a valuable tool in understanding and interfering in CK1 biology. In a similar vein, the generation of a PAWS1 transcription reporter system would be an ideal tool to screen for and identify small molecules, inhibitors or ligands, that could regulate PAWS1 transcription in a sensitive and quantitative manner.

However, one limitation of modulating protein levels is that it can potentially affect other activities, related to the global enzymatic functions of CK1α in cells, resulting in non-specific or off-target effects. To overcome these limitations, the design of

molecules that specifically target and disrupt the interaction between PAWS1 and CK1α is recommended. Ongoing efforts (by A. Bullock lab, Oxford) aiming to solve the crystal structure of PAWS1 in complex with CK1α are underway and such a structure will facilitate drug design. Drugs generated in this manner could prove to be useful in treating pathological conditions associated with CK1α. Furthermore, solving the crystal structure of the PAWS1:CK1α complex could potentially reveal the basis of how different FAM83 members interact with specific CK1 isoforms in cells.

5. PAWS1 interacts with the Calcium/Calmodulin-dependent kinase 2

5.1 Introduction

Phenotypic characterisation of the U2OS PAWS1$^{-/-}$ cell line, which was employed for studies in the previous Chapters, revealed morphological differences compared to the wild type controls (Cummins, Wu et al. 2018). Further characterisations of PAWS1$^{-/-}$ cells revealed that they displayed actin cytoskeletal defects, which severely inhibited their ability to migrate (Cummins, Wu et al. 2018). Examination of the proteins associated with PAWS1, which was presented in Chapter 3, revealed a number of proteins that are implicated in regulating cytoskeletal dynamics and cell migration. Among these, CD2AP was validated as an interactor of PAWS1 (Cummins, Wu et al. 2018). CD2AP is an adapter protein involved in the formation of cell junctions as well as the actin polymerisation during cell migration (Tang and Brieher 2013, Zhao, Bruck et al. 2013). In wild type U2OS cells, it was shown that a pool of PAWS1 interacts with CD2AP at the membrane ruffles at the cell periphery, where it appears to control actin dynamics for the initiation of lamellipodia formation and cellular migration (Cummins, Wu et al. 2018). In contrast, PAWS1$^{-/-}$ cells were shown to display defects in lamellipodia formation, which could be attributed to the absence of the CD2AP accumulation at the cell periphery (Cummins, Wu et al. 2018). Strikingly, CD2AP$^{-/-}$ U2OS cells phenocopy actin cytoskeletal and cell migration defects observed in PAWS1$^{-/-}$ cells (Cummins, Wu et al. 2018). However, the precise mechanisms that control PAWS1 association with CD2AP to subsequently modulate actin cytoskeleton and cell migration remain elusive and are still under investigation in the Sapkota lab.

In addition to CD2AP, calcium and calmodulin-dependent kinases isoform D and G (CaMK2D and CaMK2G) were identified as PAWS1 interactors. This was quite exciting because Ca^{2+} influx and efflux play major role in controlling cytoskeletal dynamics (Tsai, Kuo et al. 2015). The two major Ca^{2+} sources for cells are the extracellular space and the endoplasmic reticulum (ER). A transient increase in the intracellular Ca^{2+} concentration leads to calcium binding by regulatory proteins which then activate biological responses. The major calcium-binding protein is the evolutionarily conserved protein Calmodulin (CaM) (Cheung 1980). CaM has no enzymatic activity *per se* but functions to sense Ca^{2+} signal and transduce it to

downstream enzymes (Hoeflich and Ikura 2002). One of the best characterised downstream targets is the group of CaM-dependent kinases (CaMKs), which in turn phosphorylate and modulate the activities of key components of the cytoskeletal machinery (Hoffman, Farley et al. 2013).

CaMK2s are Ser/Thr protein kinases whose activation is primarily dependent on Ca^{2+}/CaM (Lee and Edelman 1994). Their kinase domain is followed by a regulatory domain which contains an autoinhibitory domain and a CaM-binding domain and an association domain (Fig 5-1A) (Swulius and Waxham 2008). Under basal Ca^{2+} levels, CaMK2s remain inactive via auto-inhibitory mechanisms that involve the regulatory domain, which blocks catalytic activity (Tokumitsu, Enslen et al. 1995). An increase in the intracellular Ca^{2+} concentration results in the saturation of CaM with four calcium ions followed by subsequent conformational change that allows its binding to CaMK2s, which then releases them from autoinhibition (Peersen, Madsen et al. 1997). Once activated, CaMK2s phosphorylate their substrates, which usually possess the consensus phosphorylation motif F/I/L/V/Y-x-R-x-x-S*/T* (White, Kwon et al. 1998).

CaMK2 enzymes are multifunctional, as they have many substrates in cells and they form multi-subunit complexes (Kolodziej, Hudmon et al. 2000). In mammals, there are four CaMK2 isoforms (A, B, D and G), that are encoded by four different genes (Fig 5-1). CaMK2A and CaMK2B are brain specific, whereas CaMK2D and CaMK2G are ubiquitously expressed (Swulius and Waxham 2008). All isoforms are present in the cytosol as well as the nucleus, where they can regulate gene transcription (Tokumitsu, Enslen et al. 1995, Wu and McMurray 2001). Like all the CaMKs, CaMK2s remain inactive under basal Ca^{2+} levels, due to autoinhibition. A rise in the intracellular Ca^{2+} levels, followed by Ca^{2+}-saturation of CaM results in the activation of each subunit of the CaMK2 holoenzyme. Adjacent subunits are then auto-phosphorylated at Thr287 (T286 in A isoform) generating Ca^{2+}-independent activity (Miller and Kennedy 1986, Bradshaw, Hudmon et al. 2002). This autonomous activity further increases the affinity of CaMK2 for Ca^{2+}/CaM, an event known as “CaM-trapping” (Meyer, Hanson et al. 1992). As a consequence, CaMK2 remains activated far beyond the duration of the Ca^{2+} signal that causes its initial activation.

CaMK2 isoforms regulate synaptic plasticity in the brain (Derkach, Barria et al. 1999), cell proliferation (Skelding, Rostas et al. 2011), and cardiac contraction (Hudmon, Schulman et al. 2005) although the mechanisms of their activation as well as the

substrates they target remain unclear. More recently, several reports have linked the function of CaMK2 with cell migration and invasion of cancer cells (Easley, Brown et al. 2008, Mercure, Ginnan et al. 2008, Chi, Evans et al. 2016). It has been shown that in the vascular smooth muscle cells, CaMK2D is activated in the leading edge of the lamellipodia of migrating cells and pharmacological inhibition or silencing of CaMK2D decreases migration (Mercure, Ginnan et al. 2008). In line with this, activation of CaMK2 via autophosphorylation at T287 (or T286 for A isoform) was found to increase invasion and migration of breast cancer cells, osteosarcoma and gastric cancer cells (Daft, Yuan et al. 2013, Liu, Han et al. 2014, Chi, Evans et al. 2016). On the contrary, decreased expression of CaMK2D in osteosarcoma and prostate cancer cells was associated with decreased motility and invasion (Wang, Symes et al. 2010, Daft, Yuan et al. 2013).

Moreover, CaMK2 is a transducer of the Wnt/Ca^{2+} signalling pathway (Kuhl, Sheldahl et al. 2000). Wnt ligands, such as Wnt5A and Wnt11, cause an intracellular release of Ca^{2+}, which in turn activates CaMK2 and PKC. In *Xenopus* embryos, CaMK2 is active in the cells that promote the ventral cell fates and it was shown that inhibition of CaMK2 promotes dorsal cell fates (Kuhl, Sheldahl et al. 2000). Specifically, it was shown that overexpression of the constitutively active CaMK2 T286D mutant on the dorsal side of the embryo resulted in ventralisation, whereas overexpression of the kinase dead CaMK2 K42M mutant resulted in axis duplication (Kuhl, Sheldahl et al. 2000). In human cells, suppression of Wnt5A signalling was shown to inactivate CaMK2, monitored by its phosphorylation levels at T286 (Dissanayake, Wade et al. 2007). The output of Wnt/Ca^{2+} signalling is the dephosphorylation of the transcriptional regulator nuclear factor associated with T cells (NFAT) by calcineurin, followed its nuclear translocation for the activation of transcription of its target genes (Sheldahl, Slusarski et al. 2003).

The aim of this Chapter is to study the potential roles of the association between PAWS1 and CaMK2D and G isoforms. Due to time limitations, a thorough analysis has not been possible. However, this Chapter will present preliminary data and set the basis for further investigation into the possible roles of CaMK2s in regulating PAWS1 during cell migration, proliferation and calcium signalling.

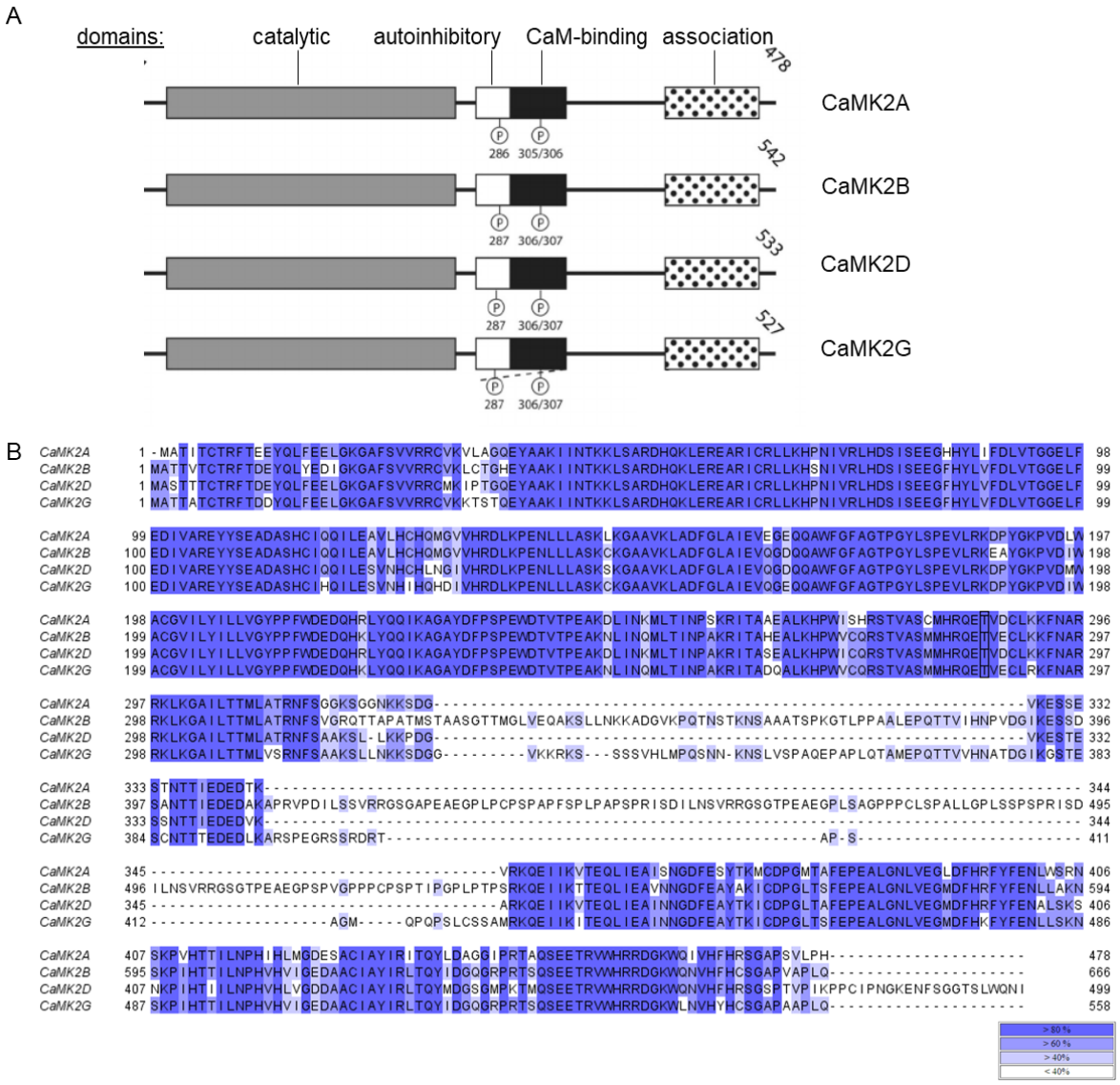

Figure 5- 1 The mammalian CaMK2 isoforms

A. Schematic illustration of the domain architecture of the CaMK2 isoforms. The catalytic domain, which is responsible for the phosphotransfer reaction to occur, is followed by the regulatory region that includes the autoinhibitory and the CaM-binding domain, and by the association domain. At basal Ca^{2+} levels, the autoinhibitory domain blocks substrate-binding or the catalytic activity of the catalytic domain. A rise in the intracellular Ca^{2+} levels, causes the binding of CaM to the CaM-binding domain, releasing autoinhibition. The association domain is present only in the CaMK2 enzymes and is required for their assembly into twelve-subunit holoenzymes (Adapted from Swulius and Waxham, 2008).

B. Sequence alignment of the mammalian CaMK2 isoforms. Alignment was performed with ClustalO in Jalview 2.10.3 and colouring indicates the % of sequence identity as shown in the box.

5.2 Results

5.2.1 PAWS1 interacts with CaMK2D and CaMK2G

As shown in Chapter 3, by mass spectrometry CK1α was identified as the major interactor of endogenous PAWS1 (Fig 3-12). CK1α was closely followed by CaMK2D and G isoforms as interactors of endogenous PAWS1, albeit the total spectral counts for CaMK2D/G were substantially lower than for CK1α (Fig. 3-12C). Similarly, CD2AP was also identified as an interactor of PAWS1 (Fig 3-12C). From these experiments, the peptide coverage of CaMK2D and CaMK2G isoforms identified in PAWS1 IPs but not in control IPs indicated a robust interaction (Figure 5-2A).

To validate the interactions between PAWS1 and CaMK2 isoforms, GFP-tagged CaMK2D and CaMK2G were transiently expressed in U2OS cells. GFP-IPs co-immunoprecipitated low levels of endogenous PAWS1 from both GFP-CaMK2D and GFP-CaMK2G expressing cells but not from GFP-control, indicating weak interaction (Fig 5-2B). Furthermore, FLAG-CaMK2D or FLAG-empty vector were transiently expressed in PAWS1$^{GFP/GFP}$ knock-in U2OS cells and the cell extracts were subjected to GFP- and FLAG-IPs (Fig 5-2C). FLAG-CaMK2D co-precipitated with GFP-PAWS1 and similarly GFP-PAWS1 was co-precipitated with FLAG-CaMK2D but not with FLAG-control (Fig 5-2C). The results from the co-IPs show that the interaction between PAWS1 and CaMK2 isoforms is rather weak and vastly weaker than the PAWS1:CK1α interaction that was described previously. There could be three possible explanations for this: first, the interaction is stimulus-dependent and so it is weak under unstimulated conditions; second, a limited pool of the PAWS1 and CaMK2 proteins contribute to the interaction; third, PAWS1 is a substrate for CaMK2D/G and so the interaction is only transient and so as soon as PAWS1 is phosphorylated, it dissociates from CaMK2D/G isoforms. Due to time constraints, focus was turned into investigating only the third possibility, that PAWS1 might be a substrate of CaMK2D/G.

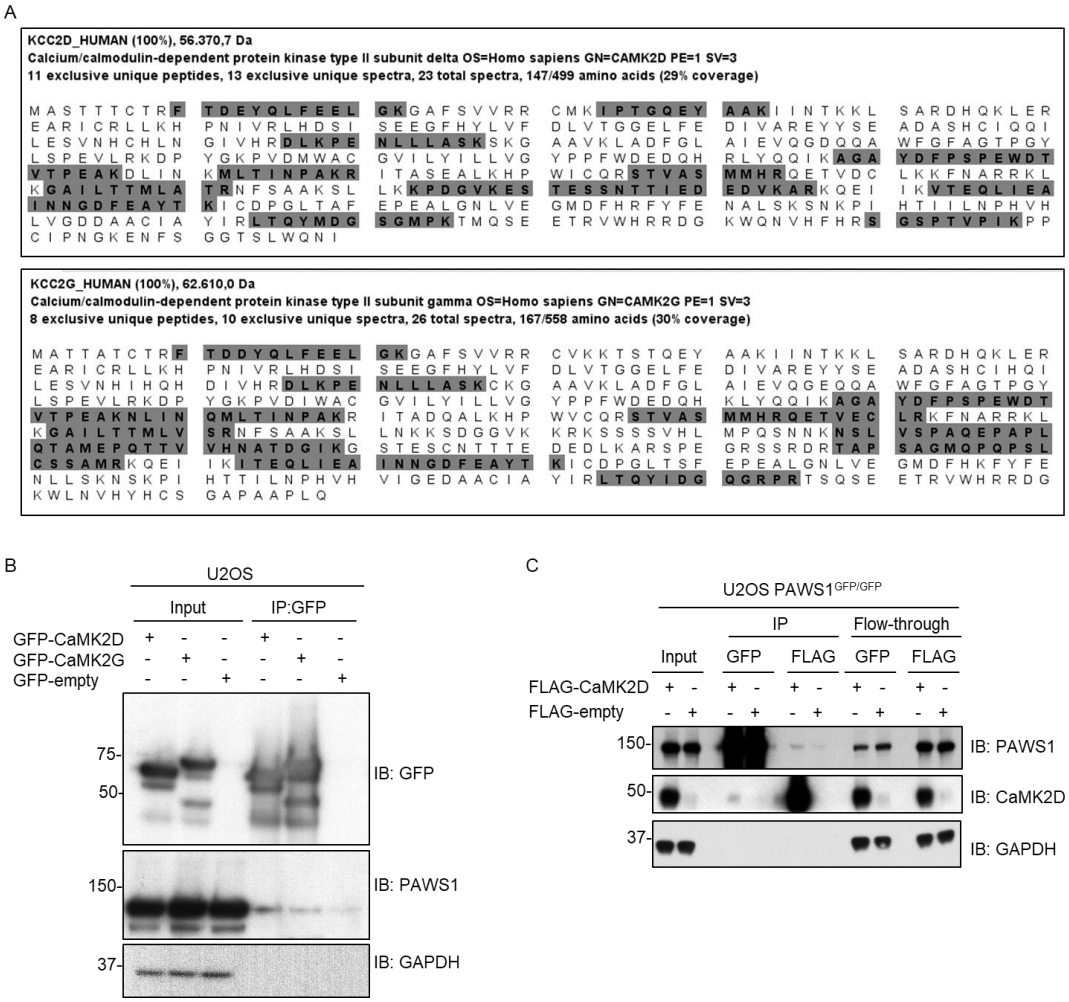

Figure 5- 2 PAWS1 interacts with CaMK2D and CaMK2G isoforms

A. The highlighted tryptic peptides on CaMK2D (top) and CaMK2G (bottom) indicate the overall protein coverage as identified by mass-spectrometry of PAWS1-GFP IPs from Fig 3-12A. The included images were obtained using Scaffold V4.3 analysis of the LC-MS/MS data.

B. U2OS cells were transfected with GFP-CaMK2D, GFP-CaMK2G or GFP-control for 48 h prior to lysis. Cell extracts (500 µg of protein) were subjected to GFP-IPs. Input extracts (10 µg of protein) and GFP-IPs (50% of the IP) were resolved by SDS-PAGE, followed by immunoblotting with the indicated antibodies.

C. U2OS PAWS1$^{GFP/GFP}$ knock-in cells were transfected with FLAG-CaMK2D or FLAG-empty for 48 h prior to lysis. Cell extracts (200 µg of protein per IP) were subjected to GFP-IPs or FLAG-IPs. Input extracts (10 µg of protein) and GFP-IPs (100% of the IP) were resolved by SDS-PAGE, followed by immunoblotting with the indicated antibodies.

5.2.3 PAWS1 is phosphorylated at S356 by CaMK2D in vitro

To test if PAWS1 was phosphorylated by CaMK2, an *in vitro* kinase assay was set up using the recombinant GST-CaMK2D protein and the full-length GST-PAWS1-6xHis, both purified from *E. coli*. A reaction with GST-CK1α and PAWS1 was employed as a positive control. As seen in Fig 5-3A, PAWS1 was phosphorylated robustly by CaMK2D while no signal was obtained in the absence of the kinase. The signal of the phosphorylated PAWS1 by CaMK2D was almost as robust as the signal from the CK1α-phosphorylated PAWS1 (Fig 5-3A). Additional bands at the molecular weight range from 75 to 37 kDa might represent CaMK2D autophosphorylation and/or degradation products of CaMK2D. In the absence of calcium and calmodulin from the reaction, PAWS1 was still phosphorylated, although the signal was substantially weaker compared to the reaction containing Ca^{2+}/CaM (Fig 5-3B). The lower molecular weight bands were still detectable in the absence of Ca^{2+}/CaM. Thus, if these products represent autophopshorylated CaMK2D, meaning that CaMK2D was still active then this could explain why PAWS1 phosphorylation was not completely abolished in the absence of Ca^{2+}/CaM (Fig 5-3B).

To identify the CaMK2D phosphorylation site on PAWS1, an *in vitro* kinase assay reaction was set up using non-radioactive ATP. The reaction sample was resolved by SDS-PAGE and the phospho-PAWS1 band, as detected by Coomassie staining, was excised, trypsin-digested and subjected to analysis by Mass spectrometry. One peptide with a single phosphorylated residue was identified, with the molecular mass of 520.753 Da. This was identical to the peptide expected for a tryptic phospho-peptide comprising residues 354-361 of PAWS1 (AKSVDEIAK), with the Ser356 being the phosphorylated residue. Indeed, analysis of PAWS1 that was transfected in U2OS and HEK93 cells by mass spectrometry, as well as global phosphoproteomics analysis in U2OS cells (Chapter 4) had also identified this pSer356 as one of the most prominent phosphorylated residues in PAWS1 (unpublished observation in the Sapkota lab), suggesting that this site is phosphorylated in cells. Excitingly, Ser356 is conserved in vertebrates and conforms to the CaMK2D/G phosphorylation consensus F/I/L/V/Y-x-R-x-x-S*/T*-F/I/L/M/V/Y-D/E motif, except that R at -3 position is replaced by a K. (LVKAKSVD).

To study the CaMK2 phosphorylation on PAWS1, a phospho-specific antibody was generated in rabbits against a short PAWS1 peptide containing pSer356 (p-PAWS1 S356) residue in the middle. In order to validate the specificity of the antibody, an in vitro kinase was set up where PAWS1 was phosphorylated *in vitro* by CaMK2D using non-

radioactive ATP. Different amounts of unphosphorylated and CaMK2D-phosphorylated PAWS1 were then spotted onto nitrocellulose membranes, which were immunoblotted with anti-p-PAWS1 S356 and anti-GST antibodies. As shown in Fig 5-4B, the anti-p-PAWS1 S356 antibody displayed a dose-dependent signal for PAWS1 phosphorylated by CaMK2D, whereas no signal was detected for the unphosphorylated PAWS1. Anti-GST blots, employed as loading controls, displayed identical signals in both cases (Fig 5-4B).

To test if the p-PAWS1 S356 antibody could recognize PAWS1 phosphorylated at Ser356 in cells, plasmids encoding wild type PAWS1, or phospho-deficient (S356A) and phospho-mimetic (S356E) mutants of PAWS1 were transiently expressed in $PAWS1^{-/-}$ cells and cell extracts were analysed by Western blotting using antibodies against total and p-PAWS1 S356. As seen in Fig 5-4C, the anti-p-PAWS1 S356 antibody recognized only $PAWS1^{WT}$ but not $PAWS1^{S356A}$ or $PAWS1^{S356E}$ indicating that the antibody selectively recognises PAWS1 phosphorylated by CaMK2D at S356 in cell extracts. Anti-PAWS1 antibody showed that the expression of wild type PAWS1 was slightly lower than the phospho-mutants Notably, when co-expressed with CaMK2D, the levels of PAWS1-pSer356 did not appear increase further (Fig 5-4C).

To determine whether PAWS1 phosphorylation at S356 in cells was indeed mediated by CaMK2D and/or CaMK2G, siRNAs were used to silence the expression of these two kinase isoforms, both individually and collectively. Upon increasing concentrations of siCaMK2D alone or in conjunction with siCaMK2G, the phosphorylation levels of PAWS1 at S356 were decreased by about 50% compared to the levels observed in untransfected cells and those that were transfected with non-targeting siRNAs (Fig5-5). Due to the lack of an antibody that recognizes endogenous CaMK2G, it was not possible to determine the efficiency of the siCaMK2G. Nevertheless, no difference in p-PAWS1 S356 levels were observed between the untransfected control and siCaMK2G transfected cells, suggesting that either the CaMK2G silencing was not efficient enough or PAWS1 phosphorylation at S356 is specifically mediated by CaMK2D isoform.

Following validation of the p-PAWS1 S356 antibody for detection of endogenous PAWS1 phosphorylated at S356, it was possible to test whether activating or inhibiting the kinase activity of CaMK2 in cells affected the phosphorylation of PAWS1 at S356. For this, the calcium ionophore A23187 (Reed and Lardy 1972) and the calcium chelator BAPTA-AM (Wie, Koh et al. 2001) were used. To monitor the activation of CaMK2 the

phospho-specific antibody recognizing the autophosphorylation site T286 (pCaMK2 T286) was used. It should be noted that this antibody cannot distinguish between different CaMK2 isoforms. Elevated level of pPAWS1 S356 was observed upon Ca^{2+} ionophore treatment for 1 min, whereas no difference in pCaMK2 T286 was observed (Fig 5-6). BAPTA-AM treatment resulted in a slight decrease in the levels of pPAWS1 S356 levels (Fig 5-6). Rather surprisingly, the levels of pCaMK2 T286 were significantly increased upon treatment with BAPTA-AM (Fig 5-6) because the opposite outcome was expected, as chelating the calcium ions in cells should result in CaMK2 inhibition, which would mean decreased autophosphorylation at T286.

To investigate this peculiar result further, U2OS cells were subjected in a time course treatment of different calcium ionophores and inhibitors and CaMK2 activation was monitored by Western blotting (Fig 5-7). The levels of pCaMK2 T286 increased in a time-dependent manner after treatment with the calcium ionophores Ionomycin (Enyeart, Liu et al. 2011) and A23187, as well as with the calcium chelator BAPTA-AM, the calcium channel blocker SKF 96365 (Singh, Hildebrand et al. 2010) and the CaMK2 inhibitor autocamtide-3 derived inhibitory peptide (AC3-I) (Chen, Otmakhov et al. 2001). However, the most striking observation to emerge from this experiment was the effect of DMSO on CaMK2 activation. An elevation in the levels of pCaMK2 T286 was detected after 30 and 60 min of treatment with DMSO control (Fig 5-7). Therefore, the above findings are somewhat affected by the fact that all the compounds used were dissolved in DMSO, in accordance with the manufacture's guidelines. The effects of DMSO on calcium signalling have been underestimated in the existing literature despite some studies that have reported that 1% (v/v) DMSO in the culture medium could elevate intracellular Ca^{2+} levels (Brown and Rydqvist 1990, Morley and Whitfield 1993). Due to time limitations, the issues with the above compounds on calcium signalling have not been resolved. However, it would be recommended to dissolve these compounds either in water, or in other solvents that do not affect calcium signalling.

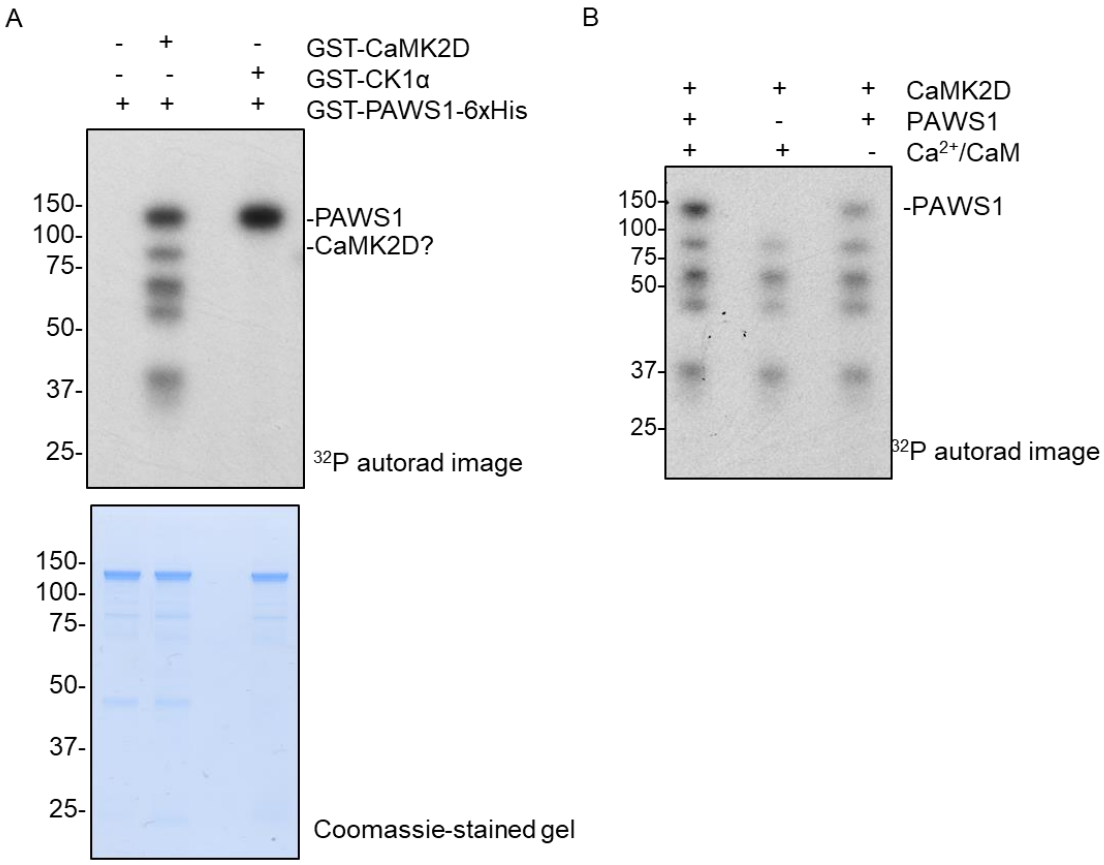

Figure 5- 3 PAWS is phosphorylated by CaMK2D *in vitro*

A. *In vitro* kinase assay with GST-CaMK2D (200 ng) and GST-PAWS1-6xHis (2 µg) in the presence of ^{32}P-ATP (500 cpm/pmol). Phosphorylation of PAWS1 by CK1α was performed as a positive control. The reaction was stopped after 30 min at 30 °C and the samples were resolved by SDS-PAGE, the gel was Coomassie stained and radioactivity was analysed by autoradiography.

B. Same as (A), except that the reactions were performed in the presence or absence of $CaCl_2$ (200 mM) and Calmodulin (CaM) (40 µM) and gels were analysed by autoradiography.

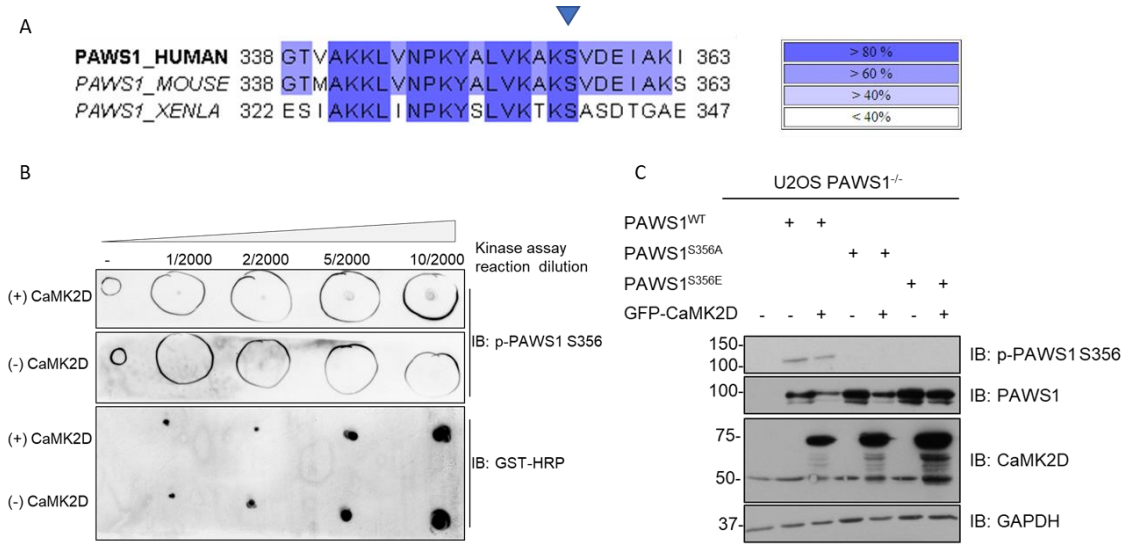

Figure 5- 4 Validation of CaMK2D-phosphorylation of PAWS1 at S356 with a pPAWS1 S356 antibody

A. Sequence alignment of PAWS1 from human, mouse and *Xenopus laevis* (XNLA) around the S356 phosphorylation residue, indicated by the blue arrow. Alignment was performed with ClustalO in Jalview 2.10.3 and colouring indicates the % of sequence identity as shown in the box.

B. A phospho-specific antibody against 15 residues surrounding PAWS1 phosho-S356 was generated by immunising rabbits and was purified by first passing sera through the dephospho-peptide dolumn and then affinity-purified on the phospho-S356 peptide immunogen (by the DSTT antibody production team). A kinase assay was set up as in 5-3A but with non-radioactive ATP. Reaction mix was diluted as indicated and spotted on a nitrocellulose membrane, which was probed with the indicated antibodies.

C. PAWS1$^{-/-}$ U2OS cells were transfected with plasmids encoding PAWS1^{WT}, PAWS1^{S356A} or PAWS1^{S356E} with or without the plasmid encoding GFP-CaMK2D for 48 h prior to lysis. Cell extracts (20 µg of protein) were resolved by SDS-PAGE, followed by immunoblotting with the indicated antibodies.

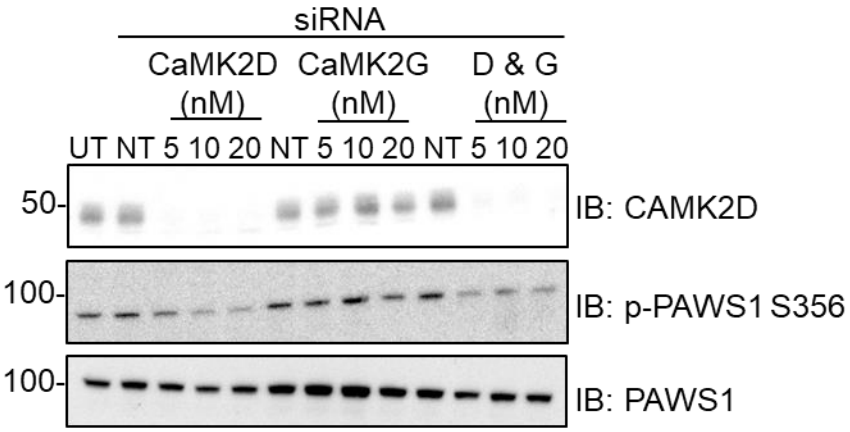

Figure 5- 5 Validation of the PAWS1 S356 by CaMK2D in cells

CaMK2D and CaMK2G expression was silenced in U2OS cells with indicated amounts of siRNA for 48 h prior to lysis. Cell extracts (20 µg of protein) were resolved by SDS-PAGE, followed by immunoblotting with the indicated antibodies. (UT: Untreated, NT: Non-targeting RNA).

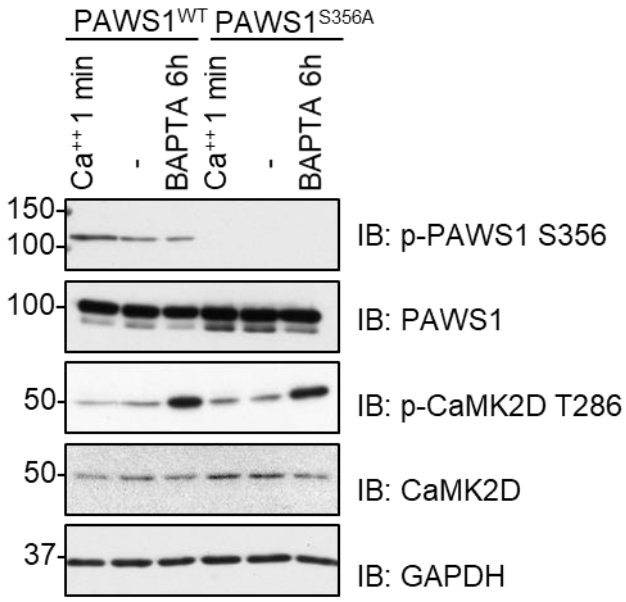

Figure 5- 6 PAWS1 does not appear to affect the calcium-induced activation of CaMK2D

PAWS1$^{-/-}$ U2OS cells stably restored with PAWS1^{WT} and PAWS1^{S356A} were treated with the calcium ionophore A23187 for 1 min or the calcium chelator BAPTA-AM for 6 h prior to lysis. Cell extracts (20 µg of protein) were resolved by SDS-PAGE, followed by immunoblotting with the indicated antibodies.

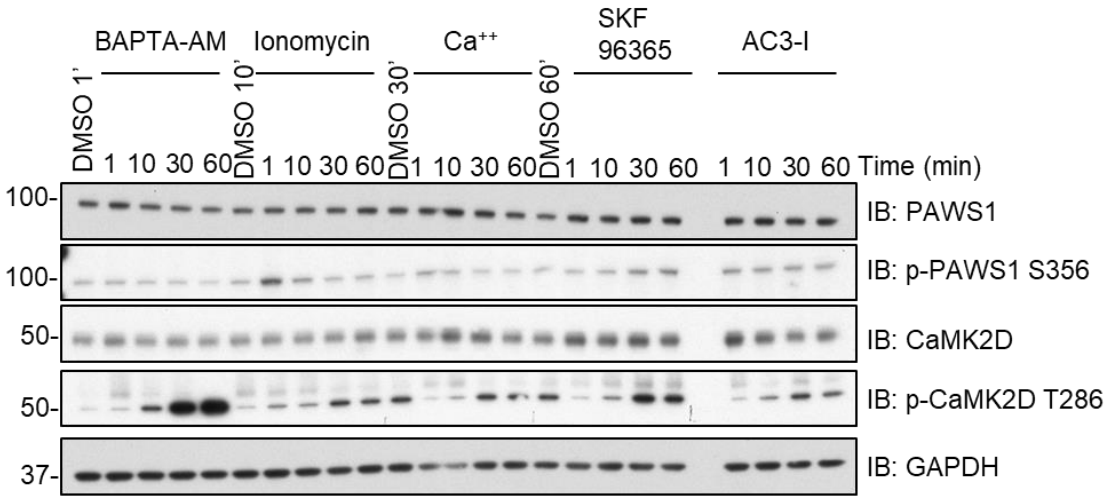

Figure 5- 7 DMSO control induces calcium-responses in U2OS cells

U2OS cells were treated with the indicated DMSO control, or calcium chelator BAPTA-AM, the ionophores Ionomycin and A23187, and the calcium channel blocker SKF 96365 or the CaMK2 inhibitor autocamtide-3 derived inhibitory peptide (AC3-I) for the indicated time points prior to lysis. Cell extracts (15 µg of protein) were resolved by SDS-PAGE, followed by immunoblotting with the indicated antibodies.

5.2.4 Biological role of PAWS1 S356 phosphorylation in cells

To study the potential physiological roles of PAWS1 phosphorylation at S356 in cells, PAWS1$^{-/-}$ cells were stably restored with PAWS1^{WT}, PAWS1^{S356A} or PAWS1^{S356E} (Fig 5-8). Since PAWS1$^{-/-}$ cells were shown to display migratory defects (Cummins et al., 2018), the first objective was to test if PAWS1 phospho-deficient (PAWS1^{S356A}) and phosho-mimetic (PAWS1^{S356E}) mutants could rescue the migration defects to the same degree as PAWS1^{WT}. For this, cells were cultured to confluency in adjacent chambers separated by a spacer. Upon removal of the spacer, a uniform gap was formed and cell migration onto the gap was monitored by imaging for up to 12 h (Fig 5-9). PAWS1^{WT} and PAWS1^{S356E} cells completely closed the gap within 12 h, whereas PAWS1^{S356A} migrated into the gap more slowly and failed to fill the gap even after 12 h (Fig 5-9). These results suggested that phosphorylation of PAWS1 at S356 is critical for cell migration, and could provide new insights into the CaMK2D function in regulating cell migration via phosphorylation of its novel substrate PAWS1.

Signaling cascades that regulate cell migration often regulate cell proliferation, (Collins, Ricketts et al. 1999, De Donatis, Comito et al. 2008) and CaMK2 isoforms have been implicated in cancer cell proliferation (Wang, Zhao et al. 2015). Thus, the next aim was to evaluate whether phosphorylation of PAWS1 at S356 could impact cell proliferation. A proliferation assay based on the reduction of MTS tetrazolium compound by metabolically active cells to generate a colored formazan product which is soluble in cell culture medium, was used to monitor cell proliferation in PAWS1$^{-/-}$ cells that were stably restored with PAWS1^{WT}, PAWS1^{S356A} or PAWS1^{S356E}. Formazan production is proportional to the number of living cells, so the measurement of the absorbance of formazan gave an estimation of cell viability. Cells were seeded in a 96-well plate at different densities and left for 16 h before being subjected to the MTS assay. It was found that the intensity of the produced colour was proportional to the cell density (Fig 5-10). No significant differences were observed among PAWS1^{WT}, PAWS1^{S356A} and PAWS1^{S356E}, in any of the cell densities tested, suggesting that phosphorylation of PAWS1 by CaMK2 at S356 is not involved in the regulation of cell proliferation in U2OS cells (Fig 5-10).

Next, the involvement of PAWS1 phosphorylation at S356 in Ca^{2+} signalling activation was investigated by monitoring the Ca^{2+}-induced nuclear translocation of NFAT in U2OS wild type, PAWS1$^{-/-}$, PAWS1^{WT}, PAWS1^{S356A} cells (Fig 5-11). Cells were transiently transfected with NFAT-mCherry for 24 h and cells were treated with or

without the calcium ionophore A23187 for 5 min. Cells were then fixed and analysed with fluorescence microscopy. In the untreated cells, NFAT-mCherry displayed cytosolic staining (Fig 5-11). Ca^{2+} stimulation resulted in the nuclear translocation of NFAT within 5 min independent of PAWS1 expression in all cell lines. This result indicated that PAWS1 is not involved in sensing intracellular Ca^{2+} fluxes nor in inducing Ca^{2+}-mediated nuclear localization of NFAT. Similarly, PAWS1 phosphorylation at S356 was not found to be required in the downstream responses of Ca^{2+} signalling (Fig 5-11).

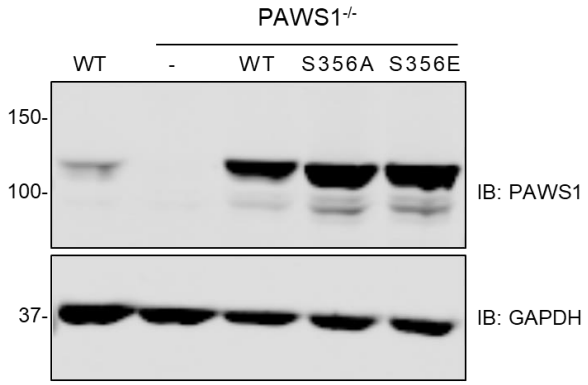

Figure 5- 8 Generation of PAWS1^{S356A} and PAWS1^{S356E} stable cell lines

U2OS PAWS1$^{-/-}$ cells were stably integrated with a vector encoding PAWS1^{WT}, PAWS1^{S356A}, PAWS1^{S356E}. Cell extracts (15 µg of protein) were resolved by SDS-PAGE, followed by immunoblotting with the indicated antibodies. Expression levels were compared to endogenous PAWS1 levels from wild type U2OS extracts.

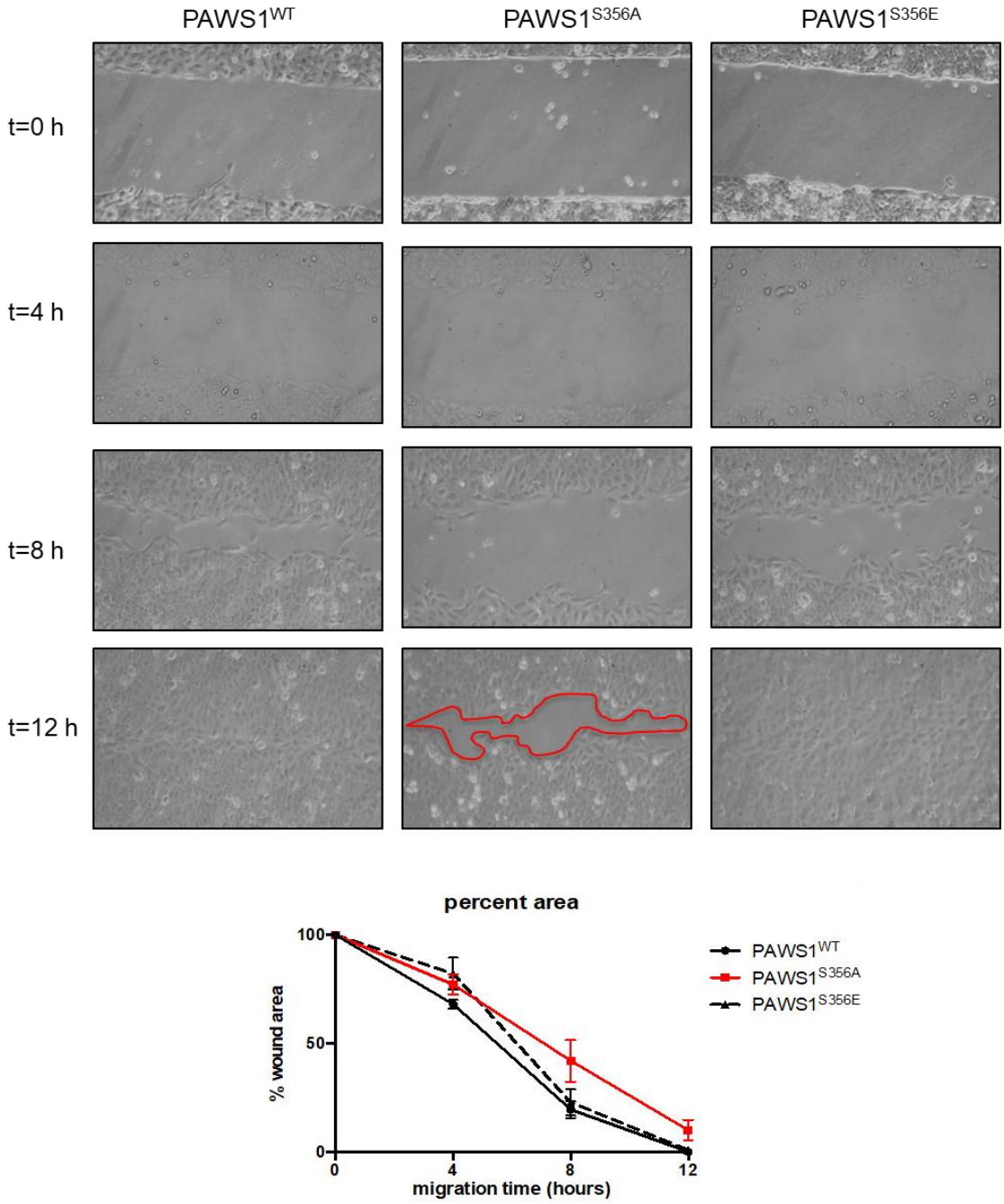

Figure 5- 9 Mutation of PAWS1 S356 to A prevents rescue of migration defect in U2OS PAWS1$^{-/-}$ cells

Representative images of wound healing migration assay of PAWS1^{WT}, PAWS1^{S356A}, PAWS1^{S356E} cells at 0, 4, 8, and 12 h following removal of the insert separating wells of confluent cells. The percentage of wound (gap) closure was quantified and plotted as shown (n=3; Error bars represent ±SEM).

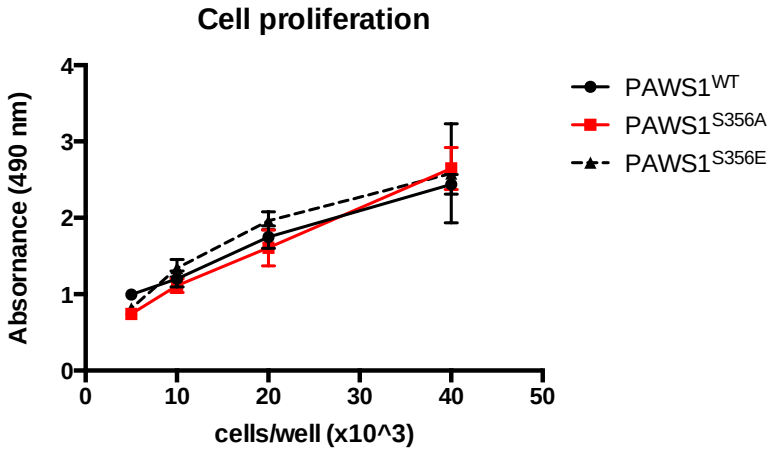

Figure 5- 10 Mutation of PAWS1 S356 to A or E does not affect cell proliferation

$PAWS1^{WT}$, $PAWS1^{S356A}$, $PAWS1^{S356E}$ cells were ceded in different densities and cell viability was quantified using the MTS cell proliferation assay kit (Promega). (n=3; Error bars represent ±SEM).

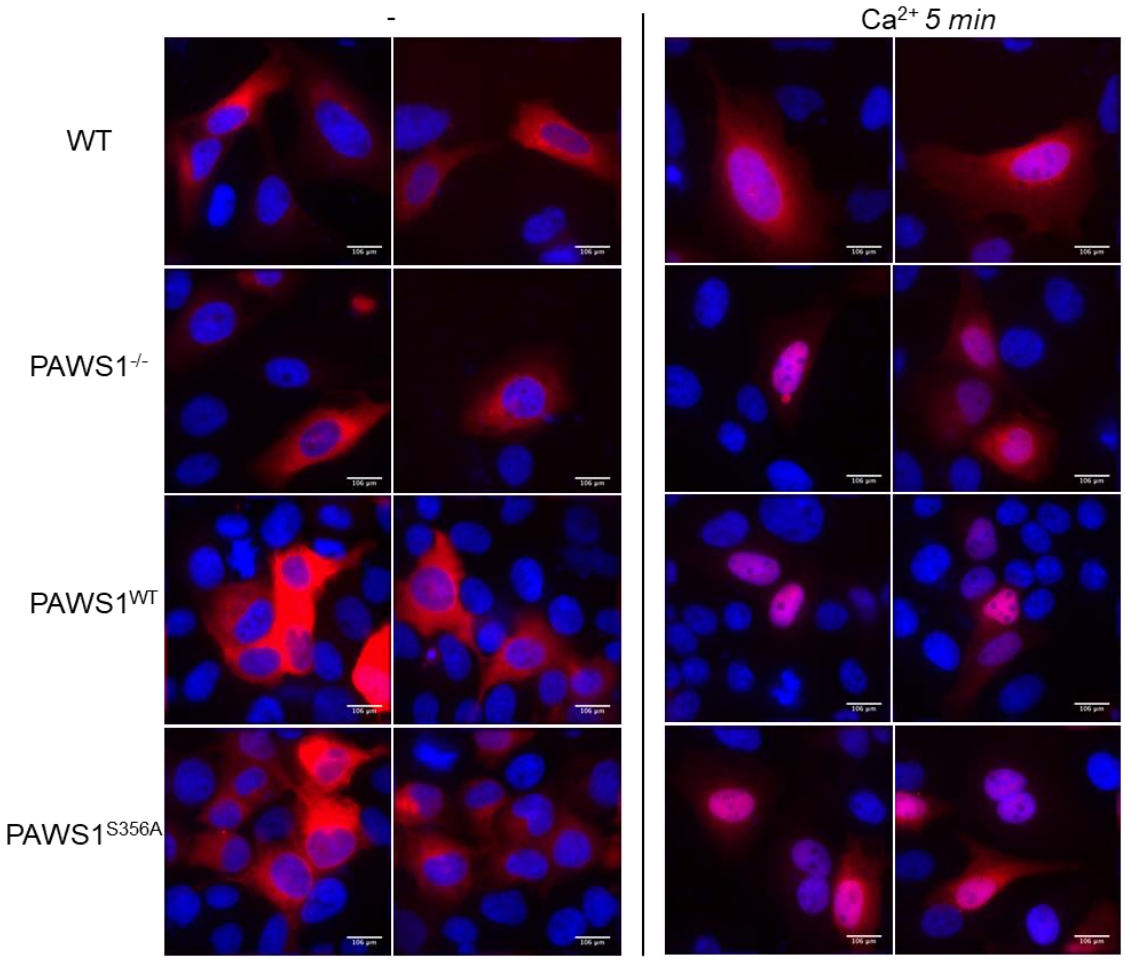

Figure 5- 11 PAWS1 does not affect the calcium-induced nuclear localisation of NFAT

U2OS wild type (WT), PAWS1^{WT}, PAWS1^{S356A}, PAWS1^{S356E} cells were transfected with NFAT-mCherry for 24 h and treated with the calcium ionophore A23187 (Ca^{2+}) or DMSO control (-) for 5 min. Cells were then fixed and analysed with fluorescence microscopy for NFAT-mCherry (red) and DAPI (blue). Scale bars represent 106 µm.

5.3 Discussion

The data presented in this Chapter has demonstrated that PAWS1 interacts with CaMK2D and CaMK2G isoforms, albeit with weak affinity. The observation that PAWS1 is phosphorylated by CaMK2D *in vitro* and in cells at S356, suggests that PAWS1 is likely to be a substrate for CaMK2D isoforms. However, the exact signalling cues and mechanisms that govern the interaction between PAWS1 and CamK2D/G and the phosphorylation of PAWS1 at S356 remain to be defined. Considerably more work will be needed to determine whether the phosphorylation of PAWS1 at S356 occurs constitutively or is stimulus-dependent.

It has been shown that PAWS1 controls actin cytoskeleton dynamics and cell migration through its association with the SH3 adaptor CD2AP (Cummins, Wu et al. 2018). Thus, PAWS1 deficiency in U2OS cells causes defects in actin cytoskeleton and cell migration. The precise signalling and molecular events that prompt PAWS1 to control cytoskeleton dynamics remain elusive. Interestingly, calcium signalling is thought to play crucial roles in cytoskeleton dynamics and cell migration (Prevarskaya, Skryma et al. 2011, Tsai, Kuo et al. 2015). The observations that both $PAWS1^{WT}$ and the phospho-mimetic $PAWS1^{S356E}$ mutant can rescue the cell migration defects caused by PAWS1 deficiency but that the phospho-deficient $PAWS1^{S356A}$ cannot, indicate an intriguing possibility that phosphorylation of PAWS1 at S356 by CaMK2 isoforms could be involved in mediating actin cytoskeleton organisation to facilitate cell migration.

Dynamic association of PAWS1 with CD2AP in the leading edge of the migrating cell was shown to be involved in cell motility. Previous reports have shown that CaMK2 isoforms also localise in the periphery of the cell and inhibition of their activity is linked to decreased migration (Mercure, Ginnan et al. 2008). It would therefore be exciting to test if CaMK2 co-localises with PAWS1 and CD2AP at the cell periphery, phosphorylates the pool of PAWS1 that associated with CD2AP, or that phosphorylation at S356 modulates PAWS1 association with CD2AP. If PAWS1:CD2AP complex is not affected by the phosphorylation of S356, a proteomic approach on p-PAWS1 S356 could reveal proteins that read and relay the pSer356 signal on PAWS1.

In addition to U2OS cells described above, a good alternative cell line to study the effect of PAWS1 in cell migration would be the prostate cancer PC3 cells, which naturally lack PAWS1 expression (Vogt, Dingwell et al. 2014). PC3 cells are derived from bone metastatic cancer and are widely used in wound healing assays as they are

highly aggressive and motile and they were shown to express high levels of CaMK2 isoforms (Mamaeva, Kim et al. 2009). Re-introduction of PAWS1^{WT}, PAWS1^{S356A} and PAWS1^{S356E} in PC3 cells would allow one to test if PAWS1 affects migration as well as the kinase activity of CaMK2D by immunoprecipitation followed by kinase assay towards a peptide substrate.

Furthermore, despite the weak nature of the PAWS1:CaMK2D/G interaction, it would be recommended to identify the residues on PAWS1 that mediate its association with CaMK2D/G. CaMK2-interacting deficient PAWS1 mutants could then be tested for their ability to restore the phenotypes that are associated with PAWS1 deficiency in U2OS and PC3 cells, such as cell migration and actin cytoskeleton organisation.

In the previous Chapters, it was uncovered that PAWS1 functions in canonical Wnt signalling via its association with CK1α. The robust nature of PAWS1:CK1α interaction cannot be neglected, when considering any new functions of PAWS1. The fact that CaMK2 is a player of the non-canonical Wnt signalling cascade makes the possibility of PAWS1 being a potential link between canonical and non-canonical Wnt signalling an intriguing one, which should be explored. In *Xenopus* embryos, CaMK2 activity is required for induction of the ventral cell fates, whereas inhibition of CaMK2 promotes dorsal cell fates (Kuhl, Sheldahl et al. 2000). Thus, it could be hypothesised that PAWS1 might exert some of its functions by inhibiting CaMK2 activity in the ventral side when overexpressed in *Xenopus* embryos. However, this hypothesis has not been tested yet. A second assumption would be that PAWS1 phosphorylation at S356 by CaMK2D might be involved in its interaction with CK1α and its ability to induce axis duplication. However, injection of PAWS1^{S356A} mRNA in *Xenopus* embryos did not inhibit the formation of a complete secondary body axis (personal communication with K. Dingwell, The Francis Crick Institute, London).

To sum up, the preliminary results presented in this Chapter have thrown up many questions that need further investigation. The most important limitation of this study was the lack of optimised tools to study Ca^{2+} signalling in cells. Once this is transcended, several assays including live cell imaging in response to Ca^{2+} stimuli and Ca^{2+} channel blockers or CaMK2 inhibitors can be performed to explore the role of PAWS1 phosphorylation by CaMK2 in more detail.

6. The pathogenic mutations on PAWS1 gene and their association with skin disorders

6.1 Introduction

While the majority of this thesis has focused on the biochemical analysis of PAWS1, several studies have highlighted more clinical roles for PAWS1 (Drogemuller, Jagannathan et al. 2014, Sayyab, Viluma et al. 2016, Maruthappu, McGinty et al. 2017). Indeed, with PAWS1 mutations being reported in pathological conditions of skin and hair, the potential clinical implications of PAWS1 research cannot be ignored. Therefore, a more thorough analysis of these disease-relevant PAWS1 mutations in this final Chapter was warranted.

To begin with, a recessive missense mutation in the PAWS1 gene resulting in R52P substitution was identified in dogs suffering from hereditary footpad hyperkeratosis (HFH) (Drogemuller, Jagannathan et al. 2014). The same mutation has since been reported in more dogs with HFH (Sayyab, Viluma et al. 2016). More recently, a novel recessive missense mutation in the PAWS1 gene resulting in A34E substitution has been reported in patients with palmoplantar keratoderma (PPK) (Maruthappu, McGinty et al. 2017) (Fig 6-1). Both sets of mutations in dogs and humans cause identical symptoms, characterised by thickening of footpads, abnormal hair growth and morphology, and epidermal hyperplasia (Drogemuller, Jagannathan et al. 2014, Sayyab, Viluma et al. 2016, Maruthappu, McGinty et al. 2017). Interestingly, mice displaying spontaneous "wooly" phenotype, which was characterised by rough or matted appearance of the hair, were found to harbour homozygous mutations in the PAWS1 gene leading to truncation of PAWS1 (Radden, Child et al. 2013). Furthermore, internal analysis of the exome sequencing data from patients with various skin diseases in collaboration with I. McLean (University of Dundee) identified an autosomal dominant mutation in the PAWS1 gene leading to G640R substitution in patients with hereditary benign trichilemmal cysts, which originate from hair follicles (unpublished data). Remarkably, all of the above pathogenic mutations in PAWS1 are linked to skin diseases. However, the molecular mechanisms that underpin the pathogenicity by PAWS1 mutations remain unelucidated.

As mentioned in the Introduction to the thesis, Wnt signalling plays pivotal role in skin and hair homeostasis and development. Hyperactivation of Wnt signalling is linked to the development of skin tumours (Malanchi, Peinado et al. 2008, Yang, Andl et

al. 2008). Wnt signalling is crucial in the maintenance of the skin stem cells in humans and mediates hair differentiation (Huelsken, Vogel et al. 2001). Interestingly, patients with mutations in the Wnt genes have also been reported to display palmoplantar hyperkeratosis and hair growth abnormalities (Adaimy, Chouery et al. 2007, Petrof, Fong et al. 2011). Given the role of PAWS1 in Wnt signalling that has been described in Chapter 3, it is tempting to speculate that the pathogenic PAWS1 mutations interfere with Wnt signalling, by either influencing PAWS1 interaction with CK1α or the transcription of PAWS1-dependent genes. Remarkably, a recent study reported that deletion of CK1α from keratinocytes of mice resulted in epidermal thickening and skin hyperpigmentation (Chang, Kuo et al. 2017), symptoms that closely resemble those caused by PAWS1 mutations R52P and A34E in dogs and humans respectively ((Drogemuller, Jagannathan et al. 2014, Sayyab, Viluma et al. 2016, Maruthappu, McGinty et al. 2017).

The key aim of this Chapter was to establish the effect of the pathogenic PAWS1 mutations on its function and delineate the molecular mechanisms by which PAWS1 mutations cause pathogenicity. In light of the knowledge accumulated on PAWS1 function in this thesis, these aims are now feasible. However, at the time this project was started, limited functional assays were available for PAWS1. Furthermore, due to time constraints of the PhD, most of the data presented here is preliminary in nature and will provide a framework for further research on this area.

6.2 Results

6.2.1 Pathogenic PAWS1 mutants are defective in mediating PAWS1-dependent transcription in PC3 cells

Prior to establishing the role of PAWS1 in Wnt signalling and CK1α biology, PAWS1 was reported to influence the transcription of ~800 genes in PC3 cells (Vogt PhD thesis, http://discovery.dundee.ac.uk). In order to study the role of the pathogenic PAWS1 mutants in gene transcription, prostate cancer PC3 cells, which lack PAWS1 expression, were restored with $PAWS1^{WT}$ or the pathogenic $PAWS1^{R52P}$ and $PAWS1^{G640R}$ mutants, by retroviral infection (Fig 6-2A), to limit expression to near-endogenous levels seen in other cells (Vogt, Dingwell et al. 2014). qPCR was performed for some of the top target genes that were previously (Vogt, Dingwell et al. 2014) identified to be regulated by PAWS1 (Figure 6-2B). Interestingly, while $PAWS1^{WT}$ led to significant increase in the transcription of the transforming growth factor beta induced (TGFBI) and matrix metalloproteinase 13 (MMP13) genes compared to control PC3 cells, the pathogenic $PAWS1^{R52P}$ and $PAWS1^{G640R}$ mutants did not (Fig 6-2B). These results that the pathogenic mutants of PAWS1 mirrored the transcriptional profiles in control PC3 cells, which are devoid of PAWS1, suggested a possible loss of PAWS1 function caused by the mutations. However, as PC3 cells are metastatic prostate cancer cells and do not resemble primary epidermal keratinocytes and hail follicular cells that these mutations affect, it is not possible to predict whether the pathogenesis involves the misregulated transcription of TGFBI and MMP13. MMP13 is a matrix metalloproteinase that functions in the turnover of connective tissue components (Knauper, Will et al. 1996). TGFBI is a secreted protein that inhibits cell adhesion (Skonier, Bennett et al. 1994). The expression of other PAWS1-target genes, including LGR5, CCNA1 and Androgen Receptor (AR) were not significantly affected by the pathogenic mutants (Figure 6-2B).

The experiments in PC3 cells were repeated when the $PAWS1^{A34E}$ mutation was identified in human patients (through personal communication with D. Kelsell, Blizzard Intitute, London) PC3 cells were stably restored with $PAWS1^{WT}$ or the pathogenic $PAWS1^{A34E}$ mutant by retroviral infection and the transcription of PAWS1-dependent genes LGR5, MMP13 and AR assessed (Fig 6-3). As before, restoration of $PAWS1^{WT}$ in PC3 cells activated the transcription of LGR5 and MMP13 and inhibited the transcription of AR compared to control PC3 cells. However, restoration of $PAWS1^{A34E}$ in PC3 cells mirrored the transcription of MMP13 and AR seen in control cells, while the transcription of LGR5 was enhanced even beyond that caused by $PAWS1^{WT}$ (Fig 6-3B). Interestingly,

PAWS1^{A34E} protein displayed a difference in its electrophoretic mobility, as it appeared at a slightly lower apparent molecular weight than PAWS1^{WT} (Fig 6-3A), suggesting that PAWS1^{A34E} mutant might lack or harbour different post-translational modifications compared to PAWS1^{WT} or display distinct structural features that could explain loss of possible functions. However, due to time limitations of the PhD, further characterisation of these mutants was not possible and this project has now been undertaken by another member of the Sapkota lab (Dr K. Wu).

Figure 6- 1 Representative phenotypes of the pathogenic PAWS1 mutations

A. The affected paw of a dog suffering from hereditary footpad hyperkeratosis carrying PAWS1^{R52P} mutation (left) compared to a paw from a healthy dog (right) (adopted from Drogemuller et al., 2014).

B. The affected soles and palms of two siblings carrying with palmoplantar keratoderma carrying PAWS1^{A34E} mutation (adopted from Maruthappu et al., 2017).

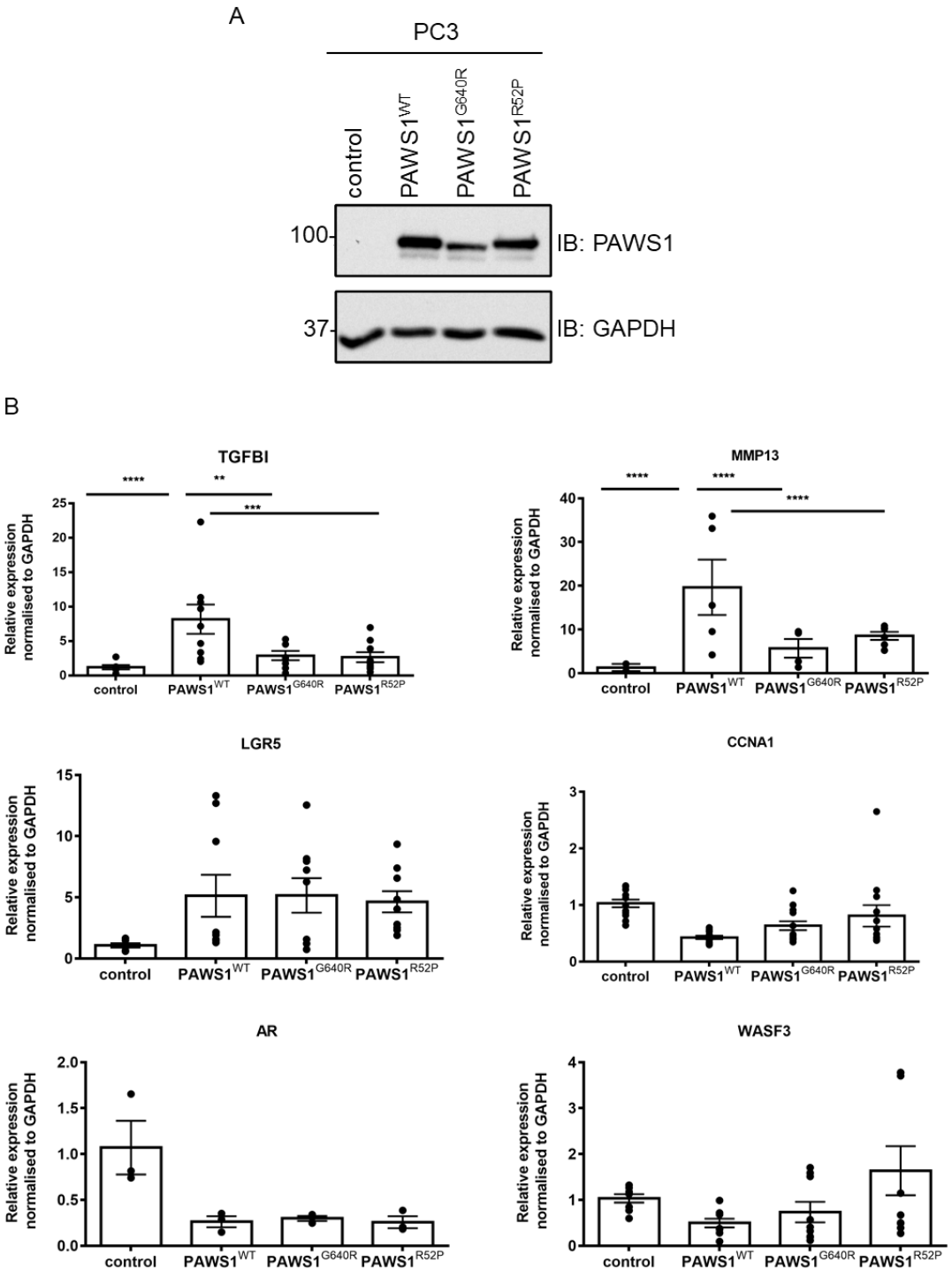

Figure 6- 2 Pathogenic PAWS1 mutants appear to affect the transcription of PAWS1-regulated genes in PC3 cells.

A. Extracts (20 µg protein) from control PC3 cells or those stably expressing $PAWS1^{WT}$, $PAWS1^{R52P}$ or $PAWS1^{G640R}$ were resolved by SDS-PAGE and analysed by immunoblotting using the indicated antibodies.

B. RNA from control PC3 cells or those stably expressing $PAWS1^{WT}$, $PAWS1^{R52P}$ or $PAWS1^{G640R}$ PC3 cells was isolated and the relative expression of the indicated genes was analysed by qPCR. The results show the fold change in gene expression relative to the controls. (n=3; Error bars represent ±SEM; ****:p<0.0001, ***:p<0.0002 **:p<0.002).

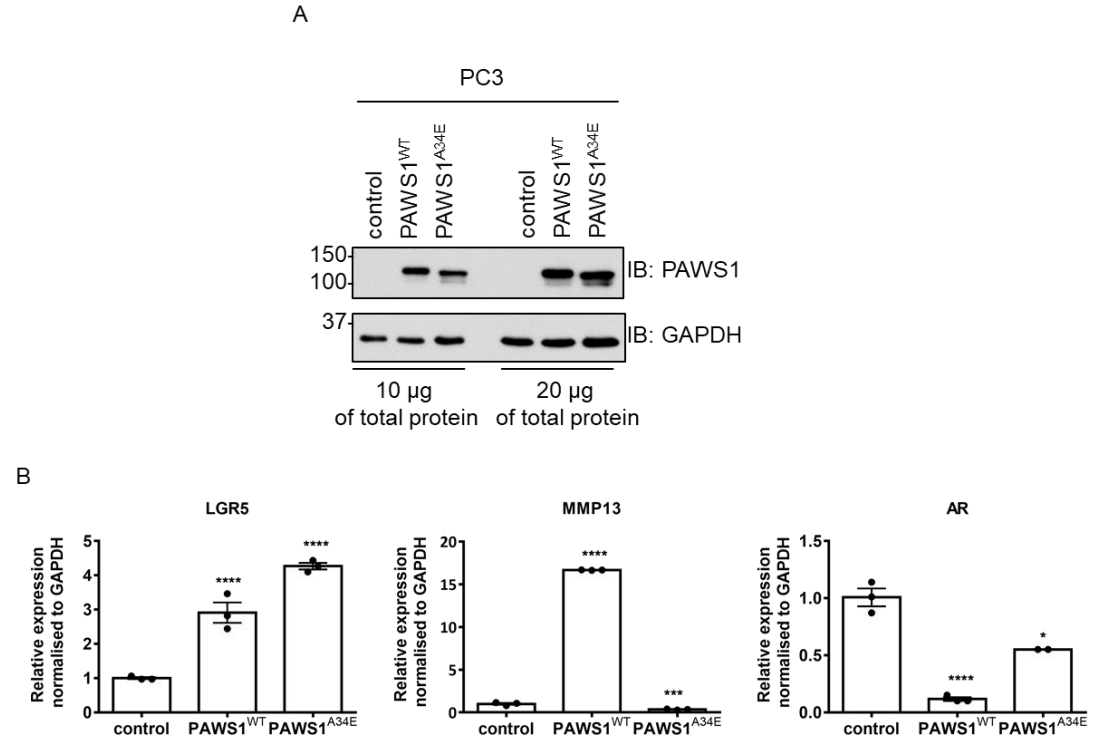

Figure 6- 3 PAWS1^{A34E} mutant affects the transcription of some PAWS1-regulated genes.

A. Extracts (10 or 20 µg protein) from control PC3 cells or those stably expressing PAWS1^{WT} or PAWS1^{A34E} were resolved by SDS-PAGE and analysed by immunoblotting using the indicated antibodies.

B. RNA from control control PC3 cells or those stably expressing PAWS1^{WT} or PAWS1^{A34E} was isolated and the relative expression of the indicated genes was analysed by qPCR. The results show the fold change in gene expression relative to the controls. (n=3; Error bars represent ±SEM; ****: $p<0.0001$, ***:$p<0.0002$, *:$p<0.033$).

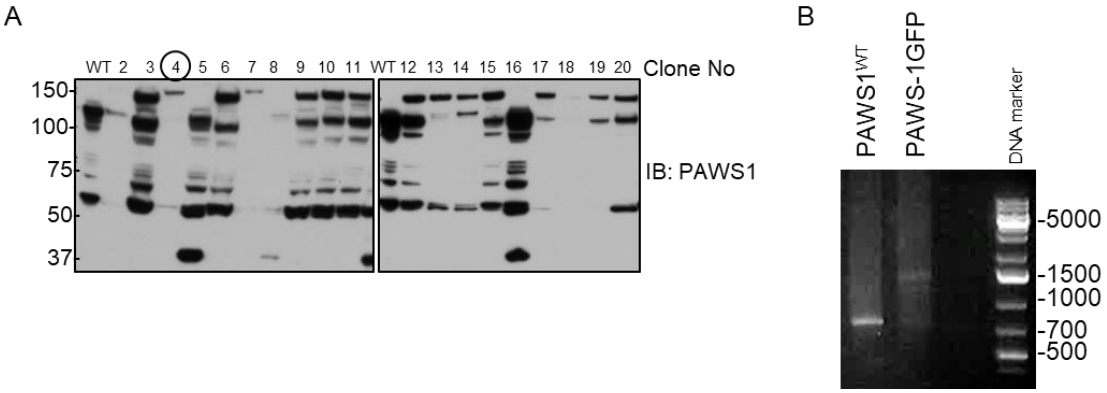

Figure 6- 4 Generation of PAWS1-GFP knock-in HaCaT cells using CRISPR/Cas9 genome editing

A. Extracts (20 μg protein) from wild type HaCaT cells (WT) or PAWS1-GFP knock-in clones were resolved by SDS-PAGE, followed by immunoblotting with anti-PAWS1. Clone 4 was selected for further analysis.

B. DNA was extracted from HaCaT wild type ($PAWS1^{WT}$) and PAWS1-GFP knock-in cells (clone 4) and a pair of primers was used to amplify the genomic region by PCR, as described in Fig 3-11D, followed by PCR followed by agarose gel electrophoresis.

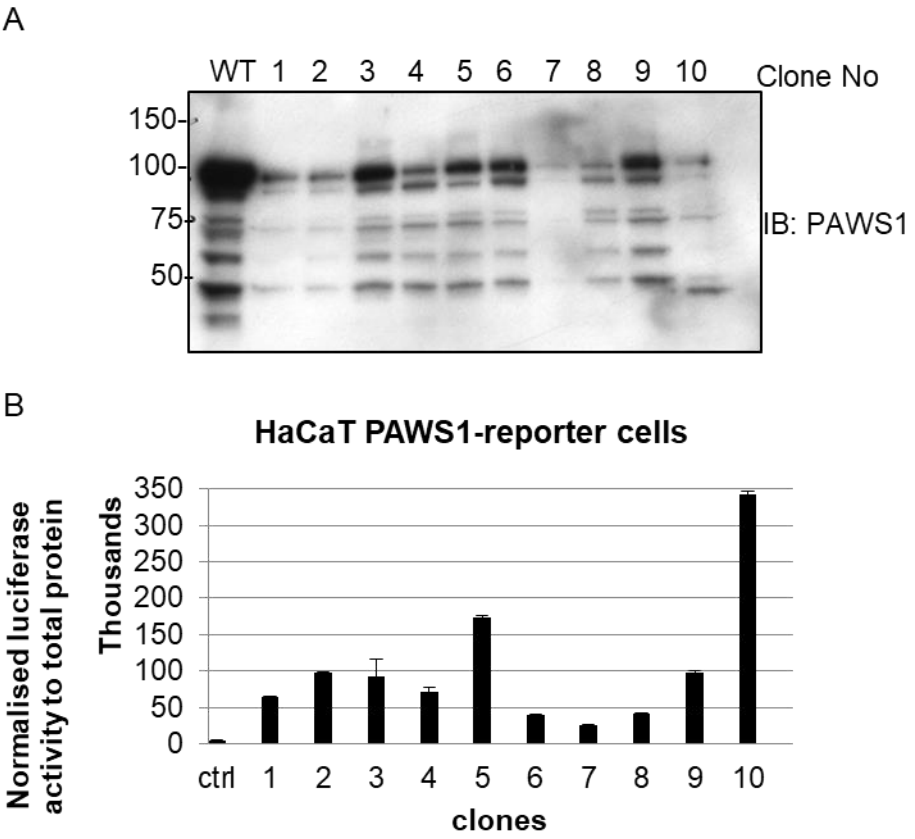

Figure 6- 5 Generation of endogenous PAWS1-transcriptional reporter HaCaT cells by CRISPR/Cas9 genome editing

A. Extracts (20 µg protein) from wild type HaCaT cells (WT) or 10 GFP-positive single cell clones selected with FACS, were resolved by SDS-PAGE, followed by immunoblotting with anti-PAWS1.

B. Measurement of luciferase activities under basal conditions of cell clones from (A).

6.3 Discussion

As described above, there is now an accumulating body of evidence suggesting that PAWS1 mutations cause skin diseases (Radden, Child et al. 2013, Drogemuller, Jagannathan et al. 2014, Sayyab, Viluma et al. 2016, Maruthappu, McGinty et al. 2017). How these mutations cause disease phenotypes remain to be defined and the lack of functional assays for PAWS1 has limited progress in this regard. The preliminary evidence presented here suggests that the three pathogenic mutations of PAWS1 described to date, namely A34E, R52P and G640R, potentially confer context-dependent loss of PAWS1 function.

By exploiting PAWS1-dependent transcription in PC3 cells, it is evident that the transcription of some of these genes is affected by all pathogenic mutants. However, PC3 prostate cancer cells do not represent the physiologically relevant epidermal keratinocytes (A34E and R52P) and hail follicular cells (G640R) that the PAWS1 mutations appear to impact in patients. Therefore, the physiological roles of these mutations should be addressed in physiologically relevant cell systems. With this in mind, HaCaT keratinocytes were chosen in the Sapkota lab to establish tools and assays to study the function of these mutations further. In this context, the endogenous PAWS1 gene was modified by an insertion of a GFP tag at the C-terminus, to allow proteomic approach to identify PAWS1-interacting proteins in keratinocytes (Fig 6-5). In similar vein, ongoing work by Dr. K. Wu in the Sapkota lab has established PAWS1$^{-/-}$ HaCaT cells by CRISPR/Cas9, and he has stably introduced the pathogenic mutants of PAWS1, similar to those done in PC3 cells. These cells will be useful in investigating the molecular mechanisms by which PAWS1 mutations might cause pathogenesis.

In light of the fact that PAWS1 associates with CK1α to mediate Wnt signalling, the ability of the pathogenic mutants to impact CK1α binding and Wnt signalling should be tested. Two of the pathogenic mutants, A34E and R52P, lie at the DUF1669 domain, which has been shown in Chapter 3 to mediate CK1α binding. Preliminary findings by K. Wu showed that R52P and A34E mutants block the interaction between PAWS1 and CK1α, suggesting that the pathological phenotypes might arise from defects in Wnt signalling. Moreover, recently it has been shown that deletion of CK1α from mouse keratinocytes results in skin disease (Chang, Kuo et al. 2017) with phenotypes resembling those described for these PAWS1 pathogenic mutants (Drogemuller, Jagannathan et al. 2014, Sayyab, Viluma et al. 2016, Maruthappu, McGinty et al. 2017). These are exciting correlations that now put PAWS1 at the heart of regulation of CK1α biology and Wnt

signalling. Future experiments will establish whether PAWS1 mutants affect the CK1α kinase activity, localisation and protein abundance of CK1α in cells.

Given the importance of PAWS1 in skin biology, understanding how PAWS1 is regulated transcriptionally or post-translationally could offer potential opportunities for therapeutic interventions. With this in mind, to facilitate studies on transcriptional regulation of PAWS1, HaCaT cells have been generated in which a transcriptional reporter cassette encompassing Luciferase-IRES-GFP-2A has been inserted at the start codon of the PAWS1 gene (Fig 6-4, 6-5). The benefits of using an endogenous PAWS1-transcriptional reporter with intact chromatin architecture have already been discussed in Chapter 4. These reporter cells will be useful in identifying stimuli that regulate PAWS1 transcription and can be used for high throughput chemical or genetic screens to identify novel regulators of PAWS1 gene transcription. In summary, the collection of tools that have been developed above, are going to be very useful in answering questions on how PAWS1 functions in keratinocyte biology and how mutations cause skin diseases.

7. Conclusion and future perspectives

In conclusion, one of the key discoveries of this thesis has been the identification of PAWS1 as a novel regulator of the Wnt signalling pathway. The thesis provides evidence that the association of PAWS1 with CK1α is critical for PAWS1 to modulate Wnt signalling. CK1α is a known regulator of Wnt signalling and phosphorylates many components of the pathway, however, how its activity and substrate specificity is regulated is poorly understood (Cruciat 2014). Although the precise molecular mechanisms by which the PAWS1:CK1α complex regulates Wnt signalling remain to be defined, the observations that PAWS1 interacts and co-localises with CK1α independently of Wnt stimulation and does not impact intrinsic CK1α kinase activity have led to the hypothesis that PAWS1 directs CK1α to or sequesters CK1α away from specific subcellular compartments and substrates to regulate Wnt signalling.

PAWS1 is a member of the poorly characterised FAM83 family of proteins, which share the conserved DUF1669 domain of unknown function. Research on the protein function of PAWS1 in cells was initiated in the Sapkota lab following its discovery as an interactor of SMAD1 (Vogt, Dingwell et al. 2014). Focusing on the BMP signalling, it was shown that PAWS1 regulates the transcription of only a subset of non-canonical, SMAD4-independent BMP-target genes (Vogt, Dingwell et al. 2014). Additional data presented in this thesis in human cells and *Xenopus* embryos corroborates with these findings, and also shows that canonical BMP signalling is not affected by PAWS1. Given the role of the BMP pathway during embryonic development, the impact of PAWS1 on *Xenopus* embryogenesis was assessed, in collaboration with Jim Smith lab (The Francis Crick Institute, London). Remarkably, PAWS1, when injected at the 4-cell stage *Xenopus* embryos was shown to induce a complete secondary body axis at the tadpole stage. Such axis-duplication phenotypes are often the result of either canonical BMP signalling inhibition or canonical Wnt signalling activation (De Robertis and Kuroda 2004, Hashiguchi and Mullins 2013). With no apparent inhibition of the canonical BMP signalling pathway by PAWS1, the focus quickly turned to a possible role in Wnt signalling activation.

Evidence obtained from *Xenopus* embryos and human cells established that overexpression of PAWS1 activates Wnt-transcriptional responses. In PAWS1$^{-/-}$ U2OS cells, Wnt-transcriptional responses were attenuated. Although the body of literature on Wnt signalling has grown exponentially over the years, there are still many unanswered

questions regarding the mechanisms that govern the key steps of Wnt signal transduction. Among the most tantalising questions are: (1) how is the β-catenin destruction complex regulated?; (2) how does the stabilised β-catenin translocate to the nucleus upon Wnt stimulation?; (3) how does Wnt signalling co-ordinate changes in cell fate, shape and polarity?; (4) how does Wnt signalling modulate the behaviour of cancer cells?; (5) is it possible to interfere with Wnt signalling by specifically targeting the key individual components of the pathway? Although this thesis did not specifically deal with answering the above questions, the results presented in the first two chapters establish PAWS1 as a novel component of Wnt signalling in cells and development. Nevertheless, the identification of new players of the Wnt signalling not only provides new insights into dissecting the complex nature of the pathway, but also opens up potential therapeutic avenues for treatment of cancers caused by aberrant Wnt signalling.

In attempting to establish the mechanisms by which PAWS1 regulates Wnt signalling, one of the most striking findings made in the thesis, was the discovery that PAWS1 interacts with CK1α. After mapping the interaction sites between PAWS1 and CK1α, it was demonstrated that the association between PAWS1 with CK1α is necessary to modulate Wnt signalling. However, further research is required to address the precise mechanisms for the coordinated actions of PAWS1 and CK1α in Wnt signalling regulation.

CK1 isoforms have long been regarded as critical components of Wnt signalling, as they have been known to exert both positive and negative regulation on the pathway (Sakanaka, Leong et al. 1999, McKay, Peters et al. 2001, Amit, Hatzubai et al. 2002, Liu, Li et al. 2002, Elyada, Pribluda et al. 2011). There is still considerable disagreement in the field over which CK1 isoforms control the phosphorylation of specific components within the Wnt signalling cascade (Del Valle-Perez, Arques et al. 2011, Cruciat 2014). Part of this stems from the fact that very little is known about the regulation of CK1 isoforms in cells (Knippschild, Kruger et al. 2014, Schittek and Sinnberg 2014). PAWS1 interacts selectively with CK1α and CK1αL isoforms, but not CK1δ and CK1ε, to activate Wnt signalling in *Xenopus* embryos and in human cells. Like PAWS1, developmental studies in *Xenopus* have shown that overexpression of CK1α alone can also induce axis duplication (Peters, McKay et al. 1999, McKay, Peters et al. 2001); (Chapter 3), suggesting a positive regulation of this isoform in the Wnt pathway. However, contrasting evidence demonstrated that CK1α was also responsible for the phosphorylation of β-catenin at S45, which promotes its subsequent phosphorylation at S33/37/T41 by

GSK3, thereby inducing its ubiquitylation and degradation (Liu, Li et al. 2002). Nevertheless, other studies reported that both CK1δ and CK1ε could also phosphorylate β-catenin at S45 (Sakanaka, Leong et al. 1999, Amit, Hatzubai et al. 2002). The negative role of CK1α in Wnt signalling has been further supported by the observations that conditional knockout of CK1α from the intestinal epithelium of mice leads to activation of Wnt signalling, by blocking the phosphorylation of β-catenin at S45, resulting in the stabilisation of β-catenin (Elyada, Pribluda et al. 2011). Interestingly, the levels of pSer45-β-catenin in PAWS1$^{-/-}$ U2OS cells were comparable to those seen in wild type cells, suggesting CK1α bound to PAWS1 is unlikely to play a key role in the phosphorylation of β-catenin at S45. The data presented in this thesis suggests that PAWS1 and CK1α coordinate to regulate Wnt signalling but the influence of CK1δ and CK1ε on Wnt signalling remains unaffected by PAWS1. This corroborates with the hypothesis that different CK1 isoforms target specific sets of substrates in cells and are uniquely regulated in driving specific cellular processes, including Wnt signalling.

One of the major questions that this thesis attempted to address, was how the association of PAWS1 with CK1α activated Wnt signalling. Using *Xenopus* embryos, through the assessment of axis-duplication and Wnt-transcriptional responses in animal caps, it was found that the PAWS1:CK1α complex acts either on the β-catenin destruction complex or somewhere downstream of it. However, it is evident from the data included here that PAWS1 does not associate with any components of the destruction complex, and does not appear to impact the CK1α-mediated phosphorylation of β-catenin at S45. Although PAWS1 and Axin were shown to form robust complexes with CK1α and GSK3β respectively, neither of them appeared to bind β-catenin or the other Wnt pathway components robustly. This was slightly unexpected, as the generally accepted model suggests that CK1α and Axin are core components of the β-catenin destruction complex (Ikeda, Kishida et al. 1998, Liu, Li et al. 2002, Li, Ng et al. 2012). Further research is required to determine whether this data presented here are specific to U2OS cells, or applicable more globally. Consistent with observations made here, evidence from mechanistic studies on the β-catenin phosphorylation by CK1, also suggests that CK1 isoforms do not form stable interactions with β-catenin in cells (Bustos, Ferrarese et al. 2006). On the other hand, it should be noted that the majority of the existing studies on the involvement of CK1α in β-catenin phosphorylation lack definitive *in vivo* evidence and are mostly based on overexpression systems or *in vitro* studies (Ikeda, Kishida et al. 1998, Amit, Hatzubai et al. 2002, Liu, Li et al. 2002, Marin, Bustos et al. 2003, Bustos,

Ferrarese et al. 2006). Interactions that are observed with overexpressed proteins might not reflect the true physiological conditions, as they may represent forced activation of signalling pathways caused by imbalances in the equilibrium of the signalling components.

The nuclear localisation of the active β-catenin is fundamental to the Wnt-transcriptional response (Polakis 2012). Although the PAWS1:CK1α complex did not appear to affect the composition of the destruction complex or the phosphorylation of β-catenin at S45, the nuclear accumulation of the active β-catenin was promoted by PAWS1 overexpression in *Xenopus* embryos and attenuated in PAWS1$^{-/-}$ cells. Little is known about the nucleo-cytoplasmic shuttling of β-catenin in response to Wnt stimulation and it is not clear what factors mediate this process. Therefore, the identification of the PAWS1:CK1α complex as a regulator of the nuclear accumulation of β-catenin upon Wnt activation is a potential significant contribution to this field.

A key question that still remains unanswered is how the PAWS1:CK1α complex regulates the nuclear accumulation of β-catenin and whether this sufficiently explains the role of the PAWS1:CK1α complex in Wnt signalling. Because of the robustness of the complex, independent of Wnt signalling, PAWS1 is likely to influence the activity of CK1α against key substrates. However, because PAWS1 immunoprecipitates CK1α kinase activity from extracts and does not influence kinase activity in vitro, it is unlikely that PAWS1 affects intrinsic catalytic activity of CK1α in cells. Another observation was that loss of PAWS1 from U2OS cells resulted in a decrease in CK1α protein levels. Reciprocal depletion of CK1α also resulted in reduction of PAWS1 protein levels, suggesting each protein regulates the integrity of the PAWS1:CK1α complex in cells. While precisely how the stability of the PAWS1:CK1α complex is regulated is currently not known, specific subcellular distribution of the PAWS1:CK1α complex in response to different signalling cues is likely to regulate specific CK1α substrates. A comprehensive landscape of PAWS1-dependent CK1α substrates in response to Wnt signalling is likely to reveal key mechanistic insights into how the PAWS1:CK1α complex regulates the nuclear accumulation of β-catenin and therefore, Wnt signalling responses. Recently generated phospho-proteomic data on U2OS wild type and PAWS1$^{-/-}$ cells has identified many candidates that could uncover the PAWS1-dependent CK1α substrates that may be essential for mediating Wnt signalling. In the same vein, non-Wnt targets of CK1α that are PAWS1-dependent could provide novel insights into PAWS1 function beyond Wnt signalling. As discussed extensively in Chapter 4 (section 4.3), validation of the PAWS1-

dependent CK1α substrates may establish the molecular mechanisms through which the PAWS1:CK1α complex regulates Wnt signalling, or indeed other CK1α-dependent functions in cells.

The interaction between PAWS1 and CK1α was mapped to two conserved residues within the DUF1669 domain, which are conserved in all FAM83 proteins. Excitingly, all members of the FAM83 family can associate with CK1α, while half of them also interact with CK1δ and CK1ε isoforms. Furthermore, it has been shown that different FAM83 members colocalise with the interacting CK1 isoforms in distinct subcellular compartments (Fulcher LJ, Bozatzi P et al. 2018); *In Press*). Remarkably, the conserved point mutations on the FAM83 protein sequence that abolish their association with CK1, disrupt not only the colocalization of FAM83 protein with specific CK1 isoforms in cells, but also the subcellular distribution of the respective FAM83 proteins themselves. Thus, other FAM83:CK1 complexes might act redundantly or in a coordinated fashion to mediate cellular processes, including Wnt signalling. For example, a recent report demonstrated that FAM83H recruits CK1 to nuclear speckles in colorectal cancer cells, although the downstream biology of this event has not been elucidated yet (Kuga, Sasaki et al. 2016).

To date, one of the main reasons that have hindered research on PAWS1, and on FAM83 proteins in general, is the lack of information on their biochemical properties. The DUF1669 domain that unites the family members, from the data presented here, has emerged as an anchor for CK1 isoforms, and in doing so, may act to potentially regulate both CK1 isoform subcellular localisation and substrate specificity in cells. Preliminary proteomics data have already indicated that each FAM83 members have unique sets of binding partners. Therefore, FAM83 proteins might prove to be elusive regulatory components of CK1 isoforms, thereby helping to explain how these constitutively active kinases can contribute to the regulation of the myriad of cellular processes that they are known to be implicated in. The hypothesis that different FAM83 members serve to recruit CK1 isoforms to specific subcellular locations and substrates in response to distinct signalling cues opens up many exciting new avenues for future research.

The DUF1669 domain contains a pseudo-PLD-like catalytic motif, but it is still unclear whether it possesses any function in the PLD pathway, such as binding to phospho-lipids. Preliminary structural insights of this domain suggest that the predicted PLD-like pocket is located away from the surface that contains the two residues that mediate the interaction with CK1 isoforms. Furthermore, the only proteins that have been

identified as interactors of the DUF1669 domains from proteomic studies in the Sapkota lab are the different isoforms of CK1. These observations raise interesting possibilities for investigating whether the binding of certain phospho-lipids to the PLD-like pocket of the DUF1669 domains can influence the ability of FAM83 members to bind CK1 isoforms or influence their catalytic activity or substrate specificity. Such possibilities could potentially explain the differences in the binding specificity and/or affinity of different FAM83 members for distinct CK1 isoforms.

CK1 proteins have been associated with cancer and neurodegenerative diseases but the pleiotropic nature of CK1 isoforms, has limited the exploration of CK1 inhibition in therapeutics (Perez, Gil et al. 2011, Cozza and Pinna 2016). The current inhibitors, including CK1-7, IC261, D4476, suffer from selectivity issues and display off-target effects, related to other CK1 isoforms and protein kinases (Table 1-2). FAM83 proteins, as novel CK1 regulators in cells, provide us with novel therapeutic opportunities to target specific CK1 isoforms in diseases. One remaining challenge is to establish the molecular bases for the FAM83:CK1 interaction through structural biology studies. Then, the development of small molecules that potentially disrupt the FAM83:CK1 association will be more feasible and could prove useful in targeting specific CK1 isoforms in distinct subcellular compartments.

Other than its role in Wnt signalling, this thesis has demonstrated that PAWS1 associates with the calcium/calmodulin-dependent kinases CaMK2D and CaMK2G, implying a role of PAWS1 in calcium signalling. In parallel to this work, it was discovered that the loss of PAWS1 results in migratory defects in human cells. Calcium signalling is known to be implicated in cytoskeletal reorganisation which orchestrates cell movement (Tsai, Kuo et al. 2015). Migration of cancerous cells from the primary tumour to other tissues is the main cause of death in patients with tumours (Mehlen and Puisieux 2006, Taketo 2011). The cancerous cells must therefore undergo changes, which allow them to migrate via the extracellular matrix into the bloodstream. This process partly depends on the intracellular concentration of Ca^{2+}, which forms a gradient across the cells (Prevarskaya, Skryma et al. 2011, Tsai, Kuo et al. 2015). As the gradient increases, the focal adhesion proteins disassemble, and the cell retracts. (Prevarskaya, Skryma et al. 2011). Therefore, aberrant Ca^{2+} signalling plays a critical role in metastasis of cancerous cells.

Phosphorylation of PAWS1 at S356, potentially by CaMK2 was found to be required for U2OS cells to migrate in a wound healing assay. However, the mechanisms

that control cell migration downstream of CaMK2-phosphorylation of PAWS1 are yet to be defined. An appealing hypothesis is that PAWS1 regulates the transcription of certain genes that are involved in cell movement. Unpublished data from the lab (J. Vogt) showed that introduction of the phospho-mutant $PAWS1^{S356A}$ in PC3 prostate cancer cells attenuates PAWS1-dependent gene transcription. One of those genes, NEDD9 has been implicated in cell migration, invasion and metastasis of cancer cells (Feng, Zhao et al. 2015, Kozyulina, Loskutov et al. 2015). The emerging evidence that PAWS1 is involved in cell migration raises the intriguing question whether PAWS1 expression in certain cancer types correlates with proliferative and migratory advantage in cancer cells.

Recent characterisation of the U2OS $PAWS1^{-/-}$ cells (Cummins, Wu et al. 2018), revealed that PAWS1 deficiency impacts cell morphology and cytoskeletal dynamics due to the loss of the PAWS1:CD2AP interaction. It remains to be shown whether CaMK2 isoforms are part of the same PAWS1:CD2AP complex and if PAWS1 phosphorylation by CaMK2 affects its association and co-localisation with CD2AP in cells. $PAWS1^{-/-}$ cells display disorganised actin distribution compared to U2OS wild type cells (Cummins, Wu et al. 2018). It would be therefore interesting to investigate whether rescuing the cells with CaMK2-phosphorylation-deficient mutant, $PAWS1^{S356A}$, can restore actin organisation, as $PAWS1^{WT}$ rescue did (Cummins, Wu et al. 2018). Although no direct association between CaMK2 and CD2AP has been mentioned in the literature, they are both known to interact with actin in order to regulate actin polymerisation and cytoskeletal stabilisation (Bruck, Huber et al. 2006, Hoffman, Farley et al. 2013). Future experiments aiming to address if PAWS1 can associate with CaMK2 and CD2AP in cells in the presence or absence of Ca^{2+}, through live cell imaging, could shed some light into the role of PAWS1 phosphorylation at S356 in actin dynamics. Furthermore, in light of the constitutive nature of the PAWS1:CK1α complex, the role of PAWS1 in actin cytoskeleton and cell migration should be investigated in this context.

CaMK2 is a central component of the non-canonical Wnt signalling, which regulates tissue mobility during development and metastasis of cancerous cells (Gujral, Chan et al. 2014, Asem, Buechler et al. 2016, Sandsmark, Hansen et al. 2017). Given the critical role of PAWS1 in the canonical Wnt signalling pathway, it would be interesting to explore whether PAWS1 affects the non-canonical Wnt pathway, as well. Wnt5A has been widely used in literature as an activator of the non-canonical Wnt signalling, although it has been reported to activate or de-activate β-catenin signalling, depending on which membrane receptors it binds to (He, Saint-Jeannet et al. 1997, Nishita, Enomoto et

al. 2010). It is therefore very important to study the expression of Wnt receptors in the cell system of choice before proceeding with further investigations. Upon non-canonical Wnt activation, intracellular Ca^{2+} is released and CaMK2 is activated, which results in cell motility via reorganisation of the actin cytoskeleton and subsequent filopodia formation (Nishita, Yoo et al. 2006, O'Connell, Fiori et al. 2009). One intriguing experiment would be to monitor PAWS1 phosphorylation by CaMK2 at S356 upon Wnt5A stimulation and assess the impact on actin distribution and cell migration. In parallel, it would be interesting to perform live-cell imaging, to monitor Ca^{2+} release in response to Wnt ligands in PAWS1$^{-/-}$, PAWS1^{WT} and PAWS1^{S356A} cells. Nevertheless, uncovering the intricate mechanisms of PAWS1 function with respect to its association with and phosphorylation by CaMK2, could open up therapeutic opportunities against aggressive metastatic tumours.

During the course of this PhD research, it was exciting when first reports of PAWS1 mutations in hereditary footpad hyperkeratosis in dogs and humans emerged (Drogemuller, Jagannathan et al. 2014, Sayyab, Viluma et al. 2016, Maruthappu, McGinty et al. 2017). Interestingly, misregulation of Wnt signalling and CK1α are also associated with similar skin abnormalities (Adaimy, Chouery et al. 2007, Chang, Kuo et al. 2017). The findings that PAWS1 interacts with two protein kinases CK1α and CaMK2 isoforms, which are involved in the canonical and non-canonical Wnt signalling respectively, raises the possibility that these diseases may arise from perturbations in the Wnt signalling pathway. Indeed, two of the hyperkeratosis mutants disrupt interaction of PAWS1 with CK1α (Unpublished data from K. Wu). It would be interesting to investigate whether rescuing the expression of PAWS1 and its pathogenic mutants in PAWS1$^{-/-}$ cells can restore Wnt signalling, actin organisation or cell migratory defects. This would provide important clues on the molecular aetiology of the observed phenotypes, and might open up potential therapeutic opportunities for patients with keratodermas. Moreover, a proteomic approach to identify potential differences in the binding partners of PAWS1 and its pathogenic mutants, would provide a better understanding of the impact that these mutations have at the molecular level. However, in order to achieve this, it is essential to generate cell lines expressing the PAWS1 mutants at the endogenous levels, by exploiting the CRISPR/Cas9 technology to knock-in these mutations on the PAWS1 locus Further studies could also assess the levels of expression of PAWS1 protein in the affected skin tissues from patients that carry the pathogenic mutations, to understand if the pathogenesis is due to PAWS1 loss- or gain-of function. Skin diseases,

including hyperkeratosis, are mainly characterised by defects of the epithelial keratin cytoskeleton (McLean and Moore 2011). Of note, another FAM83 member, FAM83H, has been reported to regulate the keratin cytoskeleton through its association with CK1 (Kuga, Kume et al. 2013), although to date, no FAM83H mutations have been associated with skin diseases.

In the beginning of this PhD, not much was known about the biological function of PAWS1. Overall, this thesis has identified PAWS1 as a novel component of the canonical Wnt signalling pathway. Through its interaction with CK1α, PAWS1 might present a new intersection in the Wnt pathway which could provide valuable insights into further delineating the details of regulation of Wnt signalling. Nevertheless, the findings presented here will aid further research aiming to understand how PAWS1 functions in cells and how it controls CK1 biology alone or together with other FAM83 members, in health and disease.

References

Adaimy, L., E. Chouery, H. Megarbane, S. Mroueh, V. Delague, E. Nicolas, H. Belguith, P. de Mazancourt and A. Megarbane (2007). "Mutation in WNT10A is associated with an autosomal recessive ectodermal dysplasia: the odonto-onycho-dermal dysplasia." Am J Hum Genet 81(4): 821-828.

Adrain, C. and M. Freeman (2012). "New lives for old: evolution of pseudoenzyme function illustrated by iRhoms." Nat Rev Mol Cell Biol 13(8): 489-498.

Agius, E., M. Oelgeschlager, O. Wessely, C. Kemp and E. M. De Robertis (2000). "Endodermal Nodal-related signals and mesoderm induction in Xenopus." Development 127(6): 1173-1183.

Altucci, L. and H. Gronemeyer (2001). "The promise of retinoids to fight against cancer." Nat Rev Cancer 1(3): 181-193.

Amit, S., A. Hatzubai, Y. Birman, J. S. Andersen, E. Ben-Shushan, M. Mann, Y. Ben-Neriah and I. Alkalay (2002). "Axin-mediated CKI phosphorylation of beta-catenin at Ser 45: a molecular switch for the Wnt pathway." Genes Dev 16(9): 1066-1076.

Andl, T., S. T. Reddy, T. Gaddapara and S. E. Millar (2002). "WNT signals are required for the initiation of hair follicle development." Dev Cell 2(5): 643-653.

Arce, L., N. N. Yokoyama and M. L. Waterman (2006). "Diversity of LEF/TCF action in development and disease." Oncogene 25(57): 7492-7504.

Asem, M. S., S. Buechler, R. B. Wates, D. L. Miller and M. S. Stack (2016). "Wnt5a Signaling in Cancer." Cancers (Basel) 8(9).

Bain, J., L. Plater, M. Elliott, N. Shpiro, C. J. Hastie, H. McLauchlan, I. Klevernic, J. S. Arthur, D. R. Alessi and P. Cohen (2007). "The selectivity of protein kinase inhibitors: a further update." Biochem J 408(3): 297-315.

Baker, J. C., R. S. Beddington and R. M. Harland (1999). "Wnt signaling in Xenopus embryos inhibits bmp4 expression and activates neural development." Genes Dev 13(23): 3149-3159.

Banziger, C., D. Soldini, C. Schutt, P. Zipperlen, G. Hausmann and K. Basler (2006). "Wntless, a conserved membrane protein dedicated to the secretion of Wnt proteins from signaling cells." Cell 125(3): 509-522.

Barakat, M. T., E. W. Humke and M. P. Scott (2010). "Learning from Jekyll to control Hyde: Hedgehog signaling in development and cancer." Trends Mol Med 16(8): 337-348.

Bartscherer, K., N. Pelte, D. Ingelfinger and M. Boutros (2006). "Secretion of Wnt ligands requires Evi, a conserved transmembrane protein." Cell 125(3): 523-533.

Baum, B. and M. Georgiou (2011). "Dynamics of adherens junctions in epithelial establishment, maintenance, and remodeling." J Cell Biol 192(6): 907-917.

Beck, S. E. and J. M. Carethers (2007). "BMP suppresses PTEN expression via RAS/ERK signaling." Cancer Biol Ther 6(8): 1313-1317.

Behrend, L., D. M. Milne, M. Stoter, W. Deppert, L. E. Campbell, D. W. Meek and U. Knippschild (2000). "IC261, a specific inhibitor of the protein kinases casein kinase 1-delta and -epsilon, triggers the mitotic checkpoint and induces p53-dependent postmitotic effects." Oncogene 19(47): 5303-5313.

Behrend, L., M. Stoter, M. Kurth, G. Rutter, J. Heukeshoven, W. Deppert and U. Knippschild (2000). "Interaction of casein kinase 1 delta (CK1delta) with post-Golgi structures, microtubules and the spindle apparatus." Eur J Cell Biol 79(4): 240-251.

Bettayeb, K., N. Oumata, A. Echalier, Y. Ferandin, J. A. Endicott, H. Galons and L. Meijer (2008). "CR8, a potent and selective, roscovitine-derived inhibitor of cyclin-dependent kinases." Oncogene 27(44): 5797-5807.

Beyaert, R., B. Vanhaesebroeck, W. Declercq, J. Van Lint, P. Vandenabele, P. Agostinis, J. R. Vandenheede and W. Fiers (1995). "Casein kinase-1 phosphorylates the p75 tumor necrosis factor receptor and negatively regulates tumor necrosis factor signaling for apoptosis." J Biol Chem 270(40): 23293-23299.

Bhattacharya, S., W. C. HuangFu, J. Liu, S. Veeranki, D. P. Baker, C. Koumenis, J. A. Diehl and S. Y. Fuchs (2010). "Inducible priming phosphorylation promotes ligand-independent degradation of the IFNAR1 chain of type I interferon receptor." J Biol Chem 285(4): 2318-2325.

Bibian, M., R. J. Rahaim, J. Y. Choi, Y. Noguchi, S. Schurer, W. Chen, S. Nakanishi, K. Licht, L. H. Rosenberg, L. Li, Y. Feng, M. D. Cameron, D. R. Duckett, J. L. Cleveland and W. R. Roush (2013). "Development of highly selective casein kinase 1delta/1epsilon (CK1delta/epsilon) inhibitors with potent antiproliferative properties." Bioorg Med Chem Lett 23(15): 4374-4380.

Bier, E. and E. M. De Robertis (2015). "EMBRYO DEVELOPMENT. BMP gradients: A paradigm for morphogen-mediated developmental patterning." Science 348(6242): aaa5838.

Bilic, J., Y. L. Huang, G. Davidson, T. Zimmermann, C. M. Cruciat, M. Bienz and C. Niehrs (2007). "Wnt induces LRP6 signalosomes and promotes dishevelled-dependent LRP6 phosphorylation." Science 316(5831): 1619-1622.

Bischof, J., J. Leban, M. Zaja, A. Grothey, B. Radunsky, O. Othersen, S. Strobl, D. Vitt and U. Knippschild (2012). "2-Benzamido-N-(1H-benzo[d]imidazol-2-yl)thiazole-4-carboxamide derivatives as potent inhibitors of CK1delta/epsilon." Amino Acids 43(4): 1577-1591.

Bischof, J., S. J. Randoll, N. Sussner, D. Henne-Bruns, L. A. Pinna and U. Knippschild (2013). "CK1delta kinase activity is modulated by Chk1-mediated phosphorylation." PLoS One 8(7): e68803.

Bland, J. M. and D. G. Altman (1995). "Multiple significance tests: the Bonferroni method." Bmj 310(6973): 170.

Bouwmeester, T., S. Kim, Y. Sasai, B. Lu and E. M. De Robertis (1996). "Cerberus is a head-inducing secreted factor expressed in the anterior endoderm of Spemann's organizer." Nature 382(6592): 595-601.

Bovolenta, P., J. Rodriguez and P. Esteve (2006). "Frizzled/RYK mediated signalling in axon guidance." Development 133(22): 4399-4408.

Bradshaw, J. M., A. Hudmon and H. Schulman (2002). "Chemical quenched flow kinetic studies indicate an intraholoenzyme autophosphorylation mechanism for Ca2+/calmodulin-dependent protein kinase II." J Biol Chem 277(23): 20991-20998.

Bramblett, G. T., M. Goedert, R. Jakes, S. E. Merrick, J. Q. Trojanowski and V. M. Lee (1993). "Abnormal tau phosphorylation at Ser396 in Alzheimer's disease recapitulates development and contributes to reduced microtubule binding." Neuron 10(6): 1089-1099.

Brockman, J. L., S. D. Gross, M. R. Sussman and R. A. Anderson (1992). "Cell cycle-dependent localization of casein kinase I to mitotic spindles." Proc Natl Acad Sci U S A 89(20): 9454-9458.

Brockschmidt, C., H. Hirner, N. Huber, T. Eismann, A. Hillenbrand, G. Giamas, B. Radunsky, O. Ammerpohl, B. Bohm, D. Henne-Bruns, H. Kalthoff, F. Leithauser, A. Trauzold and U. Knippschild (2008). "Anti-apoptotic and growth-stimulatory functions of CK1 delta and epsilon in ductal adenocarcinoma of the pancreas are inhibited by IC261 in vitro and in vivo." Gut 57(6): 799-806.

Brown, H. M. and B. Rydqvist (1990). "Dimethyl sulfoxide elevates intracellular Ca2+ and mimics effects of increased light intensity in a photoreceptor." Pflugers Arch 415(4): 395-398.

Bruck, S., T. B. Huber, R. J. Ingham, K. Kim, H. Niederstrasser, P. M. Allen, T. Pawson, J. A. Cooper and A. S. Shaw (2006). "Identification of a novel inhibitory actin-capping protein binding motif in CD2-associated protein." J Biol Chem 281(28): 19196-19203.

Bu, Q., Z. Li, J. Zhang, F. Xu, J. Liu and H. Liu (2017). "The crystal structure of full-length Sizzled from Xenopus laevis yields insights into Wnt-antagonistic function of secreted Frizzled-related proteins." J Biol Chem 292(39): 16055-16069.

Budini, M., G. Jacob, A. Jedlicki, C. Perez, C. C. Allende and J. E. Allende (2009). "Autophosphorylation of carboxy-terminal residues inhibits the activity of protein kinase CK1alpha." J Cell Biochem 106(3): 399-408.

Burnett, G. and E. P. Kennedy (1954). "The enzymatic phosphorylation of proteins." J Biol Chem 211(2): 969-980.

Bustos, V. H., A. Ferrarese, A. Venerando, O. Marin, J. E. Allende and L. A. Pinna (2006). "The first armadillo repeat is involved in the recognition and regulation of beta-catenin phosphorylation by protein kinase CK1." Proc Natl Acad Sci U S A 103(52): 19725-19730.

Campbell, D. G. and N. A. Morrice (2002). "Identification of protein phosphorylation sites by a combination of mass spectrometry and solid phase Edman sequencing." J Biomol Tech 13(3): 119-130.

Cavallo, R. A., R. T. Cox, M. M. Moline, J. Roose, G. A. Polevoy, H. Clevers, M. Peifer and A. Bejsovec (1998). "Drosophila Tcf and Groucho interact to repress Wingless signalling activity." Nature 395(6702): 604-608.

Chang, C. H., C. J. Kuo, T. Ito, Y. Y. Su, S. T. Jiang, M. H. Chiu, Y. H. Lin, A. Nist, M. Mernberger, T. Stiewe, S. Ito, K. Wakamatsu, Y. A. Hsueh, S. Y. Shieh, I. Snir-Alkalay and Y. Ben-Neriah (2017). "CK1alpha ablation in keratinocytes induces p53-dependent, sunburn-protective skin hyperpigmentation." Proc Natl Acad Sci U S A 114(38): E8035-e8044.

Chen, H. X., N. Otmakhov, S. Strack, R. J. Colbran and J. E. Lisman (2001). "Is persistent activity of calcium/calmodulin-dependent kinase required for the maintenance of LTP?" J Neurophysiol 85(4): 1368-1376.

Chen, L., C. Li, Y. Pan and J. Chen (2005). "Regulation of p53-MDMX interaction by casein kinase 1 alpha." Mol Cell Biol 25(15): 6509-6520.

Chen, Y., N. Sasai, G. Ma, T. Yue, J. Jia, J. Briscoe and J. Jiang (2011). "Sonic Hedgehog dependent phosphorylation by CK1alpha and GRK2 is required for ciliary accumulation and activation of smoothened." PLoS Biol 9(6): e1001083.

Cheng, J., A. J. Syder, Q. C. Yu, A. Letai, A. S. Paller and E. Fuchs (1992). "The genetic basis of epidermolytic hyperkeratosis: a disorder of differentiation-specific epidermal keratin genes." Cell 70(5): 811-819.

Cheong, J. K. and D. M. Virshup (2011). "Casein kinase 1: Complexity in the family." Int J Biochem Cell Biol 43(4): 465-469.

Cheong, J. K., F. Zhang, P. J. Chua, B. H. Bay, A. Thorburn and D. M. Virshup (2015). "Casein kinase 1alpha-dependent feedback loop controls autophagy in RAS-driven cancers." J Clin Invest 125(4): 1401-1418.

Chergui, K., P. Svenningsson and P. Greengard (2005). "Physiological role for casein kinase 1 in glutamatergic synaptic transmission." J Neurosci 25(28): 6601-6609.

Cheung, W. Y. (1980). "Calmodulin plays a pivotal role in cellular regulation." Science 207(4426): 19-27.

Chi, M., H. Evans, J. Gilchrist, J. Mayhew, A. Hoffman, E. A. Pearsall, H. Jankowski, J. S. Brzozowski and K. A. Skelding (2016). "Phosphorylation of calcium/calmodulin-stimulated protein kinase II at T286 enhances invasion and migration of human breast cancer cells." Sci Rep 6: 33132.

Chicoine, J., P. Benoit, C. Gamberi, M. Paliouras, M. Simonelig and P. Lasko (2007). "Bicaudal-C recruits CCR4-NOT deadenylase to target mRNAs and regulates oogenesis, cytoskeletal organization, and its own expression." Dev Cell 13(5): 691-704.

Chijiwa, T., M. Hagiwara and H. Hidaka (1989). "A newly synthesized selective casein kinase I inhibitor, N-(2-aminoethyl)-5-chloroisoquinoline-8-sulfonamide, and affinity purification of casein kinase I from bovine testis." J Biol Chem 264(9): 4924-4927.

Choi, S. Y., P. Huang, G. M. Jenkins, D. C. Chan, J. Schiller and M. A. Frohman (2006). "A common lipid links Mfn-mediated mitochondrial fusion and SNARE-regulated exocytosis." Nat Cell Biol 8(11): 1255-1262.

Cipriano, R., B. L. Bryson, K. L. Miskimen, C. A. Bartel, W. Hernandez-Sanchez, R. C. Bruntz, S. A. Scott, C. W. Lindsley, H. A. Brown and M. W. Jackson (2014). "Hyperactivation of EGFR and downstream effector phospholipase D1 by oncogenic FAM83B." Oncogene 33(25): 3298-3306.

Cipriano, R., J. Graham, K. L. Miskimen, B. L. Bryson, R. C. Bruntz, S. A. Scott, H. A. Brown, G. R. Stark and M. W. Jackson (2012). "FAM83B mediates EGFR- and RAS-driven oncogenic transformation." J Clin Invest 122(9): 3197-3210.

Cipriano, R., K. L. Miskimen, B. L. Bryson, C. R. Foy, C. A. Bartel and M. W. Jackson (2013). "FAM83B-mediated activation of PI3K/AKT and MAPK signaling cooperates to promote epithelial cell transformation and resistance to targeted therapies." Oncotarget 4(5): 729-738.

Cipriano, R., K. L. Miskimen, B. L. Bryson, C. R. Foy, C. A. Bartel and M. W. Jackson (2014). "Conserved oncogenic behavior of the FAM83 family regulates MAPK signaling in human cancer." Mol Cancer Res 12(8): 1156-1165.

Collins, L. R., W. A. Ricketts, L. Yeh and D. Cheresh (1999). "Bifurcation of cell migratory and proliferative signaling by the adaptor protein Shc." J Cell Biol 147(7): 1561-1568.

Cong, F., L. Schweizer and H. Varmus (2004). "Casein kinase Iepsilon modulates the signaling specificities of dishevelled." Mol Cell Biol 24(5): 2000-2011.

Cong, F. and H. Varmus (2004). "Nuclear-cytoplasmic shuttling of Axin regulates subcellular localization of beta-catenin." Proc Natl Acad Sci U S A 101(9): 2882-2887.

Cong, L., F. A. Ran, D. Cox, S. Lin, R. Barretto, N. Habib, P. D. Hsu, X. Wu, W. Jiang, L. A. Marraffini and F. Zhang (2013). "Multiplex genome engineering using CRISPR/Cas systems." Science 339(6121): 819-823.

Cooper, S. (2000). "The continuum model and G1-control of the mammalian cell cycle." Prog Cell Cycle Res 4: 27-39.

Cordingley, M. G., P. L. Callahan, V. V. Sardana, V. M. Garsky and R. J. Colonno (1990). "Substrate requirements of human rhinovirus 3C protease for peptide cleavage in vitro." J Biol Chem 265(16): 9062-9065.

Cozza, G., A. Gianoncelli, M. Montopoli, L. Caparrotta, A. Venerando, F. Meggio, L. A. Pinna, G. Zagotto and S. Moro (2008). "Identification of novel protein kinase CK1 delta (CK1delta) inhibitors through structure-based virtual screening." Bioorg Med Chem Lett 18(20): 5672-5675.

Cozza, G. and L. A. Pinna (2016). "Casein kinases as potential therapeutic targets." Expert Opin Ther Targets 20(3): 319-340.

Cruciat, C. M. (2014). "Casein kinase 1 and Wnt/beta-catenin signaling." Curr Opin Cell Biol 31: 46-55.

Cruciat, C. M., C. Dolde, R. E. de Groot, B. Ohkawara, C. Reinhard, H. C. Korswagen and C. Niehrs (2013). "RNA helicase DDX3 is a regulatory subunit of casein kinase 1 in Wnt-beta-catenin signaling." Science 339(6126): 1436-1441.

Cruciat, C. M. and C. Niehrs (2013). "Secreted and transmembrane wnt inhibitors and activators." Cold Spring Harb Perspect Biol 5(3): a015081.

Cui, X. and G. A. Churchill (2003). "Statistical tests for differential expression in cDNA microarray experiments." Genome Biol 4(4): 210.

Cummins, T. D., K. Z. L. Wu, P. Bozatzi, K. S. Dingwell, T. J. Macartney, N. T. Wood, J. Varghese, R. Gourlay, D. G. Campbell, A. Prescott, E. Griffis, J. C. Smith and G. P. Sapkota (2018). "PAWS1 controls cytoskeletal dynamics and cell migration through association with the SH3 adaptor CD2AP." J Cell Sci 131(1).

Daft, P. G., K. Yuan, J. M. Warram, M. J. Klein, G. P. Siegal and M. Zayzafoon (2013). "Alpha-CaMKII plays a critical role in determining the aggressive behavior of human osteosarcoma." Mol Cancer Res 11(4): 349-359.

Davidson, G., W. Wu, J. Shen, J. Bilic, U. Fenger, P. Stannek, A. Glinka and C. Niehrs (2005). "Casein kinase 1 gamma couples Wnt receptor activation to cytoplasmic signal transduction." Nature 438(7069): 867-872.

De Boer, M. L., V. A. Mordvinov, M. A. Thomas and C. J. Sanderson (1999). "Role of nuclear factor of activated T cells (NFAT) in the expression of interleukin-5 and other cytokines involved in the regulation of hemopoetic cells." Int J Biochem Cell Biol 31(10): 1221-1236.

De Donatis, A., G. Comito, F. Buricchi, M. C. Vinci, A. Parenti, A. Caselli, G. Camici, G. Manao, G. Ramponi and P. Cirri (2008). "Proliferation versus migration in platelet-derived growth factor signaling: the key role of endocytosis." J Biol Chem 283(29): 19948-19956.

de Groot, R. E., R. S. Ganji, O. Bernatik, B. Lloyd-Lewis, K. Seipel, K. Sedova, Z. Zdrahal, V. M. Dhople, T. C. Dale, H. C. Korswagen and V. Bryja (2014). "Huwe1-mediated ubiquitylation of dishevelled defines a negative feedback loop in the Wnt signaling pathway." Sci Signal 7(317): ra26.

De Robertis, E. M. and H. Kuroda (2004). "Dorsal-ventral patterning and neural induction in Xenopus embryos." Annu Rev Cell Dev Biol 20: 285-308.

DeBruine, Z. J., H. E. Xu and K. Melcher (2017). "Assembly and architecture of the Wnt/beta-catenin signalosome at the membrane." Br J Pharmacol 174(24): 4564-4574.

Del Valle-Perez, B., O. Arques, M. Vinyoles, A. G. de Herreros and M. Dunach (2011). "Coordinated action of CK1 isoforms in canonical Wnt signaling." Mol Cell Biol 31(14): 2877-2888.

Delehouze, C., K. Godl, N. Loaec, C. Bruyere, N. Desban, N. Oumata, H. Galons, T. I. Roumeliotis, E. G. Giannopoulou, J. Grenet, D. Twitchell, J. Lahti, N. Mouchet, M. D. Galibert, S. D. Garbis and L. Meijer (2014). "CDK/CK1 inhibitors roscovitine and CR8 downregulate amplified MYCN in neuroblastoma cells." Oncogene 33(50): 5675-5687.

Derkach, V., A. Barria and T. R. Soderling (1999). "Ca2+/calmodulin-kinase II enhances channel conductance of alpha-amino-3-hydroxy-5-methyl-4-isoxazolepropionate type glutamate receptors." Proc Natl Acad Sci U S A 96(6): 3269-3274.

Desagher, S., A. Osen-Sand, S. Montessuit, E. Magnenat, F. Vilbois, A. Hochmann, L. Journot, B. Antonsson and J. C. Martinou (2001). "Phosphorylation of bid by casein kinases I and II regulates its cleavage by caspase 8." Mol Cell 8(3): 601-611.

Ding, Y., M. R. Estrella, Y. Y. Hu, H. L. Chan, H. D. Zhang, J. W. Kim, J. P. Simmer and J. C. Hu (2009). "Fam83h is associated with intracellular vesicles and ADHCAI." J Dent Res 88(11): 991-996.

Dissanayake, S. K., M. Wade, C. E. Johnson, M. P. O'Connell, P. D. Leotlela, A. D. French, K. V. Shah, K. J. Hewitt, D. T. Rosenthal, F. E. Indig, Y. Jiang, B. J. Nickoloff, D. D. Taub, J. M. Trent, R. T. Moon, M. Bittner and A. T. Weeraratna (2007). "The Wnt5A/protein kinase C pathway mediates motility in melanoma cells via the inhibition of metastasis suppressors and initiation of an epithelial to mesenchymal transition." J Biol Chem 282(23): 17259-17271.

Drogemuller, M., V. Jagannathan, D. Becker, C. Drogemuller, C. Schelling, J. Plassais, C. Kaerle, C. Dufaure de Citres, A. Thomas, E. J. Muller, M. M. Welle, P. Roosje and T. Leeb (2014). "A mutation in the FAM83G gene in dogs with hereditary footpad hyperkeratosis (HFH)." PLoS Genet 10(5): e1004370.

Du, S. J., S. M. Purcell, J. L. Christian, L. L. McGrew and R. T. Moon (1995). "Identification of distinct classes and functional domains of Wnts through expression of wild-type and chimeric proteins in Xenopus embryos." Mol Cell Biol 15(5): 2625-2634.

Dunsch, A. K., D. Hammond, J. Lloyd, L. Schermelleh, U. Gruneberg and F. A. Barr (2012). "Dynein light chain 1 and a spindle-associated adaptor promote dynein asymmetry and spindle orientation." J Cell Biol 198(6): 1039-1054.

Easley, C. A. t., C. M. Brown, A. F. Horwitz and R. M. Tombes (2008). "CaMK-II promotes focal adhesion turnover and cell motility by inducing tyrosine dephosphorylation of FAK and paxillin." Cell Motil Cytoskeleton 65(8): 662-674.

Eide, E. J., M. F. Woolf, H. Kang, P. Woolf, W. Hurst, F. Camacho, E. L. Vielhaber, A. Giovanni and D. M. Virshup (2005). "Control of mammalian circadian rhythm by CKIepsilon-regulated proteasome-mediated PER2 degradation." Mol Cell Biol 25(7): 2795-2807.

Elkins, J. M., V. Fedele, M. Szklarz, K. R. Abdul Azeez, E. Salah, J. Mikolajczyk, S. Romanov, N. Sepetov, X. P. Huang, B. L. Roth, A. Al Haj Zen, D. Fourches, E. Muratov, A. Tropsha, J. Morris, B. A. Teicher, M. Kunkel, E. Polley, K. E. Lackey, F. L. Atkinson, J. P. Overington, P. Bamborough, S. Muller, D. J. Price, T. M. Willson, D. H. Drewry, S. Knapp and W. J. Zuercher (2016). "Comprehensive characterization of the Published Kinase Inhibitor Set." Nat Biotechnol 34(1): 95-103.

Elyada, E., A. Pribluda, R. E. Goldstein, Y. Morgenstern, G. Brachya, G. Cojocaru, I. Snir-Alkalay, I. Burstain, R. Haffner-Krausz, S. Jung, Z. Wiener, K. Alitalo, M. Oren, E. Pikarsky and Y. Ben-Neriah (2011). "CKIalpha ablation highlights a critical role for p53 in invasiveness control." Nature 470(7334): 409-413.

Eng, G. W. L., Edison and D. M. Virshup (2017). "Site-specific phosphorylation of casein kinase 1 delta (CK1delta) regulates its activity towards the circadian regulator PER2." PLoS One 12(5): e0177834.

Enyeart, J. J., H. Liu and J. A. Enyeart (2011). "Calcium-dependent inhibition of adrenal TREK-1 channels by angiotensin II and ionomycin." Am J Physiol Cell Physiol 301(3): C619-629.

Esseltine, J. L. and J. D. Scott (2013). "AKAP signaling complexes: pointing towards the next generation of therapeutic targets?" Trends Pharmacol Sci 34(12): 648-655.

Etchegaray, J. P., K. K. Machida, E. Noton, C. M. Constance, R. Dallmann, M. N. Di Napoli, J. P. DeBruyne, C. M. Lambert, E. A. Yu, S. M. Reppert and D. R. Weaver (2009). "Casein kinase 1 delta regulates the pace of the mammalian circadian clock." Mol Cell Biol 29(14): 3853-3866.

Ewan, K. B. and T. C. Dale (2008). "The potential for targeting oncogenic WNT/beta-catenin signaling in therapy." Curr Drug Targets 9(7): 532-547.

Feng, J., J. Zhao, H. Xie, Y. Yin, G. Luo, J. Zhang, Y. Feng and Z. Li (2015). "Involvement of NEDD9 in the invasion and migration of gastric cancer." Tumour Biol 36(5): 3621-3628.

Fish, K. J., A. Cegielska, M. E. Getman, G. M. Landes and D. M. Virshup (1995). "Isolation and characterization of human casein kinase I epsilon (CKI), a novel member of the CKI gene family." J Biol Chem 270(25): 14875-14883.

Flotow, H., P. R. Graves, A. Q. Wang, C. J. Fiol, R. W. Roeske and P. J. Roach (1990). "Phosphate groups as substrate determinants for casein kinase I action." J Biol Chem 265(24): 14264-14269.

Fohr, K. J., U. Knippschild, A. Herkommer, M. Fauler, C. Peifer, M. Georgieff and O. Adolph (2017). "State-dependent block of voltage-gated sodium channels by the casein-kinase 1 inhibitor IC261." Invest New Drugs 35(3): 277-289.

Fu, Z., T. Chakraborti, S. Morse, G. S. Bennett and G. Shaw (2001). "Four casein kinase I isoforms are differentially partitioned between nucleus and cytoplasm." Exp Cell Res 269(2): 275-286.

Fukuchi, T., M. Sakamoto, H. Tsuda, K. Maruyama, S. Nozawa and S. Hirohashi (1998). "Beta-catenin mutation in carcinoma of the uterine endometrium." Cancer Res 58(16): 3526-3528.

Fulcher LJ, Bozatzi P, Tachie-Menson T., Wu KZL, Cummins TD, Bufton JC, Pinkas DM, Dunbar K, Shrestha S, Wood NT, Weidlich S, Macartney TJ, Varghese J, Gourlay R, Campbell DG, Dingwell KS, Smith JC and B. A. a. S. GS (2018). "The FAM83 family

of proteins are anchors for Casein Kinase 1 1 isoforms through the DUF1669 domain." Science signalling In press.

Gamberi, C. and P. Lasko (2012). "The Bic-C family of developmental translational regulators." Comp Funct Genomics 2012: 141386.

Gammons, M. V., M. Renko, C. M. Johnson, T. J. Rutherford and M. Bienz (2016). "Wnt Signalosome Assembly by DEP Domain Swapping of Dishevelled." Mol Cell 64(1): 92-104.

Gao, Z. H., J. M. Seeling, V. Hill, A. Yochum and D. M. Virshup (2002). "Casein kinase I phosphorylates and destabilizes the beta-catenin degradation complex." Proc Natl Acad Sci U S A 99(3): 1182-1187.

Giamas, G., H. Hirner, L. Shoshiashvili, A. Grothey, S. Gessert, M. Kuhl, D. Henne-Bruns, C. E. Vorgias and U. Knippschild (2007). "Phosphorylation of CK1delta: identification of Ser370 as the major phosphorylation site targeted by PKA in vitro and in vivo." Biochem J 406(3): 389-398.

Gietzen, K. F. and D. M. Virshup (1999). "Identification of inhibitory autophosphorylation sites in casein kinase I epsilon." J Biol Chem 274(45): 32063-32070.

Glinka, A., W. Wu, H. Delius, A. P. Monaghan, C. Blumenstock and C. Niehrs (1998). "Dickkopf-1 is a member of a new family of secreted proteins and functions in head induction." Nature 391(6665): 357-362.

Gottardi, C. J. and B. M. Gumbiner (2004). "Distinct molecular forms of beta-catenin are targeted to adhesive or transcriptional complexes." J Cell Biol 167(2): 339-349.

Graff, J. M. (1997). "Embryonic patterning: to BMP or not to BMP, that is the question." Cell 89(2): 171-174.

Grentzmann, G., J. A. Ingram, P. J. Kelly, R. F. Gesteland and J. F. Atkins (1998). "A dual-luciferase reporter system for studying recoding signals." Rna 4(4): 479-486.

Gross, S. D. and R. A. Anderson (1998). "Casein kinase I: spatial organization and positioning of a multifunctional protein kinase family." Cell Signal 10(10): 699-711.

Grumolato, L., G. Liu, P. Mong, R. Mudbhary, R. Biswas, R. Arroyave, S. Vijayakumar, A. N. Economides and S. A. Aaronson (2010). "Canonical and noncanonical Wnts use a common mechanism to activate completely unrelated coreceptors." Genes Dev 24(22): 2517-2530.

Grzeschik, K. H., D. Bornholdt, F. Oeffner, A. Konig, M. del Carmen Boente, H. Enders, B. Fritz, M. Hertl, U. Grasshoff, K. Hofling, V. Oji, M. Paradisi, C. Schuchardt, Z. Szalai, G. Tadini, H. Traupe and R. Happle (2007). "Deficiency of PORCN, a regulator of Wnt signaling, is associated with focal dermal hypoplasia." Nat Genet 39(7): 833-835.

Gu, B., K. Watanabe, P. Sun, M. Fallahi and X. Dai (2013). "Chromatin effector Pygo2 mediates Wnt-notch crosstalk to suppress luminal/alveolar potential of mammary stem and basal cells." Cell Stem Cell 13(1): 48-61.

Gujral, T. S., M. Chan, L. Peshkin, P. K. Sorger, M. W. Kirschner and G. MacBeath (2014). "A noncanonical Frizzled2 pathway regulates epithelial-mesenchymal transition and metastasis." Cell 159(4): 844-856.

Ha, N. C., T. Tonozuka, J. L. Stamos, H. J. Choi and W. I. Weis (2004). "Mechanism of phosphorylation-dependent binding of APC to beta-catenin and its role in beta-catenin degradation." Mol Cell 15(4): 511-521.

Halekotte, J., L. Witt, C. Ianes, M. Kruger, M. Buhrmann, D. Rauh, C. Pichlo, E. Brunstein, A. Luxenburger, U. Baumann, U. Knippschild, J. Bischof and C. Peifer (2017). "Optimized 4,5-Diarylimidazoles as Potent/Selective Inhibitors of Protein Kinase CK1delta and Their Structural Relation to p38alpha MAPK." Molecules 22(4).

Hammerlein, A., J. Weiske and O. Huber (2005). "A second protein kinase CK1-mediated step negatively regulates Wnt signalling by disrupting the lymphocyte enhancer factor-1/beta-catenin complex." Cell Mol Life Sci 62(5): 606-618.

Hart, P. S., S. Becerik, D. Cogulu, G. Emingil, D. Ozdemir-Ozenen, S. T. Han, P. P. Sulima, E. Firatli and T. C. Hart (2009). "Novel FAM83H mutations in Turkish families with autosomal dominant hypocalcified amelogenesis imperfecta." Clin Genet 75(4): 401-404.

Hashiguchi, M. and M. C. Mullins (2013). "Anteroposterior and dorsoventral patterning are coordinated by an identical patterning clock." Development 140(9): 1970-1980.

He, X., J. P. Saint-Jeannet, Y. Wang, J. Nathans, I. Dawid and H. Varmus (1997). "A member of the Frizzled protein family mediating axis induction by Wnt-5A." Science 275(5306): 1652-1654.

Heasman, J., A. Crawford, K. Goldstone, P. Garner-Hamrick, B. Gumbiner, P. McCrea, C. Kintner, C. Y. Noro and C. Wylie (1994). "Overexpression of cadherins and underexpression of beta-catenin inhibit dorsal mesoderm induction in early Xenopus embryos." Cell 79(5): 791-803.

Henderson, B. R. and F. Fagotto (2002). "The ins and outs of APC and beta-catenin nuclear transport." EMBO Rep 3(9): 834-839.

Hendriksen, J., F. Fagotto, H. van der Velde, M. van Schie, J. Noordermeer and M. Fornerod (2005). "RanBP3 enhances nuclear export of active (beta)-catenin independently of CRM1." J Cell Biol 171(5): 785-797.

Hikasa, H. and S. Y. Sokol (2013). "Wnt signaling in vertebrate axis specification." Cold Spring Harb Perspect Biol 5(1): a007955.

Hoeflich, K. P. and M. Ikura (2002). "Calmodulin in action: diversity in target recognition and activation mechanisms." Cell 108(6): 739-742.

Hoekstra, M. F., R. M. Liskay, A. C. Ou, A. J. DeMaggio, D. G. Burbee and F. Heffron (1991). "HRR25, a putative protein kinase from budding yeast: association with repair of damaged DNA." Science 253(5023): 1031-1034.

Hoffman, L., M. M. Farley and M. N. Waxham (2013). "Calcium-calmodulin-dependent protein kinase II isoforms differentially impact the dynamics and structure of the actin cytoskeleton." Biochemistry 52(7): 1198-1207.

Holley, S. A., P. D. Jackson, Y. Sasai, B. Lu, E. M. De Robertis, F. M. Hoffmann and E. L. Ferguson (1995). "A conserved system for dorsal-ventral patterning in insects and vertebrates involving sog and chordin." Nature 376(6537): 249-253.

Horn, H. F. and K. H. Vousden (2007). "Coping with stress: multiple ways to activate p53." Oncogene 26(9): 1306-1316.

Hu, Y., W. Song, D. Cirstea, D. Lu, N. C. Munshi and K. C. Anderson (2015). "CSNK1alpha1 mediates malignant plasma cell survival." Leukemia 29(2): 474-482.

Huart, A. S., N. J. MacLaine, D. W. Meek and T. R. Hupp (2009). "CK1alpha plays a central role in mediating MDM2 control of p53 and E2F-1 protein stability." J Biol Chem 284(47): 32384-32394.

Hudmon, A., H. Schulman, J. Kim, J. M. Maltez, R. W. Tsien and G. S. Pitt (2005). "CaMKII tethers to L-type Ca2+ channels, establishing a local and dedicated integrator of Ca2+ signals for facilitation." J Cell Biol 171(3): 537-547.

Huelsken, J., R. Vogel, B. Erdmann, G. Cotsarelis and W. Birchmeier (2001). "beta-Catenin controls hair follicle morphogenesis and stem cell differentiation in the skin." Cell 105(4): 533-545.

Hyun, H. K., S. K. Lee, K. E. Lee, H. Y. Kang, E. J. Kim, P. H. Choung and J. W. Kim (2009). "Identification of a novel FAM83H mutation and microhardness of an affected molar in autosomal dominant hypocalcified amelogenesis imperfecta." Int Endod J 42(11): 1039-1043.

Ianes, C., P. Xu, N. Werz, Z. Meng, D. Henne-Bruns, J. Bischof and U. Knippschild (2016). "CK1delta activity is modulated by CDK2/E- and CDK5/p35-mediated phosphorylation." Amino Acids 48(2): 579-592.

Ikeda, S., S. Kishida, H. Yamamoto, H. Murai, S. Koyama and A. Kikuchi (1998). "Axin, a negative regulator of the Wnt signaling pathway, forms a complex with GSK-3beta and beta-catenin and promotes GSK-3beta-dependent phosphorylation of beta-catenin." Embo j 17(5): 1371-1384.

Ingham, P. W. and A. P. McMahon (2001). "Hedgehog signaling in animal development: paradigms and principles." Genes Dev 15(23): 3059-3087.

Inoki, K., H. Ouyang, T. Zhu, C. Lindvall, Y. Wang, X. Zhang, Q. Yang, C. Bennett, Y. Harada, K. Stankunas, C. Y. Wang, X. He, O. A. MacDougald, M. You, B. O. Williams and K. L. Guan (2006). "TSC2 integrates Wnt and energy signals via a coordinated phosphorylation by AMPK and GSK3 to regulate cell growth." Cell 126(5): 955-968.

Inouye, S. and O. Shimomura (1997). "The use of Renilla luciferase, Oplophorus luciferase, and apoaequorin as bioluminescent reporter protein in the presence of coelenterazine analogues as substrate." Biochem Biophys Res Commun 233(2): 349-353.

Ishida, W., T. Hamamoto, K. Kusanagi, K. Yagi, M. Kawabata, K. Takehara, T. K. Sampath, M. Kato and K. Miyazono (2000). "Smad6 is a Smad1/5-induced smad inhibitor. Characterization of bone morphogenetic protein-responsive element in the mouse Smad6 promoter." J Biol Chem 275(9): 6075-6079.

Itoh, K. and S. Y. Sokol (1999). "Axis determination by inhibition of Wnt signaling in Xenopus." Genes Dev 13(17): 2328-2336.

Izeradjene, K., L. Douglas, A. B. Delaney and J. A. Houghton (2004). "Casein kinase I attenuates tumor necrosis factor-related apoptosis-inducing ligand-induced apoptosis by regulating the recruitment of fas-associated death domain and procaspase-8 to the death-inducing signaling complex." Cancer Res 64(21): 8036-8044.

Jamieson, C., M. Sharma and B. R. Henderson (2011). "Regulation of beta-catenin nuclear dynamics by GSK-3beta involves a LEF-1 positive feedback loop." Traffic 12(8): 983-999.

Janda, C. Y., D. Waghray, A. M. Levin, C. Thomas and K. C. Garcia (2012). "Structural basis of Wnt recognition by Frizzled." Science 337(6090): 59-64.

Jaras, M., P. G. Miller, L. P. Chu, R. V. Puram, E. C. Fink, R. K. Schneider, F. Al-Shahrour, P. Pena, L. J. Breyfogle, K. A. Hartwell, M. E. McConkey, G. S. Cowley, D. E. Root, M. G. Kharas, A. Mullally and B. L. Ebert (2014). "Csnk1a1 inhibition has p53-dependent therapeutic efficacy in acute myeloid leukemia." J Exp Med 211(4): 605-612.
Jenkins, G. M. and M. A. Frohman (2005). "Phospholipase D: a lipid centric review." Cell Mol Life Sci 62(19-20): 2305-2316.

Jho, E. H., T. Zhang, C. Domon, C. K. Joo, J. N. Freund and F. Costantini (2002). "Wnt/beta-catenin/Tcf signaling induces the transcription of Axin2, a negative regulator of the signaling pathway." Mol Cell Biol 22(4): 1172-1183.

Joshi, T. and D. Xu (2007). "Quantitative assessment of relationship between sequence similarity and function similarity." BMC Genomics 8: 222.

Kelleher, F. C., D. Fennelly and M. Rafferty (2006). "Common critical pathways in embryogenesis and cancer." Acta Oncol 45(4): 375-388.

Kiecker, C. and C. Niehrs (2001). "A morphogen gradient of Wnt/beta-catenin signalling regulates anteroposterior neural patterning in Xenopus." Development 128(21): 4189-4201.

Kikuchi, A., H. Yamamoto, A. Sato and S. Matsumoto (2011). "New insights into the mechanism of Wnt signaling pathway activation." Int Rev Cell Mol Biol 291: 21-71.

Kim, J. H., H. S. Shin, S. H. Lee, I. Lee, Y. S. Lee, J. C. Park, Y. J. Kim, J. B. Chung and Y. C. Lee (2010). "Contrasting activity of Hedgehog and Wnt pathways according to gastric cancer cell differentiation: relevance of crosstalk mechanisms." Cancer Sci 101(2): 328-335.

Kim, J. W., S. K. Lee, Z. H. Lee, J. C. Park, K. E. Lee, M. H. Lee, J. T. Park, B. M. Seo, J. C. Hu and J. P. Simmer (2008). "FAM83H mutations in families with autosomal-dominant hypocalcified amelogenesis imperfecta." Am J Hum Genet 82(2): 489-494.

Kim, K. M., S. H. Park, J. S. Bae, S. J. Noh, G. Z. Tao, J. R. Kim, K. S. Kwon, H. S. Park, B. H. Park, H. Lee, M. J. Chung, W. S. Moon, K. G. Sylvester and K. Y. Jang (2017). "FAM83H is involved in the progression of hepatocellular carcinoma and is regulated by MYC." Sci Rep 7(1): 3274.

Kim, S. E., H. Huang, M. Zhao, X. Zhang, A. Zhang, M. V. Semonov, B. T. MacDonald, X. Zhang, J. Garcia Abreu, L. Peng and X. He (2013). "Wnt stabilization of beta-catenin reveals principles for morphogen receptor-scaffold assemblies." Science 340(6134): 867-870.

Kinoshita, E., E. Kinoshita-Kikuta, K. Takiyama and T. Koike (2006). "Phosphate-binding tag, a new tool to visualize phosphorylated proteins." Mol Cell Proteomics 5(4): 749-757.

Kinoshita, E., A. Yamada, H. Takeda, E. Kinoshita-Kikuta and T. Koike (2005). "Novel immobilized zinc(II) affinity chromatography for phosphopeptides and phosphorylated proteins." J Sep Sci 28(2): 155-162.

Kishida, M., S. Hino, T. Michiue, H. Yamamoto, S. Kishida, A. Fukui, M. Asashima and A. Kikuchi (2001). "Synergistic activation of the Wnt signaling pathway by Dvl and casein kinase Iepsilon." J Biol Chem 276(35): 33147-33155.

Klein, P. S. and D. A. Melton (1996). "A molecular mechanism for the effect of lithium on development." Proc Natl Acad Sci U S A 93(16): 8455-8459.

Klimowski, L. K., B. A. Garcia, J. Shabanowitz, D. F. Hunt and D. M. Virshup (2006). "Site-specific casein kinase 1epsilon-dependent phosphorylation of Dishevelled modulates beta-catenin signaling." Febs j 273(20): 4594-4602.

Kloss, B., J. L. Price, L. Saez, J. Blau, A. Rothenfluh, C. S. Wesley and M. W. Young (1998). "The Drosophila clock gene double-time encodes a protein closely related to human casein kinase Iepsilon." Cell 94(1): 97-107.

Knauper, V., H. Will, C. Lopez-Otin, B. Smith, S. J. Atkinson, H. Stanton, R. M. Hembry and G. Murphy (1996). "Cellular mechanisms for human procollagenase-3 (MMP-13) activation. Evidence that MT1-MMP (MMP-14) and gelatinase a (MMP-2) are able to generate active enzyme." J Biol Chem 271(29): 17124-17131.

Knippschild, U., A. Gocht, S. Wolff, N. Huber, J. Lohler and M. Stoter (2005). "The casein kinase 1 family: participation in multiple cellular processes in eukaryotes." Cell Signal 17(6): 675-689.

Knippschild, U., M. Kruger, J. Richter, P. Xu, B. Garcia-Reyes, C. Peifer, J. Halekotte, V. Bakulev and J. Bischof (2014). "The CK1 Family: Contribution to Cellular Stress Response and Its Role in Carcinogenesis." Front Oncol 4: 96.

Kolodziej, S. J., A. Hudmon, M. N. Waxham and J. K. Stoops (2000). "Three-dimensional reconstructions of calcium/calmodulin-dependent (CaM) kinase IIalpha and truncated CaM kinase IIalpha reveal a unique organization for its structural core and functional domains." J Biol Chem 275(19): 14354-14359.

Koppert, L. B., A. W. van der Velden, M. van de Wetering, M. Abbou, A. M. van den Ouweland, H. W. Tilanus, B. P. Wijnhoven and W. N. Dinjens (2004). "Frequent loss of the AXIN1 locus but absence of AXIN1 gene mutations in adenocarcinomas of the gastro-oesophageal junction with nuclear beta-catenin expression." Br J Cancer 90(4): 892-899.

Korinek, V., N. Barker, P. Moerer, E. van Donselaar, G. Huls, P. J. Peters and H. Clevers (1998). "Depletion of epithelial stem-cell compartments in the small intestine of mice lacking Tcf-4." Nat Genet 19(4): 379-383.

Kosten, J., A. Binolfi, M. Stuiver, S. Verzini, F. X. Theillet, B. Bekei, M. van Rossum and P. Selenko (2014). "Efficient modification of alpha-synuclein serine 129 by protein kinase CK1 requires phosphorylation of tyrosine 125 as a priming event." ACS Chem Neurosci 5(12): 1203-1208.

Kozyulina, P. Y., Y. V. Loskutov, V. K. Kozyreva, A. Rajulapati, R. J. Ice, B. C. Jones and E. N. Pugacheva (2015). "Prometastatic NEDD9 Regulates Individual Cell Migration via Caveolin-1-Dependent Trafficking of Integrins." Mol Cancer Res 13(3): 423-438.

Kramps, T., O. Peter, E. Brunner, D. Nellen, B. Froesch, S. Chatterjee, M. Murone, S. Zullig and K. Basler (2002). "Wnt/wingless signaling requires BCL9/legless-mediated recruitment of pygopus to the nuclear beta-catenin-TCF complex." Cell 109(1): 47-60.

Krieghoff, E., J. Behrens and B. Mayr (2006). "Nucleo-cytoplasmic distribution of beta-catenin is regulated by retention." J Cell Sci 119(Pt 7): 1453-1463.

Kronke, J., E. C. Fink, P. W. Hollenbach, K. J. MacBeth, S. N. Hurst, N. D. Udeshi, P. P. Chamberlain, D. R. Mani, H. W. Man, A. K. Gandhi, T. Svinkina, R. K. Schneider, M. McConkey, M. Jaras, E. Griffiths, M. Wetzler, L. Bullinger, B. E. Cathers, S. A. Carr, R. Chopra and B. L. Ebert (2015). "Lenalidomide induces ubiquitination and degradation of CK1alpha in del(5q) MDS." Nature 523(7559): 183-188.

Kuga, T., H. Kume, J. Adachi, N. Kawasaki, M. Shimizu, I. Hoshino, H. Matsubara, Y. Saito, Y. Nakayama and T. Tomonaga (2016). "Casein kinase 1 is recruited to nuclear speckles by FAM83H and SON." Sci Rep 6: 34472.

Kuga, T., H. Kume, N. Kawasaki, M. Sato, J. Adachi, T. Shiromizu, I. Hoshino, T. Nishimori, H. Matsubara and T. Tomonaga (2013). "A novel mechanism of keratin cytoskeleton organization through casein kinase Ialpha and FAM83H in colorectal cancer." J Cell Sci 126(Pt 20): 4721-4731.

Kuga, T., M. Sasaki, T. Mikami, Y. Miake, J. Adachi, M. Shimizu, Y. Saito, M. Koura, Y. Takeda, J. Matsuda, T. Tomonaga and Y. Nakayama (2016). "FAM83H and casein kinase I regulate the organization of the keratin cytoskeleton and formation of desmosomes." Sci Rep 6: 26557.

Kuhl, M., L. C. Sheldahl, C. C. Malbon and R. T. Moon (2000). "Ca(2+)/calmodulin-dependent protein kinase II is stimulated by Wnt and Frizzled homologs and promotes ventral cell fates in Xenopus." J Biol Chem 275(17): 12701-12711.

Kuhl, M., L. C. Sheldahl, M. Park, J. R. Miller and R. T. Moon (2000). "The Wnt/Ca2+ pathway: a new vertebrate Wnt signaling pathway takes shape." Trends Genet 16(7): 279-283.

Kuret, J., G. S. Johnson, D. Cha, E. R. Christenson, A. J. DeMaggio and M. F. Hoekstra (1997). "Casein kinase 1 is tightly associated with paired-helical filaments isolated from Alzheimer's disease brain." J Neurochem 69(6): 2506-2515.

Kweon, Y. S., K. E. Lee, J. Ko, J. C. Hu, J. P. Simmer and J. W. Kim (2013). "Effects of Fam83h overexpression on enamel and dentine formation." Arch Oral Biol 58(9): 1148-1154.

Larabell, C. A., M. Torres, B. A. Rowning, C. Yost, J. R. Miller, M. Wu, D. Kimelman and R. T. Moon (1997). "Establishment of the dorso-ventral axis in Xenopus embryos is presaged by early asymmetries in beta-catenin that are modulated by the Wnt signaling pathway." J Cell Biol 136(5): 1123-1136.

Lasa-Benito, M., O. Marin, F. Meggio and L. A. Pinna (1996). "Golgi apparatus mammary gland casein kinase: monitoring by a specific peptide substrate and definition of specificity determinants." FEBS Lett 382(1-2): 149-152.

Lee, E., A. Salic and M. W. Kirschner (2001). "Physiological regulation of [beta]-catenin stability by Tcf3 and CK1epsilon." J Cell Biol 154(5): 983-993.

Lee, J. C. and A. M. Edelman (1994). "A protein activator of Ca(2+)-calmodulin-dependent protein kinase Ia." J Biol Chem 269(3): 2158-2164.

Lee, M. J., S. K. Lee, K. E. Lee, H. Y. Kang, H. S. Jung and J. W. Kim (2009). "Expression patterns of the Fam83h gene during murine tooth development." Arch Oral Biol 54(9): 846-850.

Lee, S. K., J. C. Hu, J. D. Bartlett, K. E. Lee, B. P. Lin, J. P. Simmer and J. W. Kim (2008). "Mutational spectrum of FAM83H: the C-terminal portion is required for tooth enamel calcification." Hum Mutat 29(8): E95-99.

Lee, S. Y., R. Meier, S. Furuta, M. E. Lenburg, P. A. Kenny, R. Xu and M. J. Bissell (2012). "FAM83A confers EGFR-TKI resistance in breast cancer cells and in mice." J Clin Invest 122(9): 3211-3220.

Leiros, I., F. Secundo, C. Zambonelli, S. Servi and E. Hough (2000). "The first crystal structure of a phospholipase D." Structure 8(6): 655-667.

Leon, R. P., M. Tecklenburg and R. A. Sclafani (2008). "Functional conservation of beta-hairpin DNA binding domains in the Mcm protein of Methanobacterium thermoautotrophicum and the Mcm5 protein of Saccharomyces cerevisiae." Genetics 179(4): 1757-1768.

Leyns, L., T. Bouwmeester, S. H. Kim, S. Piccolo and E. M. De Robertis (1997). "Frzb-1 is a secreted antagonist of Wnt signaling expressed in the Spemann organizer." Cell 88(6): 747-756.

Li, B., D. Orton, L. R. Neitzel, L. Astudillo, C. Shen, J. Long, X. Chen, K. C. Kirkbride, T. Doundoulakis, M. L. Guerra, J. Zaias, D. L. Fei, J. Rodriguez-Blanco, C. Thorne, Z. Wang, K. Jin, D. M. Nguyen, L. R. Sands, F. Marchetti, M. T. Abreu, M. H. Cobb, A. J. Capobianco, E. Lee and D. J. Robbins (2017). "Differential abundance of CK1alpha

provides selectivity for pharmacological CK1alpha activators to target WNT-dependent tumors." Sci Signal 10(485).

Li, B., C. Rheaume, A. Teng, V. Bilanchone, J. E. Munguia, M. Hu, S. Jessen, S. Piccolo, M. L. Waterman and X. Dai (2007). "Developmental phenotypes and reduced Wnt signaling in mice deficient for pygopus 2." Genesis 45(5): 318-325.

Li, G., H. Yin and J. Kuret (2004). "Casein kinase 1 delta phosphorylates tau and disrupts its binding to microtubules." J Biol Chem 279(16): 15938-15945.

Li, V. S., S. S. Ng, P. J. Boersema, T. Y. Low, W. R. Karthaus, J. P. Gerlach, S. Mohammed, A. J. Heck, M. M. Maurice, T. Mahmoudi and H. Clevers (2012). "Wnt signaling through inhibition of beta-catenin degradation in an intact Axin1 complex." Cell 149(6): 1245-1256.

Lim, X. and R. Nusse (2013). "Wnt signaling in skin development, homeostasis, and disease." Cold Spring Harb Perspect Biol 5(2).

Little, S. C. and M. C. Mullins (2006). "Extracellular modulation of BMP activity in patterning the dorsoventral axis." Birth Defects Res C Embryo Today 78(3): 224-242.

Liu, C., Y. Kato, Z. Zhang, V. M. Do, B. A. Yankner and X. He (1999). "beta-Trcp couples beta-catenin phosphorylation-degradation and regulates Xenopus axis formation." Proc Natl Acad Sci U S A 96(11): 6273-6278.

Liu, C., Y. Li, M. Semenov, C. Han, G. H. Baeg, Y. Tan, Z. Zhang, X. Lin and X. He (2002). "Control of beta-catenin phosphorylation/degradation by a dual-kinase mechanism." Cell 108(6): 837-847.

Liu, W., X. Dong, M. Mai, R. S. Seelan, K. Taniguchi, K. K. Krishnadath, K. C. Halling, J. M. Cunningham, L. A. Boardman, C. Qian, E. Christensen, S. S. Schmidt, P. C. Roche, D. I. Smith and S. N. Thibodeau (2000). "Mutations in AXIN2 cause colorectal cancer with defective mismatch repair by activating beta-catenin/TCF signalling." Nat Genet 26(2): 146-147.

Liu, Z., G. Han, Y. Cao, Y. Wang and H. Gong (2014). "Calcium/calmodulindependent protein kinase II enhances metastasis of human gastric cancer by upregulating nuclear factorkappaB and Aktmediated matrix metalloproteinase9 production." Mol Med Rep 10(5): 2459-2464.

Livak, K. J. and T. D. Schmittgen (2001). "Analysis of relative gene expression data using real-time quantitative PCR and the 2(-Delta Delta C(T)) Method." Methods 25(4): 402-408.

Logan, C. Y. and R. Nusse (2004). "The Wnt signaling pathway in development and disease." Annu Rev Cell Dev Biol 20: 781-810.

Loh, K. M., R. van Amerongen and R. Nusse (2016). "Generating Cellular Diversity and Spatial Form: Wnt Signaling and the Evolution of Multicellular Animals." Dev Cell 38(6): 643-655.

Lohler, J., H. Hirner, B. Schmidt, K. Kramer, D. Fischer, D. R. Thal, F. Leithauser and U. Knippschild (2009). "Immunohistochemical characterisation of cell-type specific expression of CK1delta in various tissues of young adult BALB/c mice." PLoS One 4(1): e4174.

Longenecker, K. L., P. J. Roach and T. D. Hurley (1998). "Crystallographic studies of casein kinase I delta toward a structural understanding of auto-inhibition." Acta Crystallogr D Biol Crystallogr 54(Pt 3): 473-475.

Lopez-Rovira, T., E. Chalaux, J. Massague, J. L. Rosa and F. Ventura (2002). "Direct binding of Smad1 and Smad4 to two distinct motifs mediates bone morphogenetic protein-specific transcriptional activation of Id1 gene." J Biol Chem 277(5): 3176-3185.

Lu, Z., S. Ghosh, Z. Wang and T. Hunter (2003). "Downregulation of caveolin-1 function by EGF leads to the loss of E-cadherin, increased transcriptional activity of beta-catenin, and enhanced tumor cell invasion." Cancer Cell 4(6): 499-515.

Luo, M., T. T. Gamage, B. W. Arentson, K. N. Schlasner, D. F. Becker and J. J. Tanner (2016). "Structures of Proline Utilization A (PutA) Reveal the Fold and Functions of the Aldehyde Dehydrogenase Superfamily Domain of Unknown Function." J Biol Chem 291(46): 24065-24075.

MacDonald, B. T., C. Yokota, K. Tamai, X. Zeng and X. He (2008). "Wnt signal amplification via activity, cooperativity, and regulation of multiple intracellular PPPSP motifs in the Wnt co-receptor LRP6." J Biol Chem 283(23): 16115-16123.

Maisonneuve, C., I. Guilleret, P. Vick, T. Weber, P. Andre, T. Beyer, M. Blum and D. B. Constam (2009). "Bicaudal C, a novel regulator of Dvl signaling abutting RNA-processing bodies, controls cilia orientation and leftward flow." Development 136(17): 3019-3030.

Malanchi, I., H. Peinado, D. Kassen, T. Hussenet, D. Metzger, P. Chambon, M. Huber, D. Hohl, A. Cano, W. Birchmeier and J. Huelsken (2008). "Cutaneous cancer stem cell maintenance is dependent on beta-catenin signalling." Nature 452(7187): 650-653.

Mali, P., L. Yang, K. M. Esvelt, J. Aach, M. Guell, J. E. DiCarlo, J. E. Norville and G. M. Church (2013). "RNA-guided human genome engineering via Cas9." Science 339(6121): 823-826.

Mamaeva, O. A., J. Kim, G. Feng and J. M. McDonald (2009). "Calcium/calmodulin-dependent kinase II regulates notch-1 signaling in prostate cancer cells." J Cell Biochem 106(1): 25-32.

Manning, G., D. B. Whyte, R. Martinez, T. Hunter and S. Sudarsanam (2002). "The protein kinase complement of the human genome." Science 298(5600): 1912-1934.

Mao, Y., J. Liu, D. Zhang and B. Li (2016). "miR-143 inhibits tumor progression by targeting FAM83F in esophageal squamous cell carcinoma." Tumour Biol 37(7): 9009-9022.

Marin, O., V. H. Bustos, L. Cesaro, F. Meggio, M. A. Pagano, M. Antonelli, C. C. Allende, L. A. Pinna and J. E. Allende (2003). "A noncanonical sequence phosphorylated

by casein kinase 1 in beta-catenin may play a role in casein kinase 1 targeting of important signaling proteins." Proc Natl Acad Sci U S A 100(18): 10193-10200.

Maruthappu, T., L. A. McGinty, D. C. Blaydon, B. Fell, A. Maatta, R. Duit, T. Hawkins, K. M. Braun, M. A. Simpson, E. A. O'Toole and D. P. Kelsell (2017). "Recessive mutation in FAM83G associated with palmoplantar keratoderma and exuberant scalp hair." J Invest Dermatol.

Mashhoon, N., A. J. DeMaggio, V. Tereshko, S. C. Bergmeier, M. Egli, M. F. Hoekstra and J. Kuret (2000). "Crystal structure of a conformation-selective casein kinase-1 inhibitor." J Biol Chem 275(26): 20052-20060.

Massague, J., S. W. Blain and R. S. Lo (2000). "TGFbeta signaling in growth control, cancer, and heritable disorders." Cell 103(2): 295-309.

McCrea, P. D., W. M. Brieher and B. M. Gumbiner (1993). "Induction of a secondary body axis in Xenopus by antibodies to beta-catenin." J Cell Biol 123(2): 477-484.

McKay, R. M., J. M. Peters and J. M. Graff (2001). "The casein kinase I family in Wnt signaling." Dev Biol 235(2): 388-396.

McLean, W. H. and C. B. Moore (2011). "Keratin disorders: from gene to therapy." Hum Mol Genet 20(R2): R189-197.

Mehlen, P. and A. Puisieux (2006). "Metastasis: a question of life or death." Nat Rev Cancer 6(6): 449-458.

Meng, Q. J., L. Logunova, E. S. Maywood, M. Gallego, J. Lebiecki, T. M. Brown, M. Sladek, A. S. Semikhodskii, N. R. J. Glossop, H. D. Piggins, J. E. Chesham, D. A. Bechtold, S. H. Yoo, J. S. Takahashi, D. M. Virshup, R. P. Boot-Handford, M. H. Hastings and A. S. I. Loudon (2008). "Setting clock speed in mammals: the CK1 epsilon tau mutation in mice accelerates circadian pacemakers by selectively destabilizing PERIOD proteins." Neuron 58(1): 78-88.

Mercure, M. Z., R. Ginnan and H. A. Singer (2008). "CaM kinase II delta2-dependent regulation of vascular smooth muscle cell polarization and migration." Am J Physiol Cell Physiol 294(6): C1465-1475.

Meyer, T., P. I. Hanson, L. Stryer and H. Schulman (1992). "Calmodulin trapping by calcium-calmodulin-dependent protein kinase." Science 256(5060): 1199-1202.

Miller, S. G. and M. B. Kennedy (1986). "Regulation of brain type II Ca2+/calmodulin-dependent protein kinase by autophosphorylation: a Ca2+-triggered molecular switch." Cell 44(6): 861-870.

Miyoshi, Y., K. Iwao, Y. Nagasawa, T. Aihara, Y. Sasaki, S. Imaoka, M. Murata, T. Shimano and Y. Nakamura (1998). "Activation of the beta-catenin gene in primary hepatocellular carcinomas by somatic alterations involving exon 3." Cancer Res 58(12): 2524-2527.

Morley, P. and J. F. Whitfield (1993). "The differentiation inducer, dimethyl sulfoxide, transiently increases the intracellular calcium ion concentration in various cell types." J Cell Physiol 156(2): 219-225.

Munoz, I. M., P. Szyniarowski, R. Toth, J. Rouse and C. Lachaud (2014). "Improved genome editing in human cell lines using the CRISPR method." PLoS One 9(10): e109752.

Murphy, J. M., H. Farhan and P. A. Eyers (2017). "Bio-Zombie: the rise of pseudoenzymes in biology." Biochem Soc Trans 45(2): 537-544.

Nakajo, S., T. Hagiwara, K. Nakaya and Y. Nakamura (1987). "Tissue distribution of casein kinases." Biochem Int 14(1): 701-707.

Nelson, R. K. and M. A. Frohman (2015). "Physiological and pathophysiological roles for phospholipase D." J Lipid Res 56(12): 2229-2237.

Niehrs, C. (2012). "The complex world of WNT receptor signalling." Nat Rev Mol Cell Biol 13(12): 767-779.

Nishita, M., M. Enomoto, K. Yamagata and Y. Minami (2010). "Cell/tissue-tropic functions of Wnt5a signaling in normal and cancer cells." Trends Cell Biol 20(6): 346-354.

Nishita, M., S. K. Yoo, A. Nomachi, S. Kani, N. Sougawa, Y. Ohta, S. Takada, A. Kikuchi and Y. Minami (2006). "Filopodia formation mediated by receptor tyrosine kinase Ror2 is required for Wnt5a-induced cell migration." J Cell Biol 175(4): 555-562.

Nusse, R. and H. Varmus (2012). "Three decades of Wnts: a personal perspective on how a scientific field developed." Embo j 31(12): 2670-2684.

O'Connell, M. P., J. L. Fiori, K. M. Baugher, F. E. Indig, A. D. French, T. C. Camilli, B. P. Frank, R. Earley, K. S. Hoek, J. H. Hasskamp, E. G. Elias, D. D. Taub, M. Bernier and A. T. Weeraratna (2009). "Wnt5A activates the calpain-mediated cleavage of filamin A." J Invest Dermatol 129(7): 1782-1789.

Okamura, H., C. Garcia-Rodriguez, H. Martinson, J. Qin, D. M. Virshup and A. Rao (2004). "A conserved docking motif for CK1 binding controls the nuclear localization of NFAT1." Mol Cell Biol 24(10): 4184-4195.

Ori, A., M. Iskar, K. Buczak, P. Kastritis, L. Parca, A. Andres-Pons, S. Singer, P. Bork and M. Beck (2016). "Spatiotemporal variation of mammalian protein complex stoichiometries." Genome Biol 17: 47.

Oumata, N., K. Bettayeb, Y. Ferandin, L. Demange, A. Lopez-Giral, M. L. Goddard, V. Myrianthopoulos, E. Mikros, M. Flajolet, P. Greengard, L. Meijer and H. Galons (2008). "Roscovitine-derived, dual-specificity inhibitors of cyclin-dependent kinases and casein kinases 1." J Med Chem 51(17): 5229-5242.

Palacios, J. and C. Gamallo (1998). "Mutations in the beta-catenin gene (CTNNB1) in endometrioid ovarian carcinomas." Cancer Res 58(7): 1344-1347.

Park, S., S. Blaser, M. A. Marchal, D. W. Houston and M. D. Sheets (2016). "A gradient of maternal Bicaudal-C controls vertebrate embryogenesis via translational repression of mRNAs encoding cell fate regulators." Development 143(5): 864-871.

Park, W. S., R. R. Oh, J. Y. Park, S. H. Lee, M. S. Shin, Y. S. Kim, S. Y. Kim, H. K. Lee, P. J. Kim, S. T. Oh, N. J. Yoo and J. Y. Lee (1999). "Frequent somatic mutations of the beta-catenin gene in intestinal-type gastric cancer." Cancer Res 59(17): 4257-4260.

Peersen, O. B., T. S. Madsen and J. J. Falke (1997). "Intermolecular tuning of calmodulin by target peptides and proteins: differential effects on Ca2+ binding and implications for kinase activation." Protein Sci 6(4): 794-807.

Pera, E. M. and E. M. De Robertis (2000). "A direct screen for secreted proteins in Xenopus embryos identifies distinct activities for the Wnt antagonists Crescent and Frzb-1." Mech Dev 96(2): 183-195.

Perez, D. I., C. Gil and A. Martinez (2011). "Protein kinases CK1 and CK2 as new targets for neurodegenerative diseases." Med Res Rev 31(6): 924-954.

Perez-Pena, J., A. Alcaraz-Sanabria, C. Nieto-Jimenez, R. Paez, V. Corrales-Sanchez, L. Serrano-Oviedo, V. B. Wali, G. A. Patwardhan, E. Amir, B. Gyorffy, A. Pandiella and A. Ocana (2017). "Mitotic read-out genes confer poor outcome in luminal A breast cancer tumors." Oncotarget 8(13): 21733-21740.

Perron, J. C. and J. Dodd (2009). "ActRIIA and BMPRII Type II BMP receptor subunits selectively required for Smad4-independent BMP7-evoked chemotaxis." PLoS One 4(12): e8198.

Peters, J. M., R. M. McKay, J. P. McKay and J. M. Graff (1999). "Casein kinase I transduces Wnt signals." Nature 401(6751): 345-350.

Petrof, G., K. Fong, J. E. Lai-Cheong, S. E. Cockayne and J. A. McGrath (2011). "Schopf-Schulz-Passarge syndrome resulting from a homozygous nonsense mutation, p.Cys107X, in WNT10A." Australas J Dermatol 52(3): 224-226.

Piccolo, S., E. Agius, L. Leyns, S. Bhattacharyya, H. Grunz, T. Bouwmeester and E. M. De Robertis (1999). "The head inducer Cerberus is a multifunctional antagonist of Nodal, BMP and Wnt signals." Nature 397(6721): 707-710.

Pinna, L. A., G. Clari, V. Moret and N. Siliprandi (1969). "Isolation and enzymatic phosphorylation of rat liver cytosol phosphoproteins." FEBS Lett 5(1): 77-80.

Polakis, P. (2012). "Drugging Wnt signalling in cancer." Embo j 31(12): 2737-2746.
Prevarskaya, N., R. Skryma and Y. Shuba (2011). "Calcium in tumour metastasis: new roles for known actors." Nat Rev Cancer 11(8): 609-618.

Price, M. A. and D. Kalderon (2002). "Proteolysis of the Hedgehog signaling effector Cubitus interruptus requires phosphorylation by Glycogen Synthase Kinase 3 and Casein Kinase 1." Cell 108(6): 823-835.

Radden, L. A., 2nd, K. M. Child, E. B. Adkins, D. V. Spacek, A. M. Feliciano and T. R. King (2013). "The wooly mutation (wly) on mouse chromosome 11 is associated with a genetic defect in Fam83g." BMC Res Notes 6: 189.

Reed, P. W. and H. A. Lardy (1972). "A23187: a divalent cation ionophore." J Biol Chem 247(21): 6970-6977.

Rena, G., J. Bain, M. Elliott and P. Cohen (2004). "D4476, a cell-permeant inhibitor of CK1, suppresses the site-specific phosphorylation and nuclear exclusion of FOXO1a." EMBO Rep 5(1): 60-65.

Reversade, B. and E. M. De Robertis (2005). "Regulation of ADMP and BMP2/4/7 at opposite embryonic poles generates a self-regulating morphogenetic field." Cell 123(6): 1147-1160.

Reya, T. and H. Clevers (2005). "Wnt signalling in stem cells and cancer." Nature 434(7035): 843-850.

Richter, J., J. Bischof, M. Zaja, H. Kohlhof, O. Othersen, D. Vitt, V. Alscher, I. Pospiech, B. Garcia-Reyes, S. Berg, J. Leban and U. Knippschild (2014). "Difluoro-dioxolo-benzoimidazol-benzamides as potent inhibitors of CK1delta and epsilon with nanomolar inhibitory activity on cancer cell proliferation." J Med Chem 57(19): 7933-7946.

Rivers, A., K. F. Gietzen, E. Vielhaber and D. M. Virshup (1998). "Regulation of casein kinase I epsilon and casein kinase I delta by an in vivo futile phosphorylation cycle." J Biol Chem 273(26): 15980-15984.

Robert, X. and P. Gouet (2014). "Deciphering key features in protein structures with the new ENDscript server." Nucleic Acids Res 42(Web Server issue): W320-324.

Rojas-Fernandez, A., L. Herhaus, T. Macartney, C. Lachaud, R. T. Hay and G. P. Sapkota (2015). "Rapid generation of endogenously driven transcriptional reporters in cells through CRISPR/Cas9." Sci Rep 5: 9811.

Rowles, J., C. Slaughter, C. Moomaw, J. Hsu and M. H. Cobb (1991). "Purification of casein kinase I and isolation of cDNAs encoding multiple casein kinase I-like enzymes." Proc Natl Acad Sci U S A 88(21): 9548-9552.

Rowning, B. A., J. Wells, M. Wu, J. C. Gerhart, R. T. Moon and C. A. Larabell (1997). "Microtubule-mediated transport of organelles and localization of beta-catenin to the future dorsal side of Xenopus eggs." Proc Natl Acad Sci U S A 94(4): 1224-1229.

Sakanaka, C., P. Leong, L. Xu, S. D. Harrison and L. T. Williams (1999). "Casein kinase iepsilon in the wnt pathway: regulation of beta-catenin function." Proc Natl Acad Sci U S A 96(22): 12548-12552.

Sandsmark, E., A. F. Hansen, K. M. Selnaes, H. Bertilsson, A. M. Bofin, A. J. Wright, T. Viset, E. Richardsen, F. Drablos, T. F. Bathen, M. B. Tessem and M. B. Rye (2017). "A novel non-canonical Wnt signature for prostate cancer aggressiveness." Oncotarget 8(6): 9572-9586.

Saneyoshi, T., S. Kume, Y. Amasaki and K. Mikoshiba (2002). "The Wnt/calcium pathway activates NF-AT and promotes ventral cell fate in Xenopus embryos." Nature 417(6886): 295-299.

Santamaria, A., S. Nagel, H. H. W. Sillje and E. A. Nigg (2008). "The spindle protein CHICA mediates localization of the chromokinesin Kid to the mitotic spindle." Curr Biol 18(10): 723-729.

Sasai, Y., B. Lu, H. Steinbeisser, D. Geissert, L. K. Gont and E. M. De Robertis (1994). "Xenopus chordin: a novel dorsalizing factor activated by organizer-specific homeobox genes." Cell 79(5): 779-790.

Satoh, S., Y. Daigo, Y. Furukawa, T. Kato, N. Miwa, T. Nishiwaki, T. Kawasoe, H. Ishiguro, M. Fujita, T. Tokino, Y. Sasaki, S. Imaoka, M. Murata, T. Shimano, Y. Yamaoka and Y. Nakamura (2000). "AXIN1 mutations in hepatocellular carcinomas, and growth suppression in cancer cells by virus-mediated transfer of AXIN1." Nat Genet 24(3): 245-250.

Sauer, G., R. Korner, A. Hanisch, A. Ries, E. A. Nigg and H. H. Sillje (2005). "Proteome analysis of the human mitotic spindle." Mol Cell Proteomics 4(1): 35-43.

Sayyab, S., A. Viluma, K. Bergvall, E. Brunberg, V. Jagannathan, T. Leeb, G. Andersson and T. F. Bergstrom (2016). "Whole-Genome Sequencing of a Canine Family Trio Reveals a FAM83G Variant Associated with Hereditary Footpad Hyperkeratosis." G3 (Bethesda) 6(3): 521-527.

Schambony, A. and D. Wedlich (2007). "Wnt-5A/Ror2 regulate expression of XPAPC through an alternative noncanonical signaling pathway." Dev Cell 12(5): 779-792.

Schittek, B. and T. Sinnberg (2014). "Biological functions of casein kinase 1 isoforms and putative roles in tumorigenesis." Mol Cancer 13: 231.

Schwab, C., A. J. DeMaggio, N. Ghoshal, L. I. Binder, J. Kuret and P. L. McGeer (2000). "Casein kinase 1 delta is associated with pathological accumulation of tau in several neurodegenerative diseases." Neurobiol Aging 21(4): 503-510.

Schwarz-Romond, T., M. Fiedler, N. Shibata, P. J. Butler, A. Kikuchi, Y. Higuchi and M. Bienz (2007). "The DIX domain of Dishevelled confers Wnt signaling by dynamic polymerization." Nat Struct Mol Biol 14(6): 484-492.

Schwarz-Romond, T., C. Merrifield, B. J. Nichols and M. Bienz (2005). "The Wnt signalling effector Dishevelled forms dynamic protein assemblies rather than stable associations with cytoplasmic vesicles." J Cell Sci 118(Pt 22): 5269-5277.

Semenov, M. V., R. Habas, B. T. Macdonald and X. He (2007). "SnapShot: Noncanonical Wnt Signaling Pathways." Cell 131(7): 1378.

Shanware, N. P., J. A. Hutchinson, S. H. Kim, L. Zhan, M. J. Bowler and R. S. Tibbetts (2011). "Casein kinase 1-dependent phosphorylation of familial advanced sleep phase syndrome-associated residues controls PERIOD 2 stability." J Biol Chem 286(14): 12766-12774.

Sharma, M., M. Johnson, M. Brocardo, C. Jamieson and B. R. Henderson (2014). "Wnt signaling proteins associate with the nuclear pore complex: implications for cancer." Adv Exp Med Biol 773: 353-372.

Sheehan, D. (2011). "Introduction to Proteins: Structure, Function and Motion. By Amit Kessel and Nir Ben-Tal." ChemBioChem 12(10): 1603-1604.

Sheldahl, L. C., D. C. Slusarski, P. Pandur, J. R. Miller, M. Kuhl and R. T. Moon (2003). "Dishevelled activates Ca2+ flux, PKC, and CamKII in vertebrate embryos." J Cell Biol 161(4): 769-777.

Shi, Q., S. Li, S. Li, A. Jiang, Y. Chen and J. Jiang (2014). "Hedgehog-induced phosphorylation by CK1 sustains the activity of Ci/Gli activator." Proc Natl Acad Sci U S A 111(52): E5651-5660.

Shi, Y. and J. Massague (2003). "Mechanisms of TGF-beta signaling from cell membrane to the nucleus." Cell 113(6): 685-700.

Sillibourne, J. E., D. M. Milne, M. Takahashi, Y. Ono and D. W. Meek (2002). "Centrosomal anchoring of the protein kinase CK1delta mediated by attachment to the large, coiled-coil scaffolding protein CG-NAP/AKAP450." J Mol Biol 322(4): 785-797.

Simons, M. and M. Mlodzik (2008). "Planar cell polarity signaling: from fly development to human disease." Annu Rev Genet 42: 517-540.

Singh, A., M. E. Hildebrand, E. Garcia and T. P. Snutch (2010). "The transient receptor potential channel antagonist SKF96365 is a potent blocker of low-voltage-activated T-type calcium channels." Br J Pharmacol 160(6): 1464-1475.

Skelding, K. A., J. A. Rostas and N. M. Verrills (2011). "Controlling the cell cycle: the role of calcium/calmodulin-stimulated protein kinases I and II." Cell Cycle 10(4): 631-639.

Skonier, J., K. Bennett, V. Rothwell, S. Kosowski, G. Plowman, P. Wallace, S. Edelhoff, C. Disteche, M. Neubauer, H. Marquardt and et al. (1994). "beta ig-h3: a transforming growth factor-beta-responsive gene encoding a secreted protein that inhibits cell attachment in vitro and suppresses the growth of CHO cells in nude mice." DNA Cell Biol 13(6): 571-584.

Snijders, A. M., S. Y. Lee, B. Hang, W. Hao, M. J. Bissell and J. H. Mao (2017). "FAM83 family oncogenes are broadly involved in human cancers: an integrative multi-omics approach." Mol Oncol 11(2): 167-179.

Sparks, A. B., P. J. Morin, B. Vogelstein and K. W. Kinzler (1998). "Mutational analysis of the APC/beta-catenin/Tcf pathway in colorectal cancer." Cancer Res 58(6): 1130-1134.

Stadeli, R., R. Hoffmans and K. Basler (2006). "Transcription under the control of nuclear Arm/beta-catenin." Curr Biol 16(10): R378-385.

Stamos, J. L., M. L. Chu, M. D. Enos, N. Shah and W. I. Weis (2014). "Structural basis of GSK-3 inhibition by N-terminal phosphorylation and by the Wnt receptor LRP6." Elife 3: e01998.

Stamos, J. L. and W. I. Weis (2013). "The beta-catenin destruction complex." Cold Spring Harb Perspect Biol 5(1): a007898.

Stark, K., S. Vainio, G. Vassileva and A. P. McMahon (1994). "Epithelial transformation of metanephric mesenchyme in the developing kidney regulated by Wnt-4." Nature 372(6507): 679-683.

Stoter, M., M. Kruger, G. Banting, D. Henne-Bruns and U. Knippschild (2014). "Microtubules depolymerization caused by the CK1 inhibitor IC261 may be not mediated by CK1 blockage." PLoS One 9(6): e100090.

Stuckey, J. A. and J. E. Dixon (1999). "Crystal structure of a phospholipase D family member." Nat Struct Biol 6(3): 278-284.

Su, Y., C. Fu, S. Ishikawa, A. Stella, M. Kojima, K. Shitoh, E. M. Schreiber, B. W. Day and B. Liu (2008). "APC is essential for targeting phosphorylated beta-catenin to the SCFbeta-TrCP ubiquitin ligase." Mol Cell 32(5): 652-661.

Sunaga, N., T. Kohno, F. T. Kolligs, E. R. Fearon, R. Saito and J. Yokota (2001). "Constitutive activation of the Wnt signaling pathway by CTNNB1 (beta-catenin) mutations in a subset of human lung adenocarcinoma." Genes Chromosomes Cancer 30(3): 316-321.

Sung, T. C., R. L. Roper, Y. Zhang, S. A. Rudge, R. Temel, S. M. Hammond, A. J. Morris, B. Moss, J. Engebrecht and M. A. Frohman (1997). "Mutagenesis of phospholipase D defines a superfamily including a trans-Golgi viral protein required for poxvirus pathogenicity." Embo j 16(15): 4519-4530.

Swulius, M. T. and M. N. Waxham (2008). "Ca(2+)/calmodulin-dependent protein kinases." Cell Mol Life Sci 65(17): 2637-2657.

Tagliabracci, V. S., J. L. Engel, J. Wen, S. E. Wiley, C. A. Worby, L. N. Kinch, J. Xiao, N. V. Grishin and J. E. Dixon (2012). "Secreted kinase phosphorylates extracellular proteins that regulate biomineralization." Science 336(6085): 1150-1153.

Tagliabracci, V. S., L. A. Pinna and J. E. Dixon (2013). "Secreted protein kinases." Trends in biochemical sciences 38(3): 121-130.

Tagliabracci, V. S., J. Wen and J. Xiao (2016). "Methods to Purify and Assay Secretory Pathway Kinases." Methods Mol Biol 1496: 197-215.

Taketo, M. M. (2011). "Reflections on the spread of metastasis to cancer prevention." Cancer Prev Res (Phila) 4(3): 324-328.

Tamai, K., X. Zeng, C. Liu, X. Zhang, Y. Harada, Z. Chang and X. He (2004). "A mechanism for Wnt coreceptor activation." Mol Cell 13(1): 149-156.

Tan, C. W., B. S. Gardiner, Y. Hirokawa, M. J. Layton, D. W. Smith and A. W. Burgess (2012). "Wnt signalling pathway parameters for mammalian cells." PLoS One 7(2): e31882.

Tang, V. W. and W. M. Brieher (2013). "FSGS3/CD2AP is a barbed-end capping protein that stabilizes actin and strengthens adherens junctions." J Cell Biol 203(5): 815-833.

ten Berge, D., D. Kurek, T. Blauwkamp, W. Koole, A. Maas, E. Eroglu, R. K. Siu and R. Nusse (2011). "Embryonic stem cells require Wnt proteins to prevent differentiation to epiblast stem cells." Nat Cell Biol 13(9): 1070-1075.

Thomas, K. R. and M. R. Capecchi (1990). "Targeted disruption of the murine int-1 proto-oncogene resulting in severe abnormalities in midbrain and cerebellar development." Nature 346(6287): 847-850.

Thorne, C. A., A. J. Hanson, J. Schneider, E. Tahinci, D. Orton, C. S. Cselenyi, K. K. Jernigan, K. C. Meyers, B. I. Hang, A. G. Waterson, K. Kim, B. Melancon, V. P. Ghidu, G. A. Sulikowski, B. LaFleur, A. Salic, L. A. Lee, D. M. Miller, 3rd and E. Lee (2010). "Small-molecule inhibition of Wnt signaling through activation of casein kinase 1alpha." Nat Chem Biol 6(11): 829-836.

Tokumitsu, H., H. Enslen and T. R. Soderling (1995). "Characterization of a Ca2+/calmodulin-dependent protein kinase cascade. Molecular cloning and expression of calcium/calmodulin-dependent protein kinase kinase." J Biol Chem 270(33): 19320-19324.

Tong, S. M., Y. Chen, S. H. Ying and M. G. Feng (2016). "Three DUF1996 Proteins Localize in Vacuoles and Function in Fungal Responses to Multiple Stresses and Metal Ions." Sci Rep 6: 20566.

Tsai, F. C., G. H. Kuo, S. W. Chang and P. J. Tsai (2015). "Ca2+ signaling in cytoskeletal reorganization, cell migration, and cancer metastasis." Biomed Res Int 2015: 409245.

van de Wetering, M., R. Cavallo, D. Dooijes, M. van Beest, J. van Es, J. Loureiro, A. Ypma, D. Hursh, T. Jones, A. Bejsovec, M. Peifer, M. Mortin and H. Clevers (1997). "Armadillo coactivates transcription driven by the product of the Drosophila segment polarity gene dTCF." Cell 88(6): 789-799.

van Ooijen, G., M. Hindle, S. F. Martin, M. Barrios-Llerena, F. Sanchez, F. Y. Bouget, J. S. O'Neill, T. Le Bihan and A. J. Millar (2013). "Functional analysis of Casein Kinase 1 in a minimal circadian system." PLoS One 8(7): e70021.

Veeman, M. T., J. D. Axelrod and R. T. Moon (2003). "A second canon. Functions and mechanisms of beta-catenin-independent Wnt signaling." Dev Cell 5(3): 367-377.

Venerando, A., C. Girardi, M. Ruzzene and L. A. Pinna (2013). "Pyrvinium pamoate does not activate protein kinase CK1, but promotes Akt/PKB down-regulation and GSK3 activation." Biochem J 452(1): 131-137.

Vincent, J. P., G. F. Oster and J. C. Gerhart (1986). "Kinematics of gray crescent formation in Xenopus eggs: the displacement of subcortical cytoplasm relative to the egg surface." Dev Biol 113(2): 484-500.

Vogt, J. (2013). Dissecting the molecular mechanisms of the TGF-β/BMP signal transduction pathways: Mapping new players and critically assessing established tools. PhD, University of Dundee.

Vogt, J., K. S. Dingwell, L. Herhaus, R. Gourlay, T. Macartney, D. Campbell, J. C. Smith and G. P. Sapkota (2014). "Protein associated with SMAD1 (PAWS1/FAM83G) is a substrate for type I bone morphogenetic protein receptors and modulates bone morphogenetic protein signalling." Open Biol 4: 130210.

Walian, P. J., B. Hang and J. H. Mao (2016). "Prognostic significance of FAM83D gene expression across human cancer types." Oncotarget 7(3): 3332-3340.

Walker, P. A., L. E. Leong, P. W. Ng, S. H. Tan, S. Waller, D. Murphy and A. G. Porter (1994). "Efficient and rapid affinity purification of proteins using recombinant fusion proteases." Biotechnology (N Y) 12(6): 601-605.

Walton, K. M., K. Fisher, D. Rubitski, M. Marconi, Q. J. Meng, M. Sladek, J. Adams, M. Bass, R. Chandrasekaran, T. Butler, M. Griffor, F. Rajamohan, M. Serpa, Y. Chen, M. Claffey, M. Hastings, A. Loudon, E. Maywood, J. Ohren, A. Doran and T. T. Wager (2009). "Selective inhibition of casein kinase 1 epsilon minimally alters circadian clock period." J Pharmacol Exp Ther 330(2): 430-439.

Wang, D., S. Han, R. Peng, X. Wang, X. X. Yang, R. J. Yang, C. Y. Jiao, D. Ding, G. W. Ji and X. C. Li (2015). "FAM83D activates the MEK/ERK signaling pathway and promotes cell proliferation in hepatocellular carcinoma." Biochem Biophys Res Commun 458(2): 313-320.

Wang, Q., A. J. Symes, C. A. Kane, A. Freeman, J. Nariculam, P. Munson, C. Thrasivoulou, J. R. Masters and A. Ahmed (2010). "A novel role for Wnt/Ca2+ signaling in actin cytoskeleton remodeling and cell motility in prostate cancer." PLoS One 5(5): e10456.

Wang, S., M. Krinks, K. Lin, F. P. Luyten and M. Moos, Jr. (1997). "Frzb, a secreted protein expressed in the Spemann organizer, binds and inhibits Wnt-8." Cell 88(6): 757-766.

Wang, S. K., Y. Hu, J. Yang, C. E. Smith, A. S. Richardson, Y. Yamakoshi, Y. L. Lee, F. Seymen, M. Koruyucu, K. Gencay, M. Lee, M. Choi, J. W. Kim, J. C. Hu and J. P. Simmer (2016). "Fam83h null mice support a neomorphic mechanism for human ADHCAI." Mol Genet Genomic Med 4(1): 46-67.

Wang, Y., N. Thekdi, P. M. Smallwood, J. P. Macke and J. Nathans (2002). "Frizzled-3 is required for the development of major fiber tracts in the rostral CNS." J Neurosci 22(19): 8563-8573.

Wang, Y.-y., R. Zhao and H. Zhe (2015). "The emerging role of CaMKII in cancer." Oncotarget 6(14): 11725-11734.

Wang, Z., Y. Liu, P. Zhang, W. Zhang, W. Wang, K. Curr, G. Wei and J. H. Mao (2013). "FAM83D promotes cell proliferation and motility by downregulating tumor suppressor gene FBXW7." Oncotarget 4(12): 2476-2486.

White, R. R., Y. G. Kwon, M. Taing, D. S. Lawrence and A. M. Edelman (1998). "Definition of optimal substrate recognition motifs of Ca2+-calmodulin-dependent protein kinases IV and II reveals shared and distinctive features." J Biol Chem 273(6): 3166-3172.

Wie, M. B., J. Y. Koh, M. H. Won, J. C. Lee, T. K. Shin, C. J. Moon, H. J. Ha, S. M. Park and H. C. Kim (2001). "BAPTA/AM, an intracellular calcium chelator, induces delayed necrosis by lipoxygenase-mediated free radicals in mouse cortical cultures." Prog Neuropsychopharmacol Biol Psychiatry 25(8): 1641-1659.

Williams, C. A. C., N. S. Gray and G. M. Findlay (2017). "A Simple Method to Identify Kinases That Regulate Embryonic Stem Cell Pluripotency by High-throughput Inhibitor Screening." J Vis Exp(123).

Wilson, P. A. and A. Hemmati-Brivanlou (1995). "Induction of epidermis and inhibition of neural fate by Bmp-4." Nature 376(6538): 331-333.

Winter, M., D. Milne, S. Dias, R. Kulikov, U. Knippschild, C. Blattner and D. Meek (2004). "Protein kinase CK1delta phosphorylates key sites in the acidic domain of murine double-minute clone 2 protein (MDM2) that regulate p53 turnover." Biochemistry 43(51): 16356-16364.

Wright, J. T., S. Frazier-Bowers, D. Simmons, K. Alexander, P. Crawford, S. T. Han, P. S. Hart and T. C. Hart (2009). "Phenotypic variation in FAM83H-associated amelogenesis imperfecta." J Dent Res 88(4): 356-360.

Wu, G. and X. He (2006). "Threonine 41 in beta-catenin serves as a key phosphorylation relay residue in beta-catenin degradation." Biochemistry 45(16): 5319-5323.

Wu, X. and C. T. McMurray (2001). "Calmodulin kinase II attenuation of gene transcription by preventing cAMP response element-binding protein (CREB) dimerization and binding of the CREB-binding protein." J Biol Chem 276(3): 1735-1741.

Wu, X., X. Tu, K. S. Joeng, M. J. Hilton, D. A. Williams and F. Long (2008). "Rac1 activation controls nuclear localization of beta-catenin during canonical Wnt signaling." Cell 133(2): 340-353.

Xie, Z., W. T. Ho and J. H. Exton (2000). "Association of the N- and C-terminal domains of phospholipase D. Contribution of the conserved HKD motifs to the interaction and the requirement of the association for Ser/Thr phosphorylation of the enzyme." J Biol Chem 275(32): 24962-24969.

Xin, W., W. Wenjun, Q. Man and Z. Yuming (2017). "Novel FAM83H mutations in patients with amelogenesis imperfecta." Sci Rep 7(1): 6075.

Xu, S., C. C. Wong, E. H. Tong, S. S. Chung, J. R. Yates, 3rd, Y. Yin and B. C. Ko (2008). "Phosphorylation by casein kinase 1 regulates tonicity-induced osmotic response element-binding protein/tonicity enhancer-binding protein nucleocytoplasmic trafficking." J Biol Chem 283(25): 17624-17634.

Yang, H. and M. F. Roberts (2002). "Cloning, overexpression, and characterization of a bacterial Ca2+-dependent phospholipase D." Protein Sci 11(12): 2958-2968.

Yang, J. and R. A. Weinberg (2008). "Epithelial-mesenchymal transition: at the crossroads of development and tumor metastasis." Dev Cell 14(6): 818-829.

Yang, S. H., T. Andl, V. Grachtchouk, A. Wang, J. Liu, L. J. Syu, J. Ferris, T. S. Wang, A. B. Glick, S. E. Millar and A. A. Dlugosz (2008). "Pathological responses to oncogenic Hedgehog signaling in skin are dependent on canonical Wnt/beta3-catenin signaling." Nat Genet 40(9): 1130-1135.

Yasojima, K., J. Kuret, A. J. DeMaggio, E. McGeer and P. L. McGeer (2000). "Casein kinase 1 delta mRNA is upregulated in Alzheimer disease brain." Brain Res 865(1): 116-120.

Yim, D. G., S. Ghosh, G. R. Guy and D. M. Virshup (2015). "Casein kinase 1 regulates Sprouty2 in FGF-ERK signaling." Oncogene 34(4): 474-484.

Zeng, X., K. Tamai, B. Doble, S. Li, H. Huang, R. Habas, H. Okamura, J. Woodgett and X. He (2005). "A dual-kinase mechanism for Wnt co-receptor phosphorylation and activation." Nature 438(7069): 873-877.

Zhang, F., D. M. Virshup and J. K. Cheong (2017). "Oncogenic RAS-induced CK1alpha drives nuclear FOXO proteolysis." Oncogene.

Zhao, J., S. Bruck, S. Cemerski, L. Zhang, B. Butler, A. Dani, J. A. Cooper and A. S. Shaw (2013). "CD2AP links cortactin and capping protein at the cell periphery to facilitate formation of lamellipodia." Mol Cell Biol 33(1): 38-47.

Zhao, Y., S. Qin, L. I. Atangan, Y. Molina, Y. Okawa, H. T. Arpawong, C. Ghosn, J. H. Xiao, V. Vuligonda, G. Brown and R. A. Chandraratna (2004). "Casein kinase 1alpha interacts with retinoid X receptor and interferes with agonist-induced apoptosis." J Biol Chem 279(29): 30844-30849.

Zhou, M., H. Rebholz, C. Brocia, J. L. Warner-Schmidt, A. A. Fienberg, A. C. Nairn, P. Greengard and M. Flajolet (2010). "Forebrain overexpression of CK1delta leads to down-regulation of dopamine receptors and altered locomotor activity reminiscent of ADHD." Proc Natl Acad Sci U S A 107(9): 4401-4406.

Appendix

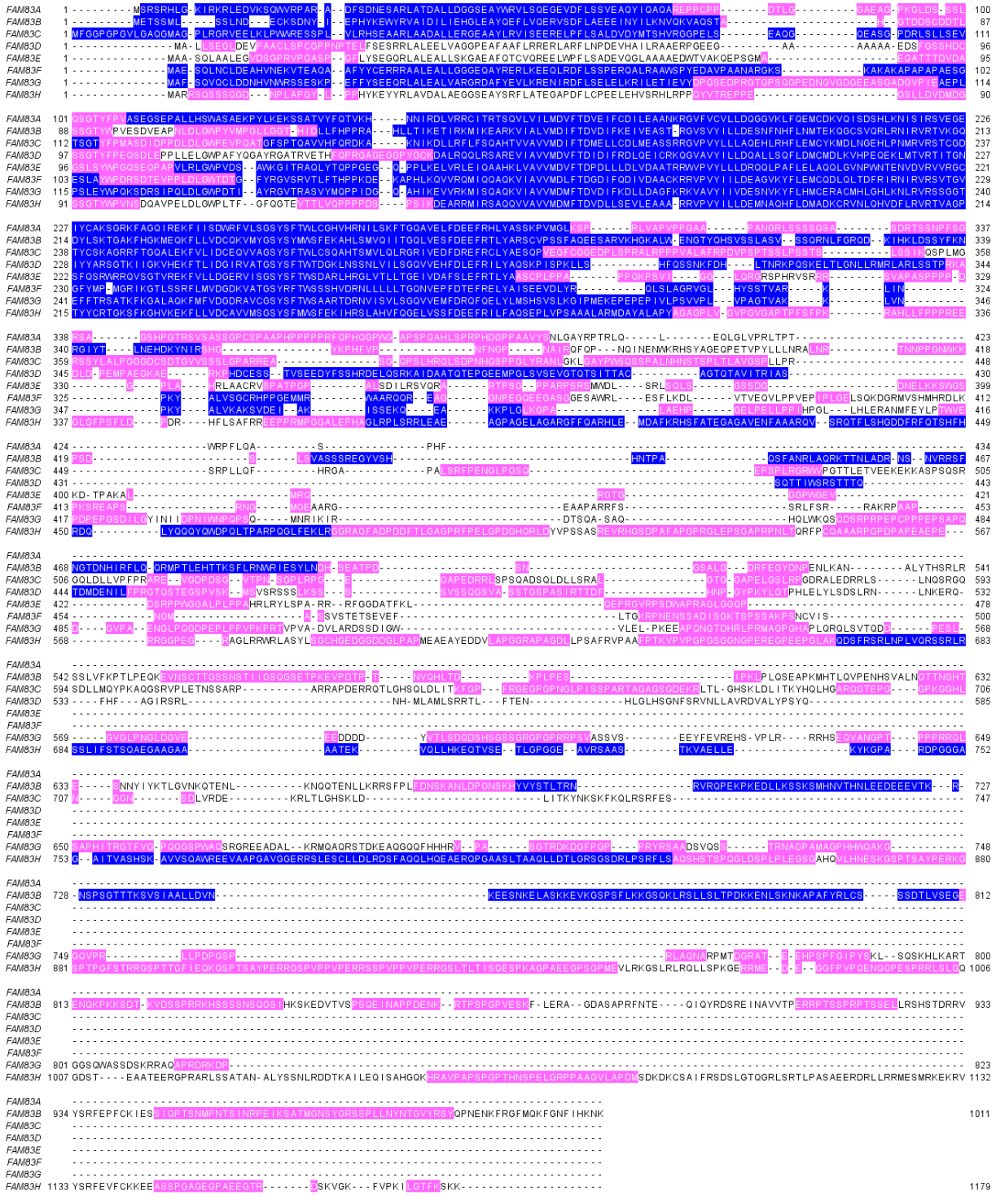

A- 1 Sequence alignment of the FAM83 proteins with disorder prediction

Multiple sequence alignment was performed with ClustalO in Jalview. Disorder prediction was done using Globplot. The highlighted sequences in blue indicate the globular regions while the disordered regions are highlighted in pink.

Uniprot ID	Phospho-peptide sequence
TRIPC	VGGKRGRAQTAPTKTSPRNAKKHDELWHDGV
RS6	QEQIAKRRRLSSLRASTSKSESSQKEQIAKRRRLSSLRASTSKSESSQK
SCX	PCHSGPAFFHAARAGSPPPPPPPPPPARDGEN
DI3L2	PGTQGHLGPEKEEEESDGEPEDSSTS
A6NGY7	TTTYEGSSMSLSRSNSREHLGGGSESDNWRD
TBCD4	VHEGSQKSQPRRRHASAPSHVQPSDSEKNRT
H14	PAGAAKKPKKATGAATPKKSAKKTPKKAKKP
PDCD5	KFNRRKVMDSDEDDDYEKTTTVKFNRRKVMDSDEDDDY
E7EVA0	KPKQKRYSQPRAGGPSDDDNADKPKGHPFAA
IRS1	KVIRADPQGCRRRHSSETFSSTPSATRVGNTPQGPGGMSAFTRVNLSPNRNQSAKVIRADPQSMVGGKPGSFRVI
F5H5B4	QESQQREVDQDDEENSEEDEMDSGTMVRAVG
KPCD3	DFGFARIIGEKSFRRSVVGTPAYLAPEVLRN;DFGFARIIGEKSFRRSVVGTPAYLAPEVLRS
SSRP1	GLKEGMNPSYDEYADSDEDQHDAYLERMKEE
B4DN89	VSRSRSRSRSRSRSRSPPPVSKRESKSRSRSSSVSRSRSRSRSRSRSRSPPPVSKRESKSRS
E9PFC1	RGPEPGVEPQDSRRRSPQEGPTWSRGRRSPR
FNBP4	KKAELRALEEGDGSVSGSSPRSDISQPASQD
USP9X	TGQRAQENYEGSEEVSPPQTKDQ
HIRP3	APGKASVSRKQAREESEESEAEPVQRTAKKV
MAP1B	LSPKSDISPLTPRESSPLYSPTFSDSTSAVK
NUCKS	PVRNRKVVDYSQFQESDDADEDYGRDSGPPT

A- 2 Identification of the CK1 phosphorylation consensus motif, D/E-x-x-S*/T* (highlighted in black) in the sequence of the phospho-peptides with a significant change higher than 2-fold in control unstimulated wild type U2OS cells from Fig 4-12A (left quadrant of the volcano plot).

Uniprot ID	Phospho-peptide sequence
BORG4	AAEKGTSKLPKSLSSSPVKKANDGEGGDEEA
AHNK	KASLGSLEGEAEAEASSPKGKFSLFKSKKPREYQRIYTTKIKPRLKSEDGVEGDLGETQSRT
BAD	NLWAAQRYGRELRRMSDEFVDSFKKGLPRPK
NKAP	MAPVSGSRSPDREASGSGGRRRSS
ADDA	GSPGKSPSKKKKKFRTPSFLKKSKKKSDS;GSPSKSPSKKKKKFRTPSFLKKNKKKEKVEA
B7Z269	NFECLRRQSSQEEVPSSPIFPHRTALPLHLM
H0YJ30	VLPRDTASLSTTPSESPRAQATSRLSTASCP
H0YE40	VEDRKPSGLNGEASKSQEMVHLVNKESSETP
C9JID5	GEVVPSGESGLRRRGSDPASGEVEASQLRRL
CX067	QKATGHADEHLAQTKSPGNSRRRKQPCRNQAGPQKATGHADEHLAQTKSPGNSRRRKQPCRN
SEPT9	RLRRLGDSSGPALKRSFEVEEVETPNSTPPRGVKNSEPSARHVDSLSQRSPKASLRRVELSGMERDRISALKRSFEVEEVETPNSTPPR
MTUS1	RRNSDNRNPSADRAVSPQRIRRVSSSAGNAA
DC1L2	TPTRASESPARGPSGSPRTQGRGGPASVPSS
ARHGG	LYQEIQERGLNTSQESDDDILDESSSPEGTQ
H0YDV5	VFICLSRRRRASAPISQWSSSRRSRSSYTHGCLSRRRRASAPISQWSSSRRSRSSYTHGLNRLSRRRRASAPISQWSSSRRSRSSYTHGL
J3KT76	ADAGSSGGTGPTEGYSPPAASTRAAARAKAR
TOIP1	RMQNDSILKSELGNQSPSTSSRQVTGQPQNA
OPTN	RQSLMEMQSRHGARTSDSDQQAYLVQRGAED
F5H593	QRVTSTPQADSEREASPLGSSVEPGTEEKSL
B1AJQ6	KEKESIARARAGSRLSAEERQREEQLVSFDS
TOP2A	EKKNKKKIKNENTEGSPQEDGVELEGLKQRL
Q5VZY9	RRSTTKSPGPSRRSKSPASTSSVNGTPGSQL
L2GL2	GNGAGPKKAPSRARNSGTQSDGEEKQPGLVM
IP6K3	KKYFLCKDKYYGRKLSVEGFRQALYQFLHNG
XIRP1	GGGSDPRIPAAPRKVSREEQALPRGLPGGWV

A- 3 Identification of the CK1 phosphorylation consensus motif, D/E-x-x-S*/T* (highlighted in black) in the sequence of the phospho-peptides with a significant change higher than 2-fold in unstimulated U2OS PAWS1$^{-/-}$ cells from Fig 4-12A (right quadrant of the volcano plot).

A- 4 Identification of the CK1 phosphorylation consensus motif, D/E-x-x-S*/T* (highlighted in black) in the sequence of the phospho-peptides with a significant change higher than 2-fold in Wnt3A-stimulated wild type U2OS cells from Fig 4-13A (left quadrant of the volcano plot).

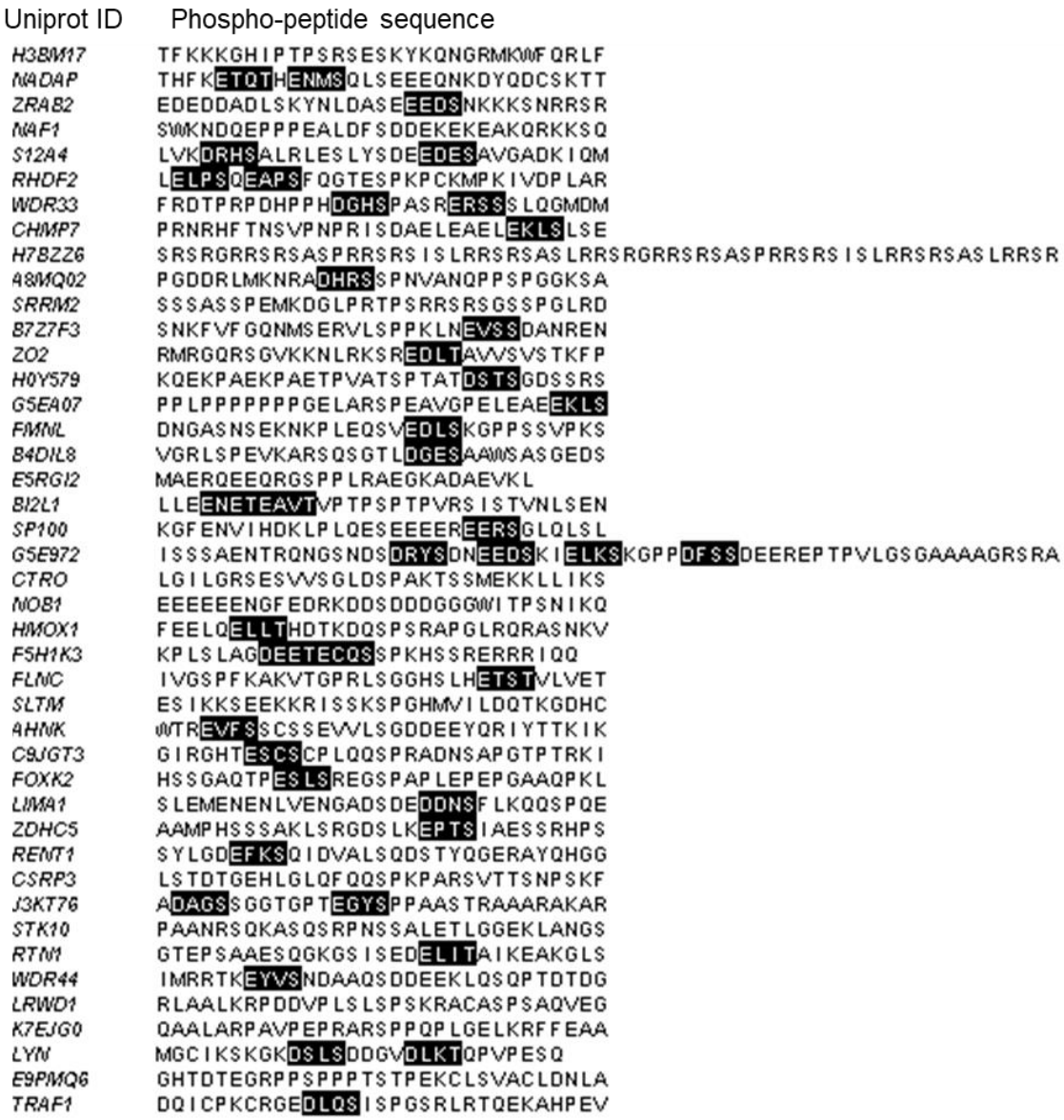

A- 5 Identification of the CK1 phosphorylation consensus motif, D/E-x-x-S*/T* (highlighted in black) in the sequence of the phospho-peptides with a significant change higher than 2-fold in Wnt3A-stimulated U2OS PAWS1$^{-/-}$ cells from Fig 4-13A (right quadrant of the volcano plot).